Technical Report Documentation Page

1. Report No.	2. Government Accession No.	3. Recipient's Catalog No.
FHWA/TX-02/1872-1		

4. Title and Subtitle	5. Report Date
DEVELOPMENT OF A NEW METHOD FOR ASSESSING ASPHALT BINDER PERFORMANCE DURABILITY	October 2001
	6. Performing Organization Code

7. Author(s)	8. Performing Organization Report No.
Charles J. Glover, Richard R. Davison, Chris H. Domke, Yonghong Ruan, Pramitha Juristyarini, Daniel B. Knorr	Report 1872-1

9. Performing Organization Name and Address	10. Work Unit No. (TRAIS)
Texas Transportation Institute The Texas A&M University System College Station, Texas 77843-3135	11. Contract or Grant No. Project No. 0-1872

12. Sponsoring Agency Name and Address	13. Type of Report and Period Covered
Texas Department of Transportation Research and Technology Implementation Office P.O. Box 5080 Austin, Texas 78763-5080	Research: September 1998 - August 2001
	14. Sponsoring Agency Code

15. Supplementary Notes

Research performed in cooperation with the Texas Department of Transportation and the U.S. Department of Transportation, Federal Highway Administration.
Research Project Title: Evaluate Non-Specification Properties for Performance Graded Asphalts Which May Affect Performance

16. Abstract

This project was a comprehensive study directed at developing an improved method of screening asphalt binders for long-term pavement performance. A new dynamic shear rheometer (DSR) function which correlates well with ductility was coupled with a new aging procedure in a tentative specification which should guard against failure caused by premature asphalt hardening and consequent fatigue cracking.

The correlation was found for unmodified asphalts between ductility (at 15 °C, 1 cm/min) below 10 cm and the DSR function $G'/(\eta'/G')$. The correlation was originally developed for DSR measurements at 15 °C and 0.005 rad/s. These conditions were shifted to 43 °C and 10 rad/s by using time-temperature superposition to produce a method that is easily accessible to standard laboratory rheological equipment and methods. The developed method is not adequate for modified asphalts.

The aging procedure that is recommended uses the pressure aging vessel (PAV) apparatus but is modified by taking advantage of the higher average aging rate when the asphalt is aged in thiner films. This, combined with somewhat longer aging, results in more extended binder aging and thus a more rigorous test of durability than the standard PAV method. At the same time, the resulting rankings of aged materials is more representative of rankings that are obtained from aging at atmospheric air pressure and 60 °C.

For modified asphalts, the results were complex. Generally for a given value of the DSR function, the ductility was better than indicated by the DSR function correlation for unmodified asphalts. Larger amounts of modifier produced increasing values of ductility for a given function value. This result was very asphalt dependent, however, so no general correlation could be found. As modified binders oxidize, the asphalt hardens and the improvement to ductility imparted by modifiers decreases. After enough aging, the improvement is gone and modified binders perform no better than their aged unmodified counterpart. A critical issue is whether the life extension produced by modifiers is life-cycle cost effective.

17. Key Words	18. Distribution Statement
Asphalt Oxidation, Ductility, Asphalt Durability, Asphalt Aging, Superpave, Maxwell Model, Failure Stress, Failure Strain, Aging Test	No restrictions. This document is available to the public through NTIS: National Technical Information Service 5285 Port Royal Road Springfield, Virginia 22161

19. Security Classif.(of this report)	20. Security Classif.(of this page)	21. No. of Pages	22. Price
Unclassified	Unclassified	222	

Form DOT F 1700.7 (8-72) Reproduction of completed page authorized

DEVELOPMENT OF A NEW METHOD FOR ASSESSING ASPHALT BINDER PERFORMANCE DURABILITY

by

Charles J. Glover
Richard R. Davison
Research Engineers
Chemical Engineering/Texas Transportation Institute

and

Chris H. Domke
Yonghong Ruan
Pramitha Juristyarini
Daniel B. Knorr
Graduate Students
Chemical Engineering/Texas Transportation Institute

Report 1872-1
Project Number 0-1872
Research Project Title: Evaluate Non-Specification Properties for Performance Graded Asphalts Which May Affect Performance

Sponsored by the
Texas Department of Transportation
In Cooperation with the
U.S. Department of Transportation
Federal Highway Administration

October 2001

TEXAS TRANSPORTATION INSTITUTE
and Chemical Engineering Department
The Texas A&M University System
College Station, Texas 77843-3135

DISCLAIMER

This research was performed in cooperation with the Texas Department of Transportation (TxDOT) and the U.S. Department of Transportation, Federal Highway Administration (FHWA). The contents of this report reflect the views of the authors, who are responsible for the facts and accuracy of the data presented herein. The contents do not necessarily reflect the official view or policies of the FHWA or TxDOT. This report does not constitute a standard, specification, or regulation, nor is it intended for construction, bidding, or permit purposes. Trade names are used solely for information and not for product endorsement. The engineer in charge of this project was Charles James Glover, Ph.D., P.E. (Texas, 48732).

ACKNOWLEDGMENTS

The authors wish to express their appreciation for contributions made by several individuals during the study. Gerald Peterson, Texas Department of Transportation project director, was very helpful with technical suggestions and in serving as study contact. The excellent staff support of the Chemical Engineering Department and the Texas Transportation Institute of the Texas A&M University system is greatly appreciated. Also, we recognize the assistance of Todd Hausman of the Center for Asphalt and Materials Chemistry for assistance with laboratory analyses and operations. Finally, the contributions of Dorothy Jordan to project administration and preparation of this report are especially valued and appreciated.

The financial support provided by the Texas Department of Transportation in cooperation with the Federal Highway Administration, the Texas Transportation Institute, the Texas Engineering Experiment Station, and the Chemical Engineering Department at Texas A&M University is also greatly appreciated.

TABLE OF CONTENTS

LIST OF FIGURES

LIST OF TABLES

CHAPTER 1. INTRODUCTION AND BACKGROUND

PROBLEM STATEMENT

Performance grade specifications (PG) are intended to predict pavement performance. By basing the specification on a model of pavement structure and pavement life, the PG system should ideally be able to ignore the content of the asphalt binder in determining the behavior of the material. In actuality, it is known that asphalts of the same grade may behave differently, displaying markedly different aging characteristics, water or stripping susceptibilities, fatigue resistance, and low-temperature strength and flexibility. Refineries will be investigating methods to meet specifications at a low cost, and in some cases, may provide products which meet specifications but do not perform as expected or desired.

The objectives of this research were as follows:

1. Determine asphalt properties which will affect the performance of hot mix asphalt concrete (HMAC). Performance should be related to general pavement behavior, such as rutting, stripping, fatigue cracking, and thermal cracking.
2. Develop methods to measure the identified properties.
3. Determine acceptable criteria for the identified properties.
4. Evaluate existing asphalts which are manufactured to meet the performance grade specifications, including modified systems such as latex, block copolymer, and tire rubber, with respect to performance-related properties and acceptable criteria previously identified.

BASIS AND THEORY OF SUPERPAVE™ SPECIFICATIONS

The Strategic Highway Research Program (SHRP) was conducted from 1988 to 1993. A significant part of this effort was a study of asphalt binder properties leading to performance-based specifications for their selection and use. Specifically, these specifications address the major failure properties of pavements, namely, rutting, fatigue cracking, and thermal cracking. The work of the SHRP program built upon early asphalt work, added new data and theory, and provided updated specifications.

The Superpave™ binder testing protocol calls for a combination of conditioning and property measurement steps (Figure 1-1). First, the binder is tested in an unaged condition at the desired maximum pavement temperature to assess the likelihood that it will produce a tender mix. This test is assessed with a dynamic shear rheometer (DSR) $G^*/\sin\delta$ measurement, and a minimum value of 1.0 kPa is required. Second, the binder is subjected to the rolling thin-film oven test (RTFOT) to mimic the binder aging that would occur in the hot-mix plant and then tested again for the likelihood of permanent deformation (rutting) (DSR, $G^*/\sin\delta$, measured at the maximum pavement temperature, a minimum value of 2.2 kPa is required). Third, the binder is subjected to the pressure aging vessel (PAV) at a high temperature and high pressure to mimic

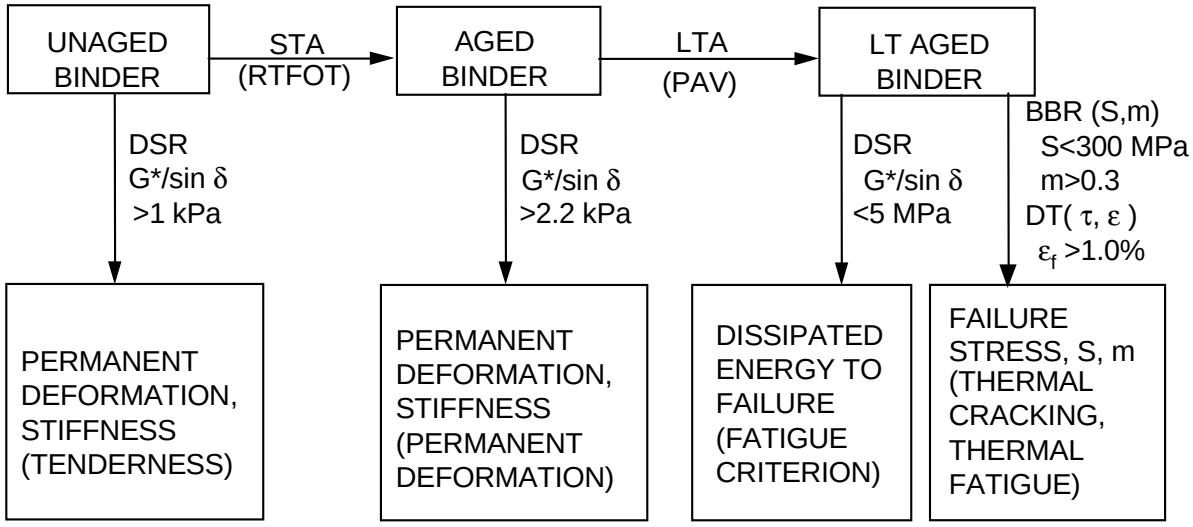

Note: DSR measurements at 10 rad/s

Figure 1-1. Superpave Asphalt Binder Test.

the aging that would occur over extended periods of time in pavement use. Then it is tested a) at moderate temperatures for a tendency to fail due to fatigue cracking (DSR, $G^*\sin\delta$, a maximum value of 5 MPa is allowed) and b) at low temperature (10 °C above the minimum pavement temperature) to obtain a stiffness (S, maximum 300 MPa allowed) and the slope (m) of the log creep stiffness versus log loading time curve to determine the likelihood that the material will fail due to low temperature cracking and thermal fatigue (bending beam rheometer, BBR, S, and m measured at 60 s loading time). Furthermore, the direct tension failure test at low temperature on this long-term aged material may be performed to provide additional information about the likelihood of low-temperature cracking failure (tested at 10 °C above the minimum pavement temperature, 1 percent strain at failure, minimum).

Thermal Cracking Specifications

Early Work

Recent work in the SHRP program leading to Superpave specifications is based upon work which occurred during the mid 1960s by Heukelom and others which led to the concept of a limiting stiffness and limiting stiffness temperature. When an asphalt reaches a certain limiting stiffness, presumably either by temperature or by oxidative aging, then it is susceptible to cracking. The early work of Heukelom (1966) produced considerable data on binder properties and especially binder stiffness, stress, and strain. From these data, he determined that over a wide range of stiffness, Log elongation at break for road bituminous binders versus Log stiffness followed two linear correlations which intersected at a stiffness of about 3 kPa (Figure 1-2). This

common relationship was found for a number of different bitumens and for a number of different rheological measurement techniques. With stiffnesses above 3 kPa, the correlation was especially good, and he extrapolated it to the theoretical glassy modulus of elasticity for bitumens of about 3 Gpa (Figure 1-3). This range of stiffnesses from 3 kPa to 3 GPa covered the failure strain range from about 10% to a little over 0.1%. From these data Heukelom also calculated failure stress data and obtained a common curve for tensile strength versus log stiffness for bituminous binders. The tensile strength at the glassy elastic limit was found to be about 3.5 MPa. This tensile strength curve passed through a maximum tensile strength of about 5.5 MPa at a stiffness value of about 40 MPa. It should be noted that while he recognized that loading time was a factor in the measurements, his measurements were made for common loading rates, and he reported simply "stiffness," bypassing the issue of dependence of stiffness on temperature and time. Nevertheless, the data are very valuable for establishing the importance of stiffness to thermal cracking.

Parallel with the work of Heukelom, Hills and Brien (1966) demonstrated a procedure for determining a cracking temperature for bituminous binders. This technique was based upon the data of Heukelom and recognized that cooling binders, while being restrained from contracting, generated tensile stresses. When these tensile stresses exceed the tensile strength of the binders, whose values as a function of stiffness were determined by Heukelom, the binders will crack. This work then, together with the work of Heukelom, establishes two concepts: the limiting stiffness and the limiting stiffness temperature. For typical coefficients of thermal expansion for asphalt binders, and for pavements, a typical thermal-induced strain is of the order of 1 percent. Therefore, when the stiffness is high enough that a 1 percent strain causes the tensile strength of the binder to be exceeded, we would expect the binder to crack. From Heukelom's data, 1 percent failure strain occurs at a (limiting) stiffness of approximately 400 MPa. Thus, in the literature, one sees limiting stiffness values that approach this value, e.g., 240 MPa at 0.5 hour loading time (McLeod, 1972), 138 MPa at 2.8 hours (Fromm and Phang, 1970), and 200 MPa at 2 hours (Readshaw, 1972). Hills and Brien (1966), as reported by Anderson et al. (1990) use a thermal expansion coefficient of $2 \times 10^{-4}/^{o}C$ to calculate thermal strains.

McLeod (1972) reports much data on thermal cracking in Ontario test roads. Using his data, Readshaw (1972) reports a critical stiffness for bitumen of 240 MPa at 0.5 hr loading time. These field data would seem to match quite well the laboratory data of Heukelom on binder stiffnesses and tensile strengths.

Work of the SHRP Program

Within the SHRP program, a number of thermal cracking theories and procedures were considered (Anderson et al., 1990), including the limiting stiffness concepts discussed above, an empirical/mechanistic model for computing thermal cracking as a function of time (Shahin-McMulin model TC-1), the program COLD, the Ruth model, statistical models, and fracture mechanics models, including the Lytton model. These latter models all attempt to do more than establish a limiting stiffness temperature; they also attempt to calculate the onset-of-cracking

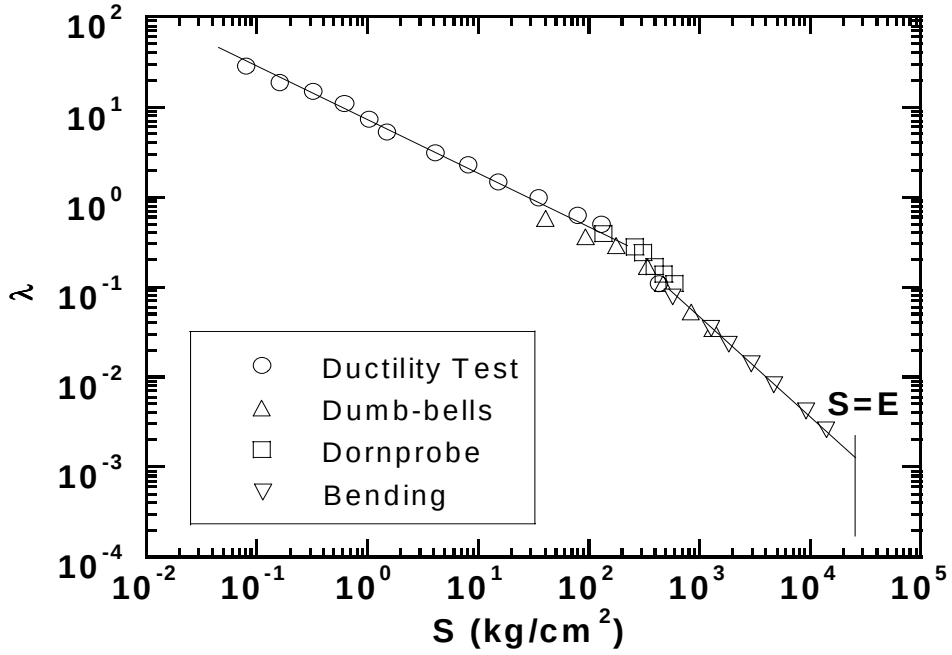

Figure 1-2. Elongation at Break (λ) as a Function of the Stiffness Modulus (S). (1 kg / cm² = 98 kPa) (Heukelom, 1966)

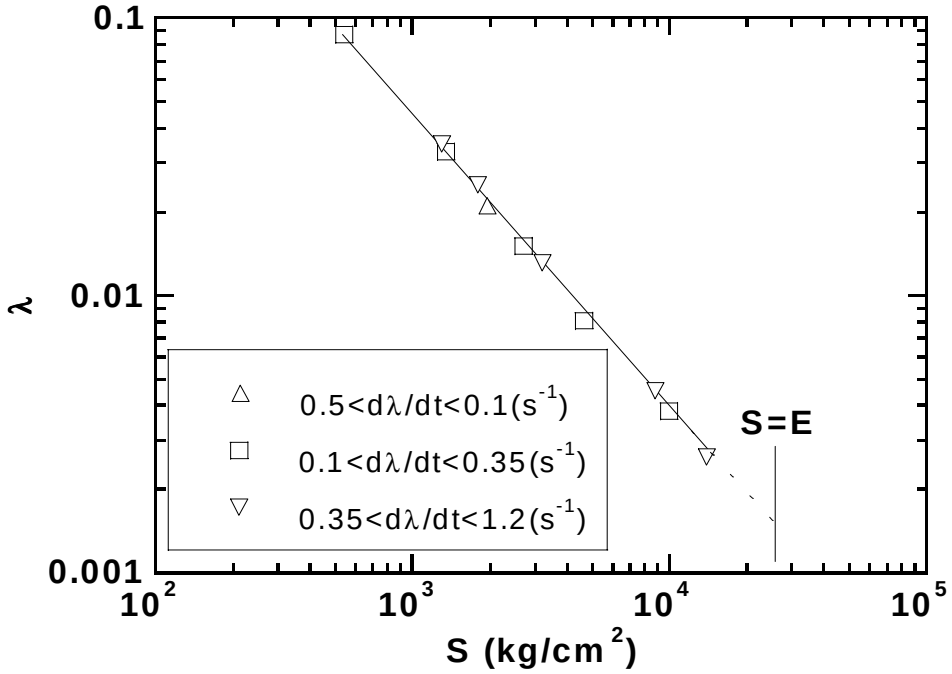

Figure 1-3. Elongation at Break (λ) as a Function of the Stiffness Modulus (S) at High Stiffnesses. (Heukelom, 1966)

time and the extent of cracking over time. All are based variously upon either empirical data, theory, or combinations of the two. These more sophisticated and detailed models, although evaluated as part of the SHRP effort, were considered to be inappropriate for specification purposes (Anderson et al., 1991). In the area of thermal cracking, the limiting stiffness of 300 MPa at a loading time of 2 hours was finally selected for the asphalt binder specification for Superpave (Anderson and Kennedy, 1993). However, this value was time-temperature shifted so that the measurement was actually made at a 10 °C higher temperature and at 60 s instead of 2 hours (i.e., a measurement made at a 10 °C above the specified pavement temperature after 60 s loading is equivalent to one made at the actual pavement temperature and after 2 hours loading) (Anderson and Kennedy, 1993). Additionally, it was specified that the magnitude of the slope of the Log(S) versus Log(t) curve must be greater than 0.3 measured at 10 °C above the minimum pavement temperature. This forces the material to still exhibit relaxation and therefore to exhibit a failure strain greater than its failure strain at its elastic limit. Based on Heukelom's work, an asphaltic material which is at its elastic limit can sustain a strain of only 0.13 percent. The values of 300 MPa and m=0.3 were based upon field data and observations of cracking (Stoffels et al., 1994).

Rutting Specifications

The tenderness and permanent deformation tests which are based on the $G^*/\sin\delta$ parameter measured at the maximum pavement temperature have been related to laboratory rutting tests conducted on compacted mixes (Anderson and Kennedy, 1993). These results have been obtained for both original asphalts and modified asphalt binders. A higher G^* (stiffness) at the maximum pavement temperature and a greater elasticity (smaller $\sin\delta$) will each contribute to a reduced tendency for the binder to deform under load, and therefore, should characterize a binder that is less susceptible to rutting.

Fatigue Cracking Specification

The fatigue cracking specification is the least supported in the literature and, evidently, the least successful. Fatigue cracking is evaluated in the Superpave system from measurements of $G^*\sin\delta$ ($=G''$), which is a measure of energy dissipation, along with the low-temperature value of the slope of the log creep stiffness versus log time curve, m (Anderson and Kennedy, 1993).

ASPHALT DURABILITY AND SUPERPAVE™

Introduction

Perhaps the greatest shortcoming of Superpave specifications for unmodified binders is in regard to the hardening of asphalt. It has been recognized for years that while asphalt roadways can fail for a variety of reasons, if they are properly constructed and designed for the loads they must carry, failure will finally occur when the binder is so oxidized that it becomes very brittle.

Thus one of the most desired properties of asphalt is that it resist the effect of weathering or aging.

For example, in a report to the Virginia Highway and Transportation Committee, Halstead (1984) said: "Thus, the durability of the asphalt cement is a major consideration. A durable asphalt is sometimes defined as one where properties are resistant to change for the worse with time. However, a better definition is that used by Petersen (1984). He defines a durable asphalt as one that 1) possesses the physical properties necessary to produce the desired initial product performance, and 2) is resistant to change in physical properties during long-term, in-use environmental aging."

Superpave™ and Fatigue Cracking

While it is assumed Superpave specifications do a creditable job of guarantying good initial properties, they do not guarantee good aging characteristics. Since this statement is strong it deserves elaboration.

The PAV was introduced to ensure that the fatigue cracking parameter $G^*\sin\delta$ and the low temperature transverse cracking parameters S and m from the bending beam would reflect aging effects. The problem is that none of these parameters is particularly sensitive to aging. This is less important for the low temperature parameters since asphalt physical properties become relatively constant at very low temperature, but it is very important for the fatigue cracking parameters. The literature is replete with studies showing that when penetration, ductility, or other rheological properties reach certain critical levels, roads fail through cracking. Many of these properties are discussed later.

Figure 1-4 is a plot of $G^*\sin\delta$ at 19 and 28 ^oC after 20, 40, and 60 hours in the PAV. Little change in $G^*\sin\delta$ with increased aging is observed. Note that very few asphalts fail this specification (i.e., exceed 5 Mpa) which implies, falsely, that fatigue cracking is not a problem. The specifications could be tightened until some asphalts fail, but that hardly deals with the problem that an aging insensitive property is being used to control for a very aging sensitive malady. In fact Figure 1-4 indicates $G^*\sin\delta$ can even go in the wrong direction with continued aging.

Asphalt Oxidation and Hardening

Before continuing this analysis it is necessary that we digress to discuss the nature of asphalt oxidation and hardening. Over the last decade, we (CMAC) have done extensive studies on asphalt oxidation.

Asphalt hardening is broken into independent parameters as indicated by equation 1-1 relative to viscosity changes with oxidation.

$$\frac{d \ln \eta_o^*}{dt} = \frac{d \ln \eta_o^*}{dCA} \frac{dCA}{dt} \qquad (1\text{-}1)$$

where η_o^* is the low shear rate limiting dynamic complex viscosity, t is time, and carbonyl area (CA) is the area under the carbonyl curve as measured by infrared analysis. We have shown the CA is a good surrogate for oxygen and much easier to measure (Liu et al., 1996). We discovered some years ago (Martin et al., 1990) that the first term in equation 1-1 was independent of aging temperature below about 100-110 ºC and was a constant for each asphalt. We called this term the hardening susceptibility (HS). It is not a measure of how fast an asphalt oxidizes, but it is a measure of its tendency to harden when it oxidizes. Obviously a low value is desirable.

Figure 1-5 shows a typical plot of how carbonyl changes with time when diffusion is eliminated. There is an initial jump that is characteristic of the asphalt and then a constant slope. The change in ln η_o^* behaves the same way, so that when ln η_o^* is plotted versus CA as in Figure 1-6, a straight line is obtained with data from all temperatures collapsing to a single line.

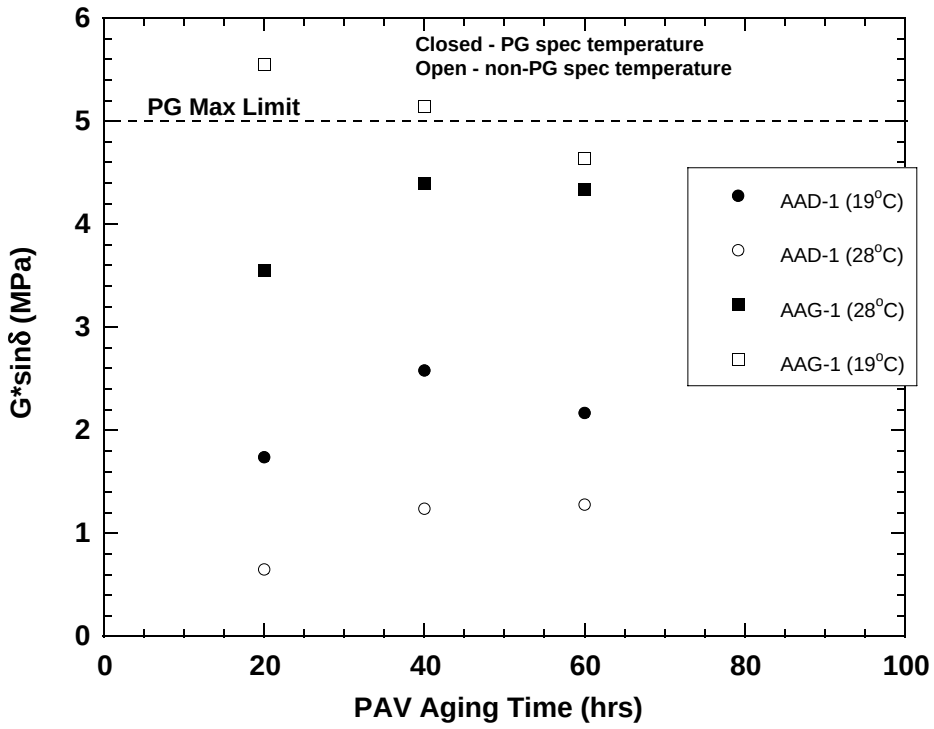

Figure 1-4. G*sinδ vs Aging Time.

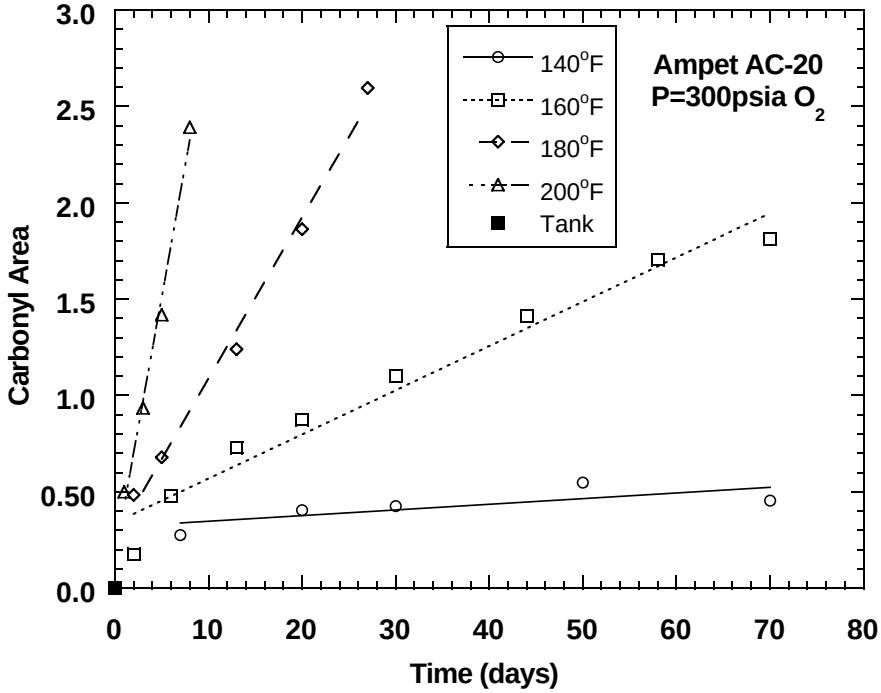

Figure 1-5. Carbonyl Area vs Aging Time.

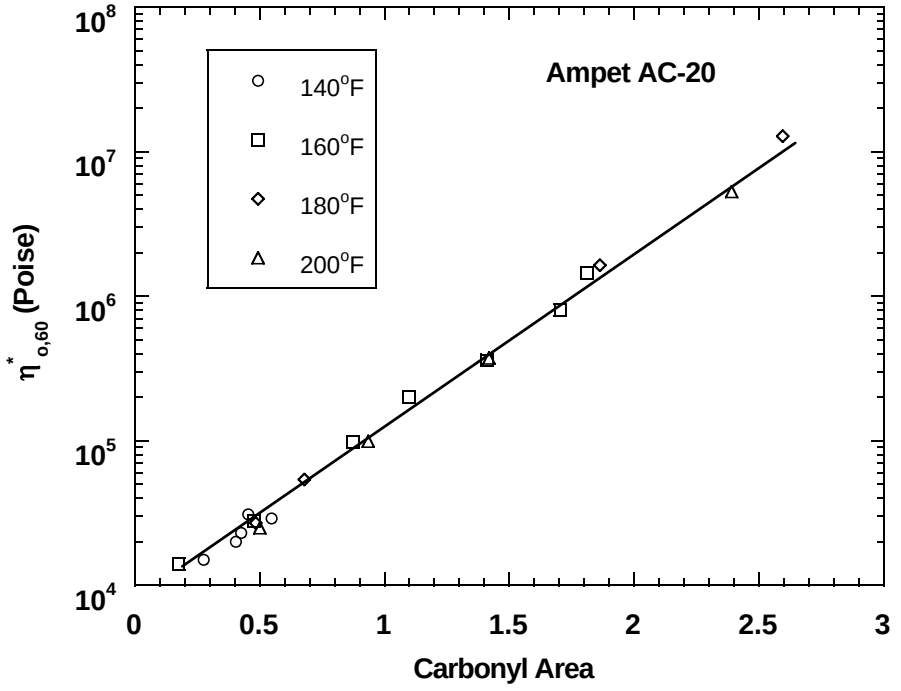

Figure 1-6. Hardening Susceptibility.

We have also done extensive studies on how to manipulate asphalt composition to affect the HS. Though as equation 1-1 shows, it is only part of the picture. It is usually the most variable term, and we also know generally how those changes affect the oxidation rate (Liu et al., 1997a; Liu et al., 1997b; Jemison et al., 1995; Stegeman et al., 1991).

The realization that asphalt hardening rate is of paramount importance is indicated by the large number of attempts to simulate road aging with short term tests. The thin film oven test (TFOT) and the rolling thin film oven test are reasonably accurate at simulating the hot-mix process, at least for conventional, unmodified materials (Jemison et al., 1991). The two tests produce almost identical results and simulate changes in viscosity as accurately as could be expected. The literature of the development and use of these tests were extensively reviewed in Davison et al. (1989). There are some differences in chemical properties between the oven tests and hot mix operation as indicated by gel permeation chromatography (GPC) and carbonyl formation, but overall, these oven tests are as good at simulating the hot mix operations as could be expected and need not be changed.

On the other hand, attempts to relate the results of these tests to road aging have generally been unsatisfactory. Many attempts have been made to alter these tests to better simulate road aging. Welborn (1984) lists 18 of these. Frequently it is stated that one of these tests is equal to so many years on the road. For instance, Huang et al. (1996) stated that the RTFOT at 185 °C can simulate one year of aging and that 168 hours in the California tilt oven is equivalent to eight years on the road. They also claim that high temperature aging is satisfactory because when, for a single asphalt, penetration is plotted versus log viscosity of oven aged, PAV aged and road aged materials, they more or less fall on the same curve. This is naive not only because asphalts differ but because the effect of voids often overwhelms other factors affecting road life (Davison et al., 1989).

The Superpave specified PAV is based on earlier work on pressure oxidation (Lee, 1968; Lee and Huang, 1973) even though Jamieson and Hattingh (1970) reports pressure oxidation at 65 °C and 300 psi oxygen did not agree with road performance. Since asphalt oxidation rates increase with pressure, it shortens the time for the test. The problem is that asphalt oxidation is not simple. The second term in equation 1 is represented by (Liu et al., 1996)

$$\frac{dCA}{dt} = AP^{\alpha}EXP\left(-\frac{E}{RT}\right) \qquad (1\text{-}2)$$

where P is pressure, T absolute temperature, and A, α and E are constants that are characteristic of each asphalt. Later we discovered that both E and HS were functions of pressure, (Figures 1-7 and 1-8) as well as the initial jump shown in Figure 1-5. This means that it is quite probable that relative hardening rates measured in the PAV will differ from those experienced on roadways. Figure 1-9 shows relative oxidation rates experienced in the PAV versus those obtained by aging asphalt in thin films in a 60 °C environmental room.

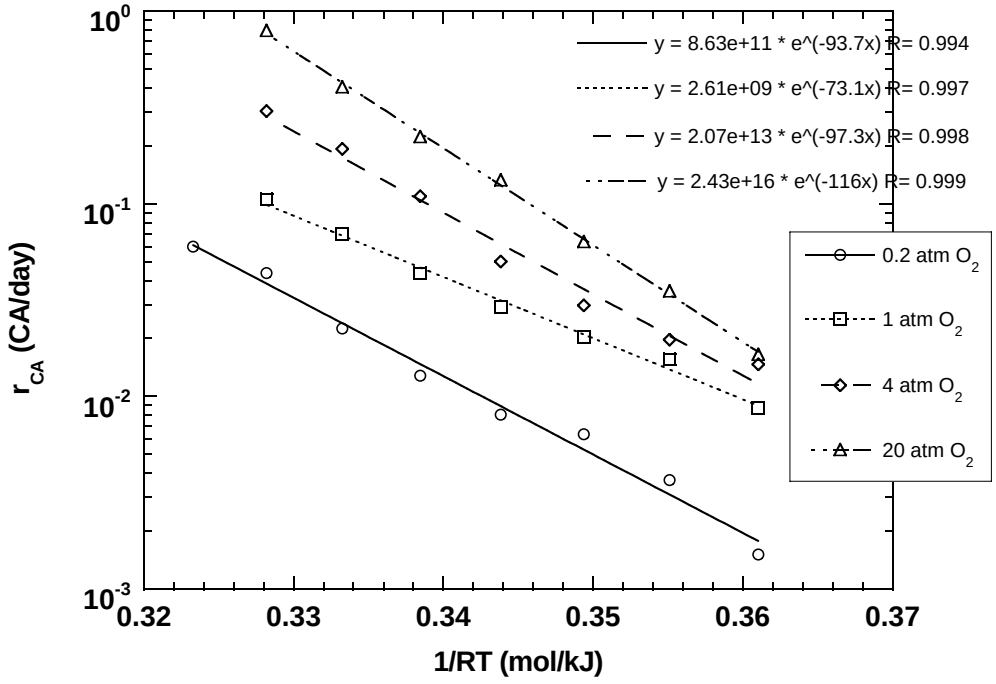

Figure 1-7. Activation Energy as a Function of Aging Pressure.

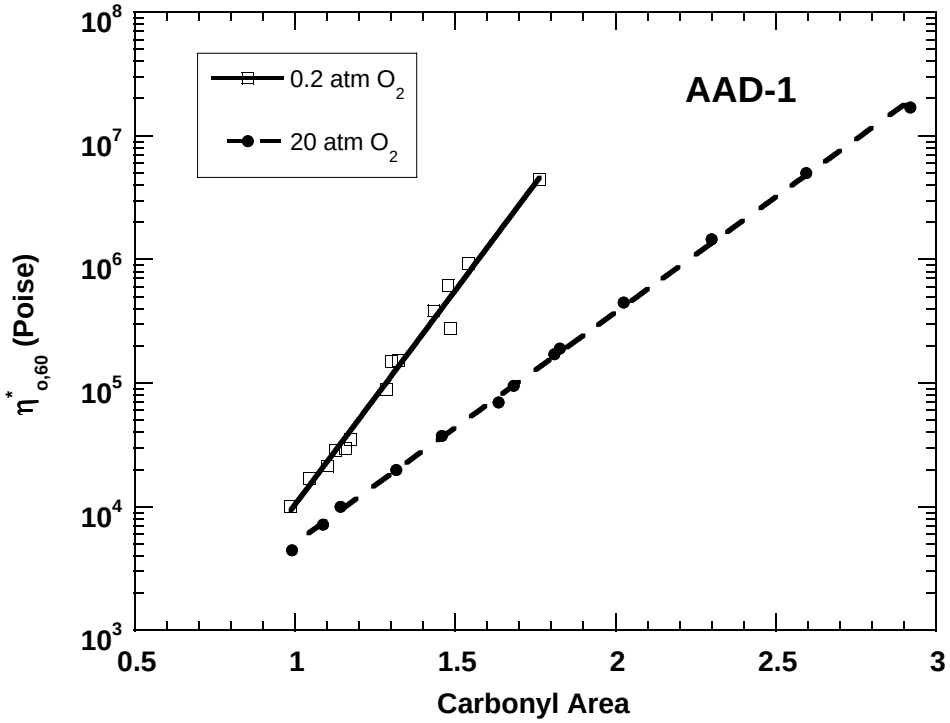

Figure 1-8. Hardening Susceptibility as a Function of Aging Pressure.

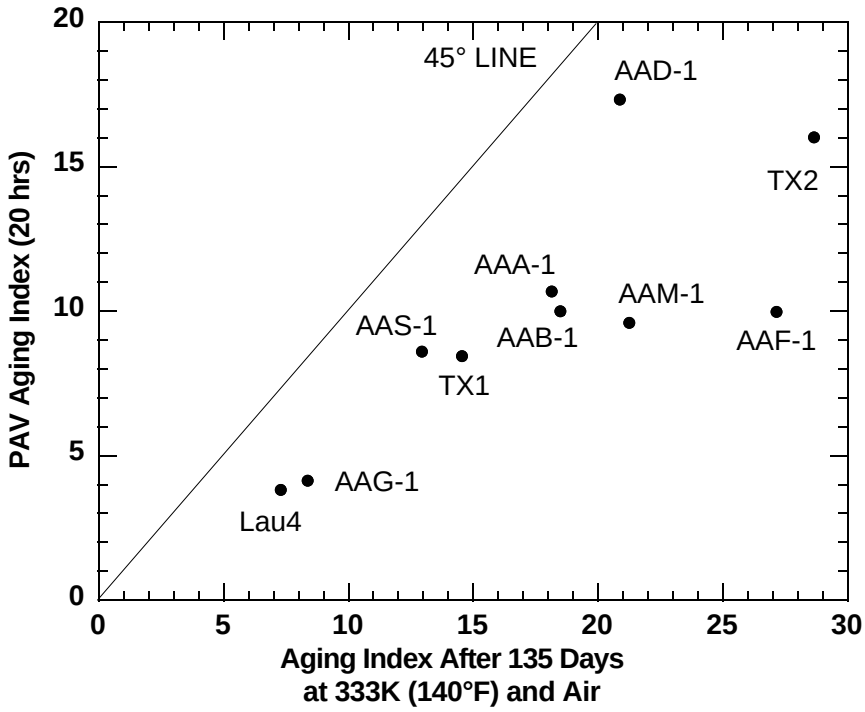

Figure 1-9. PAV Aging Index vs Environmental Room Aging Index.

While the degree of aging in the environmental room does not correspond to the 20 hours in the PAV, very large variations are still apparent. For instance, there are six asphalts that aged almost the same in the PAV, while aging in the 60 °C room varies over twofold. Similarly, AAD-1 and AAM-1 aged the same in the 60 °C room but differ nearly twofold in the PAV.

Any short-term aging test will have problems because E in equation 1-2 is asphalt dependent, but the accuracy should be improved by running at atmospheric pressure and eliminating the effect of α and the pressure dependence of E, HS, and the initial jump.

Chemistry of Asphalt Hardening

Again we will digress in order to show how asphalt composition may be manipulated to affect properties. Many attempts have been made to relate asphalt properties to chemical measurements. These attempts are reviewed in Davison et al. (1991). Generally they have not been very successful, and we have no intention of recommending a chemical specification. However, in a general sense we know how to move properties in the desired direction.

The hardening of asphalt on oxidation is almost entirely caused by the increase in asphaltene content (Lin et al., 1995a; Lin et al., 1995b). This is primarily the result of the

oxidation of polar aromatics. The presence of original asphaltenes accelerates the process. However, the asphaltenes formed by oxidation, while hardening the material, do not change the rate of hardening.

Saturates do not oxidize and they lower the viscosity and improve the low temperature grade, but in the presence of high original asphaltenes they increase the HS. Thus at high asphaltenes content, they may actually increase the viscosity (Figure 1-10).

Figure 1-11 shows the effect of recycling agent saturate content on the HS of recycling material. The top line is the result of blending agents of varying saturate content with a 85,000 poise hardened SHRP AAF-1 asphalt (Chaffin et al., 1997). The bottom line is the result of blending saturate-free agents of varying viscosity with a 55,000 poise hardened SHRP AAA-1 asphalt (Madrid, 1997). The abscissa shows the blend saturate content. The principal effect of the agents is to dilute asphaltene content and for the bottom line, saturate content also.

The Effect of Composition on Grade and Hardening

Figure 1-12 shows the result of another recycling experiment. Four hardened asphalts were mixed with four recycling agents to produce 16 blends of about 5000 poise. Three of the agents were asphaltene free and relatively low in saturates. The fourth was an AC-10 asphalt. As can be seen, there is little difference overall in the Superpave grade span: (64-22 is a ΔT of 86) but the HS is much higher when using the AC-10. The oxidation rate also probably will be higher for AC-10 blends.

One of the most interesting studies is shown in Figure 1-13 (Domke et al., 1997). In this study a vacuum tower bottom grading 64-22 was separated on a "Giant Corbett" column (Peterson et al., 1994) into asphaltenes, aromatics, and saturates. These components were reblended to form a variety of materials which were graded and aged in our reactors (Lau et al., 1992; Liu et al., 1997a) to get the HS values.

The line drawn across the top shows how one can improve the top grade as much as four levels while maintaining the bottom grade simply by adding asphaltenes to a high saturate material. Figure 1-14 shows what this does to the HS. The point in the upper right is the original vacuum tower bottom with its high HS. The point in the lower left corner shows the good HS and poor grade of the aromatic alone. Interestingly, at low asphaltenes, a little saturate actually lowers HS while improving the grade span.

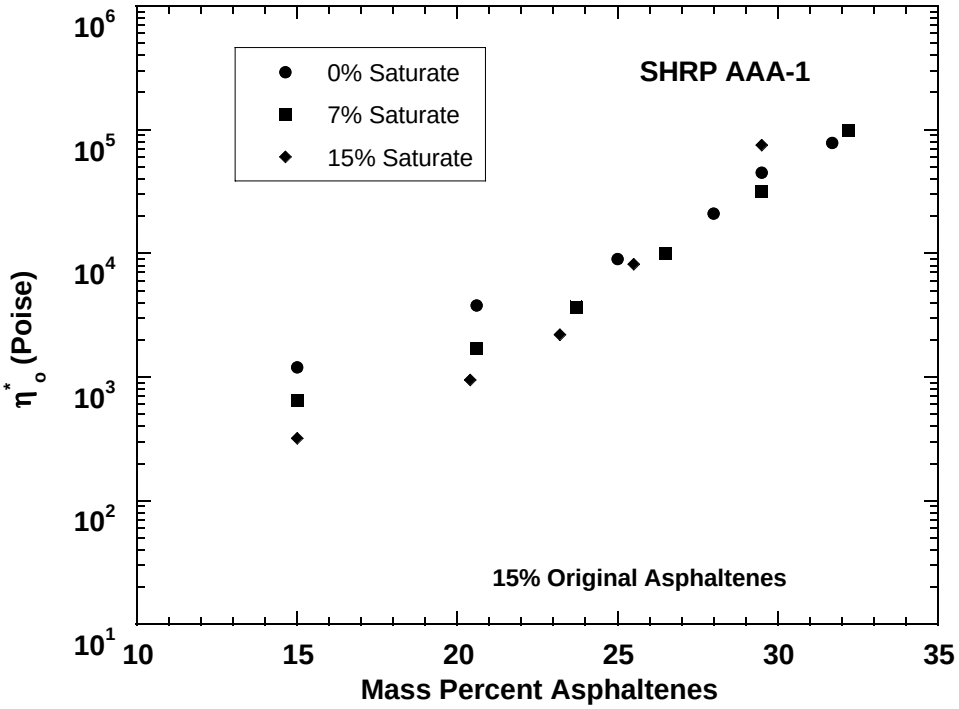

Figure 1-10. Viscosity vs Asphaltene Content at Varying Saturate Levels.

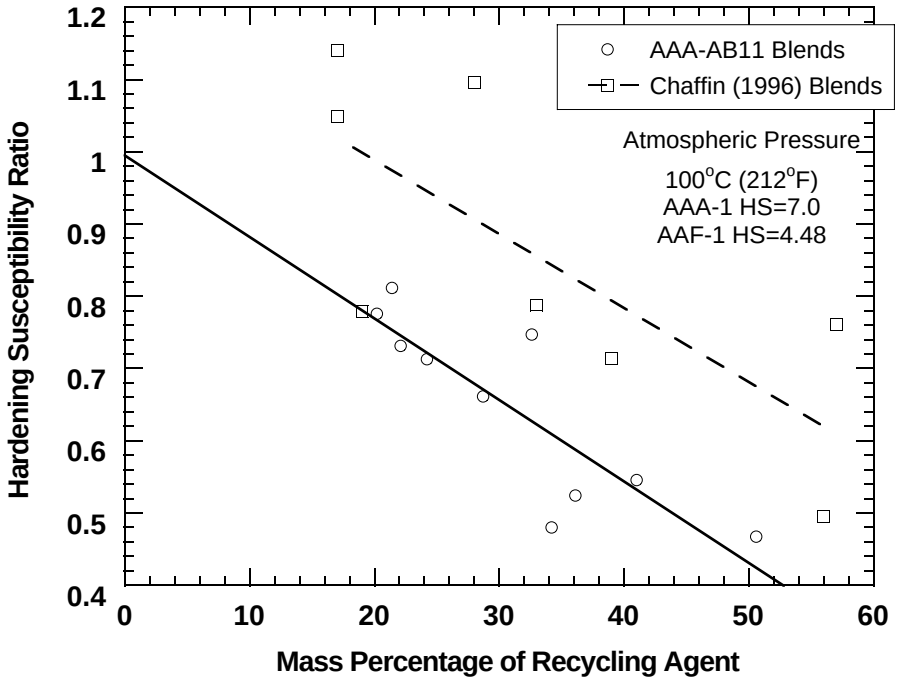

Figure 1-11. Hardening Susceptibility Ratio vs Percent of Recycling Agent.

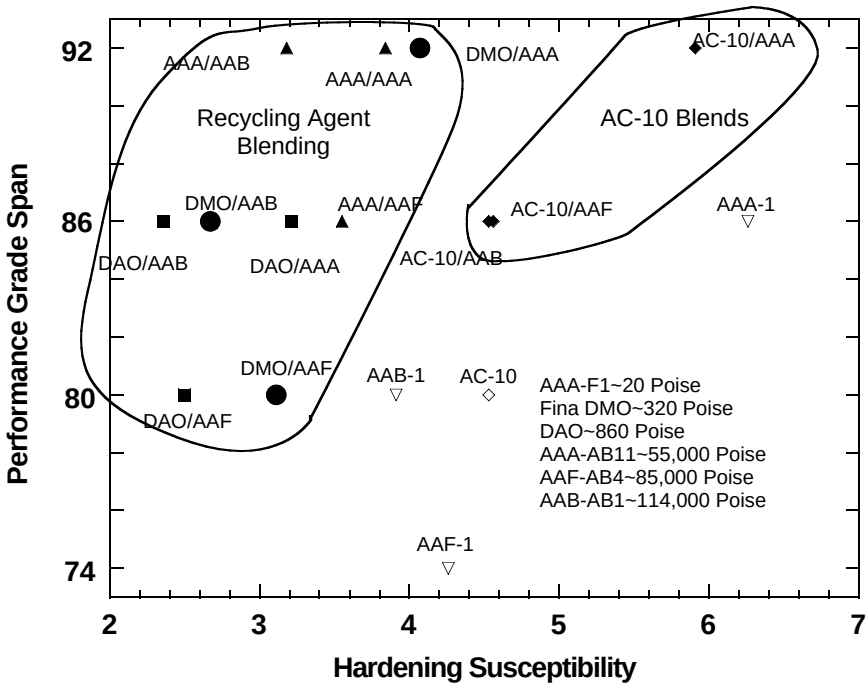

Figure 1-12. Recyling Performance Grades vs Hardening Susceptibility.

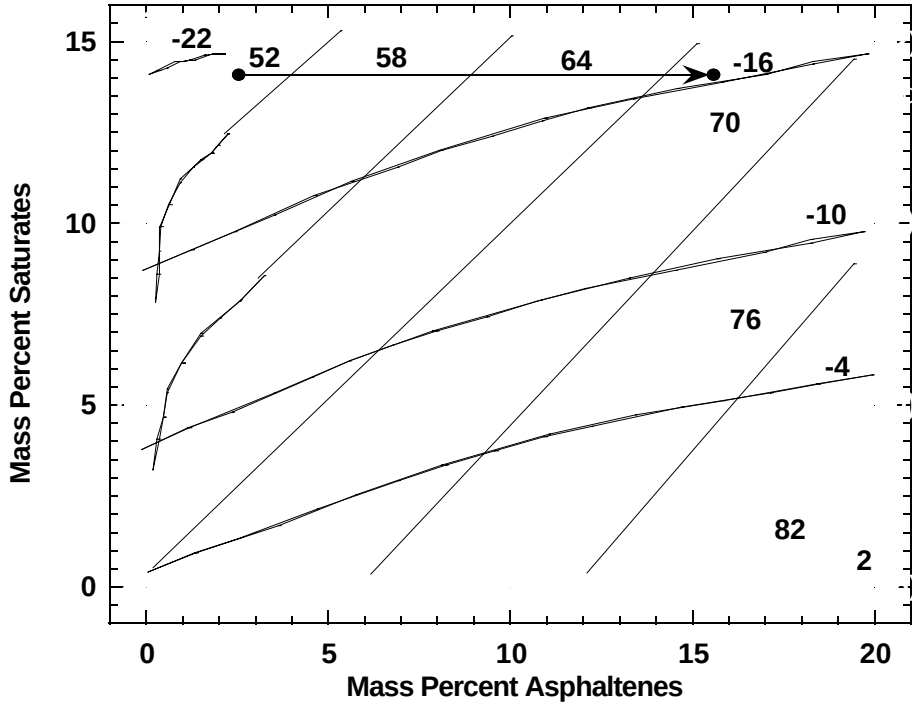

Figure 1-13. Performance Grading for VTB Aromatics Compounds.

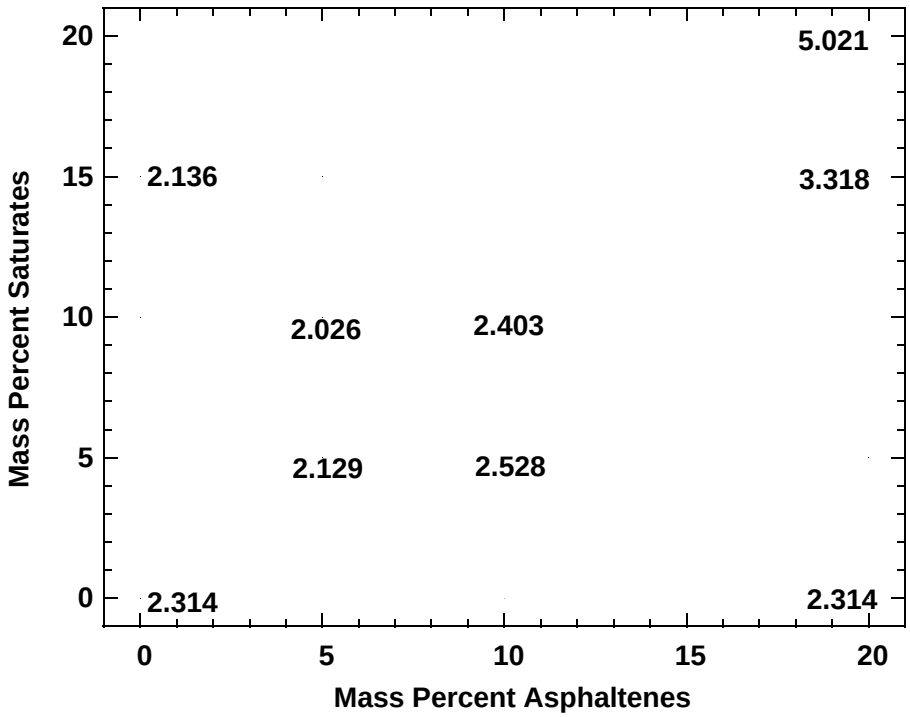

Figure 1-14. Hardening Susceptibility for VTB Aromatic Compounds.

HISTORICAL ATTEMPTS TO RELATE PROPERTIES TO PERFORMANCE

As mentioned earlier, attempts to correlate asphalt chemical properties with performance have not been very successful, but of course it is chemical composition that actually determines physical properties. However, the relationship is so complex that while we know the general effect for compositional manipulations, the magnitude of these effects are asphalt specific. For this reason one would expect changes in physical properties with aging to be better predictors of asphalt durability.

Even so, one of the most interesting and controversial proposals for specifications to reduce road aging was the suggestion by Jennings that the percent large molecular size region (LMS) as determined by GPC be used as a specification. It is controversial because LMS is primarily an indication of asphaltene formation which is the main cause of asphalt hardening but not a measure of the changes in physical properties that actually cause road failure. On the other hand, it is very easy to measure and made possible the collection of a very large body of data.

His first study was of Montana roads (Jennings et al., 1980) which was later expanded to include many parts of the country (Jennings and Pribanic, 1985). The significant findings of these studies were that in each region there was a level of LMS above which all roads were in bad condition. There were bad roadways with lower LMS, but these had likely failed for non-

binder related causes. In general, the critical LMS was higher in warmer climates, and in hotter regions some very low LMS roadways had rutted.

This work showed that, first, parameters are needed that are sensitive to aging and that have critical values that indicate failure. Then, secondly, an aging procedure is needed will indicate the rate at which individual asphalts approach these values. The work of this project was directed at meeting these needs.

The attempts to find such parameters was not new. The literature concerning these attempts is both interesting and informative. For instance, in 1937, Hubbard and Gollomb (1937) reporting on an Ohio field study stated "---that out of 9 pavements rated good or excellent all but one showed the recovered asphalt to have a penetration of 30 or higher. Out of 12 pavements rated as bad, all but two showed the recovered asphalt to have a penetration of 20 or less." In a comparison of lab and field aging of asphalts in an Iowa study, Lee (1973) suggested a critical pen of 20 and a critical viscosity of 20-30 megapoise at 25 ^{o}C.

In a study of roads in Utah, the condition of 20 controlled sections were correlated with a wide variety of effects (Anderson et al.,1976). The best correlation was the accumulated total (7 years) of 18-kip loads. Transverse cracking went up with saturate content, which is interesting considering that increasing saturates improves the low temperature Superpave grade. This is consistent, however, with the effect of saturates on hardening (Figure 1-10). Some correlation was also obtained between force ductility and transverse cracking.

Doyle (1958) reporting on the performance of Ohio test sections says, "Ductility at 25 ^{o}C shows an inconsistency as far as these two carefully observed test roads are concerned; however, ductility at 12.8 ^{o}C, 1 cm or lower does apparently correlate with results on these roads." He gave data on other roads, and one showed no cracking after 5 years for which the recovered asphalt had a ductility of 29 at 12.8 ^{o}C and 1 cm/min. Two others with considerable cracking showed ductilities of 3 and 4.

Skog (1967) aged these same asphalts and showed that the shear susceptibility versus aging time was much lower for the good road than for the two cracked roadways with low ductilities. Welborn et al. (1966) showed that there was a fairly good correlation between 60 ^{o}F ductility and shear susceptibility before and after TFOT. Kandahl and Wenger (1973) also showed a good correlation between shear susceptibility at 25 ^{o}C and 15.6 ^{o}C ductility for TFOT residues.

Kandahl and others (1975, 1977, 1984) have published a series of papers on performance of Pennsylvania test sections. Four sections were laid in 1960-61 and after 10 years all showed some cracking, while one with high voids had cracked after 5 years. All cracked between a penetration of 20-25 at viscosities ranging from about 40,000 to 70,000 poise and at ductilities between 5 and 6 cm measured at 60 ^{o}F and 5 cm/min. Of these variables only ductility gave the proper ranking in road condition after 10 years.

Six more pavements were laid in 1964, each with a different asphalt. These sections were cored periodically until 1974 or 113 months after construction. This time road condition was correlated with viscosity at 25 °C, viscosity at 60 °C, shear susceptibility at 25 °C, and ductility at 15.6 °C and 1 cm/min. Also included was the slope of low shear viscosity versus shear susceptibility. Both ductility and the viscosity-shear susceptibility slope perfectly ordered the performance rating of the six pavements.

A third set of sections were laid in 1976 and were evaluated after 6 years. Again relative rankings agreed with the ordering of ductilities measured at 60 °C and 5 cm/min. Halstead (1963) studied road conditions relative to penetration and ductility and concluded, "the amount of hardening of the asphalt during construction and in service are the primary factors affecting durability of the pavement. However, the data discussed in this report demonstrate that the accompanying decrease in ductility of the asphalt is an important secondary factor that must not be overlooked. Pavements containing asphalt with penetrations in the range normally considered satisfactory (30 to 50) but with low ductility are likely to show poorer service than those pavements containing asphalts of the same penetration but with higher ductility." In fact some of his data indicated that at very low ductility (below 6 at 25 °C) a roadway with lower penetration such as below 20 was less likely to fail than a roadway with asphalt having a penetration above 30.

Clark (1958) reported results comparing laboratory oven aging at 65.6 °C with hot-mix and road aging for 46 roadways with respect to ductility and penetration. In general, oven aging ranked the roadways correctly, but low ductility particularly was a good predictor of roadway condition and life.

A variation in the use of shear susceptibility is given by Reese and Goodrich (1993). They plotted the shear susceptibility of DSR phase angle, defined by

$$\frac{\delta_{10\,\mathrm{rad/s}} - \delta_{1\,\mathrm{rad/s}}}{\log(10\,\mathrm{rad/s}) - \log(1\,\mathrm{rad/s})} \qquad (1\text{-}3)$$

versus the viscosity shear susceptibility defined by

$$\frac{\log\ \eta_{10\,\mathrm{rad/s}} - \log\ \eta_{1\,\mathrm{rad/s}}}{\log\ (10\,\mathrm{rad/s}) - \log\ (1\,\mathrm{rad/s})} \qquad (1\text{-}4)$$

Note that the denominator in both relations is numerically equal to one so that actually it is a plot of the difference in phase angle versus the difference in log viscosity. A slightly off vertical plot for asphalts extracted from California desert roadways perfectly separated 10 uncracked sections

from 9 cracked sections. These results are easily obtained from the DSR and are not subject to the difficulty with ductility for which critical values may be small. Road aging simulation is still required.

SPECIFICATION FOR MODIFIED ASPHALTS

Modifiers present different problems and require different test procedures. We have considerable experience with asphalt rubber, and we can enumerate several problems with current testing procedures. The first is that the TFOT and RTFOT no longer simulate the hot-mix operation. For instance, with asphalt rubber, material from the RTFOT is of consistently higher viscosity than that from the TFOT because of the shorter time in RTFOT. The much shorter time in the hot-mix should yield material of even higher viscosity.

The relative reaction rates for rubber and asphalt are affected by temperature and diffusion of oxygen into rubber particles which makes reaction time an important factor. Since time is so short in the hot-mix operation, the difference between it and the oven tests may be large and probably more hardening will occur than in the oven tests because of the greater dependence of rubber reaction on diffusion. Unfortunately this is not easily confirmed because extraction of asphalt-rubber from a mix can have a major effect on the recovered binder properties. As the rubber oxidizes it is broken into smaller materials decreasing the viscosity. This is why many asphalt rubber materials pass $G^*/\sin\delta$ before RTFOT or TFOT but then fail after. Another problem is using an elevated temperature to simulate road aging. The problems are even greater than those already enumerated for unmodified binders. Figure 1-15 compares HS measured at different temperatures. For unmodified binder this is independent of temperature below about 100-110 ^oC. This temperature dependency of HS for rubber modified asphalts indicates that major changes in the reaction mechanism are encountered with changing temperatures. This varying HS with temperature makes it extremely difficult to simulate road aging at elevated temperatures.

UNDERLYING PRINCIPLES AND SCOPE OF PROBLEM

The purpose of this study was to recommend specifications for asphalt binders that will ensure that in meeting Superpave specifications, other important properties will not be sacrificed. At the same time these specifications will replace the inadequate $G^*\sin\delta$ criterion for fatigue cracking. This study also addresses the issue of how testing procedures and specifications need to be modified for asphalts containing additives such as polymers or ground tire rubber. This research then naturally falls into two areas: 1) development of specifications and methods for existing asphalts and for asphalts whose composition has been manipulated by blending and/or air blowing, and 2) development of testing methods and specifications for asphalts modified by additives.

In either event, the specification $G^*\sin\delta$ is inadequate to protect against age hardening and fatigue cracking. Since the parameters used to predict fatigue cracking must be sensitive to

oxidative hardening, the adequacy of the laboratory hardening procedures must be established. Since Superpave specifications that refineries must meet can only refer to the binder and it is difficult to study aged materials in mixes, this project does not directly address mix specifications or tests. However, because some compositional changes could negatively impact adhesion, cohesion and thus water susceptibility, these composition factors have been checked.

OUTLINE OF THE REPORT

The work of this project consisted of fundamental experimental studies in a number of areas. These studies were directed at developing an appropriate aging procedure, identifying an appropriate physical property parameter (preferably to be measured using the DSR) which would be indicative of binder durability in pavements, assessing the effect of the aging procedure on this durability parameter and on low-temperature properties, and assessments of water susceptibility. These issues would be addressed for both unmodified and modified binders.

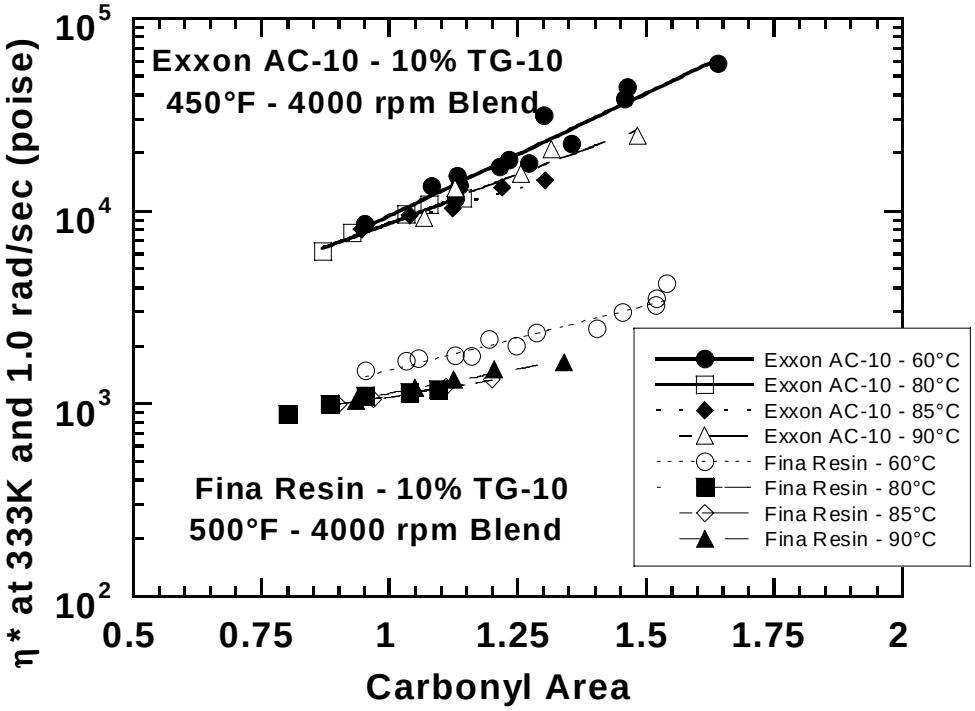

Figure 1-15. Hardening Susceptibility of Asphalt-Rubber Aged in Atmospheric Air.

Chapter 2 presents a fundamental investigation of the effect of oxidation pressure on the reaction kinetics. This information is important for devising an appropriate aging procedure for condition asphalt materials in an aging test. Chapter 3 is a study of the effect of aging on low-temperature Superpave properties and performance grades. Chapter 4 is a study of the effect of aging on asphalt durability, as measured by ductility and a newly developed surrogate DSR property. Chapter 5 presents data on the effect of modifiers on physical, chemical, and aging properties of asphalts. Chapter 6 compares various accelerated aging methods in their ability to rank asphalts in agreement with 60 °C environmental room aging. Chapter 7 provides results on adhesion and water susceptibility, as measured by the Texas DOT test, Tex 531-C. Chapter 8, based on the work of all the previous chapters, presents a recommended test protocol for unmodified asphalts and recommendations for modified materials. Finally, Chapter 9 provides an executive summary, including conclusions and recommendations.

CHAPTER 2. EFFECT OF OXYGEN PRESSURE ON ASPHALT OXIDATION KINETICS

(Pages 2-1 through 2-18 reprinted, with permission, from C. H. Domke, R. R. Davison, and C. J. Glover, "Effect of Oxygen Pressure on Asphalt Oxidation Kinetics," *Ind. Eng. Chem. Res.*, Volume 39, 2000, pp. 592-598.)

ABSTRACT

The oxidation of asphalt is a major cause of pavement failure. At a given temperature and pressure, the asphalt oxidizes in two stages: (1) a rapid-rate period followed by (2) a long period with constant oxidation rate. The degree of oxidation that occurs in the constant oxidation region is asphalt dependent and varies with oxygen pressure and with temperature. Using pavement-temperature oxidation kinetics obtained for eight asphalts in this study, it has been determined that the activation energies for the constant-rate region are dependent on the oxygen pressure and can be related to the asphaltene composition of the asphalt. An oxidation kinetic model is developed to predict the rate of oxidation in the constant rate region knowing an initial asphaltene composition variable for the asphalt.

INTRODUCTION

Millions of dollars are spent every year to build and maintain roads. A large percentage of these roads are built with asphalt. Over the lifetime of the road, an asphalt binder oxidizes and subsequently hardens eventually causing failure of the road.

Several authors have shown that carbonyl formation is a major product of oxidation (Lee and Huang, 1973; Martin et al., 1990; Lau et al., 1992; Peterson et al., 1993). The formation of carbonyl-containing compounds varies between asphalts, but for each asphalt the carbonyl content, CA, can be used as a surrogate for total oxidative changes (Liu et al., 1998b). This is because the carbonyl growth varies linearly with total oxygen increase even though the slopes vary somewhat for different asphalts.

Many accelerated aging tests have been devised to simulate the aging that occurs on the roads. Most of these tests use elevated temperatures and oxygen pressures to accelerate the aging process. However, studies have indicated that elevated temperatures and pressures may not adequately simulate the road aging conditions (Domke et al., 1999).

It would be ideal to save time and effort to produce a model that would allow for a prediction of the oxidation rate of an asphalt at a given temperature and pressure. There have been few attempts to describe the oxidation kinetics of an asphalt (Peterson et al., 1993; Liu et al., 1996). Liu et al. (1996) had described the carbonyl formation rate as a function of the temperature and pressure in an Arrhenius form:

$$r_{CA} = AP^{\alpha} \exp\left(\frac{-E}{RT}\right) \qquad (2\text{-}1)$$

For the 10 asphalts Liu et al. (1996) studied A, E, and α were calculated by determining the rates at atmospheric air (0.2 atm O_2) and 20 atm O_2 and various temperatures and fitting equation 2-1 to the data. In this study, rates have been determined for eight asphalts using the same range of temperatures, but additional oxygen pressures have been included, and additional rates were measured at the previously used conditions.

EXPERIMENTAL METHODS

Eight asphalts were used in this study: seven SHRP asphalts (AAA-1, AAB-1, AAD-1, AAF-1, AAG-1, AAM-1, and AAS-1) and one Texas asphalt, Lau4 (Lau et al., 1992). Each of these asphalts was weighed into several 4 cm x 7 cm aluminum trays using approximately 2.4 grams of material. This yielded a uniform thickness of less than 1 mm. Thin films were used to minimize the effects of diffusion (Domke et al., 1997).

The asphalts were placed in our pressure oxygen vessels (POV) (Lau et al., 1992). The POV is immersed in a triethylene glycol bath used for temperature control. Each POV holds approximately 60-70 sample trays. For each asphalt a tray was removed periodically depending on the temperature and pressure of the POV. The temperatures varied from 60 °C to 98.9 °C (140 °F>210 °F), and the oxygen pressures varied from atmospheric air (0.2 atm O_2) to 20 atm O_2.

Each sample was analyzed using a Mattson Galaxy 5000 FT-IR and the attenuated total reflectance (ATR) method described by Jemison et al. (1992). The carbonyl area was determined by finding the area under the absorbance peaks from 1650-1820 cm^{-1}. The CA was used to monitor the progress of the asphalt oxidation.

Heptane asphaltene (C7) content from Lau4 was determined by dissolving 7 grams of asphalt in 200 mL of n-heptane. After heating and stirring the sample for one hour, the solution was allowed to settle overnight. A Whatman #2 quantitative filter was used for the vacuum filtration procedure to determine the mass of the asphaltenes. The asphaltene content of the SHRP asphalts was taken from the SHRP Material Reference Library (1993).

Pentane asphaltene content for each of the eight asphalts was determined by dissolving 0.2 grams of asphalt in 20 mL of n-pentane. The samples were sonicated for 20 minutes and allowed to settle overnight. A Whatman #2 quantitative filter was used for the vacuum filtration procedure to determine the mass of the asphaltenes.

RESULTS

Reaction Rate

Lau et al. (1992) determined that the rate of carbonyl formation became constant after an initial, higher rate period. Figure 2-1 shows how pressure affects the constant oxidation rate of AAG-1 at 200 °F. The regression line determines the initial jump of the asphalt (CA_o) and the aging rate (r_{CA}) given by:

$$CA = CA_o - r_{CA} t \qquad (2\text{-}2)$$

where t is the aging time.

Figure 2-1 shows that r_{CA} increases with increasing pressure while keeping the temperature constant. The rates also increase with increasing temperature when keeping the pressure constant (Figure 2-2), a fact that is true of all eight asphalts studied (Table 2-1).

From Figures 2-1 and 2-2 it is also observed that the initial jump may be pressure dependent but, with considerable scatter, probably is temperature independent. This fact was also observed by Liu et al. (1996). Table 2-2 shows CA_o for all eight asphalts, and shows that within the scatter, that CA_o may be pressure dependent depending on the asphalt. This phenomenon will be discussed later.

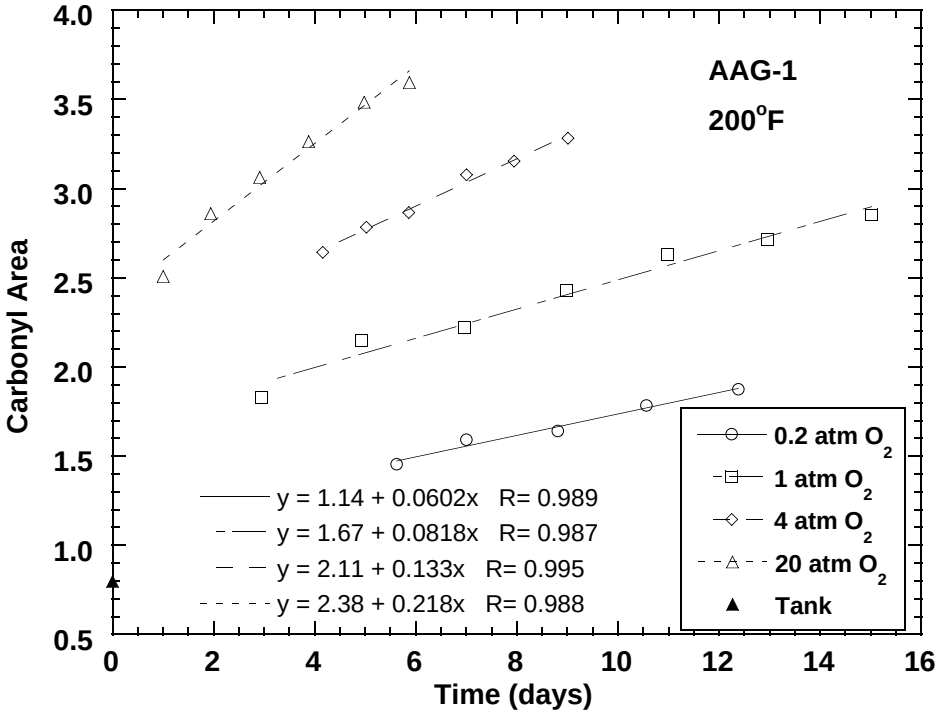

Figure 2-1. How Oxygen Pressure Affects Oxidation Rate of AAG-1.

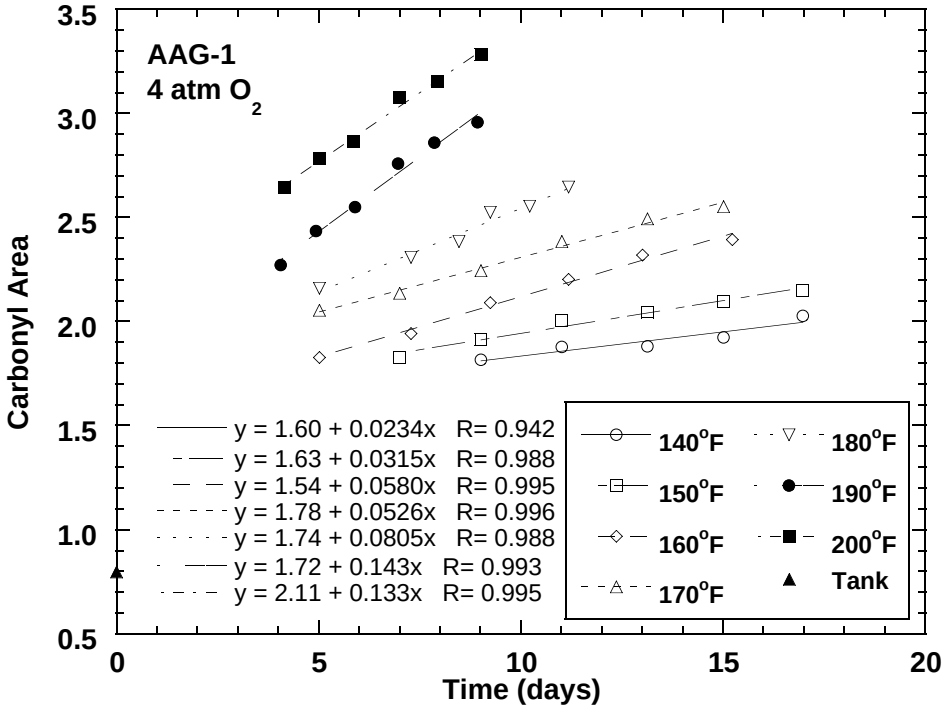

Figure 2-2. How Temperature Affects Oxidation Rate of AAG-1.

Table 2-1. Carbonyl Formation Rates x 10^3.

0.2 atm O_2

°F	AAA-1			AAB-1			AAD-1			AAF-1		
140	2.0	±	0.4	2.4	±	0.1	1.5	±	0.8	2.6	±	0.6
150	3.8	±		4.3	±		3.7	±	0.5	5.5	±	
160	6.9	±		8.1	±		6.4	±	0.8	7.2	±	
170	10.7	±	1.6	12.2	±	0.7	8.0	±	1.8	10.1	±	1.3
180	11.9	±	1.9	15.7	±	2.0	12.8	±	2.3	12.3	±	1.3
180	11.4	±	5.1	14.9	±	2.4	11.4	±	6.9	12.6	±	6.4
190	19.8	±	11.4				22.6	±	5.3	31.8	±	8.4
190	21.8			27.4			21.0			31.1		
200	44.9	±	13.5	55.5	±	15.6	42.3	±	16.2	41.7	±	36.0
210	58.7	±	7.8	80.4	±	5.6	60.0	±	8.1	65.0	±	6.5

°F	AAG-1			AAM-1			AAS-1			Lau4		
140	4.1	±	0.7	2.2	±	0.4	1.9	±	0.3	2.0	±	0.3
150	6.4	±		4.5	±		4.5	±		4.8	±	
160	10.2	±		6.4	±		6.5	±		6.7	±	
170	11.9	±	3.1	8.5	±	1.7	9.4	±	1.0	10.9	±	1.6
180	16.3	±	3.6	9.7	±	2.0	14.0	±	3.3	14.4	±	4.5
180	24.3	±	4.7	13.1	±	6.4	11.4	±	5.5	15.2	±	5.5
190	41.4	±	7.9	22.3	±	4.7						
190	42.4			33.2			23.5			26.1		
200	60.2	±	16.7	39.1	±	18.5	42.1	±	9.4	56.7	±	6.9
210	87.5	±	15.3	56.3	±	8.2	64.6	±	6.9	83.0	±	5.4

Table 2-1. Carbonyl Formation Rates x 10^3 (continued).

1 atm O_2

°F	AAA-1	AAB-1	AAD-1	AAF-1
140	6.7 ± 2.1	8.1 ± 2.2	9.4 ± 3.6	9.3 ± 3.2
150	15.3 ± 3.9	16.3 ± 3.4	15.1 ± 4.1	20.5 ± 1.8
160	18.5 ± 4.3	21.3 ± 2.8	20.3 ± 3.4	23.8 ± 3.6
170	24.6 ± 2.2	24.9 ± 4.4	25.0 ± 5.8	31.6 ± 5.0
180	34.1 ± 3.3	37.2 ± 2.8	33.7 ± 8.1	37.4 ± 7.0
190	58.6 ± 13.7	78.6 ± 5.3	70.3 ± 4.9	66.2 ± 13.1
200	89.5 ± 13.9	110.2 ± 9.5	107.6 ± 14.4	145.5 ± 25.8

°F	AAG-1	AAM-1	AAS-1	Lau4
140	24.5 ± 6.9	13.5 ± 3.6	6.6 ± 2.0	11.0 ± 1.5
150	25.9 ± 6.1	23.0 ± 4.3	14.5 ± 8.8	18.7 ± 4.1
160	30.8 ± 5.0	24.4 ± 4.2	14.7 ± 4.3	23.3 ± 3.3
170	38.6 ± 5.5	24.6 ± 3.6	22.7 ± 2.8	28.1 ± 2.1
180	42.4 ± 3.8	33.9 ± 5.3	28.8 ± 8.8	39.8 ± 9.1
190	67.3 ± 7.3	41.9 ± 9.4	67.5 ± 2.5	71.8 ± 5.8
200	81.8 ± 15.3	64.0 ± 11.1	92.3 ± 10.4	121.5 ± 19.1

4 atm O_2

°F	AAA-1	AAB-1	AAD-1	AAF-1
140	11.7 ±	13.4 ±	11.1 ±	16.1 ±
150	16.2 ± 3.0	16.6 ± 6.4	20.0 ± 4.4	26.8 ± 3.7
160	31.2 ± 5.8	25.3 ± 4.9	24.6 ± 4.3	30.7 ± 5.0
170	48.2 ± 6.1	44.4 ± 10.1	45.8 ± 4.5	39.4 ± 8.8
180	97.0 ± 19.1	110.3 ± 13.4	136.8 ± 19.9	118.3 ± 20.3
190	144.8 ± 31.5	190.9 ± 44.4	192.8 ± 18.9	156.3 ± 6.0
200	182.1 ± 38.0	295.0 ± 48.3	289.6 ± 42.2	241.7 ± 30.9

°F	AAG-1	AAM-1	AAS-1	Lau4
140	23.4 ±	18.2 ±	13.8 ±	13.7 ±
150	31.5 ± 6.8	23.0 ± 5.9	17.6 ± 2.5	18.6 ± 4.8
160	58.0 ± 8.0	25.5 ± 20.4	22.2 ± 4.6	28.6 ± 7.7
170	52.6 ± 7.0	33.9 ± 4.1	35.5 ± 2.9	43.4 ±
180	80.5 ± 17.3	59.9 ± 5.8	96.7 ±	103.3 ± 14.0
190	143.4 ± 23.4	78.7 ± 20.3	141.0 ± 19.8	153.8 ±
200	132.5 ± 18.3	109.1 ± 20.2	210.9 ± 29.4	284.5 ± 24.7

20 atm O_2

°F	AAA-1	AAB-1	AAD-1	AAF-1
140	16.2 ± 0.9	10.6 ± 0.8	16.5 ± 0.7	12.2 ± 1.8
150	29.7 ± 7.8	24.8 ± 9.0	32.9 ± 8.9	35.0 ± 11.0
160	60.4 ± 9.5	36.6 ± 5.8	63.0 ± 8.4	43.4 ± 5.4
170	121.7 ± 11.9	78.3 ± 18.1	133.2 ± 19.1	63.9 ± 6.1
180	179.5 ± 25.7	132.5 ± 11.6	223.5 ± 37.5	86.3 ± 8.0
190	349.8 ± 27.2	222.1 ± 7.6	403.9 ± 86.6	164.4 ± 16.5
200	425.7 ± 70.5	593.5 ± 75.7	726.4 ± 140.5	415.5 ± 81.5

Table 2-1. Carbonyl Formation Rates x 10^3 (continued).

°F	AAG-1			AAM-1			AAS-1			Lau4		
140	18.1	±	2.8	10.7	±	2.7	10.3	±	1.9	13.1	±	1.1
150	39.2	±	17.1	30.3	±	22.8	25.8	±	11.4	30.5	±	14.5
160	50.9	±	10.9	36.0	±	4.8	34.6	±	3.7	38.5	±	4.4
170	74.7	±	12.6	52.3	±	8.0	73.0	±	23.3	82.5	±	9.0
180	102.0	±	23.3	65.4	±	13.8	105.3	±	12.3	125.0	±	21.0
190	163.3	±	10.9	112.0	±	13.1	197.7	±	16.2	149.3	±	14.8
200	217.9	±	47.3	239.5	±	46.9	496.1	±	99.5	491.6	±	59.3

Table 2-2. CA_0 for All Asphalts.

Pressure (atm O_2)	AAA-1	AAB-1	AAD-1	AAF-1	AAG-1	AAM-1	AAS-1	Lau4
0.2	0.215	0.177	0.201	0.280	0.475	0.297	0.153	0.247
	±0.085	±0.043	±0.092	±0.069	±0.157	±0.072	±0.040	±0.029
1	0.185	0.206	0.157	0.221	0.605	0.299	0.140	0.149
	±0.086	±0.097	±0.071	±0.092	±0.172	±0.133	±0.060	±0.062
4	0.305	0.291	0.216	0.372	0.934	0.487	0.193	0.289
	±0.149	±0.064	±0.140	±0.120	±0.190	±0.145	±0.063	±0.054
20	0.254	0.374	0.194	0.580	1.490	0.669	0.128	0.093
	±0.272	±0.075	±0.141	±0.119	±0.159	±0.072	±0.054	±0.083

The oxidation rate of an asphalt can be estimated by determining a kinetic rate equation. Assuming classical kinetics, the carbonyl rate (r_{CA}) is given by equation 2-1 where A is the frequency (preexponential) factor, P is the oxygen pressure, α is the reaction order with respect to oxygen pressure, E is the activation energy, R is the universal gas constant, and T is the temperature. To find E, A, and α graphically one must plot ln r_{CA} vs 1/RT and find the slope (E) and intercept (AP^{α}) of the line. Figure 2-3 shows an example of this plot. Both E and AP^{α} vary with respect to oxygen pressure. As oxygen pressure is increased from 0.2 to 20 atm O_2, AP^{α} and E go through a minimum near 1 atm O_2. This occurs for all eight asphalts studied.

Equation 2-1 can be linearized by taking the natural logarithm of both sides

$$\ln(r_{CA}) = \ln A + \alpha \ln P - E/RT \qquad (2\text{-}3)$$

Equation 2-3 could be used to determine A, E, and α if they were independent of pressure. However, Domke et al. (1999) explain how pressure can affect the properties of an asphalt upon oxidation with a layered particle model. Figure 2-4 is taken from their work. They explain that as oxygen pressure is changed, the different diffusional fluxes of oxygen cause oxidation to occur at different layers (Figure 2-4a) of the "particle." At low pressures the oxygen would react primarily with the maltene phase of the asphalt (Figure 2-4b). As oxygen pressure is increased, the

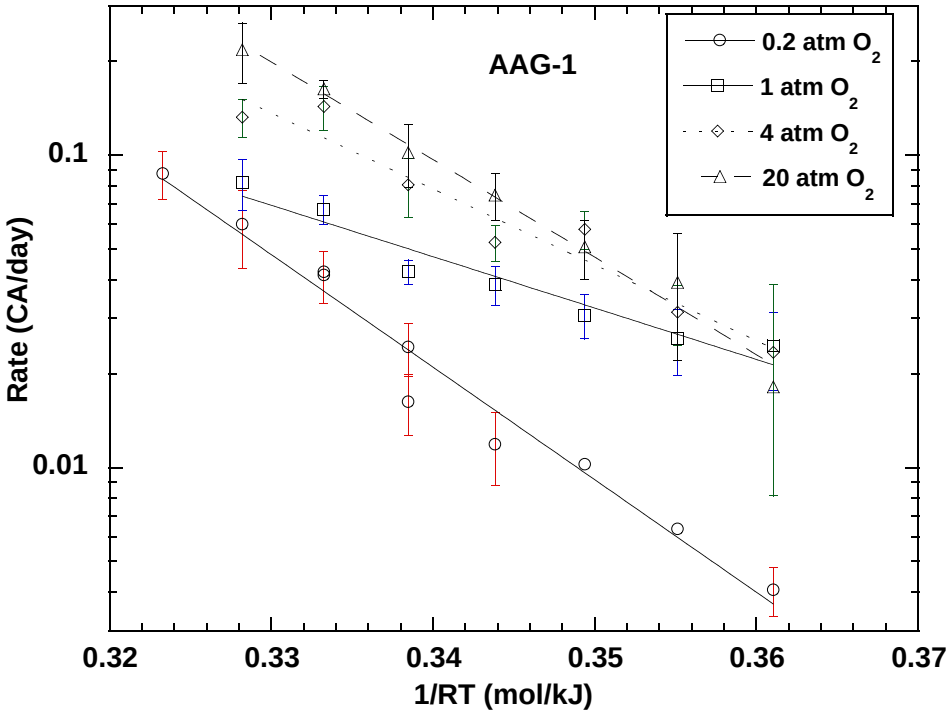

Figure 2-3. How Temperature and Pressure Affect the Oxidation Rate of AAG-1.

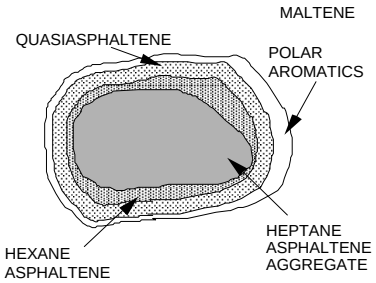

Figure 2-4a

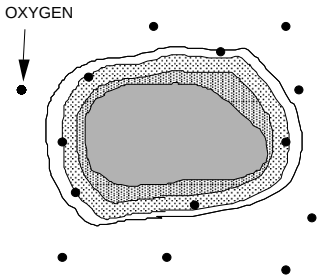

Figure 2-4b

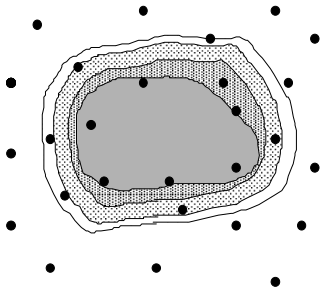

Figure 2-4c

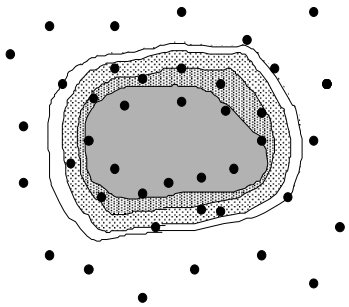

Figure 2-4d

Figure 2-4. Hypothesized Particle Model of Asphalt (Reproduced with Permission from Domke et al., 1999).

increased oxygen flux would allow for oxidation to occur with the "quasiasphaltenes" (Figure 2-4c), the hexane asphaltenes, and finally the heptane asphaltenes (Figure 2-4d). This molecular diffusion concept complicates the use of equation 2-3.

Liu et al. (1998c) showed that naphthene aromatics and polar aromatics displayed different rate constants A, E, and α. Because different molecules are reacting at different oxygen pressures, one cannot assume that the observed A, E, and α are independent of pressure. This pressure dependency causes difficulty in estimating the rate constants individually. E can be determined for each oxidation pressure; however, A and α are linked together in equation 2-1. Rather than estimating A and α separately, they were combined into one variable thus modifying equation 2-1 to:

$$r_{CA} = A' \exp\left(\frac{-E}{RT}\right) \tag{2-4}$$

where

$$A' = AP^{\alpha} \tag{2-5}$$

By combining the pressure dependent constants of A and α into one pressure dependent variable, A´, the oxidation kinetic model is simplified without damaging its integrity. Tables 2-3 and 2-4 show the values of E and ln A , respectively, for the eight asphalts at the four different oxygen pressures. It can be seen that both E and A´ go through a minimum value at 1 atm O_2. This minimum is likely tied to the layered particle model by Domke et al. (1999) and the difference in the kinetic parameters observed by Liu et al.(1998c). This is also supported by Liu et al. (1997) who determined kinetic parameters for seven fractions separated from asphalt AAF-1 by supercritical extraction. The parameters of Equation 2-3 were fitted to the data and a minimum occurred in the pressure dependency parameter, α, at fraction 4. We can speculate that the average composition reacting at 1 atm has a lower activation energy than the average material reacting at both lower and higher pressures.

Table 2-3. Activation Energy for All Asphalts at Various Pressures.

Pressure (atm O_2)	AAA-1	AAB-1	AAD-1	AAF-1	AAG-1	AAM-1	AAS-1	Lau4
0.2	85.6	90.2	92.3	82.9	83.1	84.8	88.2	86.4
	±12.7	±10.6	±11.8	±16.5	±13.4	±16.1	±13.2	±11.5
1	72.4	75.0	70.9	71.9	37.9	40.4	76.0	67.8
	±13.8	±16.7	±15.7	±21.9	±11.0	±13.5	±19.5	±15.7
4	89.9	102	105	84.7	56.0	56.4	89.8	95.0
	±13.0	±22.1	±22.5	±23.4	±15.5	±14.0	±22.1	±20.5
20	104	116	115 ±5.2	93.7	72.0	81.9	110	96.6
	±12.0	±16.3		±27.7	±15.8	±31.1	±22.2	±26.7

Table 2-4. ln (Pre-exponential Factor) for All Asphalts at Various Pressures.

Pressure (atm O_2)	AAA-1	AAB-1	AAD-1	AAF-1	AAG-1	AAM-1	AAS-1	Lau4
0.2	24.7	26.6	27.0	24.0	24.4	24.5	25.7	25.3
	±4.3	±3.6	±4.0	±5.6	±4.6	±5.5	±4.5	±3.9
1	21.3	22.3	20.9	21.4	9.8 ±3.8	10.3	22.5	19.9
	±4.8	±5.7	±5.4	±7.5		±4.7	±6.7	±5.4
4	27.9	32.1	33.1	26.3	16.5	16.2	27.9	29.8
	±4.5	±7.6	±7.8	±8.1	±5.3	±4.8	±7.6	±7.1
20	33.3	37.2	37.5	29.6	22.7	25.2	35.0	30.5
	±4.1	±5.6	±1.8	±9.5	±5.5	±10.7	±7.7	±9.2

Isokinetic Rate

An isokinetic temperature has been determined for other petroleum reactions (Liu et al., 1996; Boudart, 1991). At this temperature, all compounds in a homologous series have the same reaction rate. In order to determine the isokinetic temperature A´ vs E, data, are plotted and fit by an exponential model. The slope of the line is 1/RT, and thus the isokinetic temperature is determined. The isokinetic rate at this temperature would be the intercept of the curve-fit.

Figure 2-5 shows the A´ vs E for all oxidation pressures studied. It is interesting to see that for oxidation pressures above atmospheric pressure the data overlay extremely well. From the curve-fits in Figure 2-5 we can determine that the isokinetic temperature for atmospheric air (0.2 atm O_2) is 105 °C (221 °F) with a rate of 0.0975 CA/day. For pressures of 1 atm O_2 and higher the isokinetic temperature is calculated to be 65.7 °C (150 °F) with a rate of 0.0189 CA/day. Figures 2-6 through 2-8 show how well these calculations approximate the data. We can see that the calculated isokinetic rates appear to fall in the middle of the experimental rate data near the isokinetic temperature. We can also see that near the calculated isokinetic temperature, the oxidation rates of the asphalts are fairly close together indicating that there is a convergence in the oxidation rates, but error is also associated with the measurements.

Figures 2-6 through 2-8 also show that as oxidation rates are measured at temperatures increasingly distant from the isokinetic temperature, a larger disparity in the rates occurs. This is

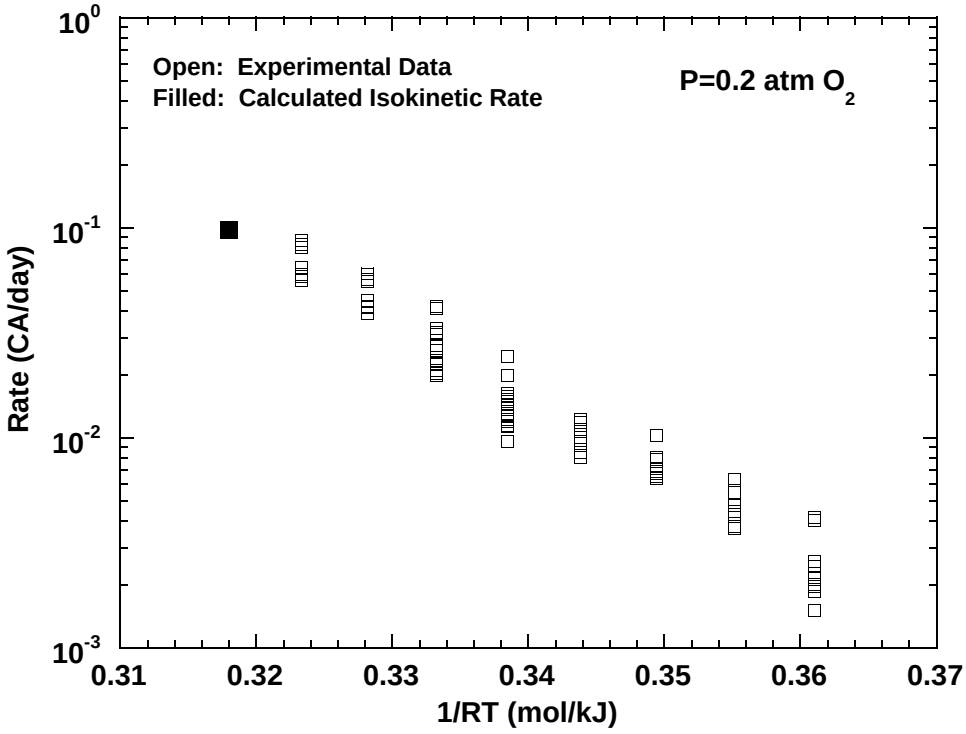

Figure 2-5. Relationship Between A' and E for Isokinetic Temperature.

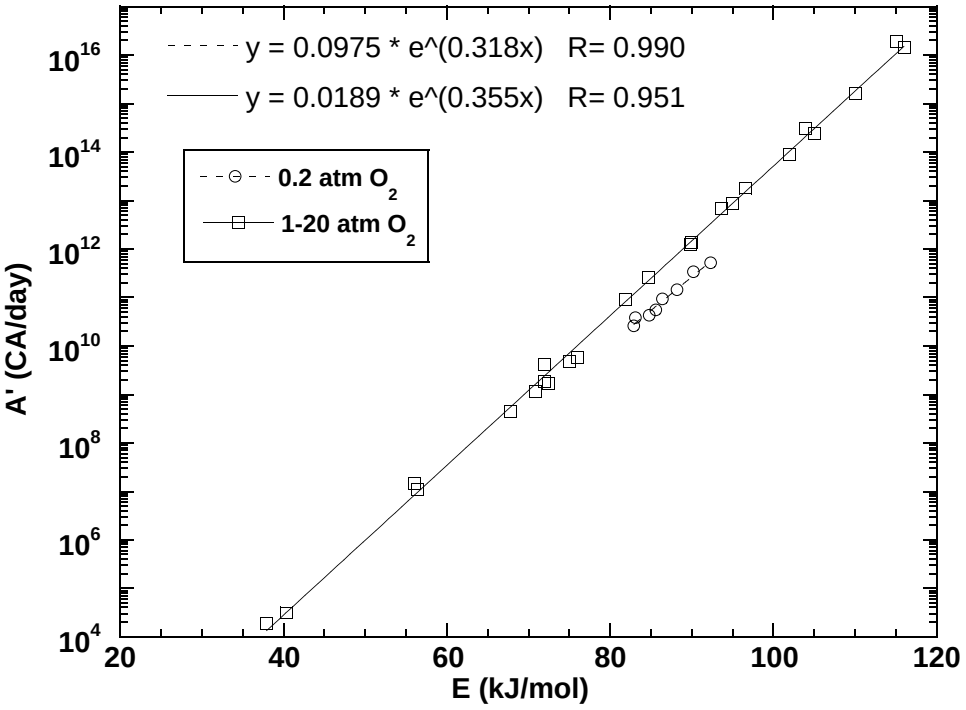

Figure 2-6. Calculated 0.2 atm O_2 Isokinetic Temperature with Experimental Results.

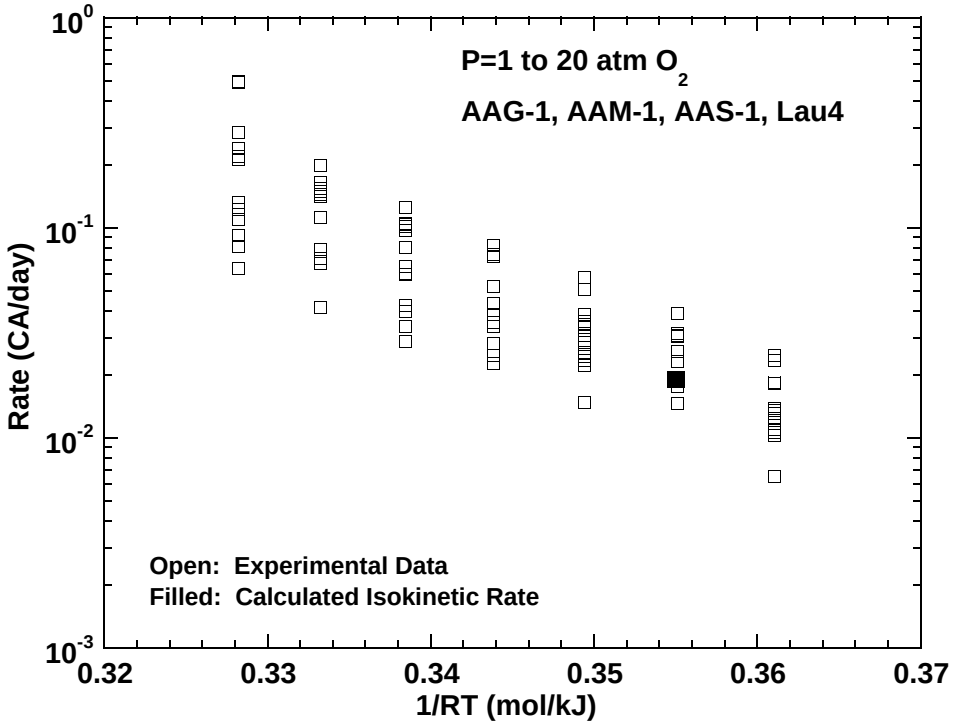

Figure 2-7. Calculated Isokinetic Temperature with Experimental Results for P=1 to 20 atm O_2 (AAA-1, AAB-1, AAD-1, AAF-1).

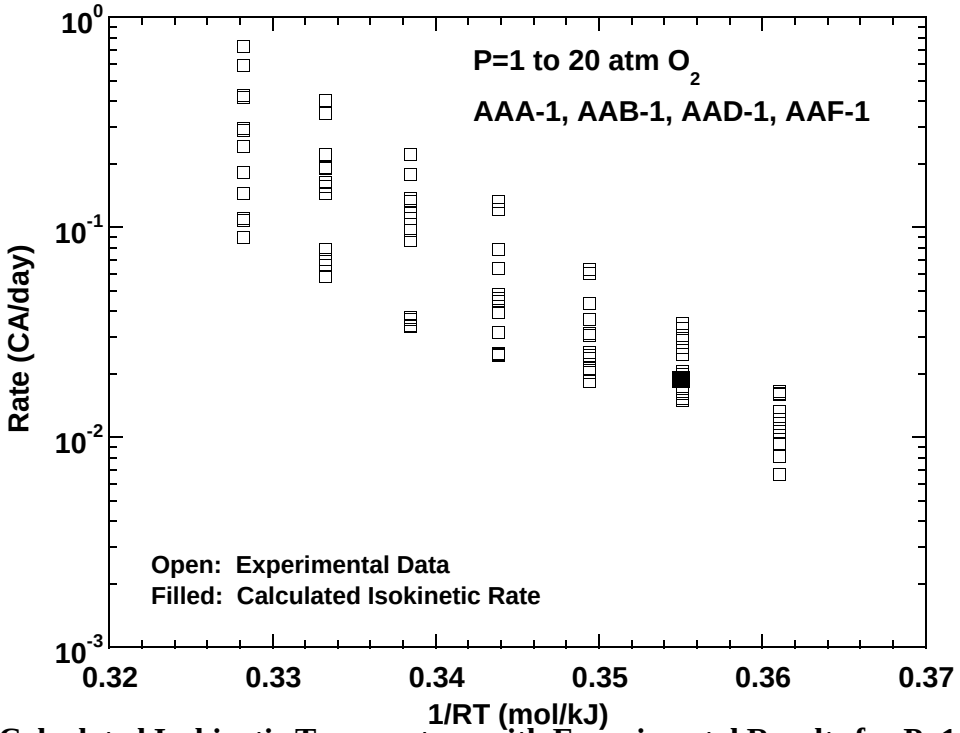

Figure 2-8. Calculated Isokinetic Temperature with Experimental Results for P=1 to 20 atm O_2 (AAG-1, AAM-1, AAS-1, Lau4).

due to the different activation energies that have been observed. Figure 2-6, which shows oxidation rates at atmospheric air, does not show this effect as well as Figures 2-7 and 2-8. This is because the activation energies at atmospheric air only range from 83-92 kJ/mol as opposed to 56-116 kJ/mol for 1 to 20 atm O_2.

The reason for the overlap of A´ vs E in Figure 2-5 (1-20 atm O_2) could be explained by the molecular diffusion hypothesis (Domke et al., 1999). As oxygen pressure is increased the asphaltenes are able to react. Once the asphaltenes can react, the overall oxidation mechanisms would be similar, thus allowing for a constant isokinetic temperature even as oxygen pressure varies.

Reaction Rate Model

Using the above results, a model can be used to estimate the kinetic parameters of the rate model in Equation 2-4. In turn A´ and E can be expressed in terms of an asphalt compositional parameter, oxygen pressure, and the results in Figure 2-5. The ratio of heptane asphaltenes (C7) to pentane asphaltenes (C5) is used as the asphalt compositional parameter (Table 2-5).

Table 2-5. Asphaltene Content of Tank Asphalts.

Asphalt	Heptane %AS	Pentane %AS	C7/C5
AAA-1	16.2	31.1	0.521
AAB-1	17.3	32.9	0.526
AAD-1	20.5	37.9	0.541
AAF-1	13.3	29.3	0.454
AAG-1	5.0	21.6	0.23
AAM-1	4.0	12.4	0.323
AAS-1	18.4	32.8	0.561
Lau4	13.6	29.7	0.458

From the data in Figure 2-9, E can be expressed in terms of the heptane:pentane asphaltene ratio and oxygen pressure. For the single pressure P=0.2 atm O_2:

$$E = 77.8 + 19.7\frac{C7}{C5} \quad \text{(for 0.2 atm } O_2\text{)} \tag{2-6}$$

For the other pressures, the data can be expressed as a single function of oxygen pressure and C7/C5 because of the single relationship between A´ and E at these higher pressures. For these pressures, the slopes from Figure 2-9 were averaged, and the intercepts were modeled as a function of oxygen pressure to find:

$$E = \left[11.3\ln(P) + 5.19\right] + 134.6\frac{C7}{C5} \quad \text{(for 1, 4, 20 atm } O_2\text{)} \tag{2-7}$$

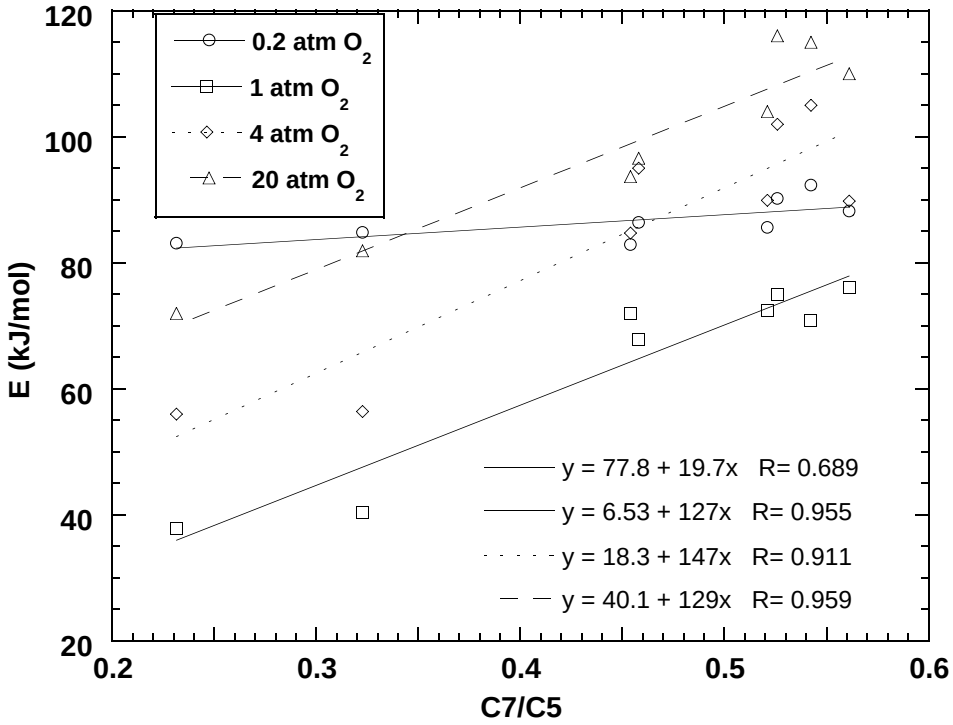

Figure 2-9. Relationship between E and Asphaltene Ratio.

Once E is known, A´ can be determined knowing the oxidation pressure by use of Figure 2-5:

$$\text{for P=0.2 atm } O_2 \quad A' = 0.0975 \exp(0.318E) \tag{2-8}$$

$$\text{for P} \geq 1 \text{ atm } O_2 \quad A' = 0.0189 \exp(0.356E) \tag{2-9}$$

It can be seen by comparing Tables 2-3, 2-4, 2-6, and 2-7 that ln A and E from the model are both within the error of the experimental data. However, when these values are substituted into equation 2-4 with the experimental error that is present, the model-calculated carbonyl formation rate for an asphalt may be in error by as much as 157percent (Table 2-8). This is because with even a small error in the rate constants in equation 4, the exponential nature of the model can cause a very large error in the model calculation of the individual oxidation rates.

Table 2-6. Model Calculations for E.

Pressure (atm O_2)	AAA-1	AAB-1	AAD-1	AAF-1	AAG-1	AAM-1	AAS-1	Lau4
0.2	88.0	88.1	88.5	86.7	82.3	84.1	88.8	86.8
1	75.3	76.0	78.2	66.3	36.4	48.6	80.7	66.8
4	91.0	81.6	93.8	81.9	52.0	64.3	96.3	82.5
20	109	110	112	100	70.1	82.4	115	101

Table 2-7. Model Calculations for ln(A′).

Pressure (atm O_2)	AAA-1	AAB-1	AAD-1	AAF-1	AAG-1	AAM-1	AAS-1	Lau4
0.2	25.7	25.7	25.8	25.3	23.9	24.5	25.9	25.3
1	22.8	23.1	23.9	19.6	9.0	13.4	24.8	19.8
4	28.4	28.6	29.4	25.2	14.6	18.9	30.3	25.4
20	34.8	35.1	35.9	31.6	21.0	25.4	36.7	31.8

It is important to note that this model predicts that the rates of two different asphalts containing the same C7/C5 asphaltene ratio would be the same. This is not necessarily the case. The individual molecules that make up the C5 and C7 asphaltenes between two different asphalts will not likely be the same let alone in the same amounts, with inevitable effect on the oxidation rates. It would be ideal to create an oxidation model that would be based on the amount of types of molecules; however, this would be extremely difficult. It is interesting that the results are unaffected by the ratio of carbonyl to oxygen content. It is lower than average for AAG-1 and above average for AAD-1, but these asphalts correlate as well as the others.

Initial Jump

Initial jump data, CA_o-CA_t, are recorded in Table 2-9, where CA_t is the carbonyl value of the tank asphalt. There is much scatter but within the scatter the results appear to be independent of temperature as reported by Liu et al. (1996) for more extensive data. Liu et al. did report pressure dependence for some asphalts and fitted the data with

$$CA_o - CA_t = \beta P^{\gamma} \qquad (2\text{-}10)$$

Table 2-8. Model-Calculated Rates x 10^3.

0.2 atm O_2

°F	AAA-1	AAB-1	AAD-1	AAF-1	AAG-1	AAM-1	AAS-1	Lau4
140	2.2	2.2	2.2	2.3	2.8	2.6	2.1	2.3
150	3.7	3.7	3.7	3.9	4.6	4.3	3.6	3.9
160	6.2	6.2	6.1	6.4	7.4	7.0	6.0	6.4
170	10.1	10.0	10.0	10.4	11.7	11.1	9.9	10.4
180	16.2	16.1	16.0	16.6	18.2	17.5	15.9	16.6
180	16.2	16.1	16.0	16.6	18.2	17.5	15.9	16.6
190	25.6		25.4	26.1	27.9	27.2		
190	25.6	25.6	25.4	26.1	27.9	27.2	25.3	26.1
200	40.0	25.6	39.8	40.5	42.3	41.6	39.6	40.5
210	61.5	39.9	61.4	62.0	63.4	62.8	61.3	61.9

1 atm O_2

°F	AAA-1	AAB-1	AAD-1	AAF-1	AAG-1	AAM-1	AAS-1	Lau4
140	12.3	12.3	12.1	13.0	15.4	14.3	11.9	12.9
150	19.2	19.2	19.2	19.2	19.1	19.1	19.3	19.2
160	29.6	29.7	30.1	28.1	23.5	25.3	30.6	28.2
170	45.0	45.3	46.5	40.6	28.7	33.1	47.9	40.8
180	67.5	68.3	70.9	58.0	34.9	43.0	73.9	58.5
190	100.0	101.4	106.5	81.9	42.2	55.4	112.6	82.9
200	146.3	148.9	158.2	114.5	50.8	70.8	169.4	116.2

4 atm O_2

°F	AAA-1	AAB-1	AAD-1	AAF-1	AAG-1	AAM-1	AAS-1	Lau4
140	11.3	11.2	11.1	11.8	14.1	13.1	10.9	11.8
150	19.3	19.3	19.3	19.3	19.1	19.2	19.3	19.3
160	32.5	32.6	33.1	30.8	25.8	27.7	33.6	30.9
170	53.9	54.3	55.7	48.6	34.4	39.6	57.3	48.9
180	87.9	88.9	92.3	75.5	45.5	56.0	96.3	76.2
190	141.2	143.3	150.5	115.7	59.7	78.2	159.1	117.1
200	223.7	227.7	241.9	175.1	77.6	108.3	259.0	177.6

20 atm O_2

°F	AAA-1	AAB-1	AAD-1	AAF-1	AAG-1	AAM-1	AAS-1	Lau4
140	10.2	10.1	10.0	10.7	12.7	11.8	9.8	10.7
150	19.4	19.4	19.4	19.3	19.2	19.3	19.4	19.3
160	36.2	36.4	36.9	34.3	28.7	30.9	37.4	34.4
170	66.4	66.9	68.6	59.9	42.4	48.8	70.7	60.2
180	119.4	120.8	125.4	102.5	61.8	76.1	130.8	103.5
190	210.9	214.0	224.8	172.8	89.1	116.9	237.6	174.8
200	366.1	372.8	396.0	286.6	127.0	177.3	424.0	290.8

Table 2-9. Initial Jump Data for All Asphalts at Various Pressures.

Pressure (atm O_2)	AAA-1	AAB-1	AAD-1	AAF-1	AAG-1	AAM-1	AAS-1	Lau4
0.2	0.215	0.177	0.201	0.280	0.475	0.297	0.153	0.247
	±0.085	±0.043	±0.092	±0.069	±0.157	±0.072	±0.040	±0.029
1	0.185	0.206	0.157	0.221	0.605	0.299	0.140	0.149
	±0.086	±0.097	±0.071	±0.092	±0.172	±0.133	±0.060	±0.062
4	0.305	0.291	0.216	0.372	0.934	0.487	0.193	0.289
	±0.149	±0.064	±0.140	±0.120	±0.190	±0.145	±0.063	±0.054
20	0.254	0.374	0.194	0.580	1.490	0.669	0.128	0.093
	±0.272	±0.075	±0.141	±0.119	±0.159	±0.072	±0.054	±0.083

Pressure dependence and composition dependence are indicated by a plot of the results in Figure 2-10. It appears however, that the pressure dependence, if any, is obscured by the scatter for the asphalts having high C7/C5 value. Perhaps the most interesting result is the high pressure dependence and high values of CA_o-CA_t at low values of C7/C5.

Values of β and γ are shown in Table 2-10 together with C7/C5 ratios. The values of β correlate rather well with C7/C5, being almost linear except that Lau4 and AAM-1 are a little low. The values for γ scatter badly. Only four asphalts AAG-1, AAM-1, AAF-1, and Lau4 show

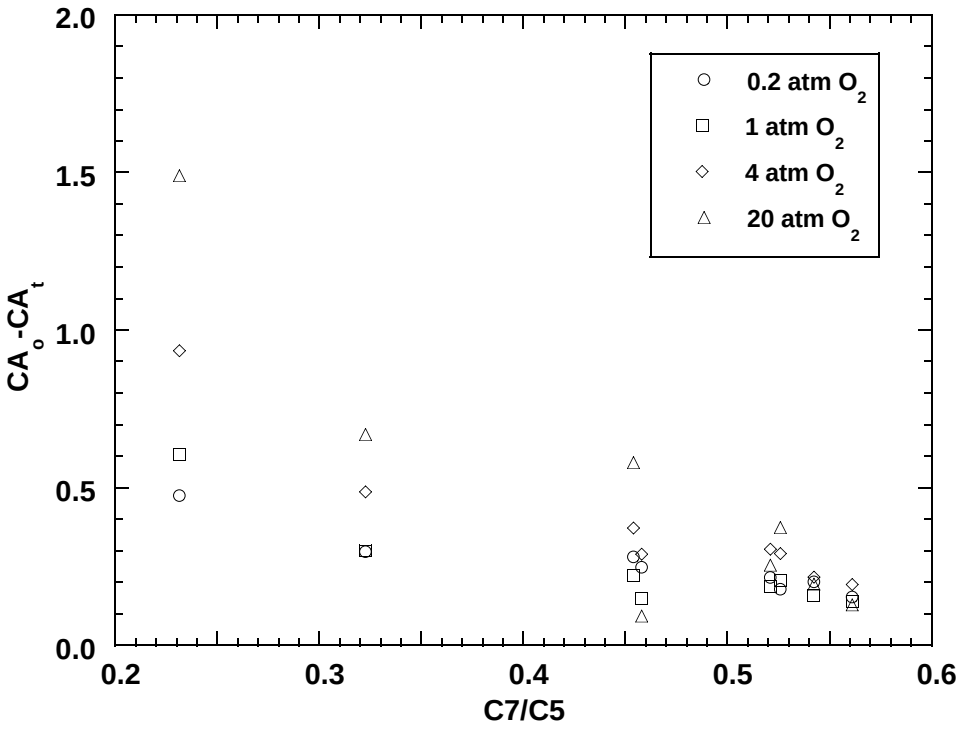

Figure 2-10. CA_0-CA_t vs Asphaltene Ratio.

Table 2-10. β, γ, and C_7/C_5 for All Asphalts.

Asphalt	β	γ	C_7/C_5
AAA-1	0.226	0.0632	0.521
AAB-1	0.223	0.17	0.526
AAD-1	0.189	0.0121	0.541
AAF-1	0.301	0.176	0.454
AAG-1	0.667	0.254	0.231
AAM-1	0.361	0.191	0.323
AAS-1	0.153	-0.0163	0.561
Lau4	0.197	-0.155	0.458

enough pressure effect on the initial jump (Figure 2-10) to be significant and the 20 atm datum for Lau4 (Table 2-9) looks bad as does the γ value. The other values of γ, except perhaps AAB-1, move in the same direction, increasing with decreasing C7/C5.

CONCLUSIONS

The oxidation kinetics of asphalts is hypothesized to be affected by oxygen diffusion through maltenes to polar aromatic and asphaltene aggregates. This causes an effect of oxygen pressure on oxidation which varies with asphaltene composition.

Several asphalts were oxidized at various temperatures and pressures to determine how the aging conditions affected their oxidation kinetics. An Arrhenius equation was assumed to fit the constant-rate region using a classical kinetics model for reactions:

$$r_{CA} = A' \exp\left(\frac{-E}{RT}\right) \qquad (2\text{-}4)$$

Thus, the oxidation rate for each asphalt was assumed to be explicit in aging temperature and effects of oxygen pressure could be included implicitly through the parameters A′ and E.

In fact, it was determined that the oxidation pressure did play a role in the kinetic model constants. In particular, the activation energy and the preexponential factor are both surprisingly a function of oxygen pressure. They appear to have a minimum value at approximately 1 atm O_2, and these values are asphalt dependent. This pressure dependency is hypothesized to be caused by molecular diffusion.

An isokinetic temperature was determined for all the asphalts studied. This isokinetic temperature also appears to be a function of oxidation pressure. For low pressures, the asphalts tested have the same model-calculated rate at one isokinetic temperature, while at higher pressures, they have a different model-calculated rate and a second isokinetic temperature.

A model was developed to relate the kinetic parameters for different asphalts to their composition. This model was based on the asphaltene content of an individual asphalt, and the

oxidation temperature and pressure. The activation energy (E) of the oxidation is determined knowing the C7:C5 asphaltene ratio and oxygen pressure (P). The preexponential factor (A′) is then determined knowing E and P.

The model-estimated parameters calculate A′ and E within experimental error for the asphalts studied. However, this error may still lead to large errors in carbonyl formation rates due to the exponential nature of the kinetic model. Model-calculated rates were sometimes in error by as much as 150%.

The extent of initial jump of CA oxidation is asphalt dependent. For all asphalts the initial jump is independent of oxidation temperature. However, for some asphalts the initial jump is pressure dependent, and for others it is within experimental error. This also appears to be due to the composition of the asphalt. It appears as though low C7:C5 asphaltene ratio asphalts had a stronger pressure dependency and a higher value of the initial jump than the higher asphaltene ratio content asphalts.

CHAPTER 3. THE EFFECT OF ASPHALT AGING TECHNIQUES ON LOW-TEMPERATURE PROPERTIES

ABSTRACT

This project includes three test phases wherein the effects of various aging techniques on asphalt low-temperature properties were investigated. In addition, two other studies were conducted: air-blowing was investigated as a possible long-term aging test, and modifier performance was compared with respect to aging.

In Phase I of this project it was shown that 38 days of aging at 60 ^{o}C and 1 atmosphere of air is approximately equivalent to 20 hours in the PAV at 100 ^{o}C after both have been RTFOT-aged. Low-temperature properties of the samples did not vary significantly between the PAV and environmental room aged material.

In Phase II of this work, a correlation was developed using the high-temperature parameter $G^{*}/\sin(\delta)$ at 58 ^{o}C and 10 rad/s to correct the low-temperature performance grade when one desires to skip the long-term aging procedure. The correlation proved to give a maximum error of ±1.6 ^{o}C for the low-temperature performance grade.

In Phase III of this project it was shown that as asphalts are aged for extended periods their relative ranks with respect to Superpave low-temperature specifications change. This indicates that the Superpave long-term aging specifications result in an arbitrary ranking of asphalts with respect to low-temperature properties.

Air-blowing was investigated as a possible alternative for long-term aging in this project. Upon examining the data obtained by long-term air-blowing, it was concluded that air-blowing is not a suitable long-term test because it did not consistently produce samples comparable to those aged in the environmental room.

To summarize the work in comparing various modifiers, the higher weight percent modified samples showed considerably better low-temperature properties. The 18% RSGF-20 modified samples showed the best improvement in low-temperature properties followed by 4%SBS and 4%SBR. Polymer modifiers, therefore, should be used in concentrations of at least 4 percent by weight, where SBS rather than SBR is recommended. If ground tire rubber is to be used, a high-cure process with 18 percent by weight rubber provides excellent benefits for both high- and low-temperature properties but faces a significant cost hurdle.

INTRODUCTION

Asphalt Aging

A significant characteristic of asphalts is the fact that they undergo oxidative aging in the presence of oxygen. Oxidative aging has a profound effect on physical properties of asphalts and therefore a great deal of research has gone into understanding the nature and effects of oxidative aging.

Oxidative aging results in changing the composition of the asphalt itself. As an asphalt undergoes oxidation, the polar aromatics transform to asphaltenes, and naphthene aromatics become polar aromatics (Liu et al., 1998). Saturates, however, do not readily oxidize in significant portions (Petersen, 1998). After naphthene aromatics become polar aromatics they may then continue to oxidize and become asphaltenes, but for limited aging times this transformation is negligible. Liu (1996) showed that the rates of reaction for the polar aromatic fraction and the naphthene aromatic fraction vary from asphalt to asphalt. Therefore, the overall amount of the aromatic fractions may increase or decrease, while the asphaltene fraction always increases, and the saturate fraction does not generally change.

The oxidative aging process begins with an initial jump region, wherein the asphalt viscosity greatly increases with oxidation time (Lau et al., 1992; Petersen et al., 1993). The initial jump region is followed by a region of slower viscosity increase at a constant rate. Petersen (1998) has presented an explanation for the two regions based on a dual sequential oxidation mechanism. Petersen suggests that the initial jump region is due to the oxidation of polycyclic hydroaromatics to hydroperoxides. The hydroperoxides then may decompose into ketones or radicals or may react with sulfur groups to form sulfoxides. Following the initial jump, the constant rate region begins wherein benzylic carbons present in the asphalt complex react with oxygen to form ketones (carbonyls).

In a general sense these mechanisms describe asphalt aging, but the mechanisms themselves and the products of the oxidation are both highly dependent upon the asphalt composition and the aging conditions. Aging conditions and composition influence oxidation primarily due to the configuration of the asphalt matrix itself. It has been shown, for example, that pressure has a profound effect on the relative size of the initial jump region while temperature has no effect at all (Lau et al., 1992). This makes sense when one considers that at atmospheric pressure there is considerable diffusion resistance to oxygen transport into the asphalt. Higher pressures allow oxygen to be transported into the asphalt more readily and therefore lead to greater overall oxidation (Domke, 1999).

Considerable work has also been done to model the rate of asphalt oxidation in terms of temperature and pressure. Lau et al. (1992) showed that the rate of asphalt oxidation can be expressed as an Arrhenius model. Lunsford (1994) expounded upon this model, adding an

oxygen pressure effect. For the constant rate region, the rate of carbonyl area formation (a measure of oxidation rate) is given as:

$$r = AP^{\alpha} \exp\left(\frac{-E(P)}{RT}\right) \qquad (3\text{-}1)$$

where P is the partial pressure of oxygen. Equation 3-1 illustrates that aging which occurs at atmospheric air pressure and a pavement temperature of 60 °C will have a significantly different rate than pressurized aging occurring at 20 atmospheres air and 100 °C.

Domke (1999) illustrated that aging conditions can also affect asphalt physical properties as he compared the 60 °C viscosities obtained by high pressure (20 atm air) aging with those obtained from asphalts in an environmental room maintained at 60 °C and 1 atm air. Domke showed that the degree of asphalt oxidation, as seen by the change in carbonyl area, differed between the two groups, proving that asphalt aging conditions have an effect on physical properties.

Upon aging, the physical properties of an asphalt may change dramatically. The viscosity of the material increases, as does its stiffness. These physical changes are due primarily to the increased amount of asphaltenes in the asphalt, although some volatilization of lighter saturates may contribute as well. As asphaltene concentration increases, the maltene concentration simultaneously decreases, resulting in larger colloidal particles with fewer solvating molecules. The resulting material tends to behave more like an elastic material at high temperatures, and more like a glassy solid at moderate to low temperatures. In service, aging leads to thermal and fatigue cracking susceptibility and is responsible, in part, for road failure.

Because the physical properties of asphalt binders are changed by oxidation, it is important to know the extent of the oxidation effect both by the hot-mix process and while in service on the road. Therefore, in order to evaluate asphalt binders, Strategic Highway Research Program researchers needed methods of asphalt aging that simulated both the hot-mix process and field aging (Anderson et al., 1991). In order to simulate the hot-mix process, researchers chose the existing rolling thin film oven test (ASTM D-2872). The RTFOT ages asphalt at elevated temperatures (325 °F) by blowing hot air over a thin film of asphalt. For field aging simulation, researchers chose to age asphalt binders in a Pressurized Aging Vessel for 20 hours at temperatures from 90 to 110 °C and a pressure of 20 atmospheres of air (Harrigan et al., 1994). SHRP goals, findings, and methods will be discussed in further detail in the following section.

Overview of SHRP (Superpave) Tests and Specifications

In 1987, the Strategic Highway Research Program was launched in order to improve asphalt pavement performance. As part of the program, researchers developed new methods for

testing asphalt binders and new specifications in accordance with the new testing methods (Anderson et al. 1994). Performing the SHRP (subsequently called Superpave) tests on an asphalt binder results in a performance grade for the binder. The PG reflects the maximum and minimum design temperatures under which the asphalt will have satisfactory performance.

Asphalt binder physical properties are critical to road performance. If an asphalt binder is too soft, rutting may occur soon after completion of the road due to traffic loads. On the other hand, if the binder is too hard or brittle, thermal cracking will occur during periods of cold weather. In addition, oxidative aging causes the binder to harden, thereby compounding its thermal cracking susceptibility over the life of the pavement (Domke, 1999). In light of these issues, SHRP formulated binder tests and specifications that determine the high-temperature and low-temperature physical properties of aged binders. In order to determine high-temperature properties, a material is aged for a short time, in the previously mentioned RTFOT test, which simulates the hot-mix process. Low-temperature properties, on the other hand, are measured using material aged in the PAV to simulate long-term aging.

Several tests are involved in obtaining the performance grade of an asphalt binder. The top grade is determined by a dynamic shear rheometer, which is used to characterize the high-temperature rheological properties of the binder. Low-temperature properties (and therefore bottom grade) are measured using a bending beam rheometer and a direct tension tester.

Overall, the Superpave standards for asphalt binder testing have provided a beneficial framework wherein binders can be evaluated and compared (Hoare and Hesp, 2000). However, Superpave standards are still relatively new and may yet be improved in some areas. Of particular concern is the long-term aging test, which takes place at pressures and temperatures well above road aging conditions. These elevated temperatures and pressures affect the mechanism of oxidation for the binder, leading to physiochemical property relations that may be different from those obtained at road aging conditions. A different mechanism for oxidation may also produce different relative aging rates between materials.

Since Superpave standards require long-term aging for low-temperature property measurement, it stands to reason that low-temperature properties are of primary interest after long-term aging. The long-term aging tests, unfortunately, are quite time consuming. The Superpave specified aging time, for example, is 20 hours within the PAV. In light of this time-consuming procedure, it would be beneficial to determine if the low-temperature properties of short-term aged material correlated with those obtained from long-term aged material. With an accurate correlation relating the physical properties of long-term aged material with those of short-term aged material, one could bypass the time-consuming long-term test. Low-temperature data collected by Domke (1999) indicate that the development of a correlation of this type may be possible.

Many previous researchers have observed that air blowing asphalt binders at elevated temperatures results in oxidation and change in physical properties (Quddus et al., 1995;

Gallagher et al., 1996). Concurrent with this project, the Center for Asphalt and Materials Chemistry has developed an alternative short-term aging procedure by air blowing to replace the existing RTFOT procedure (TxDOT project 0-1742). Also, an air-blowing procedure was sought to replace the long-term aging tests. A portion of the research reported in this chapter was devoted to establishing the validity of these new procedures.

Research Objectives

The research presented in this chapter had five primary objectives. The first objective was to compare the long-term high pressure, high-temperature aging to aging at simulated road conditions in the environmental room (Phase I). The second (Phase II) objective was to determine if long-term aging could be skipped when obtaining the performance grade of an asphalt. Third, it was hoped to gain insight into how extended aging affects the relative rankings of asphalt binders as given by the Superpave specifications (Phase III). Fourth, air-blown aging of asphalt was examined as a possible replacement for the PAV long-term aging test. Finally, the effect of modifiers on low-temperature performance was evaluated.

To accomplish the first objective, a comprehensive comparison of the RTFOT/ environmental room aged material to RTFOT/PAV aged material was performed. This comparison was intended to reveal the relative amount of road aging the PAV simulates and the accuracy with which the PAV models road conditions. In addition, the comparison revealed differences between the oxidation mechanisms for the two aging methods.

The Phase II objective of this research involved determining how the low-temperature physical properties of short-term aged material compare with those of long-term aged material. Specifically, a correlation was sought between the performance grade of long-term aged material with the apparent performance grade of short-term aged material. Hopefully, such a correlation would enable laboratories to obtain reliable performance grades for a material without running long-term aging tests.

Third, this research was intended to determine if the differing mechanisms for asphalt oxidation have significant impact on low-temperature properties. If so, the relative rankings of asphalts based on their performance grade would be entirely dependent upon the type, and perhaps length, of the aging test performed on the asphalts. For example, the degree of oxidation observed at atmospheric air concentration and 60 ^{o}C are significantly different from that observed in the PAV (Domke, 1999). These differences may result in significant differences in low-temperature properties. If this is the case, Superpave standards may need to be modified to reflect the difference.

In order to find a long-term aging test that was more representative of road conditions and yet still of reasonable length, a long-term air-blowing test was investigated. This test was intended to reflect, as much as possible, the conditions and oxidation mechanisms observed in road aging, while still accelerating the rates enough for timely testing.

The study of modifier performance used the same base asphalt with SBR, SBS, and high-cure ground tire rubber to assess their effect on low-temperature and high pavement temperature performance grade.

MATERIALS AND METHODS

Materials

Selection of Asphalts

Asphalt binders used in this project were selected from the inventory of the Center for Asphalt and Materials Chemistry (CAMC) at Texas A&M University. In order to ensure that the results of the study were not confined to a specific type of asphalt, many different asphalt binders were chosen for the study. In selecting asphalts, a wide variety of initial viscosities were sought as well as a variety of asphalt manufacturers. Table 3-1 presents the various unmodified asphalt binders used in the study as well as their initial unaged, or tank 60 ºC viscosities. The values presented in Table 3-1 tend to be higher than the literature values for the selected SHRP asphalts. The asphalts used in this study have been stored in a facility which was not temperature controlled, and some have been there for a number of years. It is conceivable, therefore, that some oxidation has taken place during storage, which would account for the higher viscosities.

Table 3-1. Unmodified Asphalt Binders and Their Unaged Viscosities Measured at 60 ºC and 0.1 rad/s.

Asphalt Binder	Unaged 60 ºC Viscosity @ 0.1 rad/s (P)
SHRP AAA-1	1081
SHRP AAD-1	1366
SHRP AAF-1	2261
SHRP AAS-1	3162
SHRP ABM-1	3313
Conoco AC-20	3870
Exxon AC-10	1203
Exxon AC-20	2267
GSAC AC-15P Base	858
Shell AC-20	2232

Preparation of Modified Samples

The 10 binders listed in Table 3-1 are unmodified materials, that is, no polymer modifiers have been added to them to enhance their rheological properties. Since the scope of this work includes modified material as well, we prepared six additional modified binders for the study. The six modified binders are listed in Table 3-2. All of the modified binders share the same base, the GSAC AC-15P base, and were modified with either styrene-butadiene rubber (SBR), styrene-butadiene-styrene block co-polymer rubber (SBS), or Rouse ground tire rubber of –20 mesh (RSGF-20).

The first pair of samples listed in Table 3-2 were modified using an SBR Latex emulsion (Sample number 140-0) received from Gulf States Asphalt Company (GSAC). The emulsion contains 72 percent solids, with the balance being water. Two percent solids by mass were added to the first sample, and four percent solids by mass to the second sample. In order to maintain the emulsion while mixing into the base asphalt, the emulsion was added drop-wise while stirring the base asphalt. To accomplish this, the base asphalt was poured into a one gallon can and heated to 325 ^{o}F. A Central Machinery drill press (model T-726) was used to mix the hot asphalt at a speed of 1550 rpm. The emulsion was then added drop-wise over a period of about 10 minutes. After the addition of the emulsion, the asphalt was stirred at 1550 rpm for 1.5 hours to ensure

Table 3-2. Modified Asphalt Binders and Their Unaged Viscosities Measured at 60 ^{o}C and 1.0 rad/s.

Asphalt Binder	Unaged 60 ^{o}C Viscosity @ 1.0 rad/s (P)
GSAC AC-15P Base W/2% SBR	1886
GSAC AC-15P Base W/4% SBR	2721
GSAC AC-15P Base W/2% SBS	1613
GSAC AC-15P Base W/4% SBS	3521
GSAC AC-15P Base W/10% RSGF-20	1750
GSAC AC-15P Base W/18% RSGF-20	2300

good mixing and to ensure the vaporization of the water in the emulsion. During the entire mixing process a nitrogen blanket was maintained on the system to prevent the asphalt from oxidizing.

The second pair of modified samples was made with 2 and 4 weight percent SBS, which was received from GSAC (D-1101 polymer, sample number 139-0). In contrast to the SBR modified material, wherein the emulsion simply needed to be mixed in, the SBS polymer had to be dissolved in the asphalt. In order to accomplish this a different procedure was used. To dissolve the polymer into the base asphalt the mixture was heated in a one gallon can to 350 ^{o}F, and mixed using a Silverson mixer (model L4RT) at 4000 rpm. The 2%SBS sample was blended for 2 hours at these conditions, and the 4%SBS sample was blended for four hours. A nitrogen blanket was maintained on the system throughout the mixing process to prevent oxidation of the binder.

The final pair of the modified samples, GSAC AC-15P Base w/10% RSGF-20 (Rouse Rubber, -20 mesh) and GSAC AC-15P Base w/18% RSGF-20, was modified using RSGF-20. These samples were cured using a high-cure process recommended by Chipps (2001) which gives adequate disintegration of the crumb rubber and thorough dispersion of the modifier throughout the base. For the first sample, 10 percent by mass RSGF-20 was added to the GSAC AC-15P base. Similarly, the second sample contains18% RSGF-20 by mass. After the rubber was added, each sample was cured in a one gallon can using a Silverson Mixer (model L4RT) for 6.5 hours at 500 ^{o}F and 8000 rpm. In order to prevent oxidation during the curing process a sparger was used to blow nitrogen through the sample. In addition, a blanket of nitrogen was maintained above the sample.

Aging Procedures

Short-Term Aging

During the road manufacturing process, asphalt is heated and mixed with aggregate, a procedure known as the hot-mix process. Asphalt hardening occurs during the hot-mix process by loss of volatile components within the asphalt and by oxidative aging due to contact with atmospheric oxygen. For laboratory purposes, it is necessary to simulate the hot-mix aging process before any other long-term aging procedure is performed on the asphalt.

There are a number of ways to simulate the hot-mix process. The most common is the rolling thin film oven test, ASTM D2872, which was developed by Hveem et al. (1963). Another hot-mix simulation, the thin film oven test, ASTM D1754, is available, but as Jemison et al. (1991) pointed out, these tests give essentially identical results. Finally, the CAMC at Texas A&M University, has developed a new air-blowing procedure to simulate the hot-mix process. In this study, the RTFOT was used for the bulk of short-term aging tests, but the new air-blowing procedure was used as well. Both the RTFOT and the new CAMC test are described in this section.

The RTFOT test simulates the hot-mix process by bringing a heated asphalt film in contact with hot air. Oxygen in the air reacts with the asphalt film, thus simulating oxidative aging, and the heating of the asphalt results in volatilization of the lighter components. The RTFOT procedure begins by pouring 35 grams of asphalt into each of eight RTFOT bottles. Within the oven, the bottles are inserted into a rack where they sit horizontally, with the mouth of the bottle facing outward. The rack itself rotates at 15 revolutions per minute, thereby passing each bottle in front of a nozzle that directs hot air into the bottle at a rate of 4 L/min. The oven temperature is maintained at 163 ^{o}C (325 ^{o}F) and the test runs for 85 minutes. For more information concerning the RTFOT test see ASTM D2872.

Figure 3-1 illustrates the apparatus used in the new air-blowing procedure developed at the CAMC. The apparatus consists of a main vessel, a temperature control system, air flow control system, and a mixer. For the prototype apparatus, the main vessel itself is made of a copper alloy with an approximately 3 1/2 inch outer diameter. The vessel has a stainless steel lid, which contains ports for the spindle, the thermocouple, and the air sparger. The vessel also was insulated with 2 inch thick fiberglass insulation. The temperature control system consists of a heating mantle (Glas-Col Model TM610), a temperature controller (Omega Model CN9000A), a variac (Staco Model 3PN1010B), and a thermocouple (Omega Part Number 010801). Temperature is continuously measured by the thermocouple, which sends a signal to the controller. The controller then varies the power sent to the heating mantle. The operator controls the maximum output to the heating mantle by adjusting the setting on the variac. Compressed air enters the system and flows through a flow controller (Cole-Parmer), which maintains a constant air flow rate. The air then proceeds into the vessel through the sparger and exits directly under the spindle. The mixing system consists of an Arrow 1750 Mixer and a spindle with four sets of six cylindrical prongs.

The procedure is straightforward. Two hundred and fifty grams of asphalt are poured into the main vessel. The vessel is then inserted into the heating mantle, and the apparatus is assembled. The temperature controller is set to 325 ^{o}F, and the Variac to about 70 percent. Once the temperature reaches about 270 ^{o}F, the Variac is adjusted to 50 percent. Once the temperature within the vessel reaches 320 ^{o}F, the air flow is turned on and controlled at a constant rate of 4L/min. The mixer is set at a constant speed of 700 rpm. When run for 75 or 80 minutes, this apparatus and procedure was found to be comparable to the RTFOT in terms of viscosity increase and carbonyl area production. The interested reader is directed to Vassiliev (2001) for details concerning the new air-blowing apparatus.

Long-Term Aging

Once asphaltic concrete is installed in road applications, the asphalt continues to age. Atmospheric oxygen reacts with the asphalt binder in periods of hot weather, thereby changing the chemical composition and material properties of the binder. As aging progresses, the binder's viscosity increases, and the binder itself becomes more brittle. This may lead to

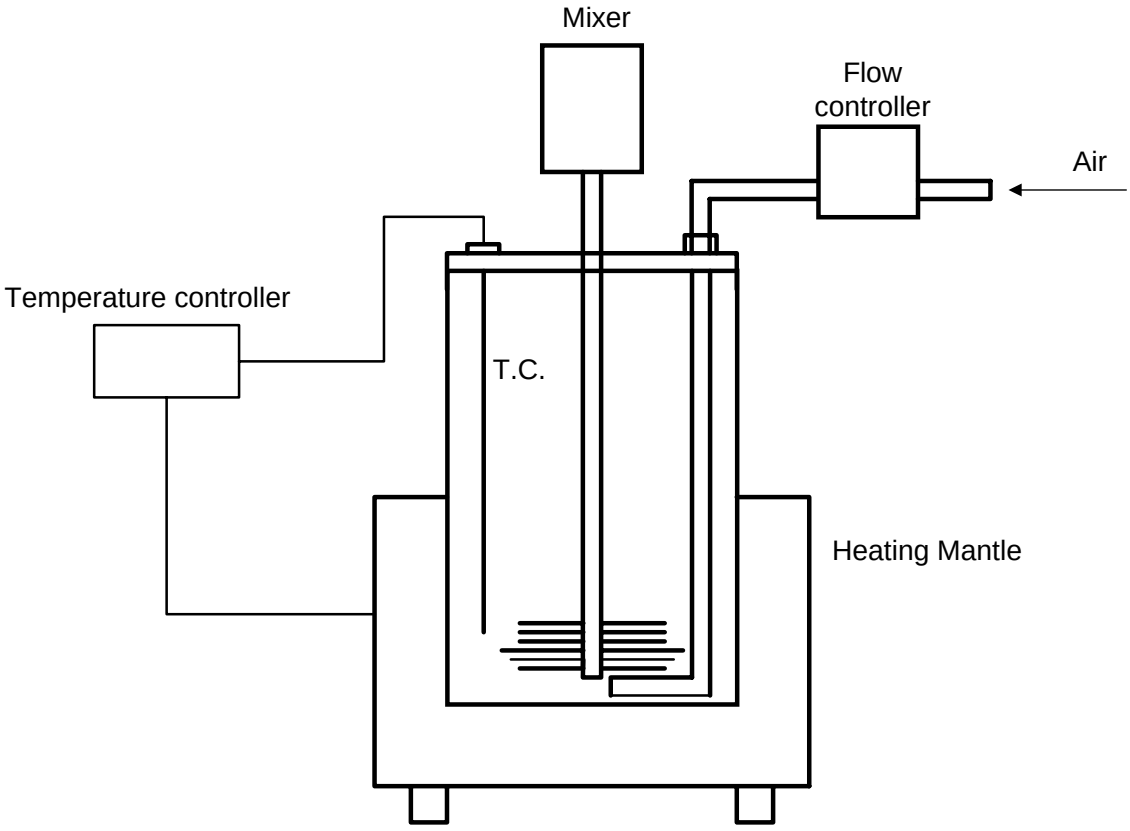

Figure 3-1. Air Blowing Short-Term Aging Apparatus.

increased thermal and fatigue cracking susceptibility of the asphaltic concrete. In order to design roads which are durable, that is, resistant to thermal and fatigue cracking, it is necessary to simulate the long-term in-service aging of asphalt binders.

As with the short-term aging simulation, several long-term aging options are available. The most common long-term aging test is performed at high temperatures and pressures using a pressure aging vessel. Asphalt binders may also be long-term aged at simulated road conditions with atmospheric pressure and temperatures similar to those encountered in summer months. Simulations of road conditions are performed in an environmental room, where temperature and humidity are held constant. Finally, asphalt binders may be air-blown at elevated temperatures in an apparatus similar to the one presented in Figure 3-1. All three of these long-term options were used during the course of this project, and as such, they are described in this section.

The PAV testing equipment consists of a pressure vessel with pressure and temperature controls, a sample rack, and a sample pan. Fifty grams of asphalt that has been RTFOT aged are poured into a sample pan giving an asphalt layer which is 3 mm thick. The sample pans are then placed onto the sample rack, which is then placed inside the vessel. Once the vessel is sealed, the temperature and pressure control systems bring the sample to the temperature and pressure

chosen by the operator. Typically, the test itself is performed at a pressure of 20 atmospheres of air and temperatures of either 90, 100 or 110 °C. For this study, all PAV tests were conducted at 100 °C. For further information regarding the PAV test, the reader is directed to AASHTO PP1.

Long-term asphalt aging can also be carried out in an environmental room, where conditions can be kept close to those seen in road service. For this study, asphalt materials were aged in an environmental room maintained at 60 °C, atmospheric pressure, and 50 percent relative humidity. These conditions were chosen because they are comparable to Texas road conditions during the summer months. Before environmental room aging, all samples are RTFOT short-term aged. Following the RTFOT, 20 grams of asphalt are poured into 5.5″ by 5.5″ aluminum trays. The resulting film of asphalt in each tray should be approximately 1.0 mm thick. The thin film of asphalt allows the oxidation to take place with little or no diffusion resistance, thereby producing a uniform sample that accurately represents aging at the environmental room conditions.

The final type of long-term aging is air-blowing. Figure 3-2 illustrates the apparatus used in the long-term air-blowing procedure. As with the short-term air-blowing apparatus, the system is comprised of a main vessel, a temperature control system, a mixer, and an air control system. The main vessel used for this apparatus is a quart can. The temperature controller receives a signal from the thermocouple and controls the power sent to the heating tape. A variac is included to allow the operator to control the maximum power sent to the heating tape. Air flow rate is controlled by a rotameter set to a specific flow rate by the operator. The air flows through the rotameter and into the sparger, which distributes the air into the asphalt sample. A Central Machinery drill press (Model T-726) with an attached impeller was used to mix the sample during the procedure.

The long-term air-blowing procedure begins by placing 250 grams of asphalt into a quart can. The apparatus is then assembled and the temperature controller is set to 325 °F. While the system achieves temperature, a nitrogen line is connected to the sparger in place of the air line. This prevents any oxidation of the asphalt prior to testing. After the system achieves temperature, the air line is connected, and the rotameter is set to a flowrate of 24,680 mL/min. The drill press is then turned on at a speed of 1550 rpm. Typically, the long-term aging test is run for 20 hours at these conditions.

High-Temperature Material Properties

High-temperature properties of binders are very important in the proper design of asphaltic concrete, for they contribute to the pavement's susceptibility to rutting. A binder having minimum hardness is desired for preventing rutting.

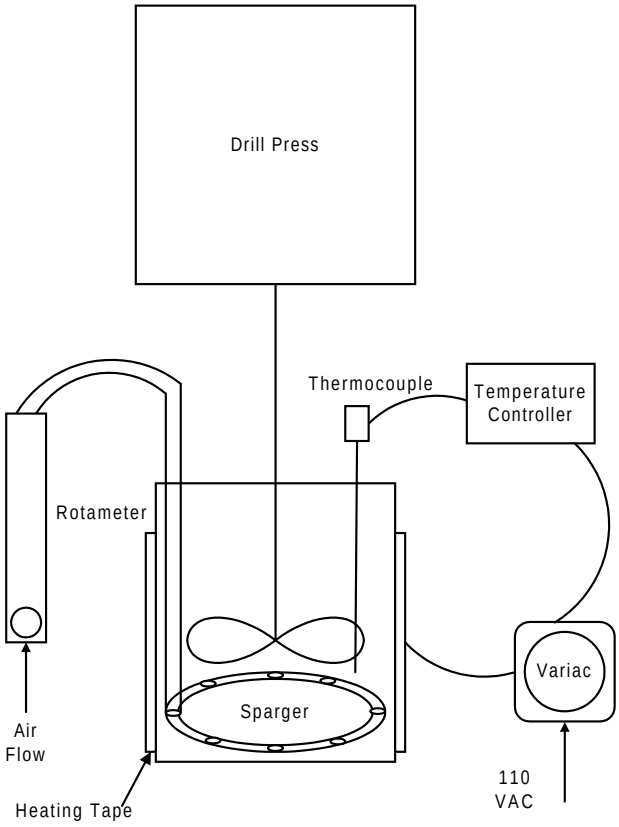

Figure 3-2. Air Blowing Long-Term Aging Apparatus.

Dynamic Shear Rheometer

In order to measure the high-temperature properties of the asphalt material, a Carri-Med CSL-500 dynamic shear rheometer was used. For all samples the 60 ºC complex viscosity was obtained by running a frequency sweep at constant torque for each material. A 2.5 cm composite plate was used with a 500 micron gap for the majority of the samples, and a 1500 micron gap for rubber-modified (RSGF-20) samples. For unmodified samples the limiting complex viscosity was taken at a strain rate of 0.1 rad/s, whereas for modified samples the value at 1.0 radians per second was recorded. Since the rubber modified materials were outside of the Newtonian flow regime at 60 ºC, the viscosity at 1.0 radians per second was chosen arbitrarily as a convenient value for comparative purposes.

All samples were also top graded according to Superpave specifications. For these measurements the frequency was fixed at 10 rad/s, and a torque sweep was performed on the material. Once the material reached the Newtonian limit, the complex shear modulus, G^*, and the phase angle, δ, were recorded. $G^*/\sin(\delta)$, an important parameter in Superpave specifications, was then calculated. Measurements of this type were conducted at two of the

following temperatures for each material: 52, 58, 64, 70 and 76 ºC. As with the 60 ºC viscosity, all runs were performed at a 500 micron gap for all samples except those modified with crumb rubber, which were performed at 1500 microns.

Low-Temperature Material Properties

Low-temperature material properties are also important for proper asphaltic concrete design. While a relatively hard asphalt is necessary to prevent rutting at high temperatures, an asphalt which is too hard will exhibit thermal cracking at low temperatures.

Bending Beam Rheometer and Direct Tension Tester

The bending beam rheometer (BBR) was used to measure the low-temperature stiffness and the m-value of an asphalt binder. The direct tension tester (DTT) was used to measure low-temperature failure strain and stress of asphalt subjected to a uniaxial load. The standard SHRP procedures were used for these tests.

From the DSR, BBR, and DTT measurements, Superpave grading of the materials was determined. Interpolation of data was used to obtain continuous gradesand values are reported as continuous grades.

Analytical Techniques for Asphalt Oxidation

Two analytical techniques were used during this study to determine the degree of asphalt aging. Infrared spectroscopy was used to determine the carbonyl area of samples after various aging techniques (Jemison et al., 1992). Gel permeation chromatography was used to determine the shift in molecular weight as a result of oxidative aging.

Methodology

For this project, the low-temperature properties of asphalt material were studied in three different test phases. First, high-pressure PAV aging was compared to road-condition aging as simulated in the 60 ºC environmental room. Second, the current standard aging procedure for obtaining the bottom grade (RTFOT/PAV 20 hours) was compared to material that was short-term aged only. Finally, some materials were PAV aged for an extended period of time, and these were compared to the conventional long-term aging times.

Figure 3-3 illustrates the methodology for the first phase of the project. All 16 asphalt binders were RTFOT aged. Following this aging the top performance grades were obtained for each asphalt using the DSR techniques previously described in this chapter. After RTFOT aging, sample Set A was PAV aged for 20 hours at 100 ºC. The bottom grade and 60 ºC viscosity of Set A was then determined. Sample Set A represents the standard Superpave method of binder aging to determine low-temperature physical properties. A second sample set, Set B, was aged in the

environmental room at 60 ºC after RTFOT aging. Periodically, the 60 ºC viscosities of the samples in Set B were obtained using the DSR and were compared to those of Set A. Once the 60 ºC viscosities of Set B were approximately equivalent to those of sample Set A, Set B was removed from the environmental room. Low-temperature properties and performance grades were then determined for both Sets A and B.

In the second phase of the project (Figure 3-4), the conventional testing method (Set A) was compared to material that had been short-term aged only. Set C consists of the short-term aged only samples that were aged by either the RTFOT method or the air-blowing method developed by Vassiliev (2001). Low-temperature properties, 60 ºC viscosities, and bottom grades for Set C were obtained and compared to those of Set A.

Figure 3-5 illustrates phase III of the project. In this phase Set D was made with five asphalts: AAF-1, AAS-1, Exxon AC-10, Exxon AC-20, and Shell AC-20. These asphalts were RTFOT aged and then aged in the PAV for 48 hours at 100 ºC. After aging, their 60 ºC viscosities were determined as well as their low-temperature physical properties and bottom performance grade. These values were compared to those of Set A.

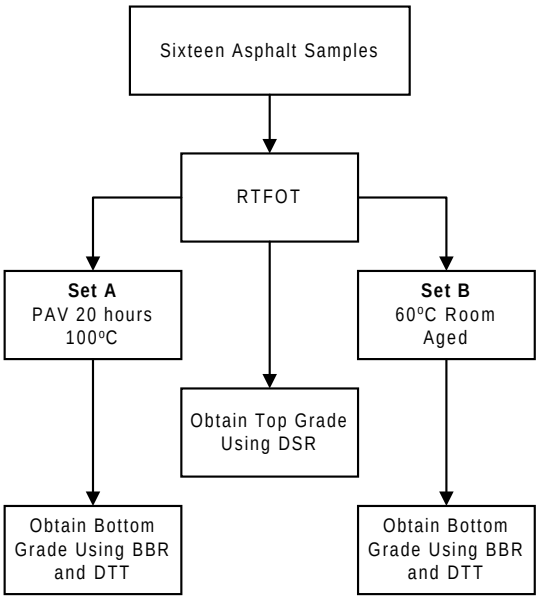

Figure 3-3. Methodology for Comparison of PAV and Environmental Room Aging.

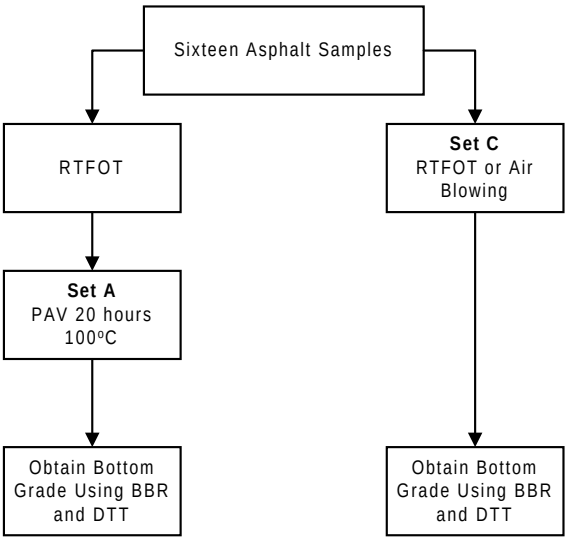

Figure 3-4. Methodology for Comparison of PAV Aged and Short-Term Aged Material.

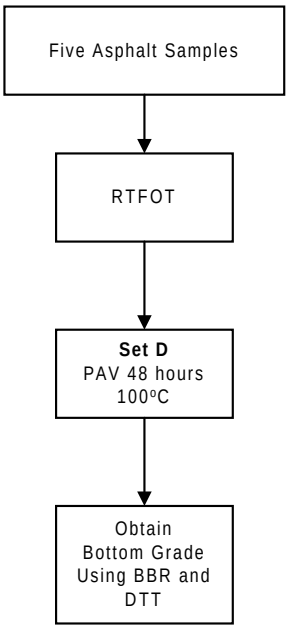

Figure 3-5. Methodology for Obtaining Extended PAV Aging Data.

RESULTS AND DISCUSSION

Phase I Results

As explained in the methodology section, sample Set B, aged in the 60 ºC environmental room was removed from the room when the viscosities of the samples, as a whole, approximately equaled that of the sample Set A values. This criterion was satisfied at an aging time of 38 days in the environmental room. Figure 3-6 shows a comparison between the 60 ºC limiting complex viscosity of unmodified members of sample Sets A and B (Figure 3-3) .

As shown in Figure 3-6, most materials fall on or near the line of equal viscosity. This indicates that an aging time of 38 days in the environmental room results in materials which have approximately equivalent viscosities to those aged in the PAV for 20 hours at 100 ºC. Also in support of this conclusion is the fact that the carbonyl areas for the same samples also show good agreement, as presented in Figure 3-7.

Figure 3-7 does seem to indicate, however, that the carbonyl area for the PAV tends to be higher than that of the environmental room. The only exceptions to this are asphalts AAD-1 and ABM-1, which showed greater carbonyl area increase in the environmental room. According to the work done by Liu (1996) and Domke et al. (1999), the hardening susceptibility of an asphalt is pressure dependent. This would explain why even though the carbonyl area of AAD-1 is quite different for Sets A and B, the viscosities are about equal. Indeed, Domke et al. (1999) showed that the hardening susceptibility for asphalts actually reaches a minimum in the vicinity of 4 atmospheres of oxygen, where the PAV operates. This is supported by Figures 3-6 and 3-7, as they indicate that although the viscosities of both sets are about equal, the carbonyl areas for the PAV tend to be slightly higher. That is, the hardening susceptibility of Set A is lower than that of Set B as a whole, presumably because it is being aged at a higher pressure.

In addition to the unmodified asphalts, modified asphalts of Sets A and B were investigated. Figure 3-8 shows the 60 ºC viscosities of modified asphalts of Sets A and B. As shown, the viscosities of the modified materials indicate good agreement between the PAV and environmental room aging. Modified samples, like the unmodifieds, were removed from the environmental room after 38 days of aging.

At this point it is important to note that the results obtained here, namely the equivalence of 38 days in the environmental room to 20 hours at 100 ºC in the PAV are in disagreement with the results obtained by Domke (1999). Domke showed that environmental room aging of 135 days gave viscosities close to those obtained from 40 hours in the PAV at 100 ºC, seeming to indicate that 20 hours in the PAV would approximate 67.5 days aging in the environmental room. This discrepancy can be easily explained since Domke did not RTFOT the samples before either aging procedure, as has been done in this project. As has been pointed out, the extent of the initial jump region of an asphalt is dependent on pressure, but not on temperature (Liu et al., 1996; Petersen, 1998; Domke et al., 2000). Therefore, since Domke did not RTFOT the

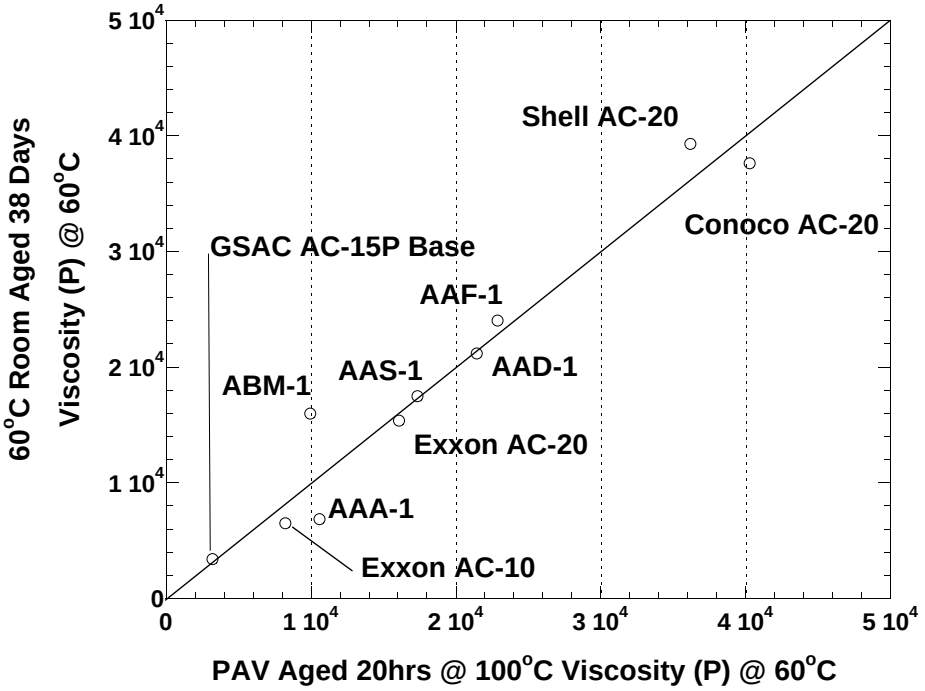

Figure 3-6. Comparison of PAV Aged and 60 ºC Room Aged 60 ºC Viscosity: Unmodified Materials.

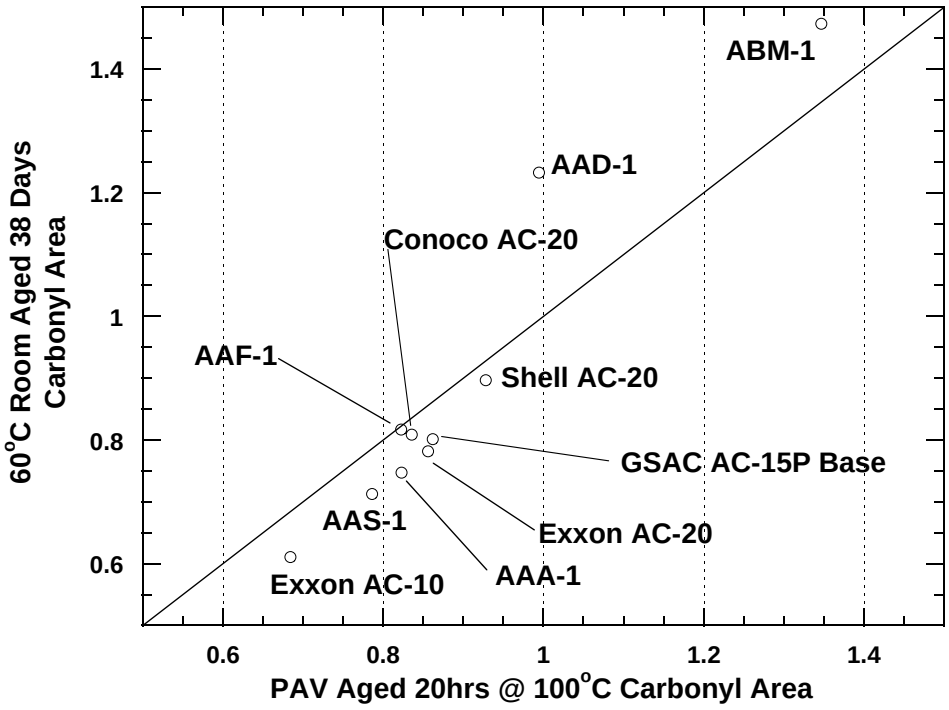

Figure 3-7. Comparison of PAV Aged and 60 ºC Room Aged Carbonyl Area: Unmodified Materials.

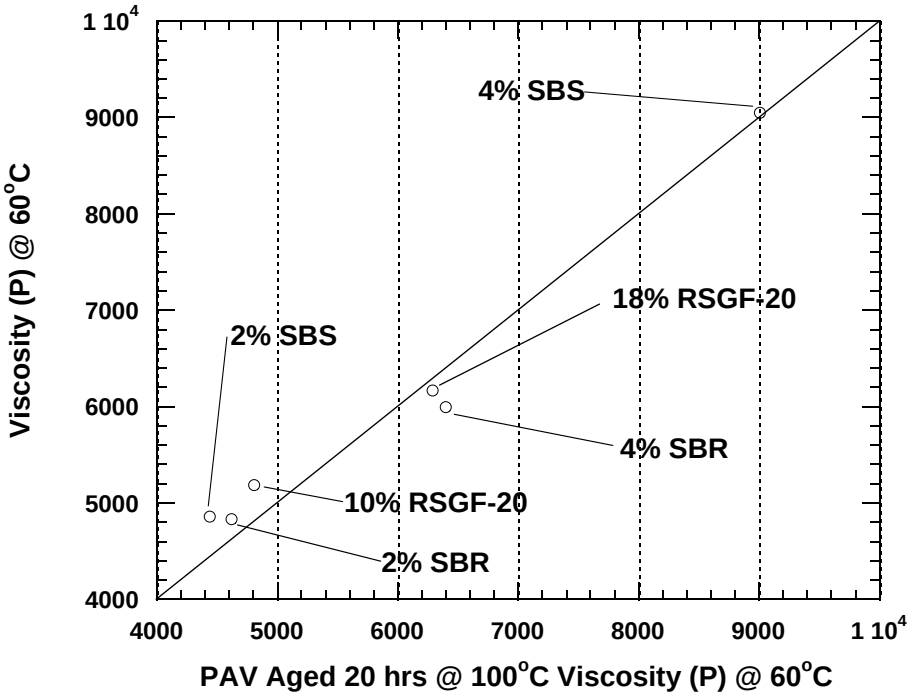

Figure 3-8. Comparison of PAV Aged and 60 ºC Room Aged 60 ºC Viscosity: Modified Material.

materials first, the initial jump regions for the environmental room samples and the PAV samples would naturally be quite different. Additionally, since increasing pressure increases the initial jump, the PAV would have a large head start on the environmental room, so that longer environmental room aging times would be necessary to match the extent of aging seen in the PAV. In this study, the initial jump regions for both sample sets A and B occurred, for the most part, in the RTFOT, so both samples had roughly the same starting point. The added pressure can, however, add to the initial jump. Presumably, each sample was in its constant rate region when long-term environmental room or PAV aging began.

If one assumes that the environmental room accurately simulates road aging during a summer in Texas, the road aging equivalent for the environmental room can be estimated. In this case and as a very rough approximation, the assumption is made that most aging occurs for four months, June through September for 8 hours per day. (A calibration based on field data will improve this calculation.) Then, for 38 days in the environmental room:

$$38\ \text{days(ER)}\ \frac{24\ \text{hours}}{1\ \text{day(ER)}}\ \frac{1\ \text{day(road)}}{8\ \text{hours}}\ \frac{1\ \text{month}}{30\ \text{days}}\ \frac{1\ \text{year(road)}}{4\ \text{months}} \cong 0.95\ \text{years} \qquad (3\text{-}2)$$

This value also applies to PAV aging for 20 hours at 100 ºC, since they have been shown to be approximately equivalent. This result is quite surprising, since the intention of the PAV in the SHRP specifications is to determine whether or not roads will fail in the long term. Clearly, the long-term aging test should simulate several years in service, so the aging time in the PAV may need to be modified.

It is important to note here that although this research is presenting 20 hours in the PAV at 100 ºC as equivalent to 38 days in the 60 ºC environmental room, this does not necessarily mean that multiples of these (e.g. 40 PAV hours and 76 days) are also equivalent. As numerous researchers have shown (Liu, 1996; Domke, 1999; Lunsford, 1994), the constant rate region of asphalt oxidation is dependent upon pressure and temperature conditions. The conditions studied in this work indicate merely an intersection of these two aging conditions with respect to carbonyl area and viscosity. Indeed, upon further aging the materials may not show such equivalence at any other point, not even, as might be expected, at 40 hours in the PAV and 76 days in the environmental room or 10 hours in the PAV and 19 days in the environmental room.

Although sample Sets A and B (Figure 3-3) look similar so far, it was still necessary to determine if their low-temperature properties and SHRP grades were considerably affected by the different aging treatments. In order to accomplish this, the stiffness and m-value for all samples were obtained using the BBR Superpave procedure. These values resulted in a continuous performance grade, wherein the passing temperature of each sample was determined by interpolation or extrapolation of the data. This procedure was repeated with DTT data by averaging the values over the four specimens tested.

Table 3-3 gives the resulting continuous bottom grades for all the asphalts included in this study. Figure 3-9 provides a comparison between sample Sets A and B for the SHRP asphalts tested. The plot shows that the BBR continuous grades for both the PAV aged material and the environmental room aged material are comparable. In fact, all the SHRP asphalts tested vary by less than 1 degree between the two sample sets. DTT data have considerably more variance, varying by as many as 5 degrees for the AAD-1 sample.

Figure 3-10 presents the same bottom continuous grade comparison for the remaining unmodified asphalts. These asphalts also indicate good agreement between the BBR continuous grades of Sets A and B, with the largest variance being for Conoco AC-20 at 1.15 ºC. In addition, the DTT data are also in good agreement, with the largest variance being that of Exxon AC-10, which showed a 4.2 ºC difference between the PAV and environmentally aged material. Considering the fact that the DTT data are notorious for scatter, the results here are well within the experimental error of the DTT equipment.

Table 3-3. Continuous Grade Values for Sample Sets A and B.

Material	PAV BBR Grade (°C)	60 °C Room BBR Grade (°C)	PAV DTT Grade (°C)	60 °C Room DTT Grade (°C)
AAA-1	-33.12	-32.51	-37.48	-35.43
AAD-1	-31.85	-31.14	-30.73	-25.25
AAF-1	-20.05	-19.42	-11.28	-12.90
AAS-1	-29.14	-29.45	-25.20	-21.71
ABM-1	-14.05	-13.67	-15.47	-17.30
Conoco AC-20	-24.60	-25.85	-27.24	-24.39
Exxon AC-10	-30.28	-30.48	-28.12	-32.32
Exxon AC-20	-24.74	-25.10	-24.07	-24.20
GSAC AC-15P Base	-27.61	-27.88	-27.00	-27.79
Shell AC-20	-28.98	-28.15	-25.43	-25.43
GSAC AC-15P w/2% SBR	-28.57	-28.29	-23.56	-25.98
GSAC AC-15P w/4% SBR	-28.95	-28.79	-30.17	-33.49
GSAC AC-15P w/2% SBS	-28.98	-28.15	-32.52	-29.23
GSAC AC-15P w/4% SBS	-28.91	-27.44	-29.66	-34.53
GSAC AC-15P w/10% RSGF-20	-29.30	-28.84	-30.87	-29.63
GSAC AC-15P w/18% RSGF-20	-30.71	-29.61	-36.95	-37.13

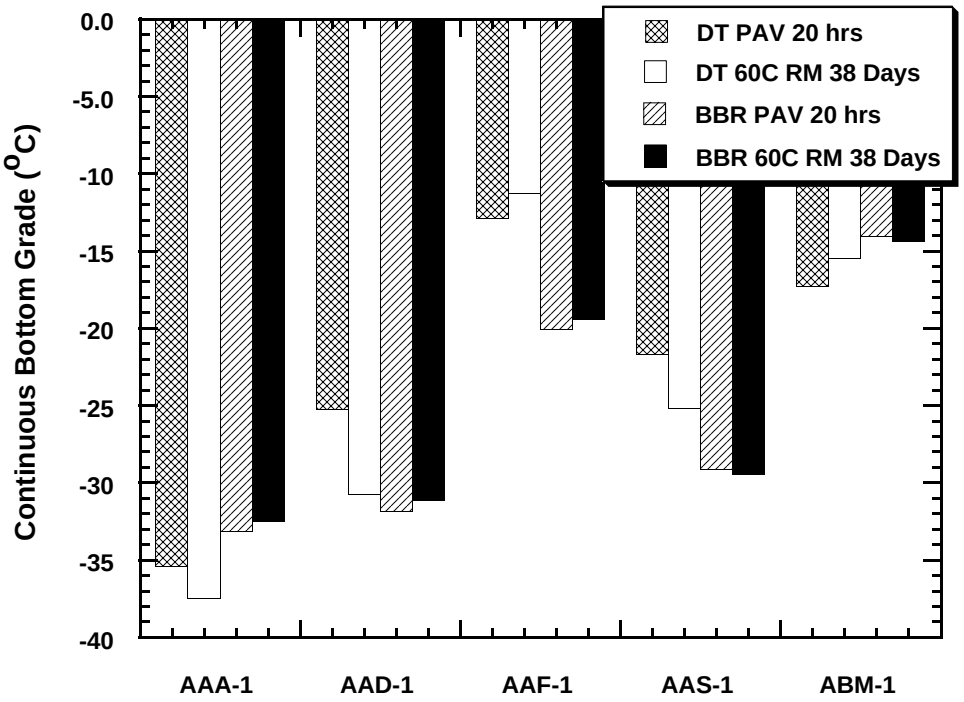

Figure 3-9. Bottom Continuous Grade Comparison for SHRP Asphalts.

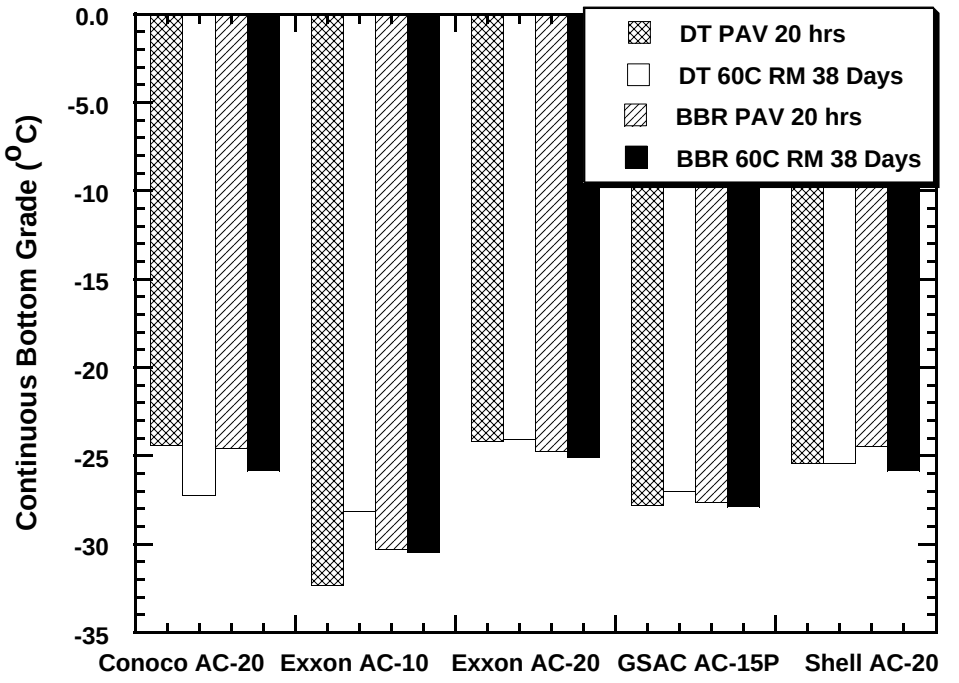

Figure 3-10. Bottom Continuous Grade Comparison for non-SHRP Asphalts.

Low-temperature physical property results for modified materials are presented in Figure 3-11. The modified materials' common base, GSAC AC-15P Base, is also included for comparative purposes. As shown, the BBR data for both Sets A and B are comparable, with the greatest variance being 1.47 °C for 4% SBS. There is considerably more scatter in the DTT data for the modified samples than for the unmodified samples. The reason is unknown.

Also of interest as far as low-temperature properties are concerned, is how the different aging mechanisms may have affected the way the asphalt is graded, particularly on the BBR. Specifically, does one method of aging make the PG limited by the m-value criterion whereas the other is limited by the stiffness criterion? Figure 3-12 presents data for m-value and S for sample Sets A and B. As seen in Figure 3-12 the data occur in pairs, which are the same material with the two different aging procedures. With the exception of data occurring very near the line, no sample seems to have changed from being S dominated or m dominated. As a group, the data show that S typically determines performance grade, rather than m.

As part of the Phase I project, the top performance grade was also obtained for all of the materials studied. Table 3-4 presents these data as well as the low-temperature performance grade obtained by the Superpave specifications for the PAV aged material. These data are intended as a characterization of the materials involved in this research and were not further investigated.

Phase II Results

In Phase II of this project the low-temperature properties for short-term aged samples (Set C) were compared with those of samples aged long term in hope of determining whether or not the long-term aging of a sample could be skipped without loss of accuracy when determining performance grade. As explained in the previous chapter, the same samples were used as in Phase I, and the samples were either RTFOT aged or air-blown according to the procedure developed by Vassiliev (2001). Table 3-5 lists the 60 °C viscosity for all of the unmodified materials and compares them to values obtained by RTFOT in Phase I. Table 3-6 presents the same data for modified materials.

For the most part the air-blowing values are comparable to the RTFOT values, the exceptions being the crumb rubber modified asphalts and AAF-1. In the case of the crumb rubber modified asphalts, the viscosity discrepancy is likely due to the fact that, unlike the RTFOT, the air-blowing apparatus allows the operator to recover most of the rubber in the sample. After RTFO aging of a sample a considerable portion of the rubber settles out during aging and remains stuck in the film of asphalt within the bottle after the test. The increased rubber concentration of the air-blown sample relative to the RTFOT would increase the viscosity while not necessarily increasing the aging of the sample. AAF-1 also seems to be quite different from the previous RTFOT value. This may be an error running the air-blowing apparatus or may simply be an outlying point. In any case, the sample was not rerun because no material was left from the original AAF-1 material used in this study.

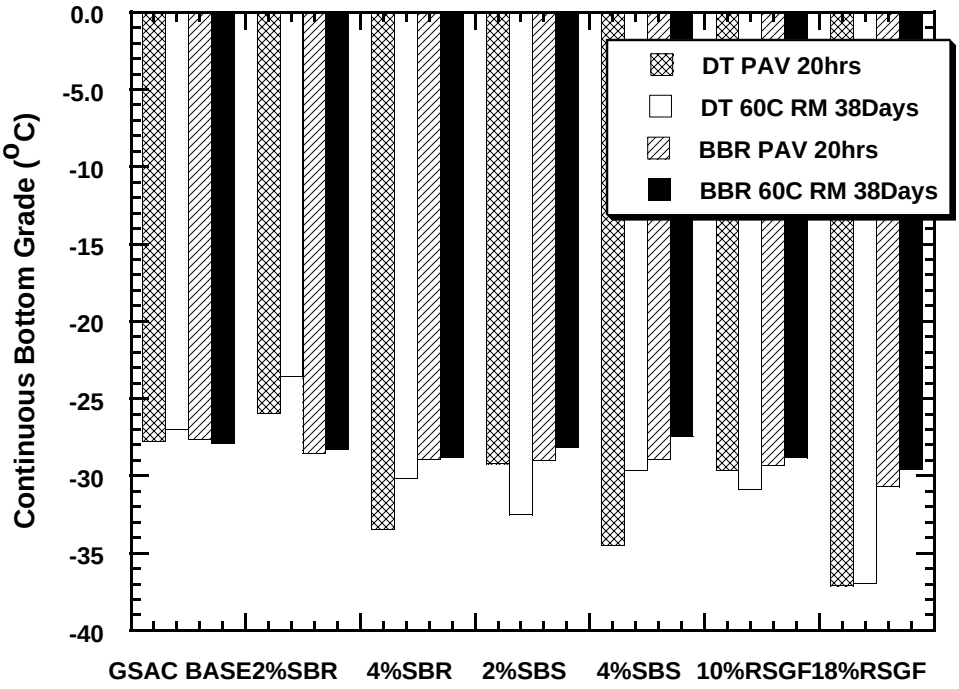

Figure 3-11. Bottom Continuous Grade Comparison for Modified Asphalts.

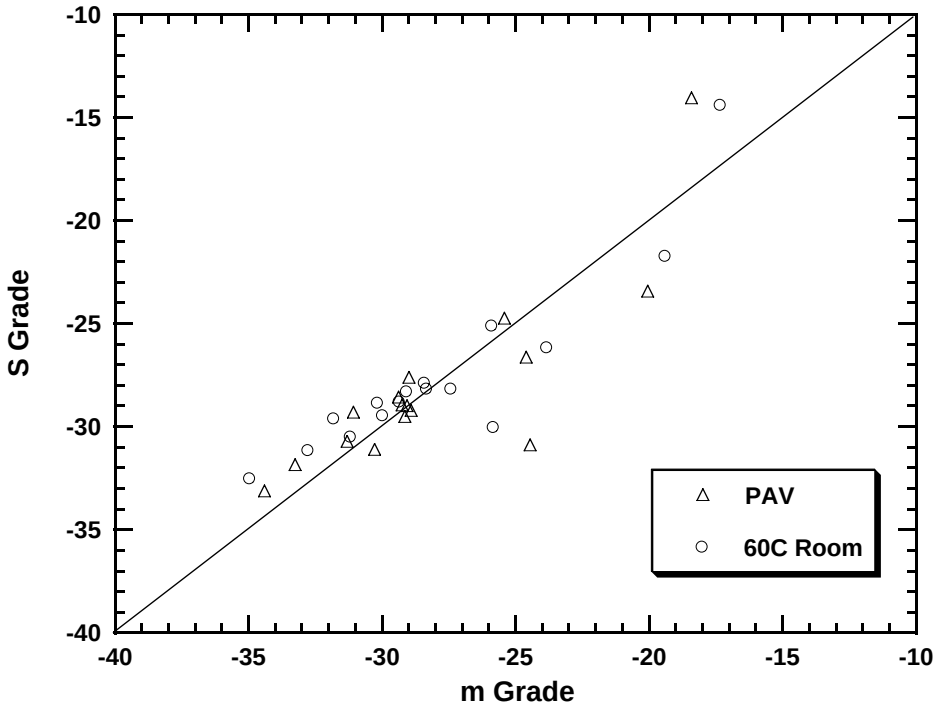

Figure 3-12. Comparison of m and S Continuous Grade for Sample Sets A&B.

Table 3-4. Overall Performance Grades.

Material	Overall PG
AAA-1	58-28
AAD-1	58-28
AAF-1	58-16
AAS-1	64-28
ABM-1	64-10
Conoco AC-20	64-22
Exxon AC-10	58-28
Exxon AC-20	64-22
GSAC AC-15P Base	52-22
Shell AC-20	64-22
GSAC AC-15P w/2% SBR	58-28
GSAC AC-15P w/4% SBR	58-28
GSAC AC-15P w/2% SBS	58-28
GSAC AC-15P w/4% SBS	58-34
GSAC AC-15P w/10% RSGF-20	58-28
GSAC AC-15P w/18% RSGF-20	58-34

Table 3-5. Comparison of 60 ºC Viscosity for Unmodified Materials Used in Phase II with RTFOT Values.

Materials	Method of Short-Term Aging	60 ºC Viscosity of Short-Term Aged Material	RTFOT 60 ºC Viscosity
AAA-1	RTFOT	2092	2177
AAD-1	Air Blown	4555	4341
AAF-1	Air Blown	5713	4723
AAS-1	Air Blown	5217	5012
ABM-1	Air Blown	5251	4937
Conoco AC-20	Air Blown	7016	6756
Exxon AC-10	RTFOT	2246	2007
Exxon AC-20	RTFOT	4630	4714
GSAC AC-15P Base	RTFOT	1266	1420
Shell AC-20	Air Blown	6505	7138

Table 3-6. Comparison of 60 ºC Viscosity for Modified Materials Used in Phase II with RTFOT Values.

Materials	Method of Short-Term Aging	60 ºC Viscosity of Short-Term Aged Material	RTFOT 60 ºC Viscosity
GSAC AC-15P w/2% SBR	RTFOT	2455	2905
GSAC AC-15P w/4% SBR	RTFOT	3651	3689
GSAC AC-15P w/2% SBS	RTFOT	2305	2191
GSAC AC-15P w/4% SBS	RTFOT	4339	4367
GSAC AC-15P w/10% RSGF-20	Air Blowing	2152	3526
GSAC AC-15P w/18% RSGF-20	Air Blowing	2572	3630

One of the first tests performed on the short-term aged samples was the bending beam rheometer determination of the continuous bottom performance grade. Figure 3-13 illustrates this comparison for the SHRP asphalts. It is interesting to note here that although the AAF-1 sample showed a higher viscosity than the RTFOT sample, the continuous bottom grade is still significantly better than the long-term aged samples. For the remainder of the samples, it is apparent that although the short-term aged material has a better grade, the grade is typically only 3 or 4 degrees better.

Figure 3-14 presents BBR data for the non-SHRP unmodified asphalts studied. Again in this plot all of the short-term aged materials provide bottom grades that are better than their long-term aged counterparts. For the three middle asphalts, Exxon AC-10, Exxon AC-20, and GSAC AC-15P Base, the continuous grades of Set C are very close to those of the long-term aged materials. Shell AC-20 and Conoco AC-20, the two asphalts which showed the highest viscosities after aging (Figure 3-6), show a considerably different grade, with Conoco AC-20 being 6.65 degrees different.

BBR data for modified materials are given in Figure 3-15, with the common base, GSAC AC-15P included as well for comparison. As shown, the modified materials behave just as the base material does, showing a better bottom grade for short-term aging, although not dramatically better. This may suggest that in the case of modified asphalts, that long-term aging could be justifiably skipped when obtaining performance grades. While the data clearly indicate that this is true for this case, an alternate conclusion may be appropriate. Rather than suggesting that all modified asphalts can be graded without long-term aging, the data suggest that the modified asphalt mimics the aging characteristics of the base. If, for example, Conoco AC-20 from Figure 3-14 was modified with these same additives, it is likely that the bottom grade difference between the short-term and long-term aged material would be just as significant as for the unmodified Conoco AC-20. Repeating the experiments with other bases and the same modifiers would allow for a more accurate assessment.

In Phase II the continuous bottom grade as obtained by the DTT was also studied for short-term aged materials. Figure 3-16 presents the results of this investigation for unmodified SHRP materials. As with the BBR measurements, all of the short-term aged material demonstrated better performance grades. The DTT data show significant differences for AAD-1, AAF-1, and AAS-1 in terms of variance from the long-term aged values. AAA-1 and ABM-1 short-term bottom grades are similar to their long-term aged counterparts.

Data for non-SHRP materials are presented in Figure 3-17. As with the SHRP materials, all show a better low-temperature PG for the short-term aged material, but some vary more drastically than others. Exxon AC-10, for example, shows a high degree of variance from the long-term aged material while Exxon AC-20 seems to show almost no difference at all.

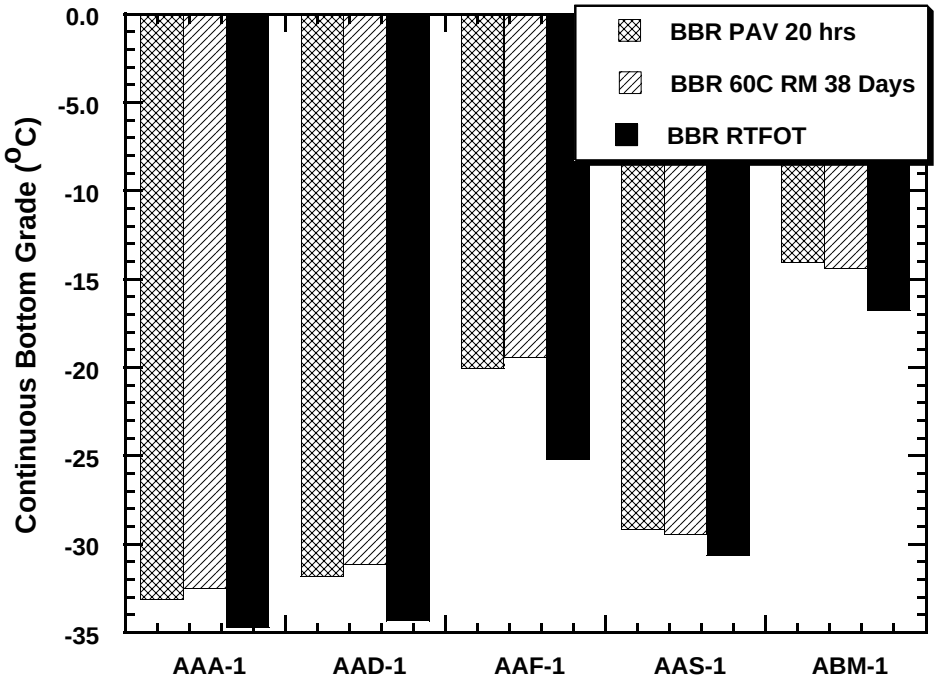

Figure 3-13. Comparison of Continuous Bottom Grade as Measured Using the BBR for Short-Term and Long-Term Aged SHRP Materials.

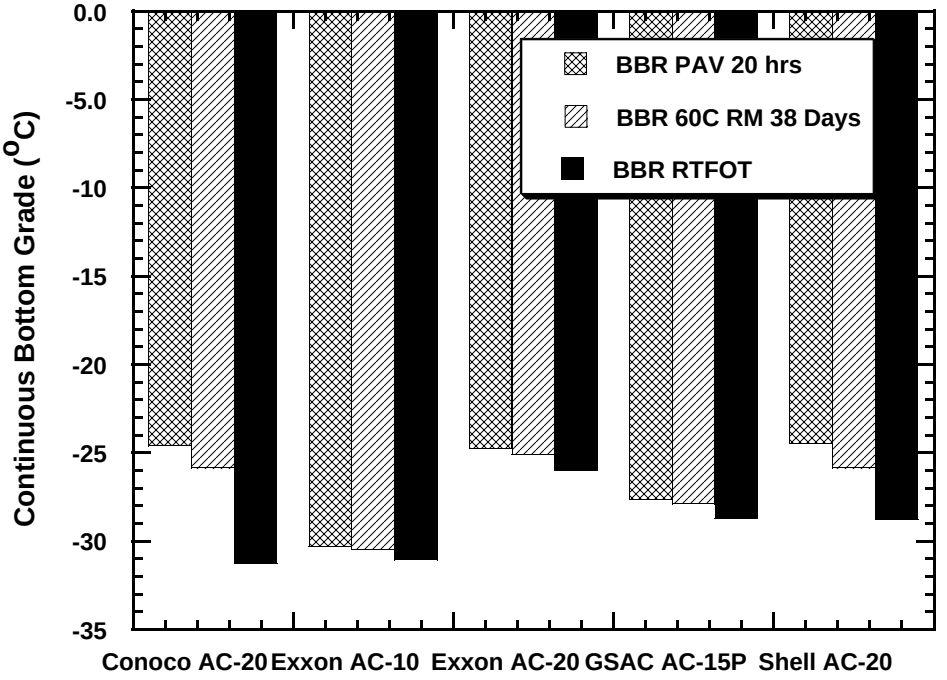

Figure 3-14. Comparison of Continuous Bottom Grade as Measured Using the BBR for Short-Term and Long-Term Aged Non-SHRP Materials.

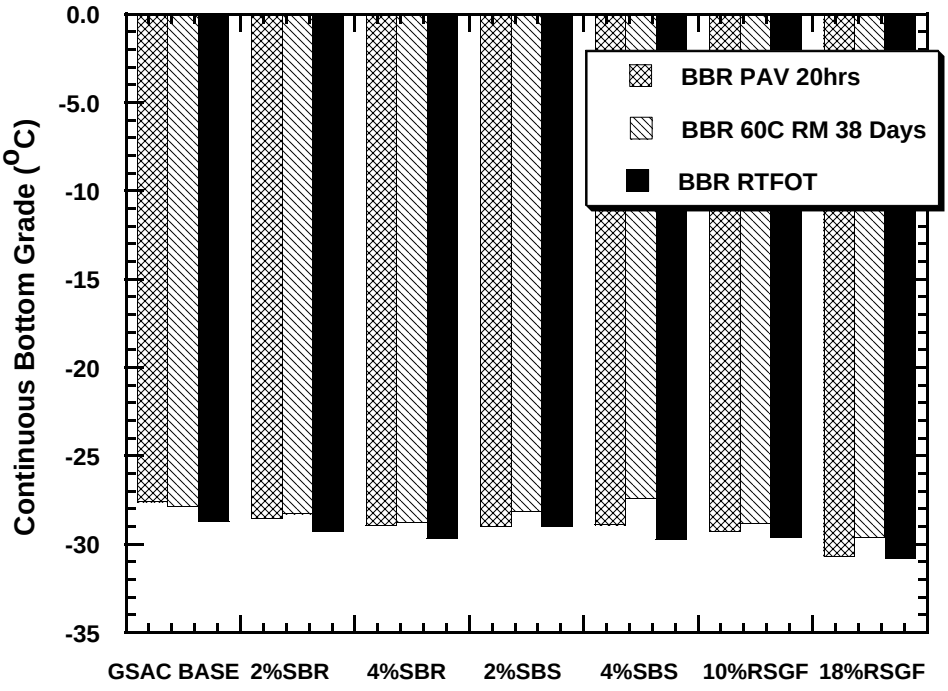

Figure 3-15. Comparison of Continuous Bottom Grade as Measured Using the BBR for Short-Term and Long-Term Aged Modified Materials.

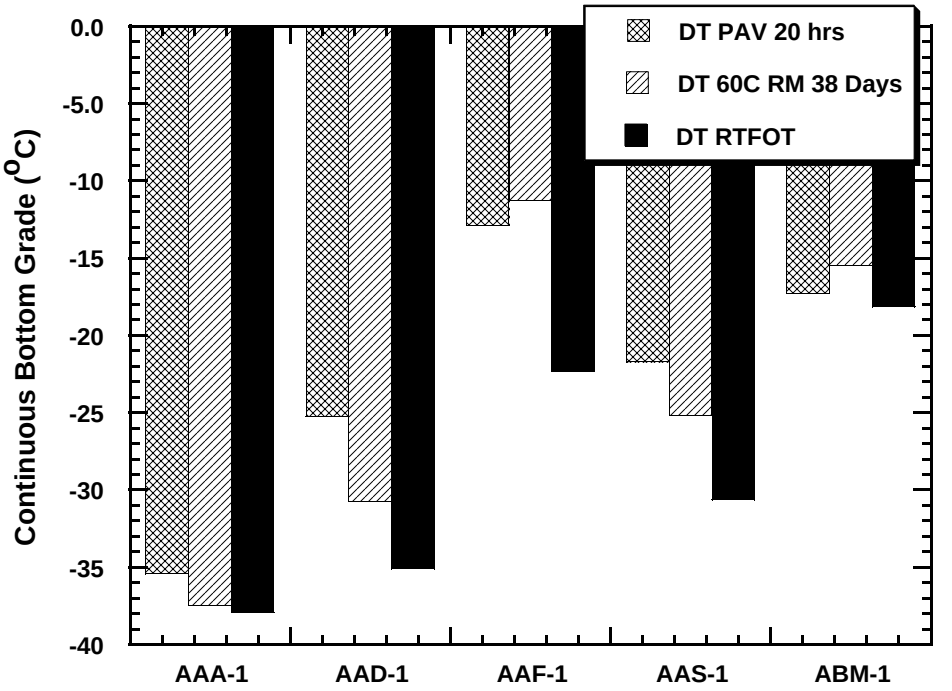

Figure 3-16. Comparison of Continuous Bottom Grade Measured Using the DTT for Short-Term and Long-Term Aged SHRP Materials.

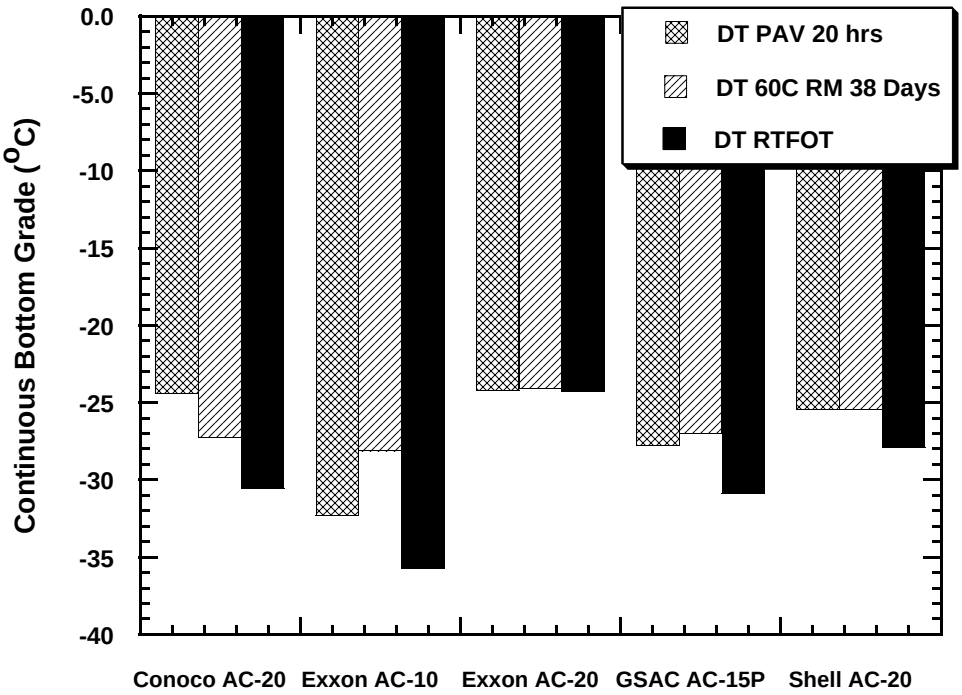

Figure 3-17. Comparison of Continuous Bottom Grade Measured Using the DTT for Short-Term and Long-Term Aged non-SHRP Materials.

DTT data for modified materials are presented in Figure 3-18. Again, this plot indicates that the modified materials behave in a similar fashion to the base material. For most of these materials, a significant difference is seen between the long-term and short-term aged materials.

A summary of the results of Phase II is presented in Figures 3-19, 3-20, and 3-21. These plots are included to enable comparison between the DTT and BBR continuous bottom grades. For the unmodified materials, the scatter in the DTT data makes it difficult to come to solid conclusions regarding the performance of the DTT data versus the BBR. For modified materials it seems that the DTT data typically give a better performance grade and therefore should be run for all modified materials.

It is also instructive to determine whether or not a correction for low-temperature performance grade can be determined by another parameter that would enable one to skip the long-term aging test. In order to do this it would be beneficial to find a parameter that may be measured while obtaining the top grade of the material. Figure 3-22 shows the difference between the PG of the PAV long-term aged set (PG_{LT}) and the PG of the short-term aged set (PG_{ST}) as measured on the BBR, as a function of the unaged viscosity of the material (Table 3-1). As can be seen from the plot, all of the softer asphalts show little difference between long-term and short-term performance grades. Harder asphalts tend to show more difference, but in some cases, such as AAS-1 and Exxon AC-20, the harder asphalts are still within 2 degrees of the

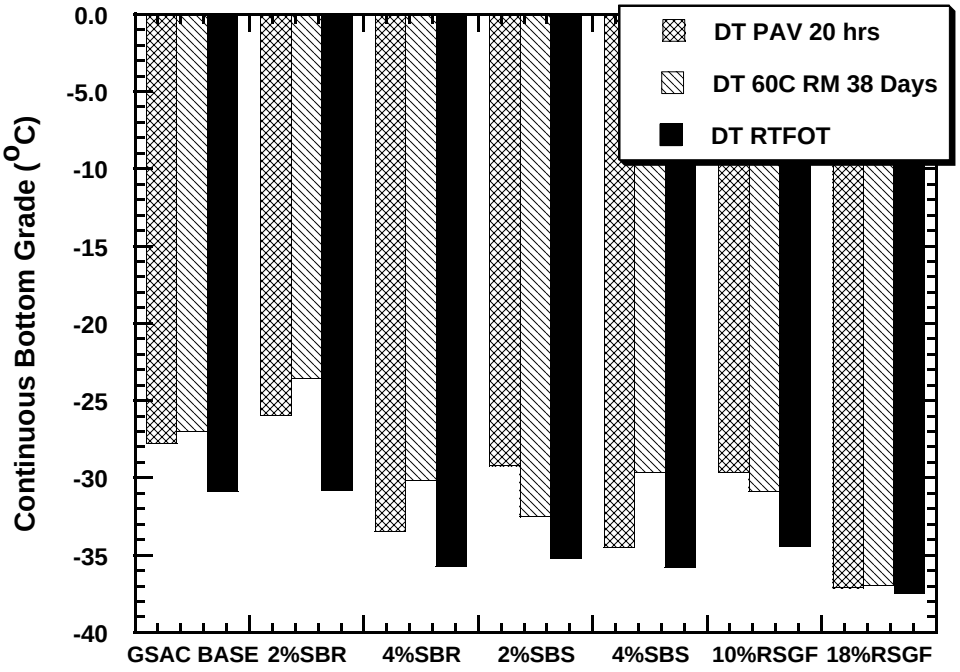

Figure 3-18. Comparison of Continuous Bottom Grade as Measured Using the DTT for Short-Term and Long-Term Aged Modified Materials.

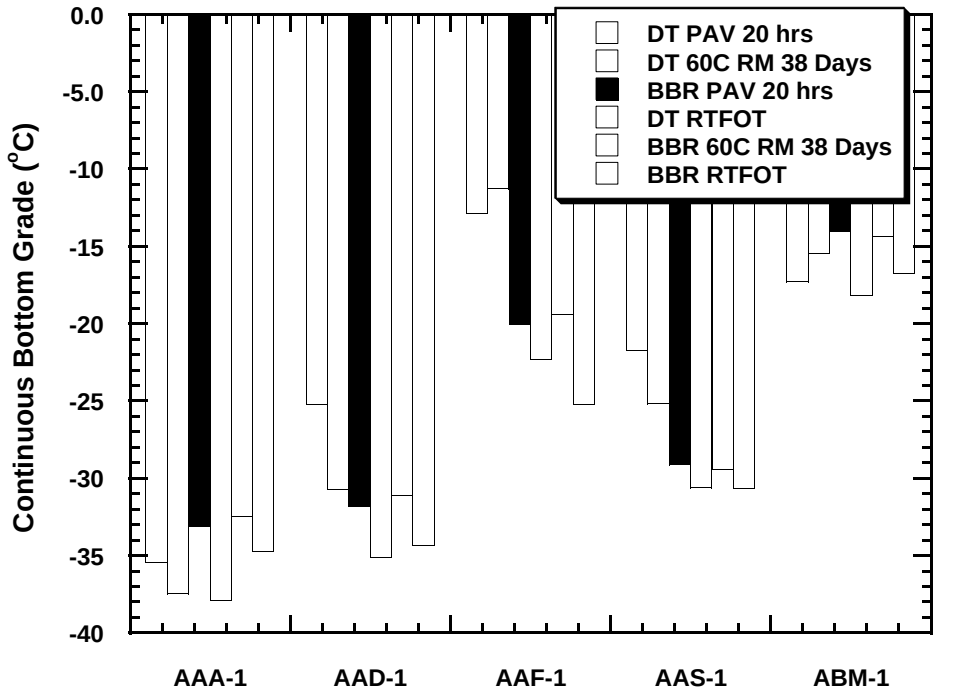

Figure 3-19. Comparison of Continuous Bottom Grade for Short-Term and Long-Term Aged SHRP Materials.

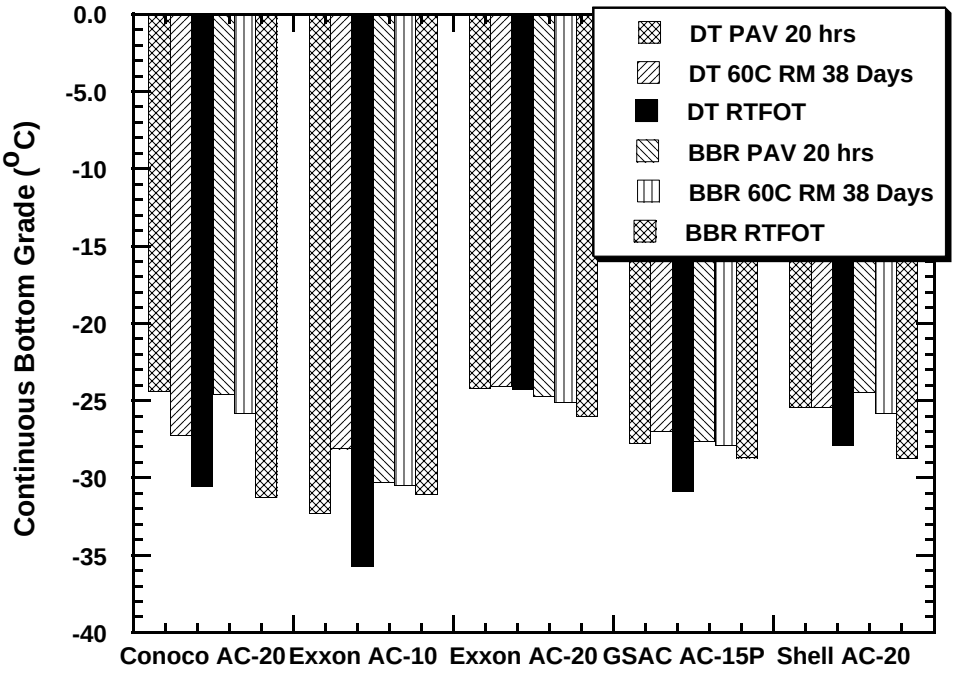

Figure 3-20. Comparison of Continuous Bottom Grade for Short-Term and Long-Term Aged non-SHRP Materials.

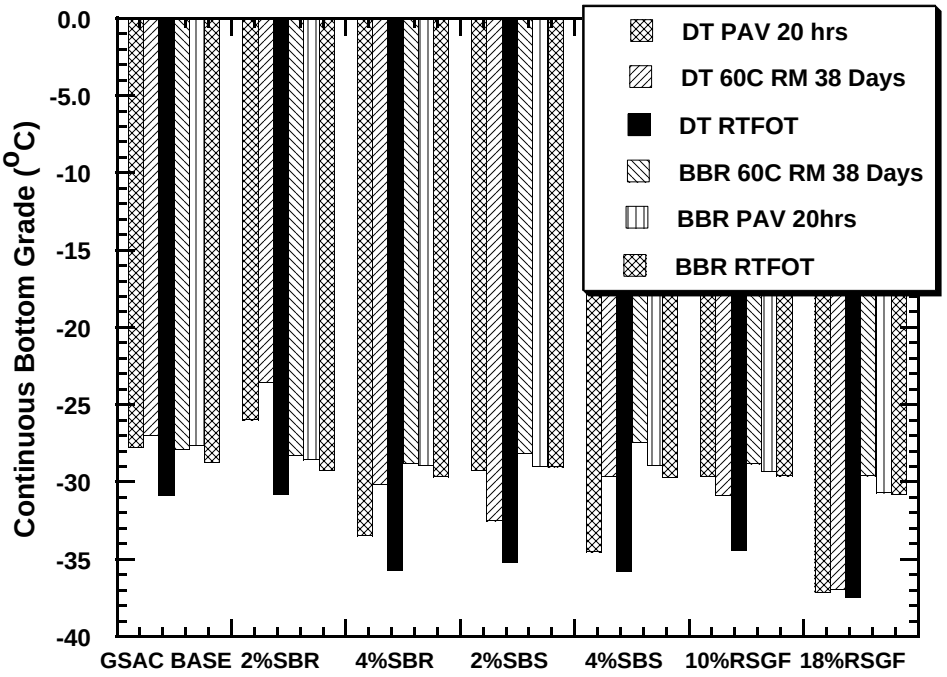

Figure 3-21. Comparison of Continuous Bottom Grade for Short-Term and Long-Term Aged Modified Materials.

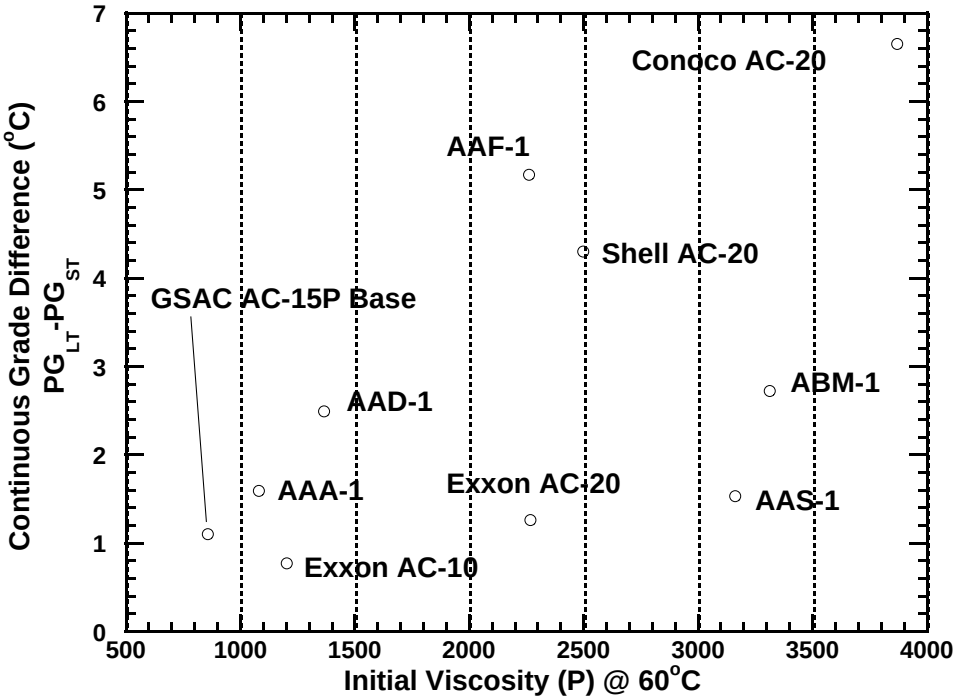

Figure 3-22. Bottom Continuous Performance Grade Difference between PAV Long-Term Aged Material and Short-Term Aged Material as a Function of Initial Viscosity.

long-term aged bottom grade. It is also interesting to note that all the asphalts studied provided grade differences of less than 7 degrees.

Figure 3-23 shows the correlation between the continuous bottom grade difference and $G^*/\sin(\delta)$ at 58 °C for the RTFOT aged material, a parameter measured to obtain the top performance grade of a material. As shown in Figure 3-23, an exponential relationship fits the data rather well. It seems that a $G^*/\sin(\delta)$ value of less than 6000 Pa would allow one to skip the long-term aging test and obtain the bottom grade on the RTFOT aged material only without gross error. This procedure is only recommended if time cannot be spared for the long-term test. The operator may also wish to performance grade the short-term aged material and simply add the given correction function value to the obtained grade. From the plot, the correction factor is obtained using the following equation:

$$C = 0.6225 \exp\left(0.0002095 G^*/\sin(\delta)\right) \quad (3\text{-}3)$$

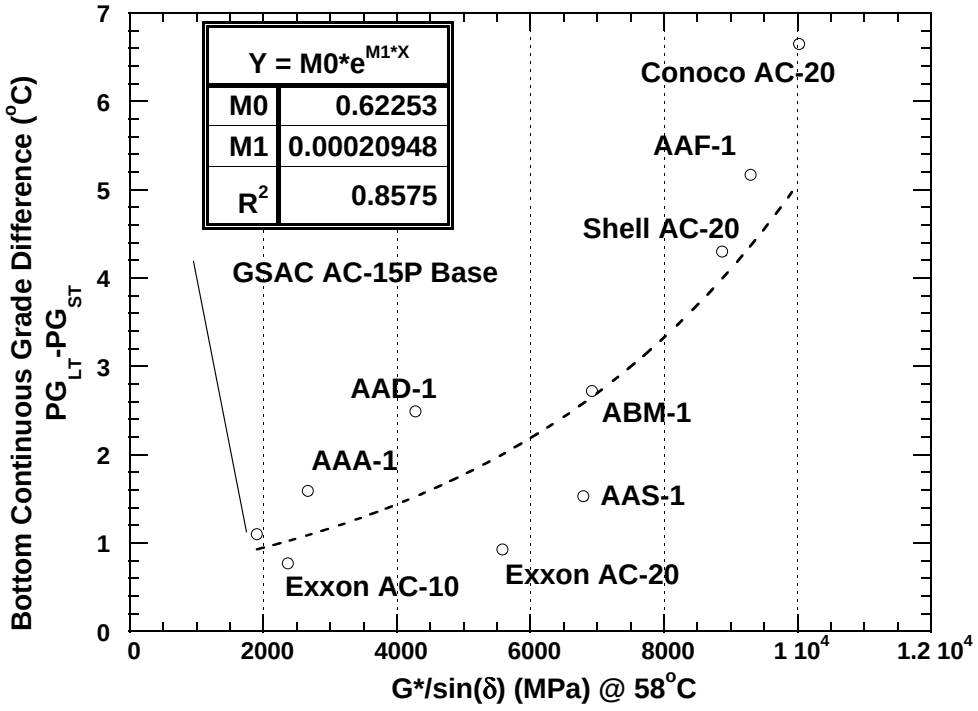

Figure 3-23. Bottom Continuous Performance Grade Difference between PAV Long-term Aged Material and Short-Term Aged Material as a Function of $G^*/\sin(\delta)$ at 58 °C and 10 rad/s.

Where $G^*/\sin(\delta)$ is measured at 58 °C and 10 rad/s on the RTFOT aged material. The low-temperature PG for the long-term aged material can be estimated from the short-term aged PG using the correction factor:

$$PG_{LT} = PG_{ST} + C \qquad (3\text{-}4)$$

Table 3-7 lists the measured low-temperature performance grades for the long-term aged materials as well as those estimated from the short-term aged materials using the correction factor. The absolute error is always within ±1.6 °C. More importantly, in all cases the estimated PG value is identical to the measured PG value, indicating that despite errors the estimation method can produce accurate low-temperature PG values. The convenience of this estimation method should not overshadow the fact that it is a rough correlation and is not intended to replace the proper SHRP specification method, which calls for long-term aging of material before low-temperature performance grading.

Table 3-7. Comparison between Estimated and Experimental PAV Bottom Performance Grades.

Material	$\frac{G}{\sin(\delta)}$	RTFO Grade (°C)	PAV Grade (°C)	PAV Grade Estimate (°C)	Error (°C)	% Error	PAV PG (°C)	Est'd PAV PG (°C)
AAA-1	2665.3	-34.71	-33.12	-33.62	0.502	-1.52%	-28	-28
AAD-1	4276.8	-34.34	-31.85	-32.82	0.965	-3.03%	-28	-28
AAF-1	9298.2	-25.22	-20.05	-20.85	0.804	-4.01%	-16	-16
AAS-1	6793.2	-30.67	-29.14	-28.09	-1.053	3.61%	-28	-28
ABM-1	6920.3	-16.77	-14.05	-14.12	0.067	-0.48%	-10	-10
Conoco AC-20	10024	-31.25	-24.6	-26.17	1.567	-6.37%	-22	-22
Exxon AC-10	2365.9	-31.05	-30.28	-30.03	-0.252	0.83%	-28	-28
Exxon AC-20	5581.9	-25.664	-24.74	-23.66	-1.080	4.37%	-22	-22
GSAC AC-15P	1901.6	-28.71	-27.61	-27.78	0.173	-0.63%	-22	-22
Shell AC-20	8870.4	-28.75	-24.45	-24.76	0.308	-1.26%	-22	-22

Phase III Results

As mentioned in the methodology section, five asphalts were aged for extended periods to determine the effect of extended aging on relative ranking of asphalts. The five asphalts studied were Exxon AC-10, Exxon AC-20, Shell AC-20, AAF-1, and AAS-1. This section presents data relating to performance grade changes with aging time, as well as changes in m-value and stiffness with aging. The section concludes with a discussion of how the m and S criteria determine performance grade for a variety of aging times.

Figure 3-24 depicts the bottom grade of each sample as a function of aging time. Zero aging time in the figure represents the continuous bottom grade of the RTFOT aged sample. As can be seen in the figure the relative rankings of asphalts do change with aging time. The Exxon AC-20 sample and the Shell AC-20 sample provide the best illustration of this phenomenon.

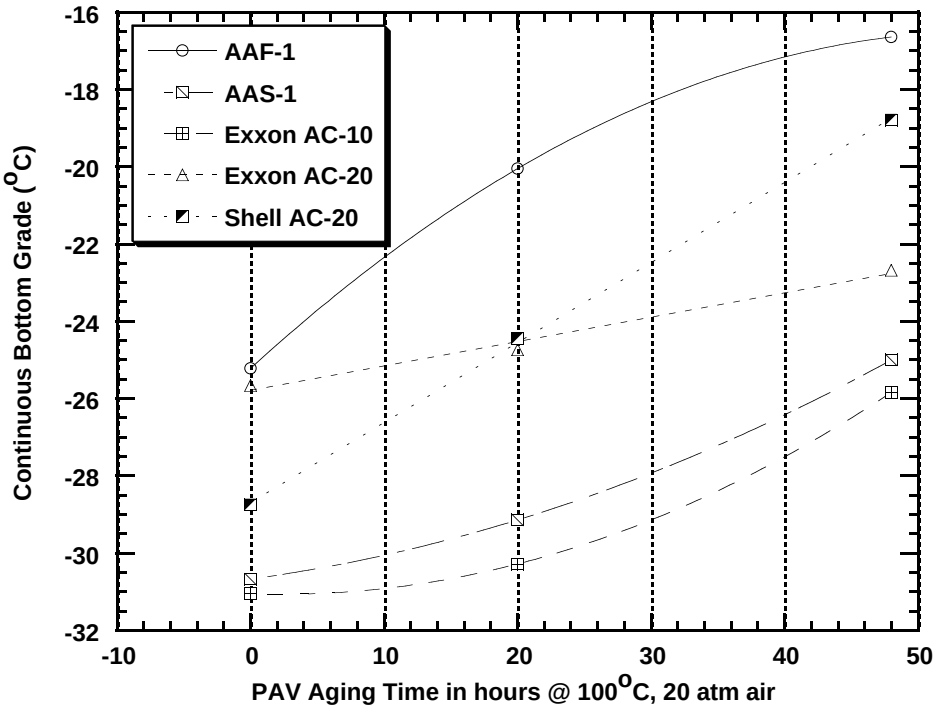

Figure 3-24. Continuous Bottom Grade as a Function of PAV Aging Time.

Before PAV aging Shell AC-20 shows a continuous bottom grade that is about 2 degrees lower than that of Exxon AC-20. After 20 hours of PAV aging, the grades are very similar, both being around −24.5 ºC. After 48 hours of PAV aging, Exxon AC-20 displays a better bottom grade by about 4 ºC.

From Figure 3-24, one may conclude that the relative ranking of asphalts will change depending upon the specified aging time. This indicates that the Superpave long-term aging specifications result in an arbitrary ranking of asphalts with respect to low-temperature properties. Figure 3-24 clearly shows that the low-temperature physical properties of Exxon AC-20 are much less affected by aging than those of Shell AC-20. Exxon AC-20 therefore is more resistant to the effects of aging on low-temperature properties, but, from the current Superpave specification, they would be given identical low-temperature grades.

Agreeing with the work of Domke (1999), Figures 3-25 through 3-28 depict how stiffness and m-value change as a function of aging time. The line in each figure indicates the Superpave specification; the sample must have an m-value greater than 0.300 and a stiffness of less than 300 MPa. Figure 3-25 shows that, for AAF-1, the m-value decreases steadily with aging time. Stiffness, as shown in Figure 3-26, increases with increased aging time. Figures 3-27 and 3-28 depict the variation of m-value and stiffness for Exxon AC-20.

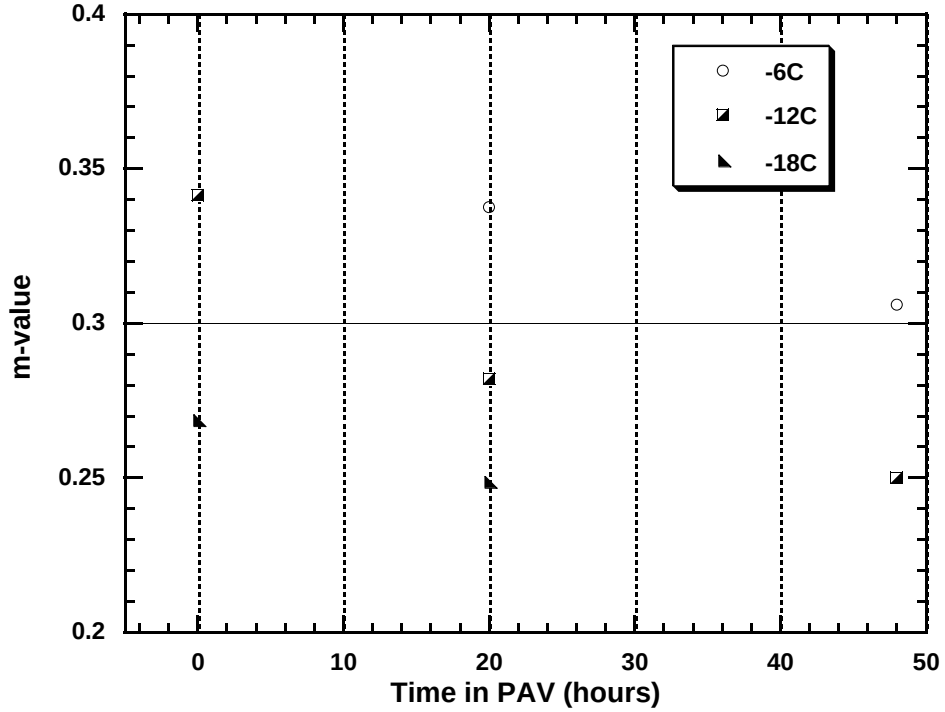

Figure 3-25. m-Value as a Function of Aging Time for AAF-1.

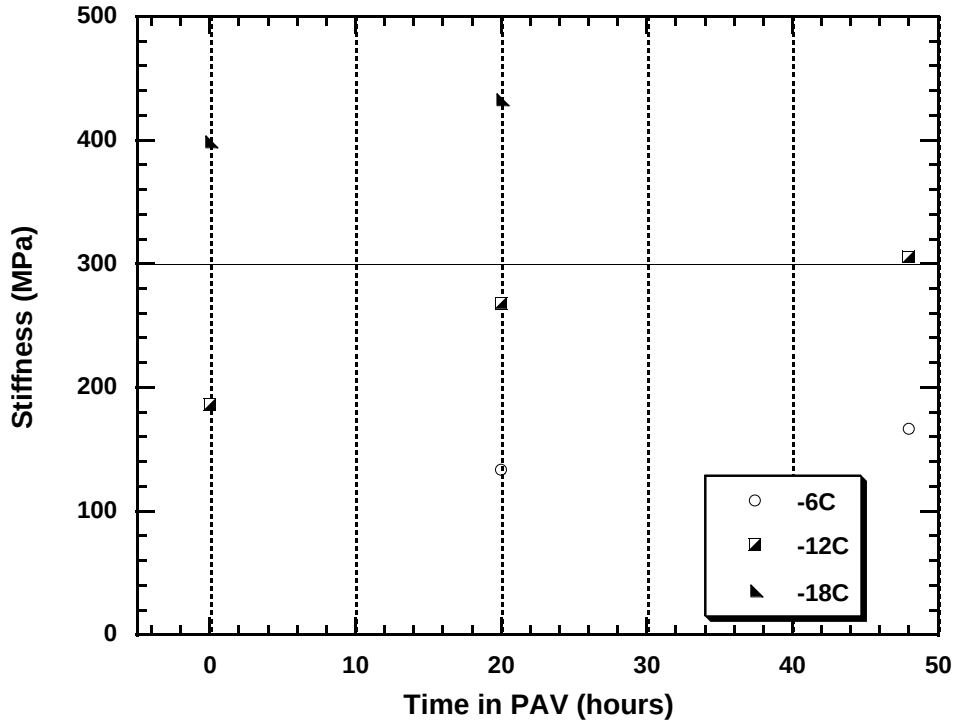

Figure 3-26. Stiffness as a Function of Aging Time for AAF-1.

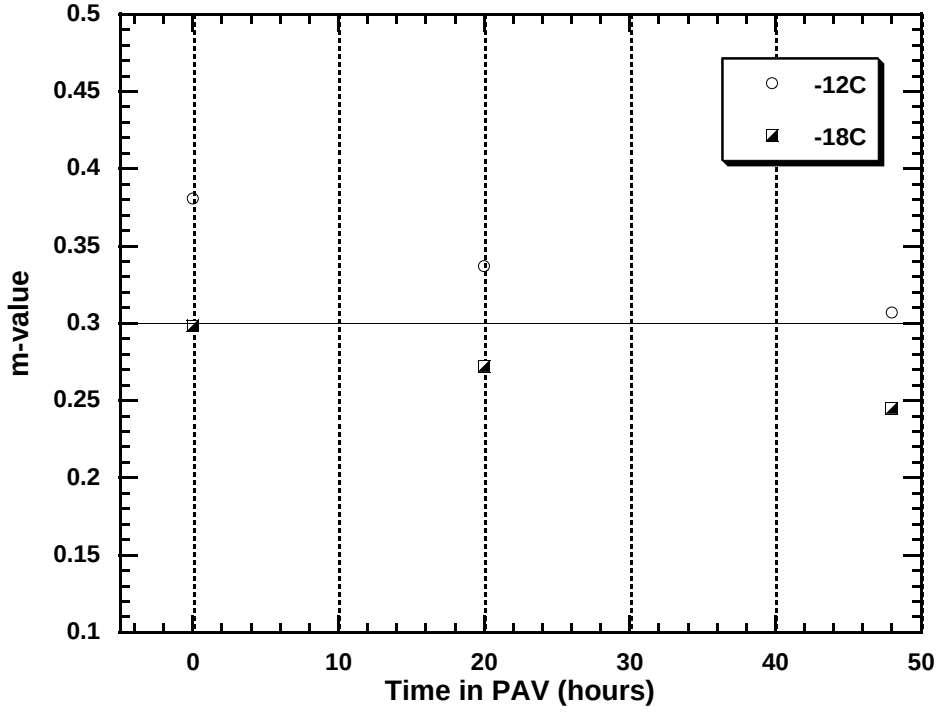

Figure 3-27. m-Value as a Function of Aging Time for Exxon AC-20.

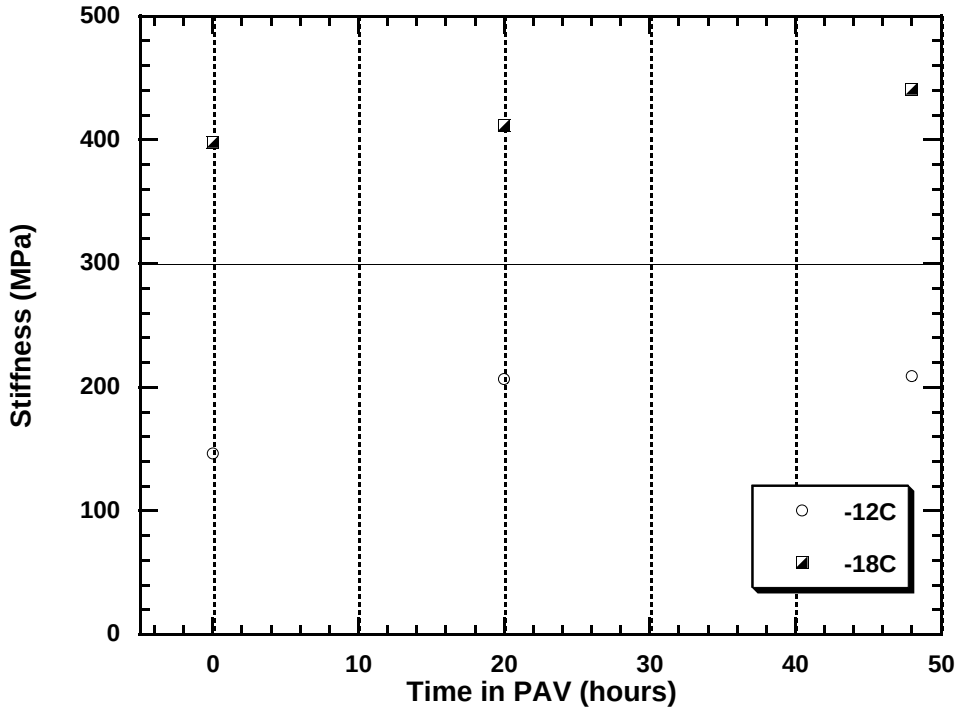

Figure 3-28. Stiffness as a Function of Aging Time for Exxon AC-20.

Another interesting result of this work is that, since the Superpave specification has two requirements which must be satisfied, the bottom PG of an asphalt is determined predominantly by stiffness at shorter aging times and m-value at longer aging times. Figure 3-29 shows that a performance grade obtained for short-term aged material is dictated by the stiffness criterion. In contrast, material aged for 48 hours in the PAV was limited by the m-value criterion. Materials aged for 20 hours in the PAV, like materials aged 38 days in the 60 °C room may be limited by either criterion, depending upon the material. Since the clutter in Figure 3-29 makes it hard to determine the change in grading for a specific asphalt, Figure 3-30 has been included. This plot depicts the change in m grade and S grade for two asphalts, AAS-1 and Exxon AC-20. As shown in Figure 3-30, the grades move linearly with aging from being limited by stiffness at short aging times, to being limited by m-value at longer aging times.

Air Blowing as a Long-Term Aging Test

Another objective of this research was to determine if a suitable long-term aging test could be developed by air-blowing asphalt. It was hypothesized that the kinetics involved in air-blowing would match those of road conditions more closely because air-blowing is carried out at atmospheric pressure. The air-blowing procedure used was described in the aging procedures section. Infrared spectroscopy and GPC were used to analyze the resulting samples to determine if they were comparable in carbonyl area and molecular weight to those obtained from 60 °C room aging and PAV aging. Ideally, an air-blowing procedure would produce viscosities, carbonyl areas and GPC results similar to those of the 60 °C room. In this project an attempt was made to find a time at which air-blowing produced carbonyl areas and viscosities similar to those obtained from RTFOT and 38 days aging in the 60 °C room. The air-blown samples were short-term aged before being air-blown for extended periods of time.

Of the asphalts used in the first three phases of this project, Exxon AC-10, Exxon AC-20 and Shell AC-20 were all air-blown for 20 hours following the short-term air-blowing procedure. Figure 3-31 depicts the carbonyl region of the Fourier transform infrared (FTIR) spectrum of Shell AC-20 for the various aging methods used. Viscosities are included in the legend for comparison. As shown, the viscosity produced by air-blowing the sample was similar to that obtained in the environmental room. The carbonyl areas, however, were quite different. This difference may indicate that a different oxidation mechanism is at work for the air-blowing procedure.

Figure 3-32 provides the FTIR spectra for Exxon AC-10 in the carbonyl region. As shown for this asphalt the carbonyl area of the air-blown sample agrees quite well with that of the 60° C room, but the viscosity obtained is still considerably different, and no better than that obtained from the PAV. Figure 3-33 shows the FTIR spectra for Exxon AC-20. As with Shell AC-20, the viscosity obtained is similar to that of the environmental room, but the carbonyl area is significantly lower.

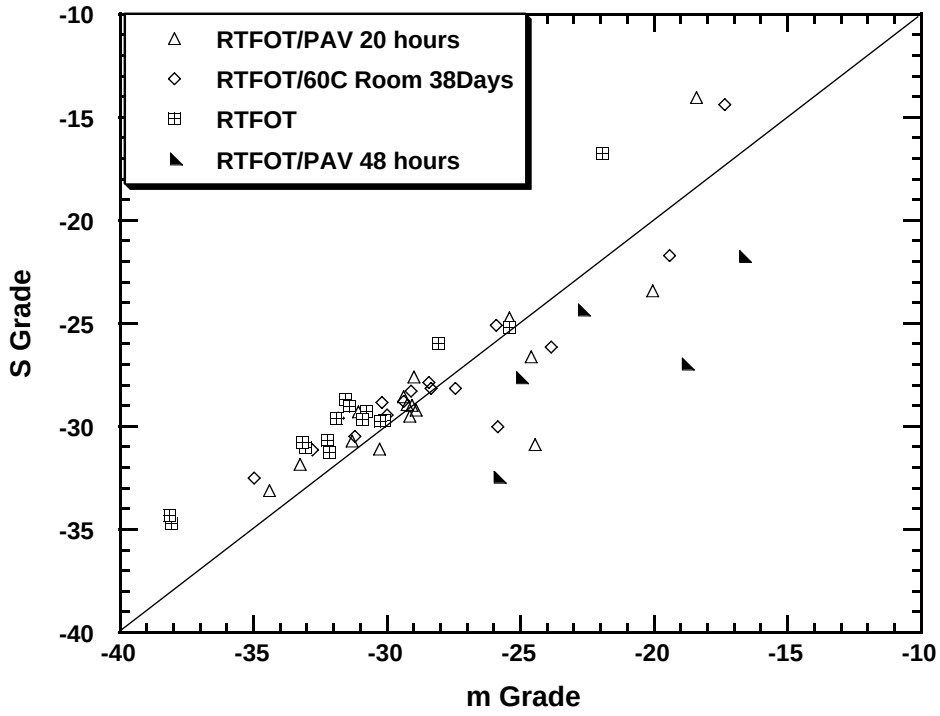

Figure 3-29. Comparison of m-Value Grade and S Grade for Materials at Various Aging Times.

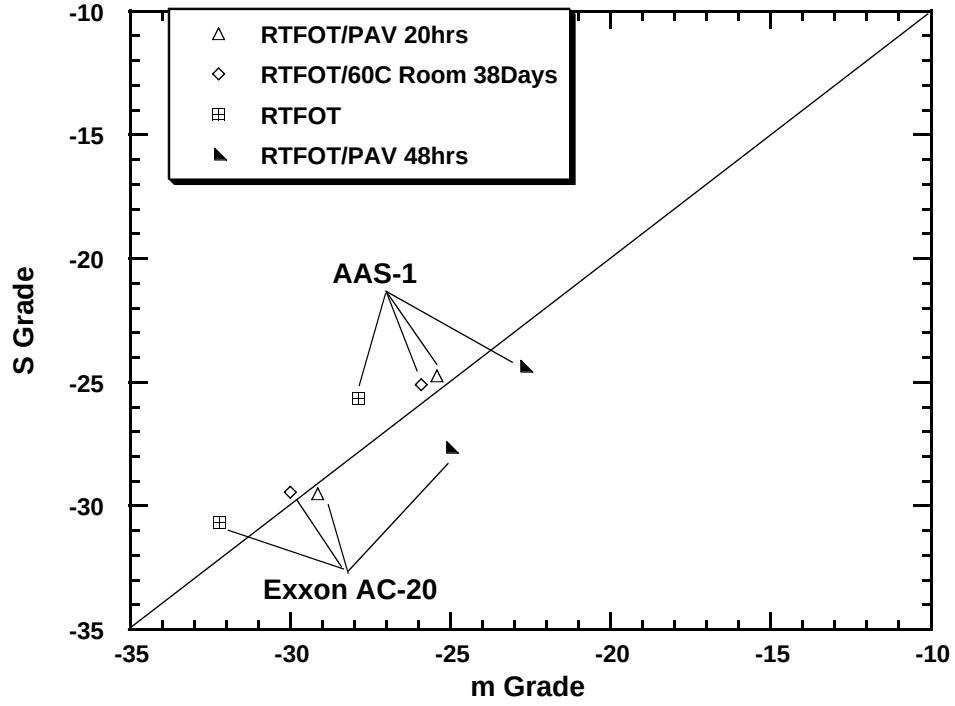

Figure 3-30. Comparison of m-Value Grade and S Grade for AAS-1 and Exxon AC-20 at Various Aging Times.

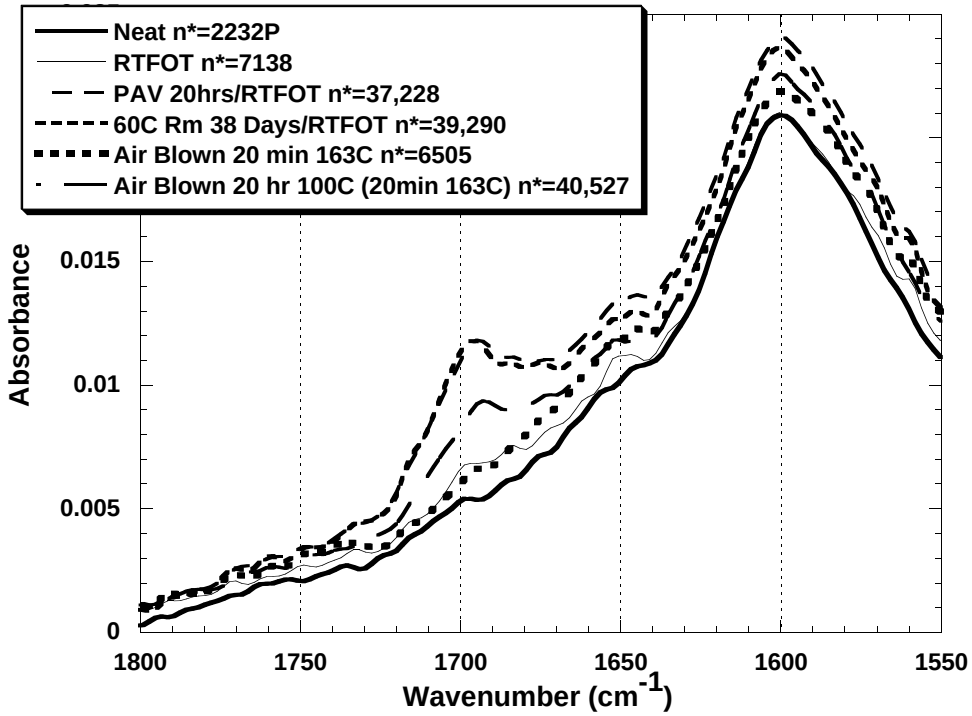

Figure 3-31. FTIR Spectra for Shell AC-20 for Various Aging Procedures.

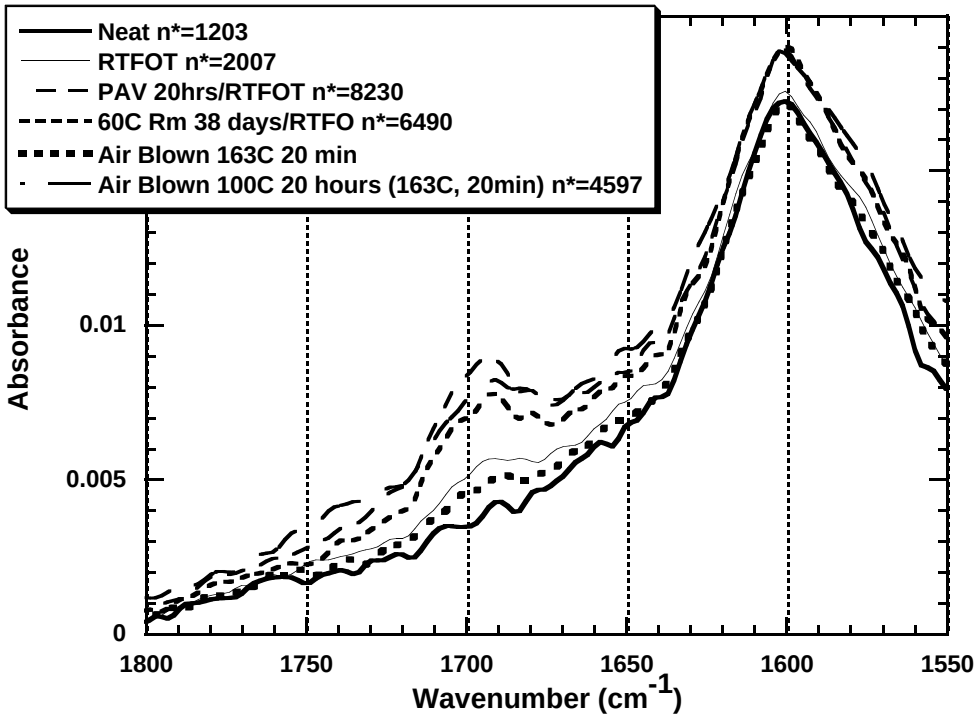

Figure 3-32. FTIR Spectra for Exxon AC-10 for Various Aging Procedures.

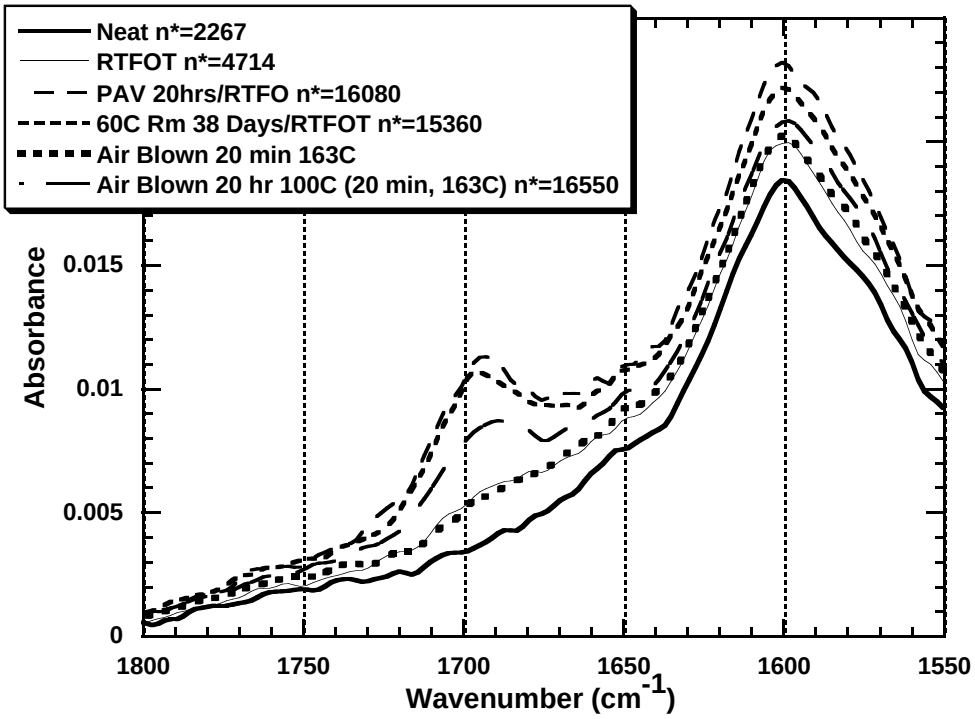

Figure 3-33. FTIR Spectra for Exxon AC-20 for Various Aging Procedures.

Several other asphalts were air-blown at various times and compared with RTFOT and 20 hour PAV aged material. As discussed in the results of Phase I, the PAV results should be similar to those obtained in the environmental room. Figure 3-34 shows that air blowing at 20 hours gives good agreement with PAV aged material both in viscosity and carbonyl area for AAS-1. Figure 3-35 indicates good agreement as well, but for an air-blowing time of 30 hours rather than 20 hours.

Since the air-blowing was taking place at elevated temperatures and high air flow rates, it was thought possible that volatilization and not oxidation was accounting for some of the viscosity increase in the samples. This would also explain why, in the cases of Exxon AC-20 and Shell AC-20, a similar viscosity was reached upon air-blowing, but a much lower carbonyl area was observed. In order to determine if this was the case, the Shell AC-20 samples were analyzed by GPC. The GPC results are presented in Figure 3-36. As shown, the air-blown sample shows asphaltene growth similar to that of the environmental room and the PAV. Also, the sample does not show significant differences in the lower molecular weight (higher time) region. Therefore, volatilization is not likely to be significantly affecting the viscosity increase.

Upon examining the data obtained by long-term air blowing of the samples, it was concluded that air-blowing is not a suitable long-term test. Air blowing did not provide carbonyl area data which were consistently in line with data obtained from the environmental room.

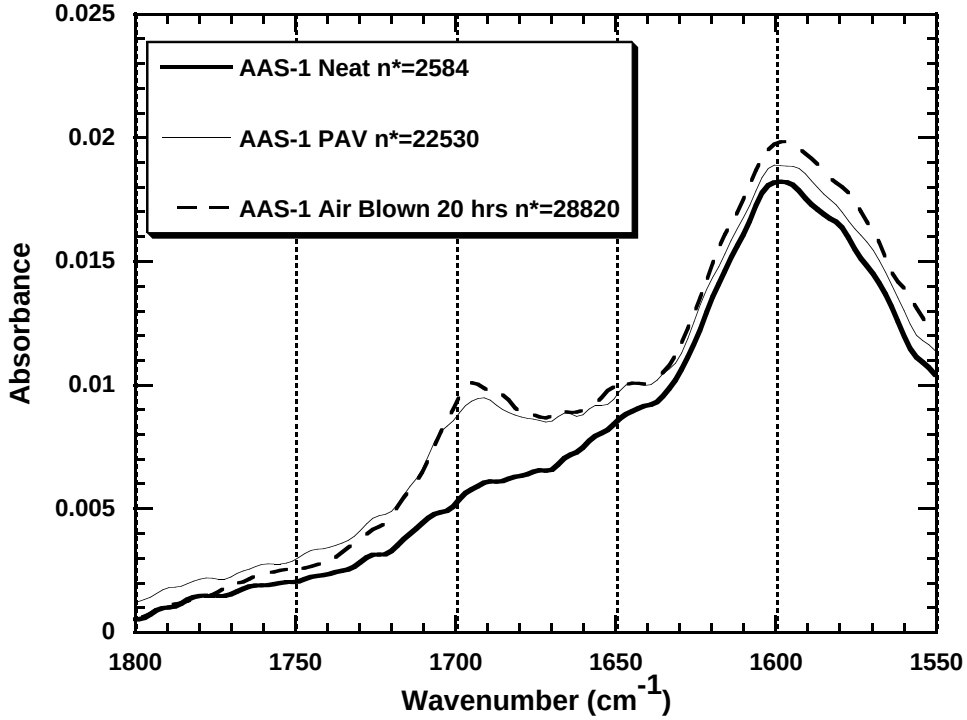

Figure 3-34. FTIR Spectra for AAS-1 for Various Aging Procedures.

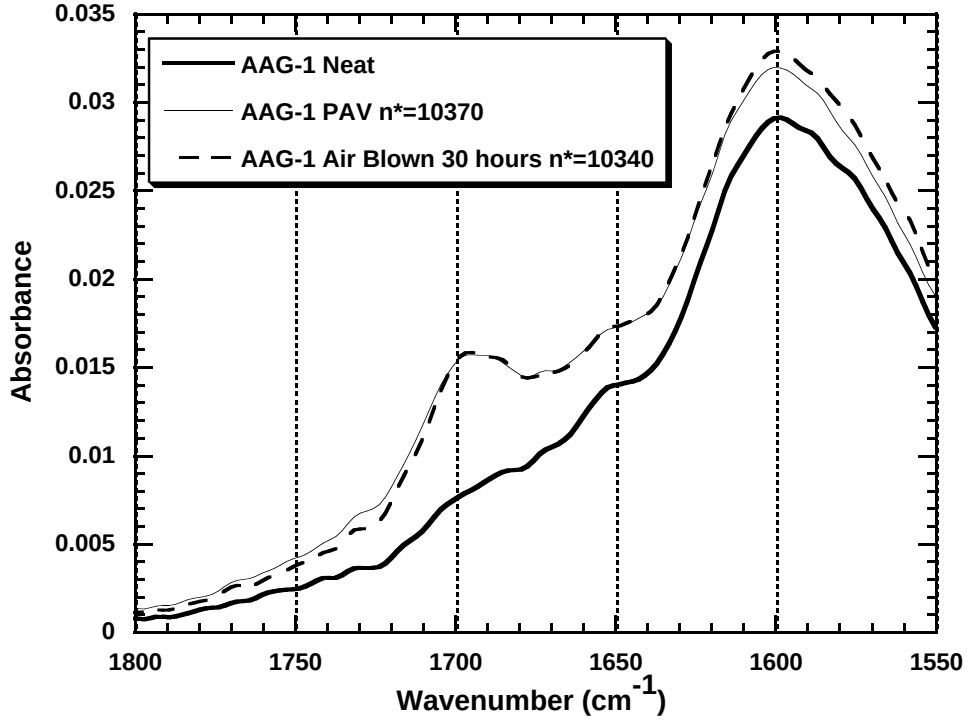

Figure 3-35. FTIR Spectra for AAG-1 for Various Aging Procedures.

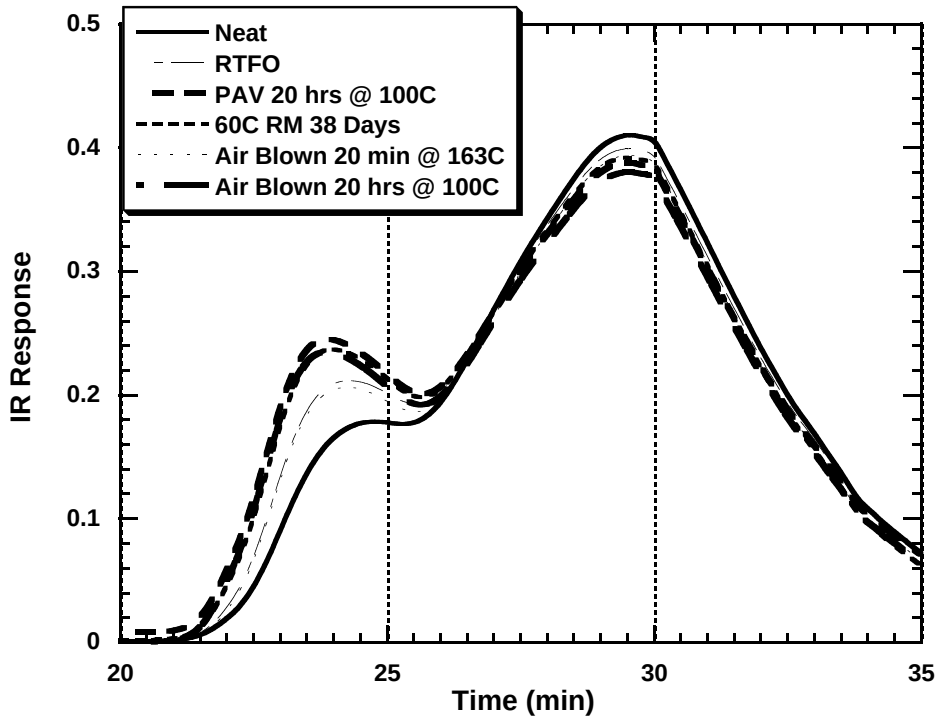

Figure 3-36. GPC Results for Shell AC-20 for Various Aging Procedures.

Several samples showed a similar viscosity while the carbonyl areas were drastically different. In addition, no time could be established where air blowing seemed to be identical to either the PAV or the environmental room aging procedures. The air-blowing test was also very difficult to run. Because high-temperature asphalt was being agitated at high rpm the apparatus could not be left on overnight unattended. This made the test tedious to monitor. In light of these problems with air blowing as a long-term aging test, the conclusion is that it would not be a suitable test.

Modifier Performance

In addition to the other results obtained in this project, some attention should be directed toward the modifiers used. All modified asphalts were made using the same base to enable a comparison between them. In this section the effect of modifiers will be discussed as it relates to the low-temperature properties and high-temperature performance grade of the material.

Beginning with the low-temperature properties, the bottom performance grades have been repeated in Figure 3-37 for convenience. A significant observation in the data of Figure 3-37 is that, although each modifier pulled the base past the –28 ºC mark, and therefore bettered its performance grade, the true impact of the modifiers on the BBR measurements does not seem to be that significant. The greatest impact on the BBR bottom continuous performance grade was

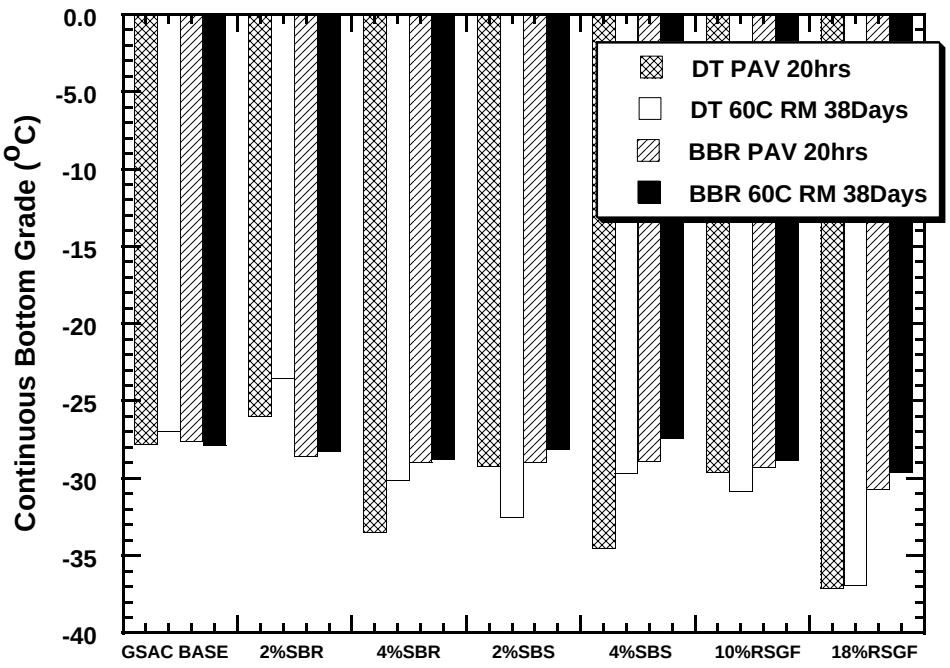

Figure 3-37. Continuous Grade Comparison for Modified Asphalts.

the 18% RSGF-20 modifier, which improved the grade 3.1 °C from the base material. The improvement seen in the remaining modifiers was modest, with most showing just over 1 degree of improvement. It seems, therefore, that modifiers have relatively little impact on the bottom grade as determined by BBR measurements.

The DTT data scatter prevents one from drawing concrete conclusions regarding modifier performance, but it seems clear that while the modifier's improvement may not be seen on the BBR, a direct tension test may allow for a better PG. The samples modified with 4% SBS and 18% RSGF-20 in Figure 3-37 illustrate this for the PAV aged materials.

Figure 3-38 presents data comparing the failure stress measured at –24 °C for each of the modified samples with that of the GSAC AC-15P base. All samples were RTFOT aged, then PAV aged for 20 hours at 100 °C. As shown in the figure, all of the modifiers increase the failure stress of the material by significant amounts. Even the smallest increases, as seen by the 2% SBR and 2% SBS modified systems show an increase from 3 to 4 MPa. The 10% RSGF-20 modified sample, while better than the 2% SBS and 2% SBR samples, clearly is inferior to the 4% SBR and 4% SBS samples, which improve failure stress by about 2 MPa. By far the best modifier in terms of raising the failure stress is the sample modified by 18% RSGF-20. This sample nearly doubles the failure stress of the base asphalt.

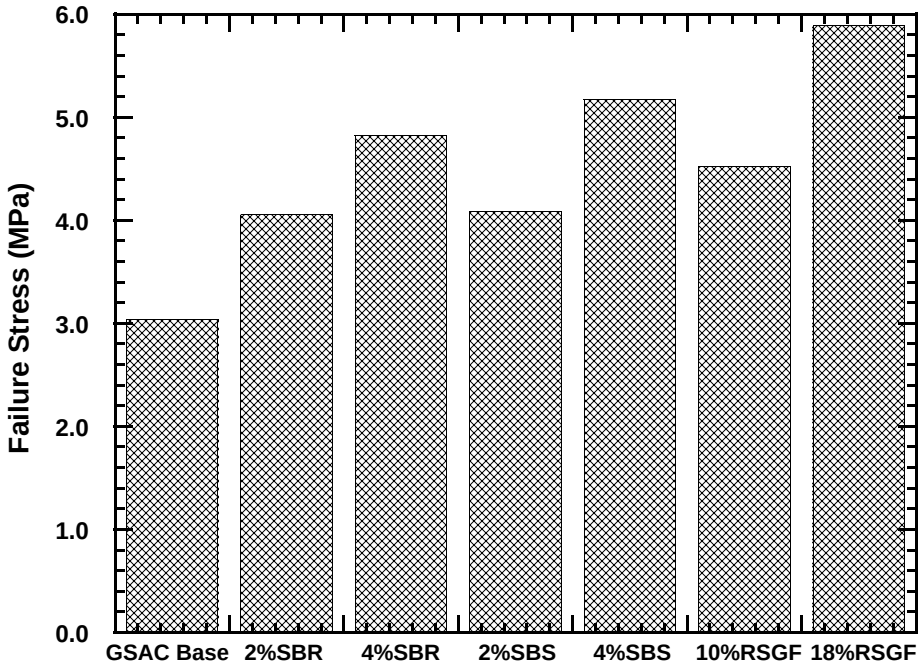

Figure 3-38. DTT Failure Stress at –24 ºC for Modified Materials.

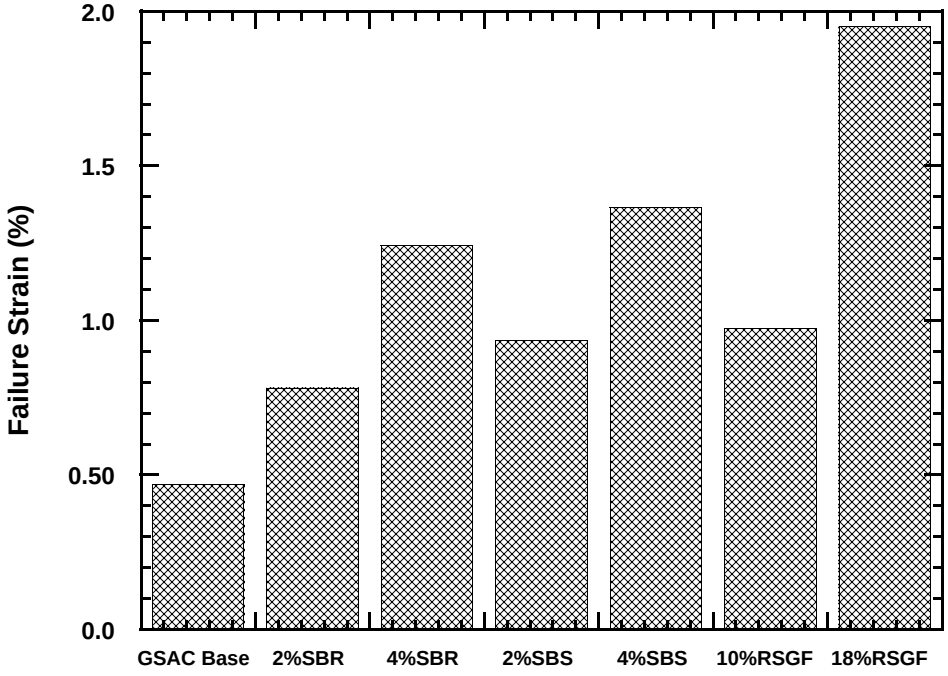

Figure 3-39. DTT Failure Strain Measured at –24 ºC for Modified Materials.

Figure 3-39 shows a comparison between the failure strain at break for modified asphalt samples. As with the failure stress, the 2%SBR, 2%SBS, and 10%RSGF-20 samples improve failure strain, but are clearly not as effective as the more heavily modified samples. In this case the improvement seen by the 18%RSGF-20 is an amazing four times the elongation at break of the base asphalt. The data presented in Figures 3-38 and 3-39 are tabulated in Table 3-8.

Table 3-8. DTT Results for Modified Samples at –24 ºC.

Material	Failure Stress at -24 ºC (MPa)	Failure Strain (%)
GSAC AC-15P	3.0340	0.46800
GS AC AC-15 w/2%SBR	4.0520	0.78100
GS AC AC-15 w/4%SBR	4.8260	1.2410
GS AC AC-15 w/2%SBS	4.0890	0.93400
GS AC AC-15 w/4%SBS	5.1730	1.3640
GS AC AC-15 w/10%RSGF-20	4.5180	0.97500
GS AC AC-15 w/18%RSGF-20	5.8910	1.9510

In addition to evaluating the direct tension data for modifiers it is interesting to note the changes in BBR data that the modifiers bring as well. Table 3-9 gives the BBR results for the modified materials and the base at −24 ºC. As can be seen in the table, all modifiers improve the stiffness of the base material, but to varying degrees. All modifiers also improve the m-value, but the changes are not as significant as the changes in the stiffness. It was hypothesized that the improvements in these DTT data could be correlated with the data obtained from the BBR. While no such correlation exists for m, stiffness correlates well with both failure stress and strain as seen in Figures 3-40 and 3-41. These data indicate that the decrease in stiffness is accompanied by increases in both the failure stress and the failure strain.

Modifiers may improve these low-temperature properties by lowering the glass transition temperature of the base material. Kumar and Gupta (1998) define the glass transition temperature as “the temperature at which a hard glassy polymer becomes a rubber material.” Asphalt, like polymers, exhibits glass transitions, and some glass transition temperatures have been measured for SHRP materials by Bahia and Anderson (1993). On a molecular level, these modifiers may prevent or help to control some of the associations between highly polar molecules which form as temperature drops, thereby lowering the glass transition temperature and improving low-temperature physical properties.

Table 3-9. BBR Results for Modified Samples at -24 ºC.

Material	Failure Stress at -24 ºC (MPa)	Failure Strain (%)
GSAC AC-15P	3.0340	0.46800
GS AC-15 w/2%SBR	4.0520	0.78100
GS AC-15 w/4%SBR	4.8260	1.2410
GS AC-15 w/2%SBS	4.0890	0.93400
GS AC-15 w/4%SBS	5.1730	1.3640
GS AC-15 w/10%RSGF-20	4.5180	0.97500
GS AC-15 w/18%RSGF-20	5.8910	1.9510

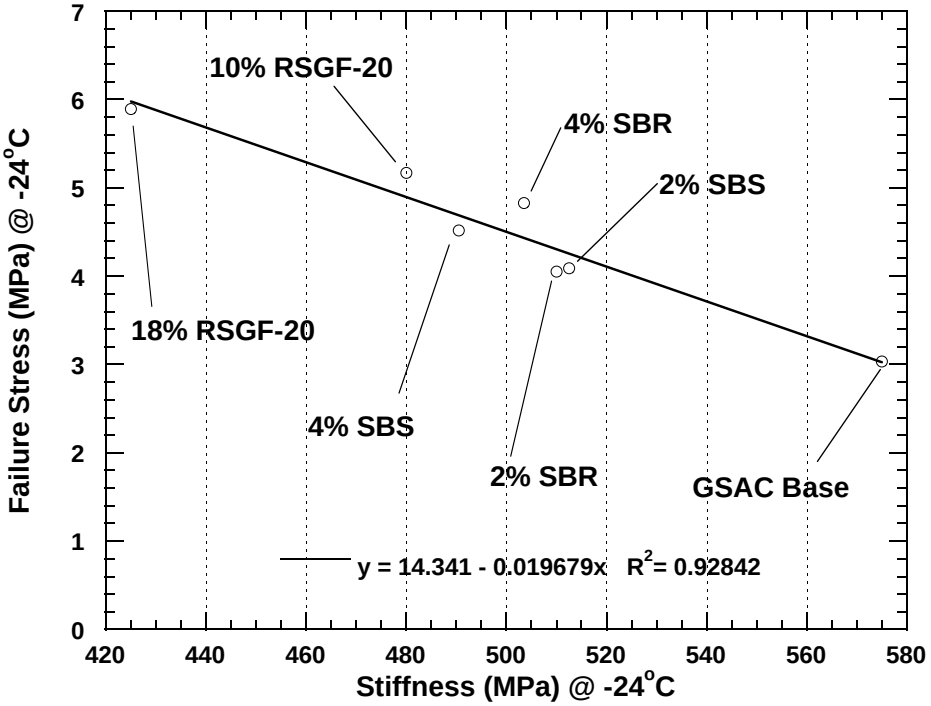

Figure 3-40. Failure Stress as a Function of Stiffness at -24 ºC for Modified Materials.

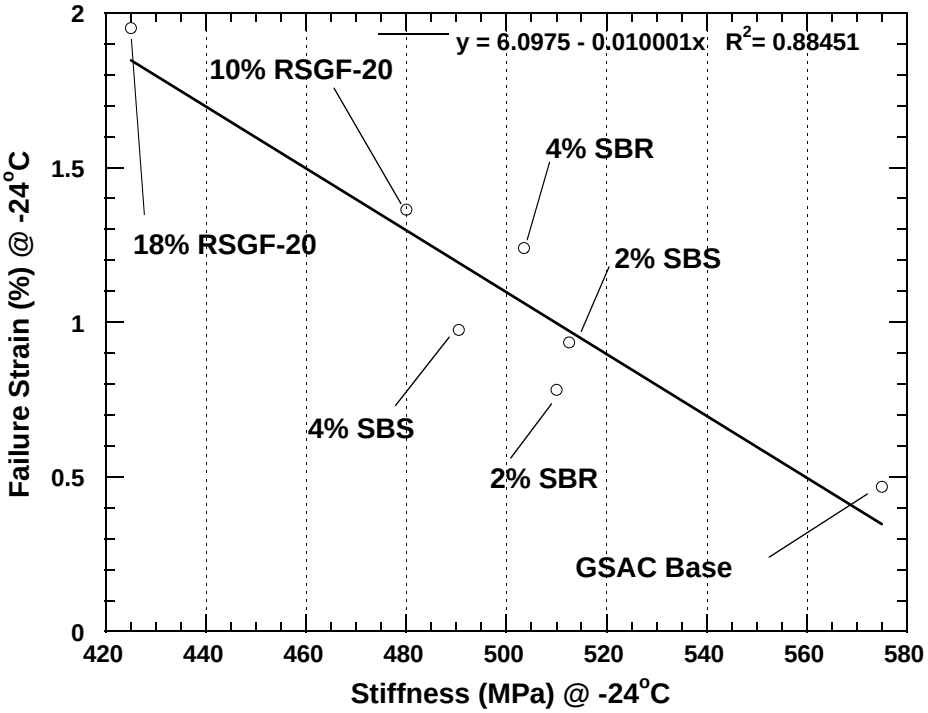

Figure 3-41. Failure Strain as a Function of Stiffness at -24 ºC for Modified Materials.

In addition to having a significant impact on low-temperature properties, modifiers also help to improve high-temperature properties and performance grades. High-temperature performance grades are determined by DSR measurement of $G^*/\sin(\delta)$ at various temperatures for unaged and RTFOT-aged materials.

Figure 3-42 illustrates $G^*/\sin(\delta)$ at 10 rad/s as measured for the unaged base and modified materials. The horizontal line on the plot indicates the SHRP specification that an unaged material must have a $G^*/\sin(\delta)$ value of 1000 Pa to pass. From the plot, 4% SBR and 4% SBS modifiers increase the value of the base $G^*/\sin(\delta)$ more than any other modifiers. They are followed closely by the 18% RSGF-20 modified material. It is interesting to note in this plot that the effect of 2% SBS at 58 ºC is similar to that of the 18% RSGF-20, but as the temperature increases to 70 ºC, 2% SBS becomes only slightly better than the base material. The remaining modifiers 2% SBR and 10% RSGF-20 showed only modest improvement to the base asphalt. The data of Figure 3-42 are also presented in Table 3-10.

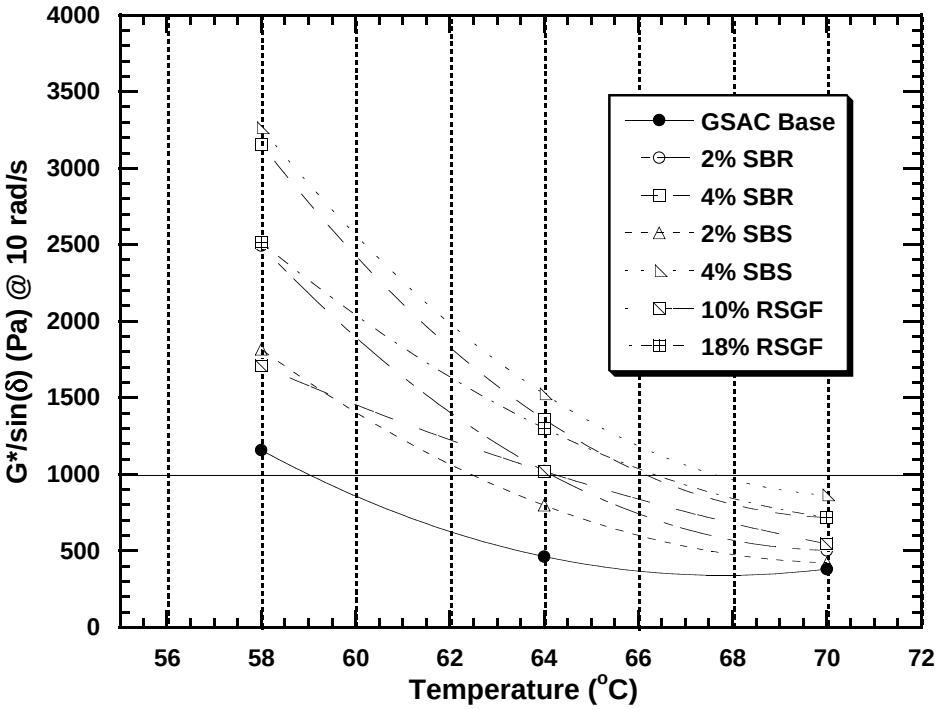

Figure 3-42. G */sin(δ) @ 10 rad/s for Unaged Modified Materials.

Table 3-10. G*/sin(δ) for Unaged Modified Materials.

Material	G*/sin(δ) (Pa) at 10 rad/s		
	58 ºC	64 ºC	70 ºC
GSAC AC-15P Base	1158.1	463.3	---
GS AC-15 w/2%SBR	2494.1	1021.3	503.7
GS AC-15 w/4%SBR	3156.4	1360.0	717.9
GS AC-15 w/2%SBS	1817.0	798.0	422.7
GS AC-15 w/4%SBS	3264.4	1525.7	864.9
GS AC-15 w10%RSGF-20	1709.1	1020.3	546.3
GS AC-15 w18%RSGF-20	2517.2	1301.7	719.4

Figure 3-43 illustrates $G^*/\sin(\delta)$ as measured for the RTFOT-aged base and modified materials. As with Figure 3-42, the horizontal line on the plot indicates the SHRP specification that a short-term aged material must have a $G^*/\sin(\delta)$ value of 2200 Pa to pass. Like the unaged material, the 4% SBR and 4% SBS modifiers increase the value of the base $G^*/\sin(\delta)$ more than any other modifiers. The 4% samples are followed by 2% SBR and 2% SBS. As before with the unaged material, the data indicate that for the 2% SBS sample, the modifier helps at lower temperatures but shows little improvement for the higher temperatures. In this case the 18% modifier does not show improvement that is as significant as that seen in the unaged material. This is likely due to the fact that after RTFOT aging, much of the ground rubber remains in the RTFOT bottle and is not collected in the sample. This loss of modifier would explain the reduced benefit. Unfortunately, the loss of modifier in a simulation does not mean that the modifier will not have benefit in service. The remaining modifier, 10% RSGF-20, showed only modest improvement to the base asphalt. The data of Figure 3-43 are also presented in Table 3-11.

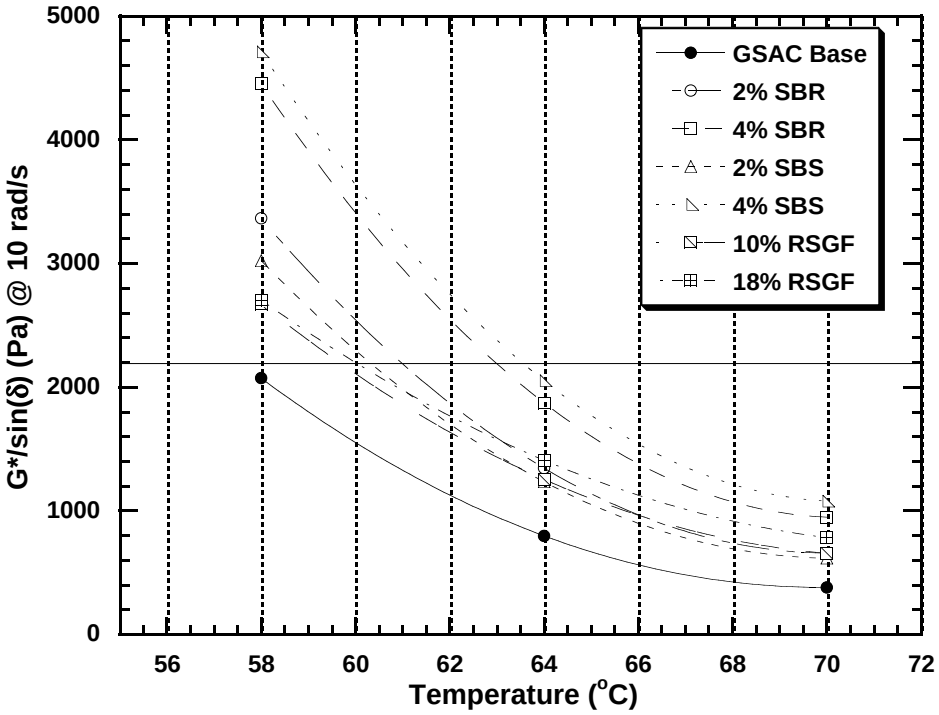

Figure 3-43. $G^*/\sin(\delta)$ for RTFOT-Aged Modified Materials.

Table 3-11. $G^*/\sin(\delta)$ for Modified Materials after RTFOT Aging.

Material	$G^*/\sin(\delta)$ (Pa) at 10 rad/s		
	58 °C	64 °C	70 °C
GSAC AC-15P	2072.7	798.0	381.4
GS AC-15P w/2%SBR	3364.9	1345.4	658.5
GS AC-15P w/4%SBR	4454.4	1873.4	949.1
GS AC-15P w/2%SBS	3024.5	1235.5	618.2
GS AC-15P w/4%SBS	4712.8	2052.5	1078.7
GS AC-15 w/10%RSGF-20	2672.2	1255.2	657.2
GS AC-15 w/18%RSGF-20	2704.7	1409.9	783.3

To summarize, the higher weight percent modified samples showed considerably better low-temperature properties. The 18% RSGF-20 modified sample showed the best improvement to low-temperature properties followed by 4% SBS and 4% SBR. For high-temperature properties 4% SBS proved to be the best modifier, followed by 4% SBR. For the base asphalt used in this project (PG 52-22), all modifiers provided a 12 °C improvement in PG to 58-28. Two modifiers, 4% SBS and 18% RSGF-20, provided an 18 °C improvement in PG to 58-34.

CONCLUSIONS AND RECOMMENDATIONS

In Phase I of this project it was shown that 38 days of aging at 60 °C and 1 atmosphere of air is approximately equivalent to 20 hours in the PAV at 100 °C, after both have been RTFOT aged. This indicates that the PAV simulates roughly one year of aging on Texas roads. Clearly this aging test should be extended or modified if the SHRP performance specifications are to accurately predict intermediate and long-term binder failure.

Low-temperature properties of the samples were found not to vary significantly between the PAV and environmental room aged material. The DTT and the BBR both gave the same performance grade for each material at each aging condition. In addition, for the BBR, the bottom grade was determined by the same parameter (S or m) for each aging procedure. Therefore, the current Superpave specification gives consistent values for PAV aged materials as well as for environmental room aged materials.

For Phase II a correlation was developed from the high-temperature parameter $G^*/\sin(\delta)$ at 58 °C and 10 rad/s to correct the low-temperature performance grade when one desires to skip the long-term aging procedure. The correction factor for the continuous bottom performance grade is given by:

$$C = 0.6225 \exp\left(0.0002095 G^{*}/\sin(\delta)\right) \quad (3\text{-}3)$$

Where the bottom continuous performance grade for long-term aged material can be estimated from that of the short-term material and the correction factor by:

$$PG_{LT} = PG_{ST} + C \quad (3\text{-}4)$$

The correlation proved to give a maximum error of ±1.6 °C for the low temperature performance grade.

In Phase III of this project it was shown that as asphalts are aged for extended periods their relative ranks with respect to Superpave low-temperature specifications change. This indicates that the Superpave long-term aging specifications result in an arbitrary ranking of asphalts with respect to low-temperature properties. In addition it was shown that as asphalts are aged for extended periods, the low-temperature grades move linearly with aging from being limited by stiffness at short aging times, to being limited by m-value at longer aging times.

Upon examining the data obtained by long-term air blowing of the samples, it was concluded that air blowing is not a suitable long-term test. Air blowing did not provide carbonyl area data which were consistently in line with data obtained from the environmental room. In addition, no time could be established where air blowing seemed to be identical to either the PAV or the environmental room aging procedures. The air-blowing test also was difficult and tedious to run. In light of these problems with air blowing as a long-term aging test, it was concluded that it would not be a suitable test.

A portion of the work in this project dealt with comparing various modifiers. To summarize, the higher weight percent modified samples showed considerably better low-temperature properties. The 18% RSGF-20 modified sample showed the best improvement to low-temperature properties followed by 4% SBS and 4% SBR. For high temperature properties 4% SBS proved to be the best modifier, followed by 4% SBR. It is recommended that polymer modifiers be used in concentrations of at least 4% by weight, where SBS rather than SBR is recommended. If ground tire rubber is to be used, a high-cure process with 18% by weight rubber provides excellent benefit for both high- and low-temperature properties.

CHAPTER 4. AN INVESTIGATION OF ASPHALT DURABILITY: RELATIONSHIPS BETWEEN DUCTILITY AND RHEOLOGICAL PROPERTIES FOR UNMODIFIED ASPHALTS

ABSTRACT

Literature reports indicate that the ductility of binders recovered from asphalt pavements correlate with cracking failure. However, ductility measurement is a time and material consuming process and is subject to reproducibility difficulties, as are all failure tests. The purpose of this study was to correlate ductility with DSR properties analogous to the SHRP procedure of using BBR S and m to screen for the thermal cracking. DSR measurements are much faster and consume much less material than ductility measurement.

Fourteen unmodified asphalts were oxidized to different levels of aging at temperatures ranging from 60 to 200 ºC. Experimental data show that the extensional flow of conventional asphalt binders can be qualitatively described with a simple elongation model using a viscoelastic Maxwell element. Based on this model, a map of the dynamic shear modulus G' versus η'/G' was used to track changes in ductility with aging. Also, ductility correlated remarkably well with $G'/(\eta'/G')$ for different binders aged at different conditions.

INTRODUCTION

Field data suggest that asphalt binder ductility correlates quite well with pavement cracking, provided it is measured at the appropriate temperature. Doyle (1958) found from the performance of Ohio test sections that while the ductility measured at 25 ºC was not a good indicator of pavement cracking, ductilities measured at 12.8 ºC, 1 cm/min or less correlated quite well. He also gave data on other roads, and one showed no cracking after 5 years for which the recovered asphalt had a ductility of 29 cm when measured at 12.8 ºC and 1 cm/min. Two others with considerable cracking showed ductilities of only 3 and 4 cm.

Four test sections were laid during 1960-61, and after 10 years all of them showed some cracking (Kandhal and Koehler, 1984; Kandhal and Wenger, 1975). Among penetration at 25 ºC, viscosity at 60 ºC, and ductility at 15.6 ºC, only ductility gave the proper ranking in road condition (cracking) after 10 years. The pavement condition was good if the ductility at 15.6 ºC was above 10 cm, and when the ductility value decreased to about 3 to 5 cm, cracking began to develop. It was also found that ductility at 15.6 ºC was more reproducible and better defined than that at higher temperature, such as 25 ºC. In 1964, six more pavements were laid, each with a different asphalt. Road cracking condition was correlated with viscosity at 25 and 60 ºC, shear susceptibility at 25 ºC, and ductility at 15.6 ºC, 1 cm/min. Among these parameters, both ductility and viscosity-shear susceptibility slope ordered the performance rating (cracking) of the six pavements correctly. A third set of test sections was laid in 1976, and again relative rankings of pavement performance agreed with the ordering of ductility measured at 15.6 ºC, 1 cm/min. Kandhal (1977) summarized results from these three test sections and concluded that when the

binder ductility decreased to 3-5 cm (measured near 15 °C), there would be serious cracking and the pavement needed resurfacing.

Clark (1958) reported results comparing laboratory oven aging with hot-mix and road aging for 46 roadways with respect to ductility and penetration and found that low-temperature ductility was a good predictor of roadway condition (cracking) and life.

Halstead (1963) showed that the pavements containing asphalts with penetration in the range normally considered satisfactory (30 to 50) but with low ductility were likely to show poorer service than pavements containing asphalts of the same penetration but with high ductility. Vallerga and Halstead (1971) studied 53 highway pavements located throughout the United States and concluded that severe raveling occurred in cold climates when the ductility at 15.6 °C, 1 cm/min decreased to 3 cm or lower.

From the above discussion we can conclude that ductility measured at reduced temperature and elongation rate (e.g., 15 °C and 1 cm/min) is a good indicator of cracking condition of asphalt binders. However, ductility measurement is a time-consuming process and requires several grams of material, according to ASTM D 113-86 (1994), 75 grams. Thus, it was the objective of this work to devise alternate measurements using viscoelastic properties to assess durability in conventional asphalt binders, similar to the concept of using bending beam rheometer S and m to indicate low-temperature thermal cracking.

METHODOLOGY

Seventeen unmodified asphalt binders were compared and evaluated through a number of physical properties. The binder materials were aged at two temperatures, 93.3 and 204 °C (200 and 400 °F), by air blowing and at a third temperature, 60 °C (140 °F), in a controlled environment room to obtain properties ranging from those of a slightly aged material to one which would be near the end of its service life. Table 4-2 summarizes the materials and their aging methods.

The air blowing was conducted by placing approximately 500 grams of asphalt binder in a 0.9-L (1 qt) can and controlling to the desired temperature. Air was blown through a sparger in the bottom of the can, and the binder was stirred continuously by a mixer at a low speed.

Physical properties measured on the aged binders were viscoelastic properties, ductility, and force ductility. The viscoelastic properties were measured with a Carri-Med CSL500 dynamic shear rheometer (DSR). Ductilities were obtained at 15 °C and an extensional speed of 1 cm/min in accordance with ASTM D113-86 (1994). The ductility sample has a 3 cm initial gauge length and a tapered throat. Ductility is recorded as the extension in centimeters of the asphalt specimen before break. Force ductility (F-D) measurements were made at 4 °C and 1 cm/min elongation speed. In this case the specimen was similar to the ductility specimen except that the initial gauge length, while still 3 cm in length, had a uniform rectangular cross-section of 1 cm by

0.5 cm. A strain gauge provided for force measurements up to 100 N. The force measurement allowed stress as a function of extension ratio to be calculated, assuming a constant cross-section and an incompressible binder. F-D measurements were made to better understand the phenomenological relationship between a material's rheological properties and ductility and thus the impact of aging on durability.

Table 4-1. List of Asphalts Studied.

Aging Method	Asphalt Binders
204 °C (400 °F) Air-blowing	DS AC-5, Exxon AC-5, Fina AC-5 Exxon AC-10, Fina AC-10, GSAC AC-10 Exxon AC-20, Fina AC-20, Shell AC-20
93.3 °C (200 °F) Air-blowing	SHRP AAA-1, AAB-1, AAD-1
60 °C (140 °F) Environmental Room	Exxon AC-30, Fina AC-5, Fina AC-10 Fina AC-20, GSAC AC-10, Neste AC-20 Wright AC-10, Wright AC-20, UR AC-10

In addition to these physical properties measurements, FTIR spectra were obtained on a number of the asphalt materials as a measure of the amount of oxidation. The area under the carbonyl absorbance band from 1650 to 1820 cm^{-1} represents the extent of oxidation in asphalt materials and is reported as carbonyl area (CA).

RESULTS AND DISCUSSION

Effect of Aging on Rheological Properties and Master Curves

Figure 4-1 shows dynamic viscosity (η') and storage modulus (G') master curves at two aging conditions at a reference temperature of 4 °C. At high frequency or low temperature the viscosity curves merge together, approaching a single asymptote. At low frequency or high temperature there is a significant increase with aging in the low shear rate, limiting viscosity.

Figure 4-2 shows typical storage modulus G' and loss modulus G'' versus aging time behavior for asphalt, and Figure 4-3 shows increases in G' and G'' with FTIR carbonyl area. From Figure 4-2, note that G'' increases less with aging time than G'. Hence, it may be said that G'' is less sensitive to aging than is G', and this is seen within the context of oxidation, as represented by the FTIR carbonyl band, by comparing the relationships in Figure 4-3. This smaller sensitivity of G'' to aging than G' means that their ratio ($\tan \delta$) and hence the phase angle, δ, decreases with aging. Phase angle master curves are shown in Figure 4-4. Thus with increased aging, asphalts tend to become more solidlike and less liquidlike at moderate temperatures. This decrease in phase angle over aging time is shown in Figure 4-5. The relationship between δ and carbonyl area (Figure 4-6) is also linear.

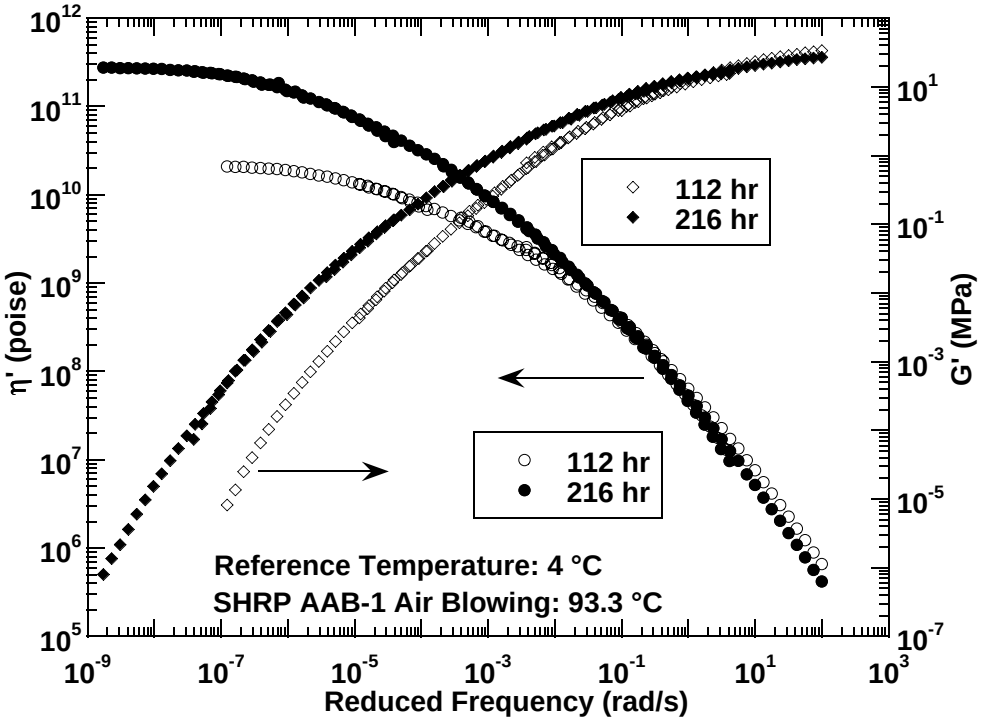

Figure 4-1. Master Curves for SHRP AAB-1 at Two Aging Times.

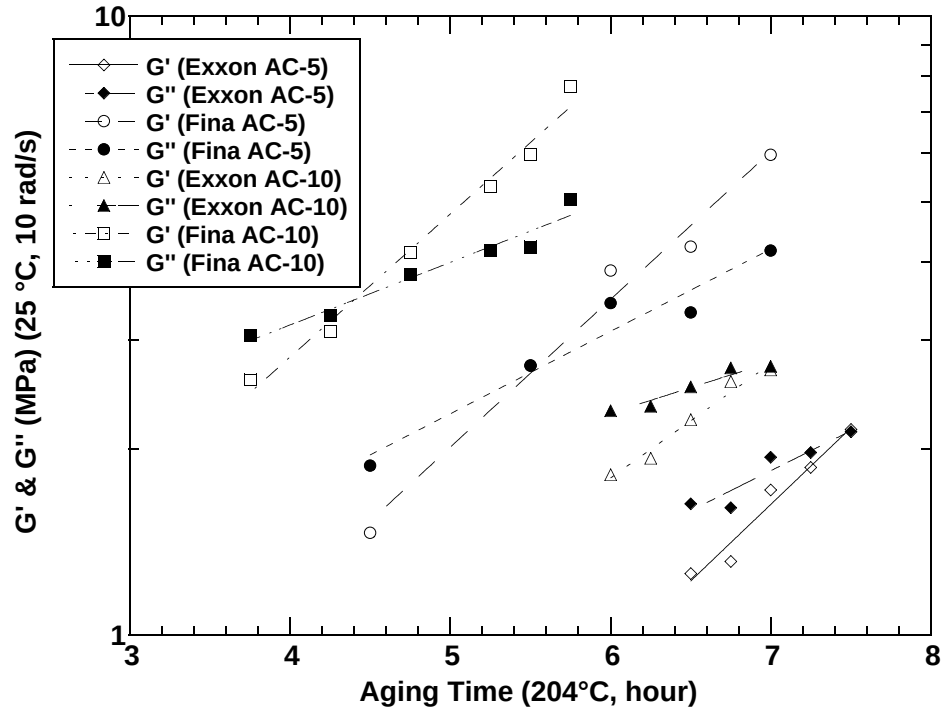

Figure 4-2. Effect of Aging on Storage and Loss Moduli.

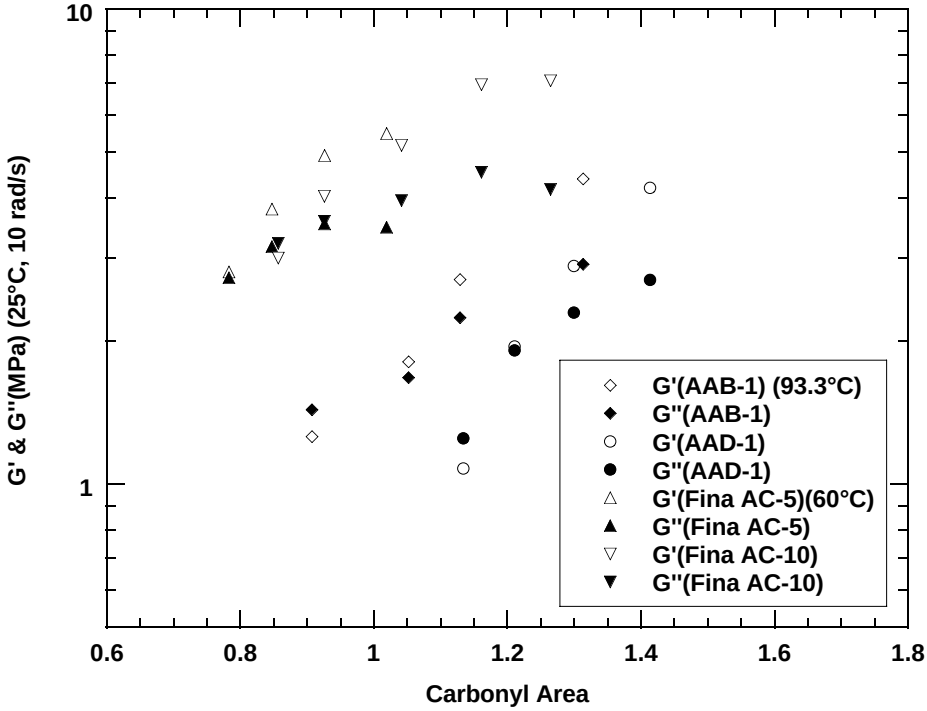

Figure 4-3. Storage and Loss Modulii Related to Oxidation Carbonyl Area.

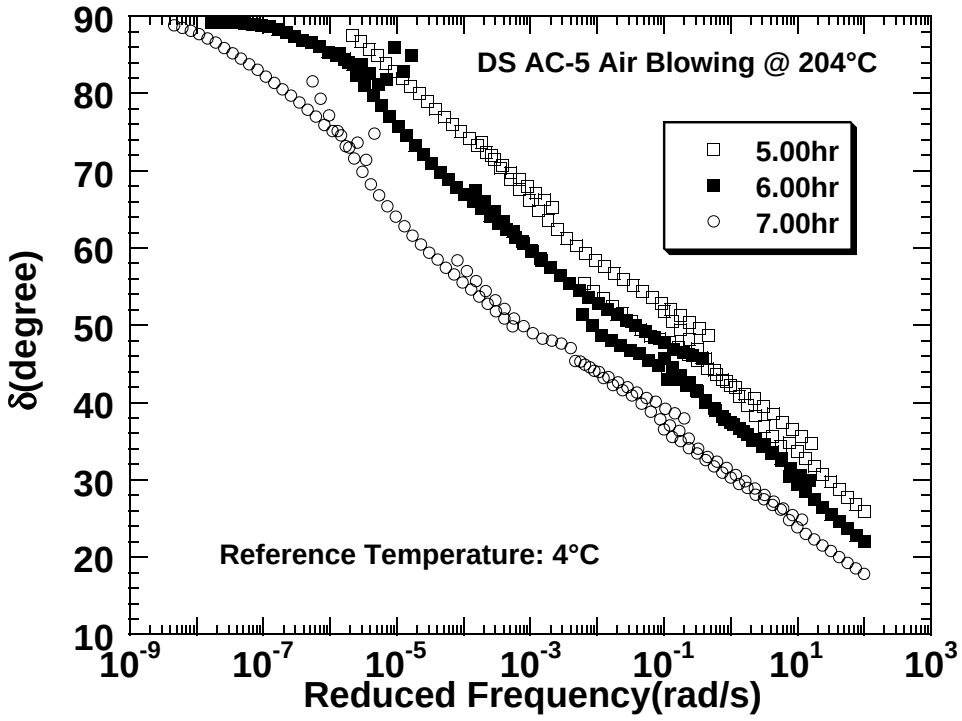

Figure 4-4. Effect of Aging on the Phase Angle Master Curve.

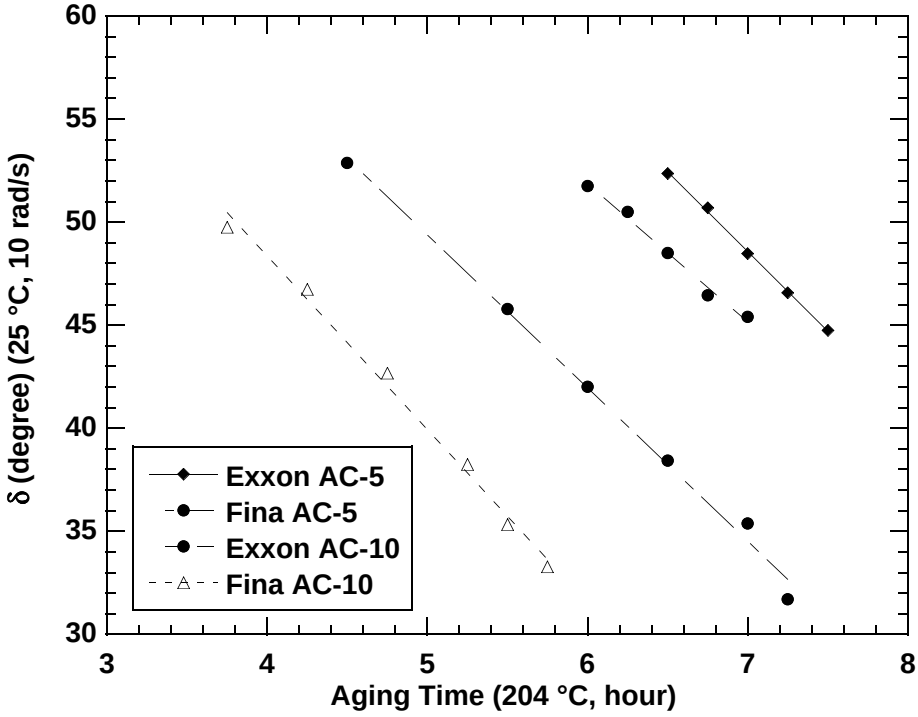

Figure 4-5. Decrease in Phase Angle (25 ºC, 10 rad/s) with Aging Time.

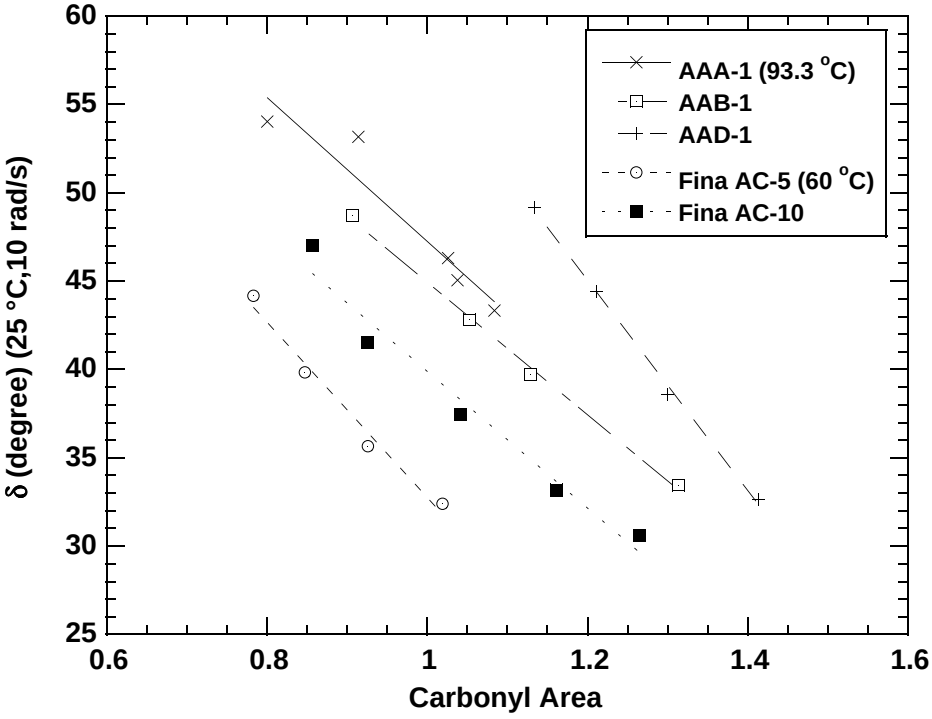

Figure 4-6. Decrease in Phase Angle with Oxidation Carbonyl Area.

The imperfections in the phase angle master curves (Figure 4-4) should be noted. Whereas G′ and η′ master curves show very consistent behavior in accordance with time-temperature superposition (TTSP) when created from measurements at different temperatures, there are obvious problems with the phase angle master curve. This has been pointed out as evidence of structuring in asphalt resulting from associations of asphaltenes and resins, associations that change with temperature, thereby bringing into question the validity of TTSP (Lesueur et al., 1996). Nevertheless, TTSP is commonly used with asphalts and we do so in this chapter.

To summarize the effect of aging on the rheological properties, aging increases the dynamic viscosity (η′) and storage modulus (G′) at intermediate frequencies (temperatures). Furthermore, G′ increases more rapidly than G″ so that the phase angle decreases with aging, thereby producing a more solidlike material over time at intermediate temperatures. These changes have a profound effect on ductility, as discussed below.

Maxwell Model

With aging, ductility decreases dramatically (Figure 4-7). This can also be seen in Figure 4-8, which shows two experimental force ductility curves for an unmodified asphalt aged to two conditions. The measurements are made at 4 ºC. The abscissa is the extension ratio so that an alpha of 3 with a gauge length of 3 cm would be a ductility of 6 cm. The ductility of the 216-hour aged sample is only about 0.45 cm.

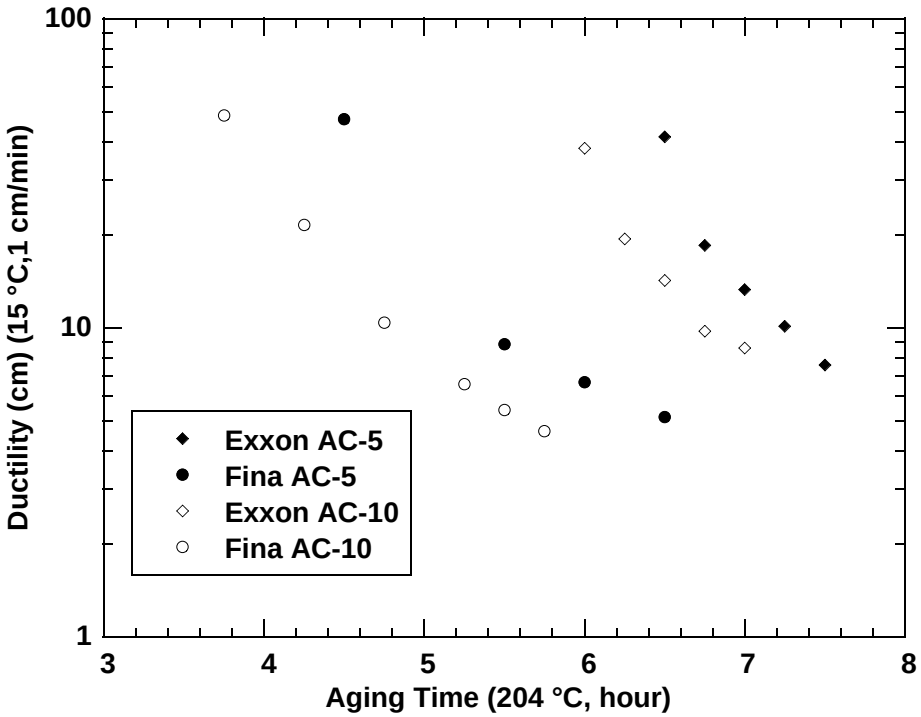

Figure 4-7. Decrease in Ductility with Aging Time.

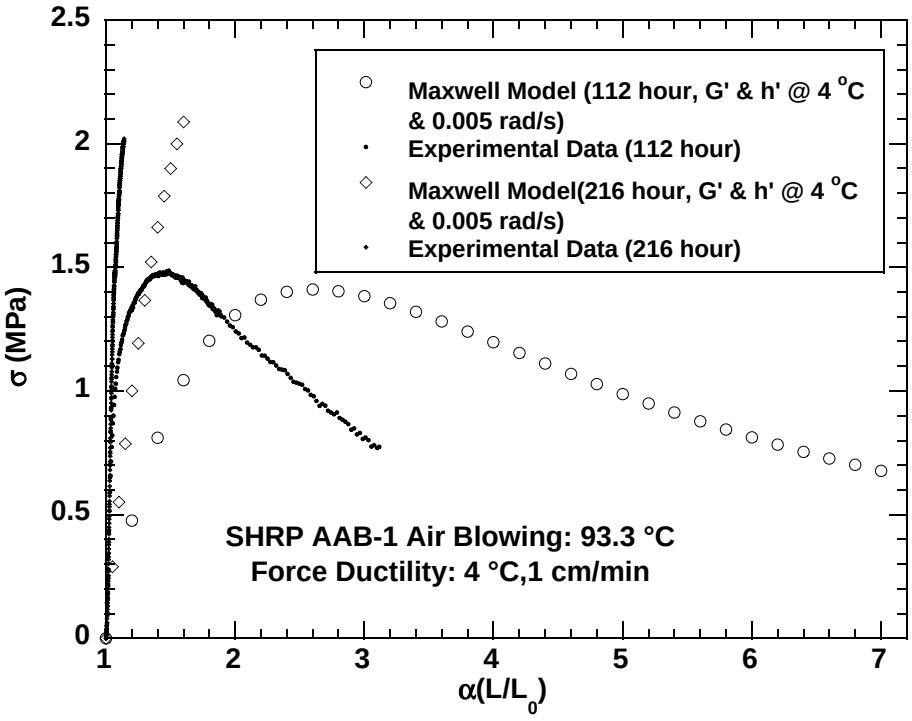

Figure 4-8. Force-Ductility Data and Maxwell Model Simulation for Two Aging Times.

As a sample is extended, the initial (short time) response is from the elastic properties of the material, and hence the initial slope is dominated largely by its elastic modulus. At longer times, i.e., larger extension ratios for the 112-hour sample, the stress actually declines with extension ratio. In this region the viscosity allows the material to flow. Furthermore, for heavilyaged asphalt samples, both the elastic modulus and viscosity are greater so that the stress reaches a higher level before the deformation can transition to flow. This is a simplistic description, but appears to embody the essential elements of these stress elongation curves.

To continue with this simplistic analysis, we have used a spring and dashpot in series (Maxwell model). Here, our emphasis is not on precise modeling of the extensional flow of asphalt binders. Previous work has shown that a multiple relaxation time model is more appropriate for such a purpose (Christensen and Anderson, 1992). Rather, our purpose is to gain sufficient insight into the nature of elongation and failure of asphalt materials, especially as they harden at low temperature or with oxidation, to provide guidance into possible correlations between ductility and linear viscoelastic rheological properties. Such a concept is similar to the use of low-temperature bending beam stiffness (S) and creep rate (d log S/dt, defined as m) together as a surrogate for the low-temperature direct-tension failure strain, as defined by the Superpave asphalt binder specifications (Asphalt Institute, 1994). Both rely upon the existence of a common failure stress in asphalt materials at the test conditions and common qualitative behavior of the stress-strain relation. In both situations, stresses build with deformation due to the elastic modulus but are relieved as the material undergoes flow. The balance between these

two phenomena determines the level of stress that is achieved as a result of deformation; the amount of stress the material can sustain without failure interacting with this balance establishes the failure strain. Such a correlation will allow failure to be estimated from DSR master curves for aged materials.

The Maxwell model represents the asphalt by a linear elastic element (linear spring) in series with a newtonian viscous element (Figure 4-9). Here we are concerned with deformation

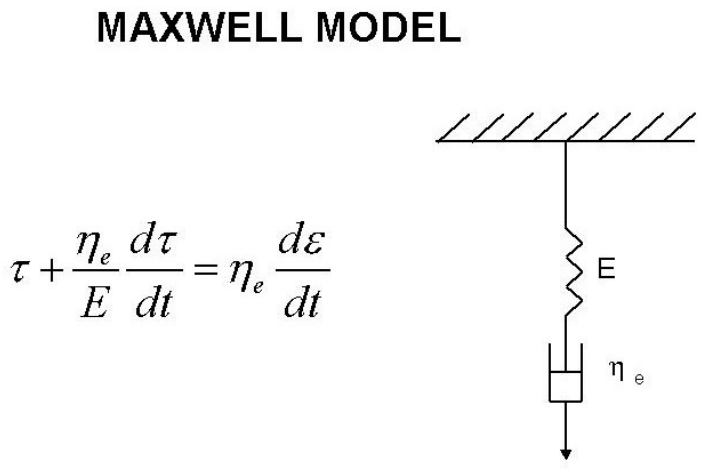

Figure 4-9. The Maxwell Model: An Elastic and Viscous Element in Series.

at constant elongation rate under uniaxial load. Because these elements are in series the stress in each is the same, but the strain rate in each depends on its own constitutive relation. Specifically, the elastic element's total stress (T) under elongation is proportional to the strain through the elastic modulus (E). Hence, the rate of strain across the spring is directly proportional to the rate of change of stress:

$$\frac{d\varepsilon_E}{dt} = \frac{1}{E}\frac{dT}{dt}. \qquad (4\text{-}1)$$

For the viscous element of an incompressible material, the rate of strain is proportional to the total stress through the elongational viscosity (η_e) (McCrum et al., 1997):

$$\frac{d\varepsilon_\eta}{dt} = \frac{1}{\eta_e} T. \qquad (4\text{-}2)$$

Combining the strain rates of these two elements gives the total strain rate as

$$\frac{d\varepsilon}{dt} = \frac{1}{\eta_e} T + \frac{1}{E}\frac{dT}{dt}, \tag{4-3}$$

which is rearranged to give

$$T + \frac{\eta_e}{E}\frac{dT}{dt} = \eta_e \frac{d\varepsilon}{dt}. \tag{4-4}$$

It is useful to transform the independent variable time to the elongation ratio. For constant elongation ratio, ($dL/dt = U_o$), $L = L_o + U_o t$. The elongation ratio $\alpha = L/L_o = 1 + U_o/L_o\, t$ so that $d\alpha/dt = U_o/L_o$, and thus

$$\frac{d\varepsilon}{d\alpha} = (d\varepsilon/dt)/(d\alpha/dt) = (U_o/L)/(U_o/L_o) = 1/\alpha, \tag{4-5}$$

leading to the differential equation for total stress as a function of elongation ratio:

$$\left(\frac{L_o}{U_o}\right)\left(\frac{E}{\eta_e}\right)\frac{T}{E} + \frac{1}{E}\frac{dT}{d\alpha} = \frac{1}{\alpha}. \tag{4-6}$$

Converting to shear modulus ($E = 2G(1 + \nu)$) and noting that $\eta_e = 3\eta$ (by Trouton's rule) then gives

$$\frac{L_o}{U_o}\,\frac{G(2(1+\nu))}{\eta}\,\frac{T}{G(2(1+\nu))} + \frac{3}{G(2(1+\nu))}\,\frac{dT}{d\alpha} = \frac{3}{\alpha}. \tag{4-7}$$

Letting $\nu = 0.5$ for an incompressible material and simplifying leads to

$$\frac{L_o}{U_o}\left(\frac{G}{\eta}\right)\frac{T}{G}+\frac{d\left(\frac{T}{G}\right)}{d\alpha}=\frac{3}{\alpha}. \qquad (4\text{-}8)$$

This can be converted to a dimensionless form by defining a dimensionless stress as $T' = T/G$ and a dimensionless "time constant" t' by $t' = (\eta/G)/(L_o/U_o)$, which gives

$$\left(\frac{T'}{t'}\right)+\frac{dT'}{d\alpha}=\frac{3}{\alpha}. \qquad (4\text{-}9)$$

This result is expressed in terms of shear modulus G and viscosity η. For the purposes of further discussion, we assume that these can be replaced by their respective dynamic shear properties, i.e., $G = G'$, $\eta = \eta'$.

With this model we can make some approximate comparisons between force-ductility data and DSR data. The data were measured at 4 °C and at an elongation rate of 1 cm/min, which is equivalent to the strain rate of approximately 0.005 s^{-1}. Using this strain rate as an angular frequency and 4 °C master curves, we obtained values for η' and G' to use in this Maxwell model.

Data and model calculations for the SHRP AAB-1 air blowing at 93.3 °C (200 °F) at both 112 and 216 hours are shown in Figure 4-8. Experimental data are from the force-ductility apparatus, and the calculations are based solely on the DSR experimental data and the Maxwell model with no empirical adjustments. While there are significant quantitative differences between the data and the calculations, the general trends are in agreement, and considering the total predictive nature of the calculations based upon the viscoelastic property data and the simplistic Maxwell model, the comparisons are really quite reasonable. Model limitations will be discussed more extensively below. The material air blown for 112 hours shows an increase in stress to a maximum followed by a relaxation, which, according to the Maxwell model, is the result of viscous flow of the material, whereas for the material air blown for 216 hours the increase in stress occurs much more rapidly (i.e., at smaller elongation ratios) so that the material breaks before it can reach a maximum in stress and a transition to viscous flow.

As noted above, the elongation model based on a Maxwell viscoelastic element is very approximate in a number of ways. First, the material's viscosity and shear modulus are assumed constant over the elongation. In fact, because the experiment is performed at a constant elongation rate, as the material lengthens the strain rate decreases. This error, while less at the small failure elongation ratios of heavily aged materials, still is a consideration. Second, like other viscoelastic materials, asphalts have many more than one relaxation time and modulus. This is likely a significant error in quantitatively modeling the extensional flow. Third, unmodified materials

tend to neck down in elongation, violating the uniform cross-section assumption of our calculations. For heavily aged materials, for which failure occurs before transition to viscous flow, this error is reasonably small.

So, in view of these model uncertainties, we would not expect to have close quantitative agreement between calculations based on the rheological properties and the experimental force-ductility data. Nevertheless, the Maxwell model qualitatively describes the extensional flow of asphalt binders, thereby providing guidance on defining physical parameters that are important for understanding and correlating the binder's extensional flow, as discussed in the next section.

Relationship between Ductility and G′, η′/G′

From this elongation model using a Maxwell element (Equation 4-8), it is seen that two rheological parameters are suggested to represent the extensional behavior of asphalt binders: the ratio of the dynamic viscosity to the storage modulus (η'/G') and the value of the storage modulus G'. Figures 4-10a and 4-10b are maps of G' versus η'/G' for materials measured at 15 °C in the DSR. Figure 4-10a shows the data with each material identified at different levels of aging, and Figure 4-10b has the data grouped by regions of ductility, also measured at 15 °C.

The general trend is clear. As an asphalt ages, it moves from the lower right to the upper left and the ductility declines dramatically along this path. For some materials this path is significantly steeper than for others. The boundaries between regions of ductility are not perfect, as one might imagine from the normal experimental scatter that is observed in any kind of failure test. These maps show clearly that ductility is not related to just one parameter, i.e., to just the ratio η'/G' or to just the modulus G' (stiffness) of the material. Rather, the ductility is dependent upon both.

As an alternate way of viewing these same data, ductility is plotted versus the ratio of G' to (η'/G') (Figure 4-11). This plot shows a good correlation between these parameters, especially for ductilities less than 10 cm. Note that it is in this region below 10 cm that Reese (1997) and Reese and Goodrich (1993) observed binder ductility as playing a significant role in binder road performance. At this level of ductility, evidently the stiffness and viscosity of the binder are great enough that the binder will fail because of excessive stresses that develop because of insufficient material flow.

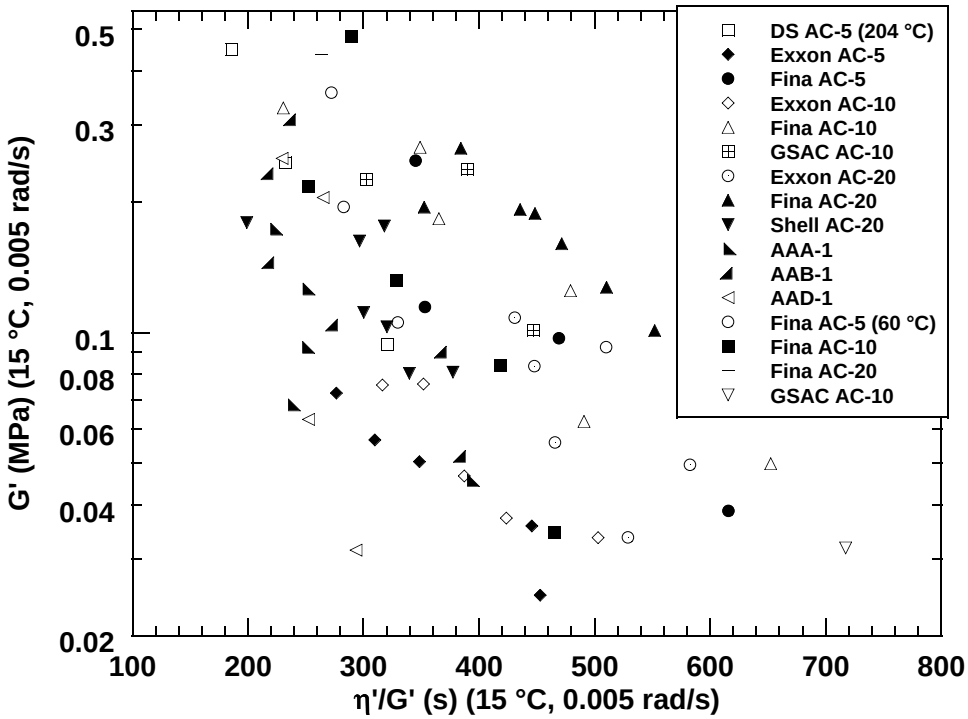

Figure 4-10a. G′ versus η′/G′ Map as Asphalts Oxidize, by Asphalt.

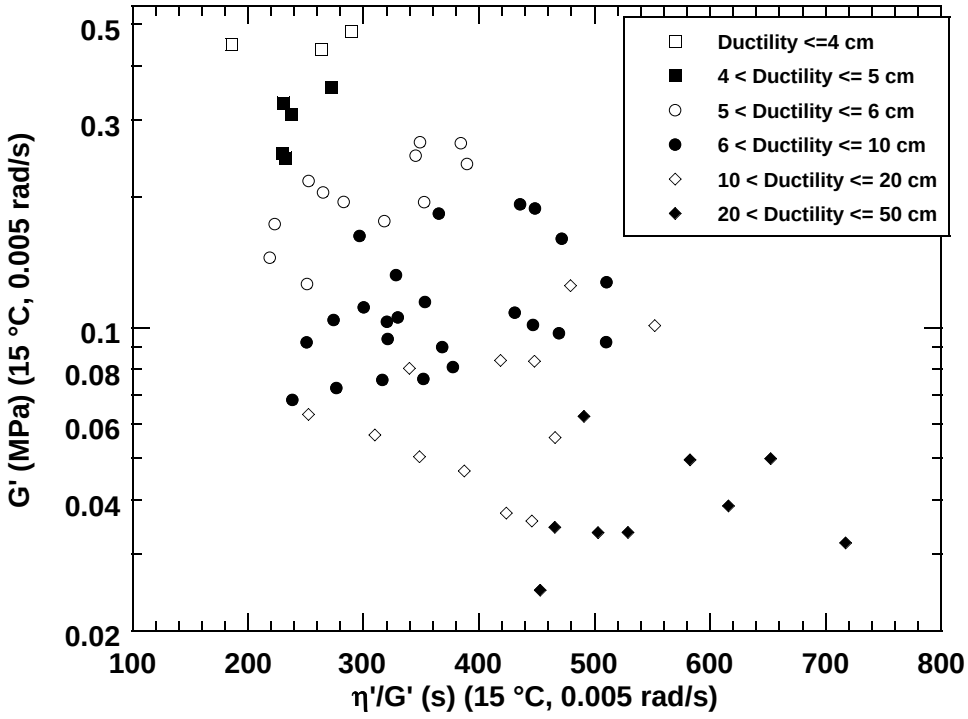

Figure 4-10b. G′ versus η′/G′ Map as Asphalts Oxidize, by Ductility Regions.

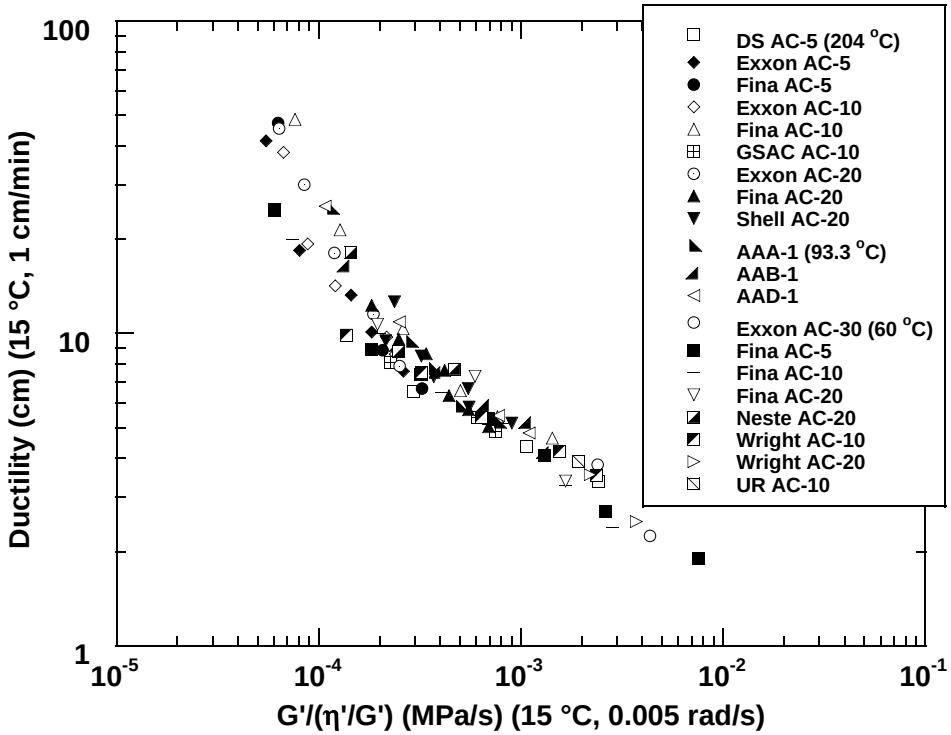

Figure 4-11. Ductility versus DSR Parameter G′/(h′′/G′), All Ductilities.

Figure 4-12 shows the linear region below 10 cm, and from this a map with curves of constant ductility is produced and is shown in Figure 4-13. Each point on the line in Figure 4-12 produces a line of constant ductility, which is also a line of constant G′ to η′/G′ ratio in Figure 4-13. This produces the ductility regions shown in the figure and the data are shown in the figure as well. That the data do not fall in the regions perfectly is the result of the scatter of the data around the line in Figure 4-12. Again, we make the observation that a whole range of values of G′ and η′/G′ can produce the same asphalt ductility.

The point of Figure 4-12 is that for conventional asphalts the function G′/(η′/G′) can serve as a surrogate for ductility, is easier to measure, and requires less material.

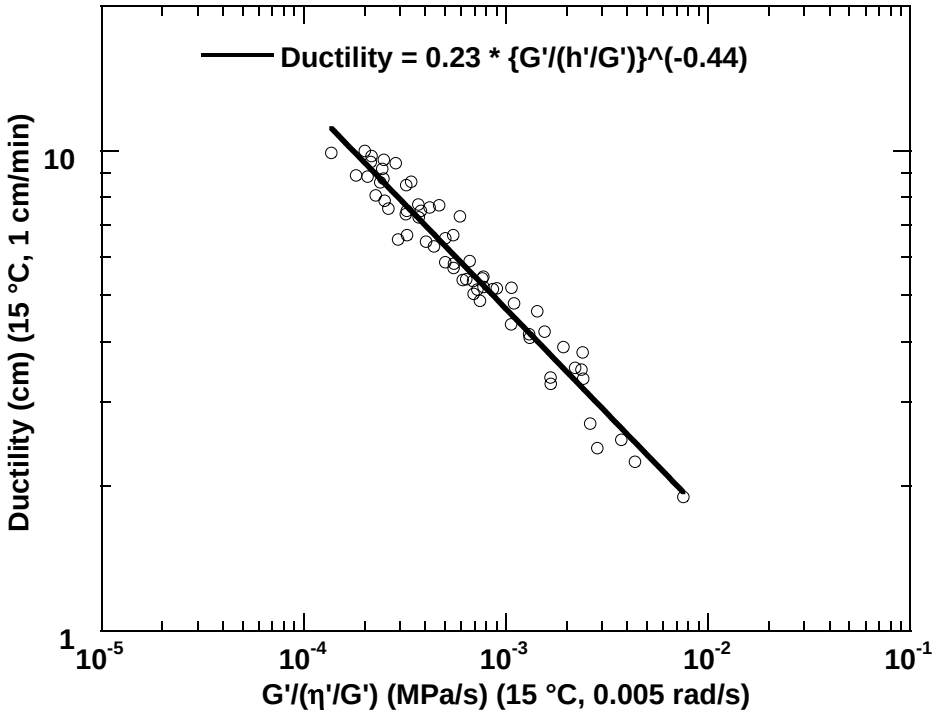

Figure 4-12. Ductility versus DSR Parameter G′/(η′/G′), Low Ductilities.

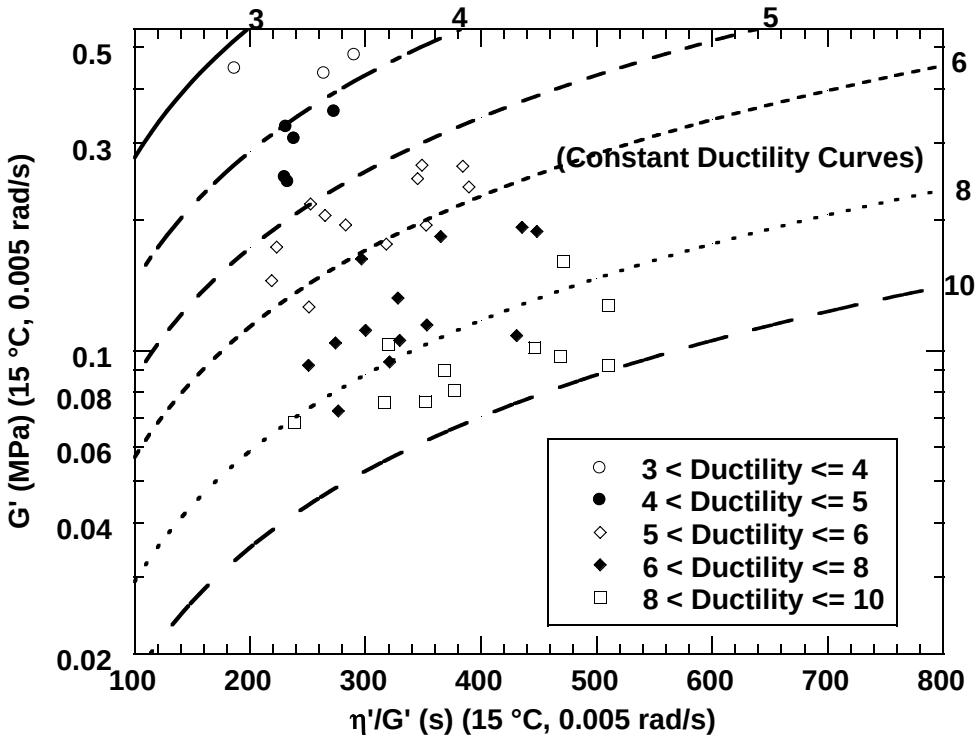

Figure 4-13. G′ versus η′/G′ Map at Low Ductilities with Lines of Constant Ductility.

Ductility-DSR Correlation at 10 rad/s

If ductility at 15 °C, 1 cm/min can be used as an indication of durability, as the literature indicates, then through the correlation of the above section, so can G′/(η′/G′) at 15 °C, 0.005 rad/s. However, this low a frequency is not accessible to most instruments except through data taken at several temperatures and over a range of several orders of magnitude in frequency, followed by use of the time-temperature superposition principle. Consequently, it is desirable to shift this correlation by using TTSP to measurements at the SHRP standard of 10 rad/s.

In accordance with TTSP, a viscoelastic property measured at two different temperatures will be the same value if the frequency of measurement is also shifted appropriately. The shift factor a_T is used to to characterize this required shift in frequency (or equivalently, time): $a_T = \omega_o/\omega_T$, where ω_o is a particular frequency of interest on the master curve for a particular reference temperature and ω_T is the frequency that gives the same value of the property at a different temperature, T. If the shift factor is known for a material, then measurements at one frequency-temperature condition can be shifted to another frequency and temperature.

The dependence of the shift factor on temperature commonly is described by using an empirical expression known as the WLF (Williams-Landel-Ferry) (Williams et al., 1955) equation:

$$\log a(T)_R = - C1(T - T_R) / (C_2 + T - T_R), \qquad (4\text{-}10)$$

where

T = the selected temperature, °C or K,
T_R = the reference temperature, °C or K,
$a(T)_R$ = the shift factor at temperature T relative to the reference temperature T_R, and
C_1, C_2 = empirically determined coefficients.

Anderson et al. (1994) found that for pavement asphalts, the appropriate WLF form was

$$\log a(T)_d = - C_1(T - T_d) / (C_2 + T - T_d), \qquad (4\text{-}11)$$

where $a(T)_d$ is the shift factor at temperature T relative to the "defining" temperature T_d. Also, they found that with fixed values of C_1 and C_2 (equal to 19 and 92, respectively) the defining temperature T_d was a characteristic parameter for each asphalt and varied from −14.5 °C to 6 °C. Their values for T_d are shown in Table 4-2.

Table 4-2. Defining Temperature T_d for PAV-Conditioned SHRP Asphalts (Anderson et al., 1994).

Sample	T_d (°C)
AAA-1	-14.5
AAB-1	-6.0
AAC-1	3.5
AAD-1	-8.7
AAF-1	5.2
AAG-1	2.7
AAK-1	-9.2
AAM-1	6.0

For our work, we used the values of C_1 and C_2 from Anderson et al. (1994) and an average of their values for T_d. Thus, all parameters in the WLF equation were fixed. From a practical point of view, this will be necessary for a test procedure on unknown asphalts. To determine the temperature T that is appropriate for DSR measurements at 10 rad/s in the sense that it would be equivalent to measurements AT 15 °C and 0.005 rad/s, we proceeded in two steps. First, the shift factor is calculated for a temperature shift from 15 °C to −2.63 °C (T_d) and from this the appropriate test frequency at the defining temperature.

$$\log a(T)_d = -19(15-(-2.63))/(92+15-(-2.63)), \quad (4\text{-}12)$$

which gives $a(T)_d = 8.8(10^{-4})$. Thus, the appropriate test frequency at −2.63 °C would be $\omega(T_d) = a(T)_d\omega(15) = 4.4(10^{-6})$ rad/s; testing at -2.63 °C and $4.4(10^{-6})$ rad/s is equivalent to testing at 15 °C and 0.005 rad/s.

Second, the shift factor from $\omega(T)_d$ to 10 rad/s, $4.4(10^{-7})$, is used to calculate the appropriate test temperature at 10 rad/s. Equation 4-11 with the appropriate substitutions gives

$$\log (4.4(10^{-7})) = -19(T-(-2.63))/(92+T-(-2.63)), \quad (4\text{-}13)$$

from which T = 43 °C. So, measurements at 43 °C and 10 rad/s should be approximately equivalent to measurements at 15 °C and 0.005 rad/s.

Figures 4-14 through 4-18 compare the DSR function $G'/(\eta'/G')$ measured at 15 °C and 0.005 rad/s to measurements at 10 rad/s and 43 °C for several asphalts. All show reasonable, although not perfect, agreement between these two conditions. It should be noted that discrepancies are not unexpected due to the simplifying assumptions that were made, i.e., that TTSP is valid, and that the constants C_1 and C_2 and the defining temperature T_d were assumed to

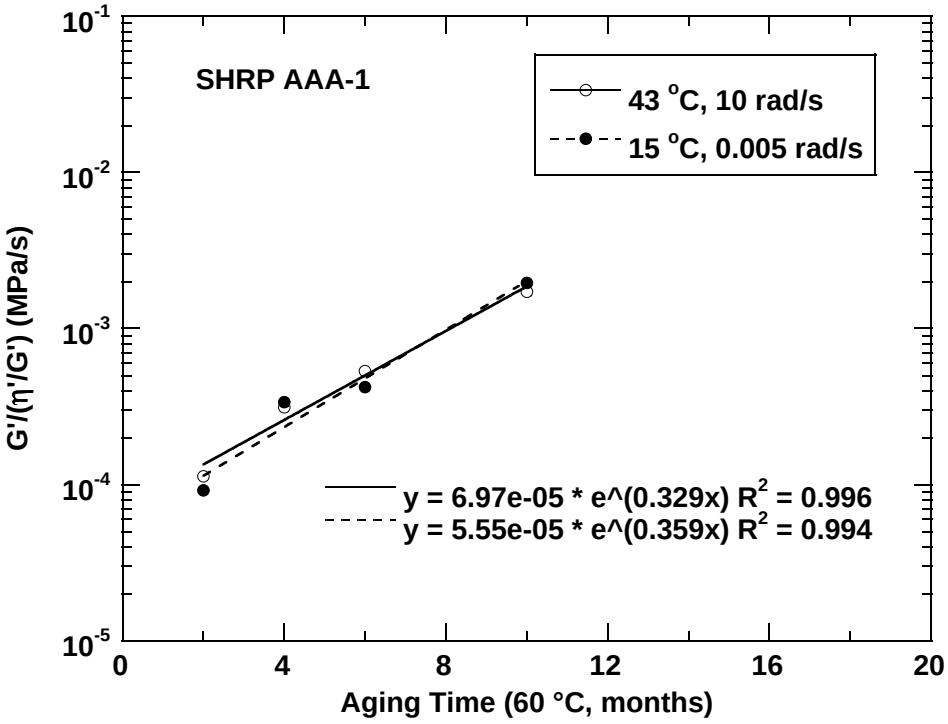

Figure 4-14. Increase in G′/(η′/G′) with Aging at Two Test Conditions: SHRP AAA-1.

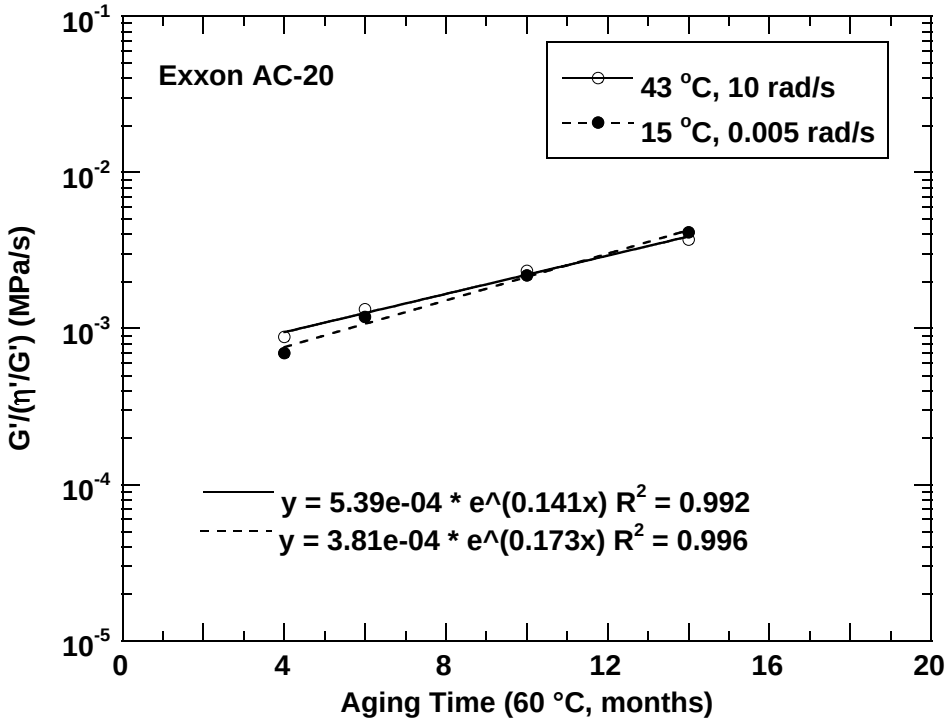

Figure 4-15. Increase in G′/(η′/G′) with Aging at Two Test Conditions: Exxon AC-20.

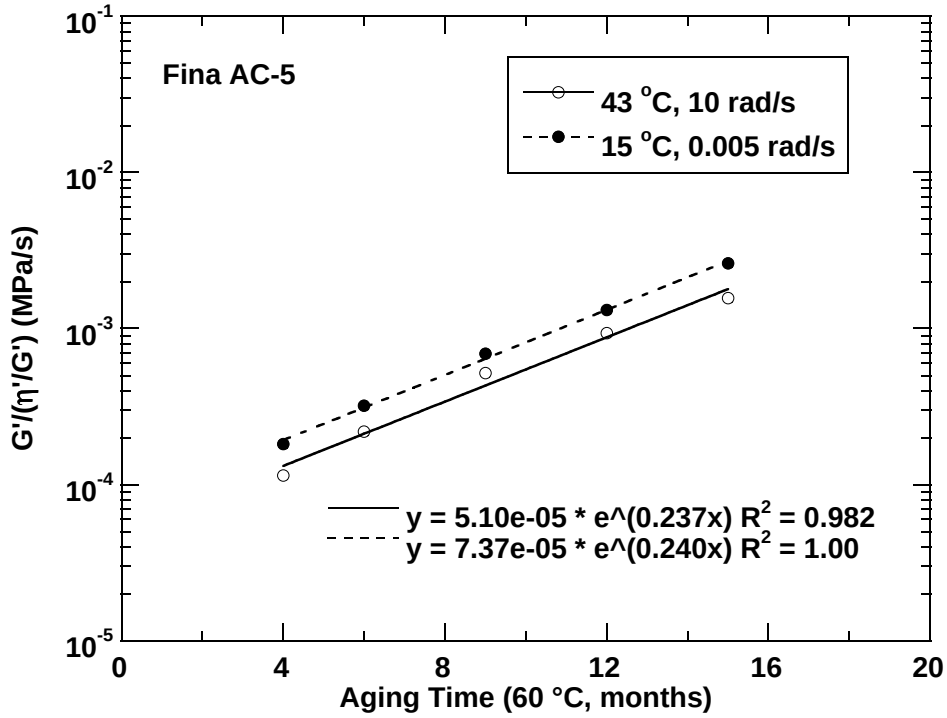

Figure 4-16. Increase in G′/(η′/G′) with Aging at Two Test Conditions: Fina AC-5.

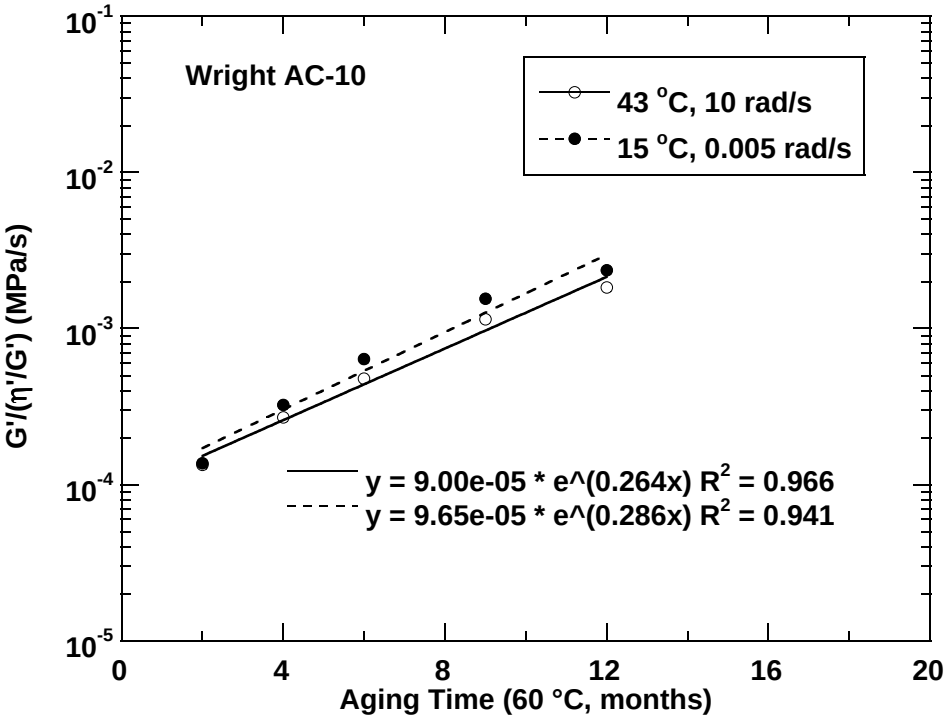

Figure 4-17. Increase in G′/(η′/G′) with Aging at Two Test Conditions: Wright AC-10.

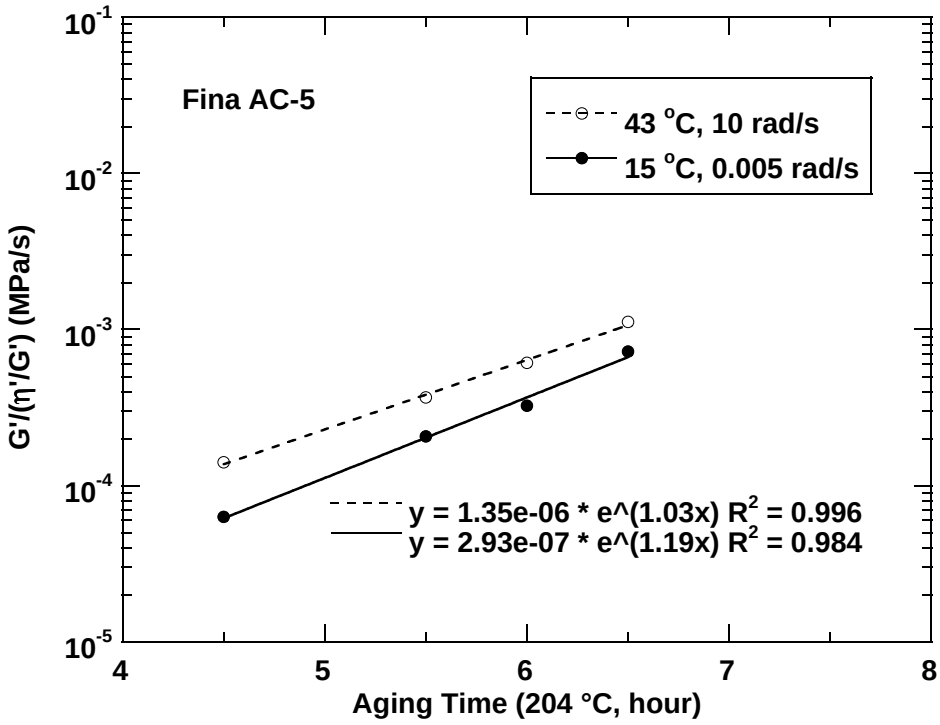

Figure 4-18. Increase in G′/(η′/G′) with Aging at Two Test Conditions: Fina AC-5.

be the same for all the asphalts. As mentioned previously, TTSP is most certainly invalid to some degree, as evidenced by the problems with the phase angle master curve, Figure 4-4. Furthermore, the fact that Anderson et al. (1994) saw a range of values for T_d suggests that our use of a single value is less than ideal. Finally, the best WLF parameters may, in fact, be different from theirs for the reason that our materials are more heavily aged than the PAV conditions that they tested. So, all things considered, the agreement between the two test conditions actually is quite good.

Figure 4-19 shows the ductility-DSR correlation for DSR properties measured at the shifted conditions of 43 °C and 10 rad/s. In the low-ductility region, again there is a good linear relationship between these two parameters, although there is somewhat more scatter than that of Figure 4-12. Note that the line shown is the same as that in Figure 4-12 and that the scatter of the 43 °C, 10 rad/s measurements bracket the line quite well.

This correlation, together with an aging procedure (Chapter 6) form a basis for a new test procedure for predicting asphalt binder durability in pavements. Chapter 8 presents this new procedure.

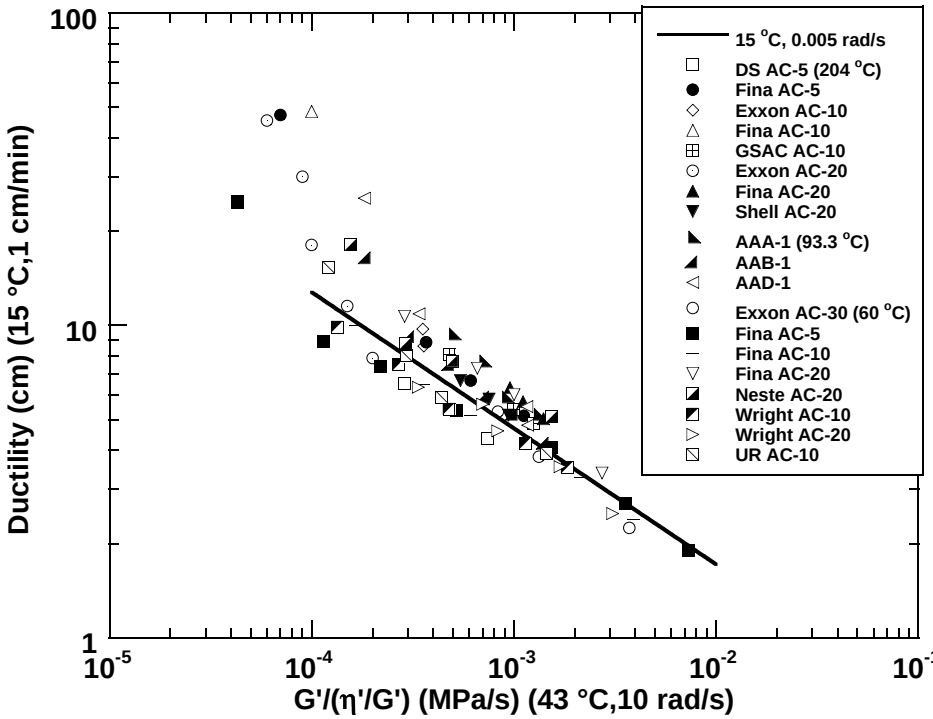

Figure 4-19. Ductility (15 °C, 0.005 rad/s) versus DSR Parameter G′/(η′/G′) (43 °C, 10 rad/s), All Ductilities.

CONCLUSION

Field tests indicate that ductility measured at low temperature is a good indicator of age-related cracking of asphalt binders. When a pavement's binder ductility decreases to a certain critical value, cracking is inevitable.

Binder ductility decreases dramatically with oxidative aging due to increases in both the viscosity and elastic modulus that result in a more solidlike material. Changes in ductility can be conceptually understood in the context of these changes in rheological properties through an elongation flow model that utilizes a simple Maxwell element.

Ductility correlates very well with G′/(η′/G′) for conventional asphalt binders aged at different conditions, especially when ductility is below 10 cm. In this region, the logarithm of ductility varies approximately linearly with the logarithm of G′/(η′/G′), and ductility measurements potentially can be replaced by G′/(η′/G′), measured at 10 rad/s, 43 °C using the DSR. This provides the basis for a new asphalt durability test, presented in Chapter 8.

CHAPTER 5. POLYMER MODIFIED ASPHALTS: OXIDATIVE AGING, RHEOLOGY, AND DUCTILITY

ABSTRACT

The effect of different polymeric modifiers on properties of asphalt binders was investigated. All samples are commercially used materials and came from the suppliers directly. Modifiers include diblock poly (styrene-b-butadiene) rubber (SBR), triblock poly (styrene-b-butadiene-b-styrene) (SBS), and tire rubber. Binder properties investigated include aging properties (hardening and oxidation). In addition, the effect of aging on modifiers was studied by means of size exclusion chromatography (SEC).

For the modifiers studied in this work, modified binders have a lower hardening rate than their corresponding base asphalts. Modified binders also have lower oxidation rate than their base materials, but the difference is not as big as for the hardening rate, and there are even some exceptions. Finally, modified binders have lower hardening susceptibility compared with their base materials.

With aging, the asphaltene content in binders increases, and modifiers such as SBR and SBS molecules will degrade.

INTRODUCTION

Asphalt is a viscoelastic material that behaves like an elastic solid at low temperature or high frequency, and like a viscous liquid at high temperature or low frequency. The purpose of asphalt modification is to minimize the effects of this behavior and thus minimize stress cracking at low temperatures and plastic deformation at high temperatures (Bouldin et al., 1991; Lewandowski, 1994).

Bouldin et al. (1992) found that polymer modification with SBS resulted in binders having superior rutting resistance compared to the straight asphalt due to a polymeric network structure which led to enhanced performance especially at elevated temperatures.

The effect of adding modifiers to asphalt was to increase molecular associations and provide elastic stability at higher temperatures, resulting in a decrease in loss tangent (Tayebali et al., 1992).

Linde and Johansson (1992) used size exclusion chromatography (SEC) to study the aging of SBS-modified binders and found that pronounced molecular size change occurred both in the bitumen and the polymer phase, resulting in changes in mechanical properties.

As for extensional properties, Srivastava et al. (1992) found that the ductility of the binder was increased by an order of magnitude by SBS. The aging of modified binders was also

less pronounced than base asphalts. The authors' explanation was that the active components of asphalt, such as naphthene and polar aromatics, carried out micro-structural interactions with the modifier (being the styrene-component of SBS) that prevented active components from oxidizing. The rubbery properties of the butadiene became evident in a ductility test. Modified binders needed more energy to deform than the base asphalt. Also, the elastic recovery of SBS-modified binder was much higher than unmodified asphalt. This resulted in an increased flexibility at low temperatures.

Muncy et al. (1987) found that SBR modification generally could improve the aging and consequent hardening characteristics of the asphalt, as indicated by the viscosity ratio, but there were some exceptions.

Shuler et al. (1987) noted that SBS was composed of glassy polystyrene end blocks and rubbery polybutadiene midblocks and that the polystyrene and polybutadiene blocks existed as two separate phases at typical pavement service temperatures. The resulting structure is a 3-D network of hard, spherical polystyrene domains in a rubbery matrix. This rubbery network imparted elastic properties to the modified binders.

Because of the importance of successes with polymer modification of asphalt binders, the purpose of the work of this chapter was to further investigate the effect of polymers on binder properties and especially the effect of oxidative aging on polymer modified properties. The work is presented in three sections. The first study addresses the effect of modifiers on aging properties, specifically on oxidation and viscosity hardening. The second part is a more detailed study of the rheology of modified binders, in the context of master curves, and the impact of aging on these properties. The third section is a study of the effect of modification on the ductility of aged binders, as it relates to the correlations of Chapter 4 and to the results of the previous sections of this chapter.

OXIDATION AND VISCOSITY HARDENING OF POLYMER MODIFIED ASPHALTS

Methodology

Dynamic viscosity was measured with a Carimed CSL500 dynamic shear rheometer.

In addition to these physical property measurements, FTIR infrared spectra were obtained on a number of asphalt materials as a measure of the amount of oxidation following the method of Jemison et al. (1992). The area under the carbonyl absorbance band (1650 to 1800 cm^{-1}) represents the extent of oxidation in asphalt materials (Liu et al., 1998) and is reported as carbonyl area (CA). A Waters HPLC-SEC system was used to measure the molecular size distribution of the asphaltic materials.

Materials used were nine conventional asphalt cements from six suppliers. These base asphalts were modified with poly(styrene-butadiene) rubber (SBR) and/or poly(syrene-butadiene-

styrene) (SBS) and in addition one of the asphalts also was modified with highly-cured ground tire rubber plus SBS. Another material, available from a high-cure rubber test section placed by our group in June, 2000 also was included in the study.

All asphaltic materials were aged at 60 ºC in a controlled environment room to simulate the long-term road aging. Aging times ranged from 2 to 18 months. Previous aging kinetics studies showed that accelerated aging at elevated temperature and pressure produces different rankings of asphalts than aging at road conditions (Domke et al., 1999; Liu et al., 1996). This is especially true of modified materials and necessitates measurements at conditions closer to actual pavement service in order to be more meaningfully related to expected pavement performance.

Results and Discussion

Asphalt Composition and Aging

Conventional asphalt binders can be separated by means of the Corbett precipitation and alumina column chromatographic procedure (ASTM D4124) into four fractions: saturates, naphthene aromatics, polar aromatics, and asphaltenes. According to Corbett (1979), asphalt can be viewed as an associated system of asphaltenes dissolved in the maltene (non-asphaltene) phase. Asphaltenes contribute to a good viscosity temperature susceptibility, and they are important viscosity builders; polar aromatics greatly contribute to ductility and the dispersion of asphaltenes; and both saturates and naphthene aromatics work against good ductility.

Pfeiffer and Saal (1998) proposed a peptization model to represent the associated nature of asphalt binder. In this model, asphaltenes (the most polar and heaviest of the asphalt constituents) form the center of some associated entities surrounded and stabilized by resins and other constituents of the maltenes. Whenever a shortage of resin occurs, attractive forces are enhanced and increase the molecular associations and ultimately extend the gel-type structure.

As an asphalt oxidizes, the heaviest naphthene aromatics convert to polar aromatics, and the heaviest polar aromatics to asphaltenes (Petersen, 1984; Liu et al., 1998a). As a result, a shortage of resin occurs and the asphaltene associations increase in size and number according to the above model. These increased associations result in the asphalt becoming stiffer and more difficult to flow and to relieve stress (Lin et al., 1998; Lin et al., 1996).

Effect of Modifiers on Oxidation of Asphalt Binders

With aging, asphalt binders harden because of these increased associations, thereby losing their ability to flow and deform under external loads (Chapter 4). After enough aging, this hardening results in serious pavement cracking. Consequently, it is important to investigate the effect of modifiers on the oxidation and hardening of asphalts. The introductory discussion indicated that polymeric modifiers could slightly improve asphalt binder's aging resistance (Dhalaan et al., 1992; Ista and Choquet, 1992; Srivastava et al., 1992; Muncy et al., 1987).

Here the parameter hardening rate (HR) is used to describe this effect. It is found that the logarithm of low shear rate dynamic viscosity (η_0^*) is linear with aging time after the "initial jump" aging period (Lau et al., 1992), and the slope of this linear relationship is called Hardening Rate,

$$\text{Hardening Rate} = \partial (\ln \eta_0^*) / \partial t \qquad (5\text{-}1)$$

where t is aging time and η_0^* typically is at 60 °C and at a sufficiently low frequency (0.1 rad/s or lower) that the material is very nearly Newtonian..

From its definition we can see that the hardening rate is a measure of how sensitive an asphalt binder's viscosity is to aging time. Obviously, binders having low hardening rates are desired.

Recognizing that η_0^* is a function of the extent of oxidation which in turn increases with time according to appropriate oxidation kinetics, i.e., $\eta_0^* = \eta_0^*(CA(t))$, the hardening rate can be expressed as the product of two derivatives:

$$\partial (\ln \eta_0^*) / \partial t = [\partial (\ln \eta_0^*)/ \partial CA] [\partial CA / \partial t] \qquad (5\text{-}2)$$

where CA is carbonyl area measured by FTIR. Carbonyl area is used as an indicator of oxidation extent because it represents the oxidation product, including ketones, carboxylic acids and anhydrides and other compounds with the C = O bond in a way that relates directly to viscosity hardening and total oxidation (Lau et al., 1992; Liu et al., 1998b).

The first term on the right side of Equation 5-2 is called the hardening susceptibility (HS), which is a characteristic property for asphalts. It indicates the sensitivity of the viscosity change due to carbonyl content increase. A desirable asphalt binder would have a comparatively low value of hardening susceptibility, which means that the binder's viscosity would increase slowly with oxidation.

The second term is the oxidation rate, and Lau et al. (1992) reported that after the initial jump period asphalt oxidation as represented by carbonyl area can be described by:

$$CA = CA_0 + r_{CA}\, t \qquad (5\text{-}3)$$

where CA_0 is the intercept, and r_{CA} is the constant reaction rate (oxidation rate) after the early time initial jump period.

Table 5-1 and Figures 5-1a, 5-1b, and 5-1c show the effect of modifiers on hardening rate, oxidation rate, and hardening susceptibility of asphalt binders. The hardening rate is the bottom-line viscosity performance indicator while the oxidation rate and the HS reflect

underlying causes of hardening. In each case in Figure 5-1a, the polymer-modified binders have a lower hardening rate than their corresponding base asphalts. In addition, the difference in hardening rate varies with the base asphalt, modifier type and modifier concentration.

Generally modified binders have a lower oxidation rate than their base materials (Figure 5-1b). However, the difference in oxidation rate between them is much smaller than the difference in hardening rate. There are even some exceptions: Fina AC-10 1 percent SBR, GSAC AC-10 3 percent SBS, and Wright AC-20 5 percent tire rubber plus from 2 to 5 percent SBS have higher oxidation rate than their corresponding base asphalts.

Similar to hardening rate, modified binders have lower hardening susceptibility than unmodified ones, i.e. the viscosity of modified binders is less sensitive to oxidation than that of base asphalts (Figure 5-1c). This is true for each material tested in this study, although the effect is relatively minor in some cases. At this point, we can only hypothesize possible reasons for this phenomenon as 1) polymer modifiers interfere with asphalt associations to the extent that in the presence of polymer, asphalt oxidation doesn't produce as much or as strong associations as in its absence and 2) with aging polymer modifiers may decompose, resulting in a decrease in viscosity enhancement on the modifiers part and perhaps even serving to increase the resin portion of the asphalt so as to improve solubilization of the asphaltenes. Due to the strong viscosity increases which occur with asphaltene production, the net effect of this such polymer degradation and asphalt oxidation would still be to increase the binder's viscosity, just not as much as the base asphalt.

The combined effect of oxidation rate and HS reductions is to produce the improved hardening rates in Table 5-1 and Figure 5-1a, but it should be noted that there are some significant differences in asphalt response to modifiers. As was noted above, the HS is reduced (compared to the base asphalt) for all of the asphalt/modifier combinations studied and the oxidation rate is reduced more often than not, but the effect is not universal. For most cases, the reductions are mild and do not generally favor either oxidation rate or HS significantly. However, for three asphalts, the comparisons are more striking. For both the Wright AC-10 and the UR AC-10, the oxidation rate has the greatest improvement (approximately 30 percent) while for the TFA AC-20, the oxidation rate improvement is marginal while the HS improvement is nearly 50 percent. Also, note that the Wright AC-20 modified by both tire rubber and SBS has by far the best improvement in HS (although the oxidation rate is actually increased). These results suggest that there can be some significant compositional effects on asphalt/polymer interactions that impact oxidation and subsequent hardening and that bear further study.

Table 5-1. Effect of Modifiers on Oxidation Properties of Asphalt Binders.

Sample	Hardening Rate (ln (poise)/day)	Oxidation Rate (day^{-1})	Hardening Susceptibility
Fina AC-5	0.00563	0.00122	4.61
Fina AC-5 2% SBR	0.00438	0.00116	3.77
Fina AC-10	0.00552	0.00139	3.96
Fina AC-10 2% SBR	0.00491	0.00132	3.71
Fina AC-20	0.01061	0.00245	4.32
Fina AC-20 1% SBR	0.00780	0.00213	3.66
Wright AC-10	0.00821	0.00153	5.38
Wright AC-10 2% SBR	0.00459	0.00093	4.94
Wright AC-10 3% SBR	0.00372	0.00093	4.01
Wright AC-10 3% SBS	0.00510	0.00102	5.02
Wright AC-20	0.00776	0.00127	6.09
Wright Ac-20 3% SBR	0.00452	0.00108	4.20
Wright AC-20 3% SBS	0.00499	0.00103	4.84
Wright AC-20 5% Tire Rubber + 2~ 5% SBS	0.00380	0.00150	2.53
TFA AC-20	0.00935	0.00118	7.90
TFA AC-20 3% SBR	0.00458	0.00101	4.52
Exxon AC-30	0.00702	0.00123	5.71
Exxon Base 1% SBR	0.00440	0.00088	4.98
UR AC-10	0.00768	0.00197	3.89
UR AC-10 3% SBR	0.00347	0.00122	2.85
GSAC AC-10	0.00438	0.00149	2.94
GSAC AC-10 3% SBS	0.00342	0.00155	2.21

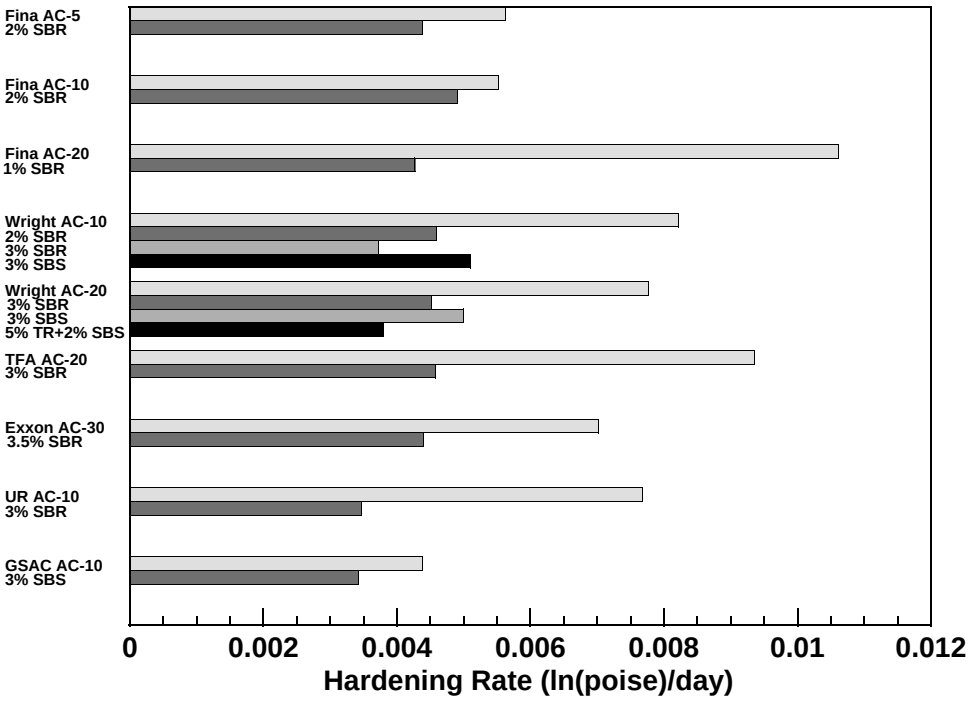

Figure 5-1a. The Effect of Modifiers on Binder Hardening Rates.

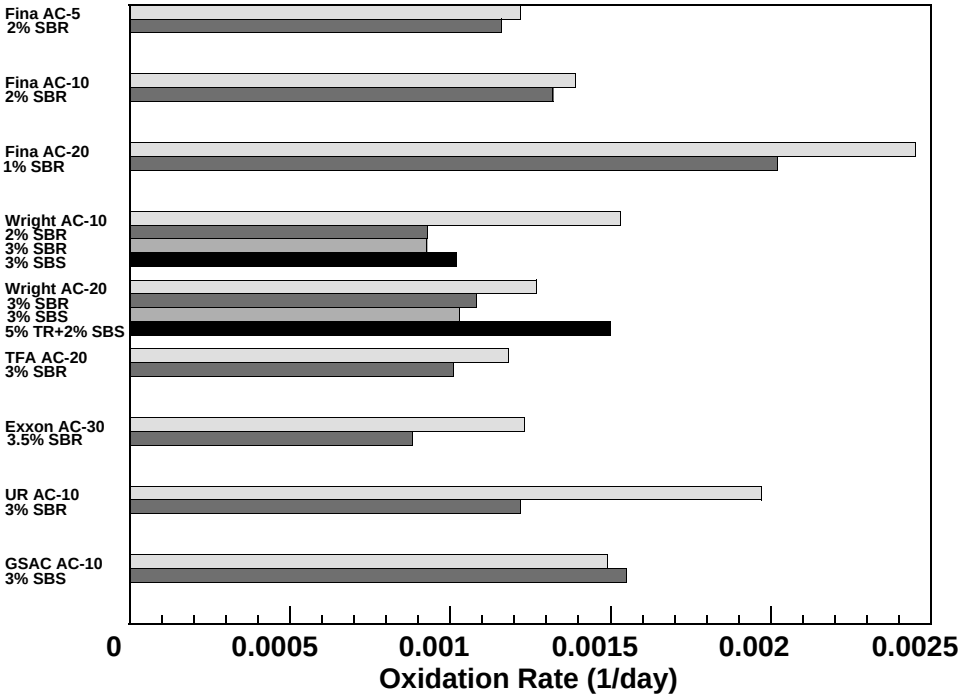

Figure 5-1b. The Effect of Modifiers on Binder Oxidation Rates.

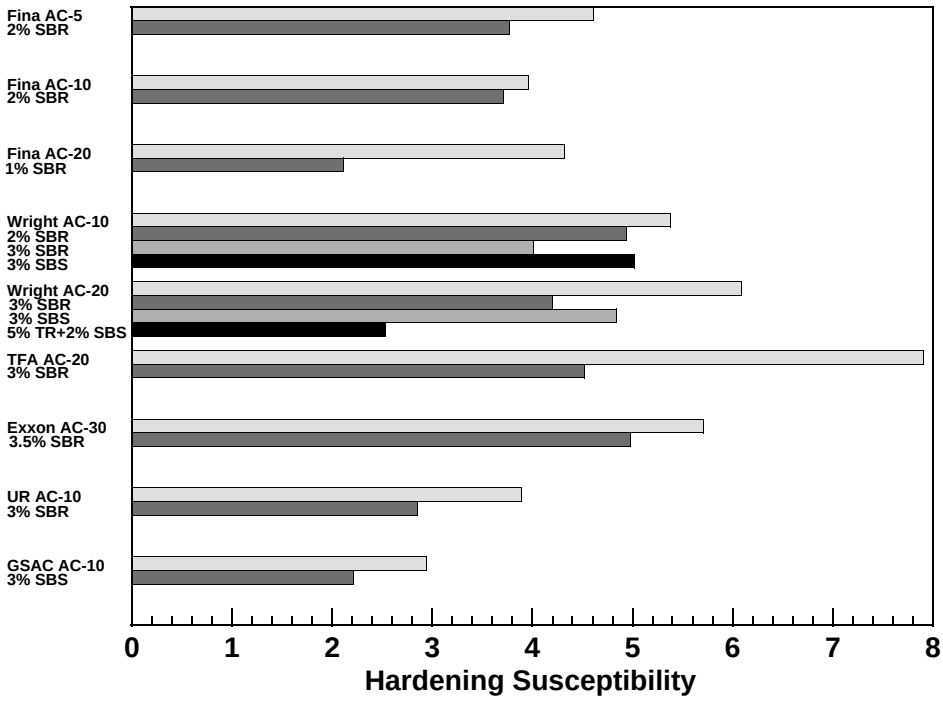

Figure 5-1c. The Effect of Modifiers on Binder Hardening Susceptibilities.

Effect of Aging on Modifiers

Linde and Johansson (1992) aged SBS-modified asphalt at 200 °C for different times and found that after a few hours, there was a significant change in the polymer phase. After 24 hours, almost all of the original SBS had been degraded to lower molecular size. The asphalt phase showed opposite behavior, larger molecular size fractions were formed.

Figure 5-2a, 5-2b, and 5-2c are SEC chromatograms for the Wright AC-10 group aged at 60 °C for 0, 6, and 12 months, respectively. In these figures, the chromatogram is the bottom plot and the top plot is the difference between the modified and unmodified chromatograms for the same amount of aging. For unaged binders (Figure 5-2a), the three peaks (from left to right) correspond to modifiers (polymers), primarily asphaltenes, and primarily maltenes. Polymer molecules elute from the column before asphaltenes, which means that both SBR and SBS molecules are larger than the associations of asphaltene. The peak of SBS is narrower and higher than that of SBR, meaning that the molecular weight distribution of SBS is narrower than SBR. In addition, the SBS peak elutes somewhat earlier than the SBR peak, indicating that the molecular weight of SBS is a little higher than that of SBR.

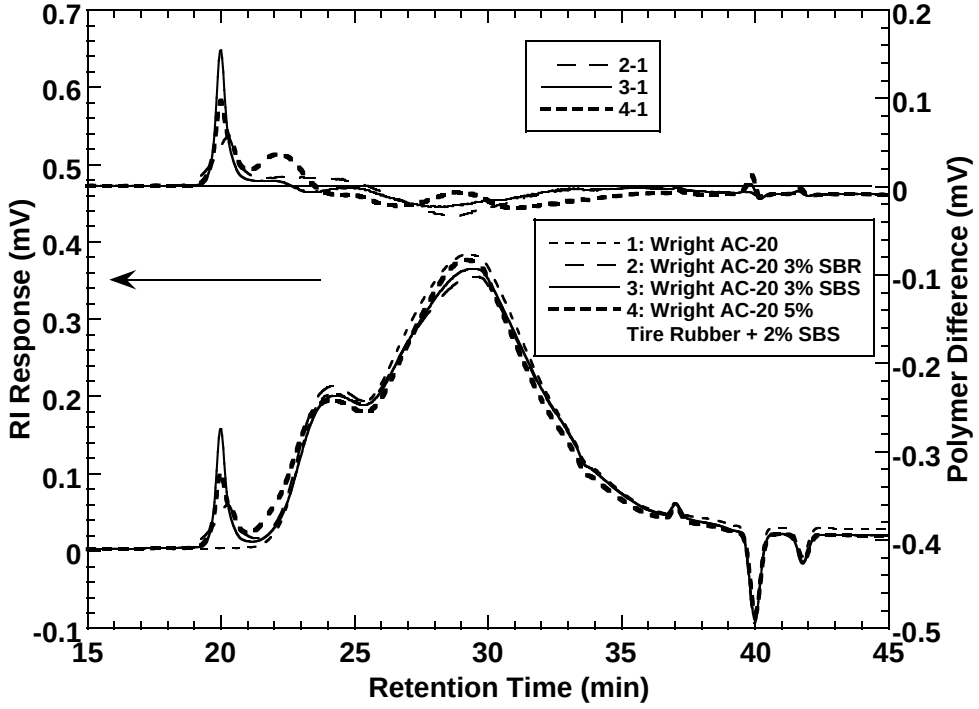

Figure 5-2a. SEC Chromatograms for Wright AC-10/SBR or SBS: Unaged.

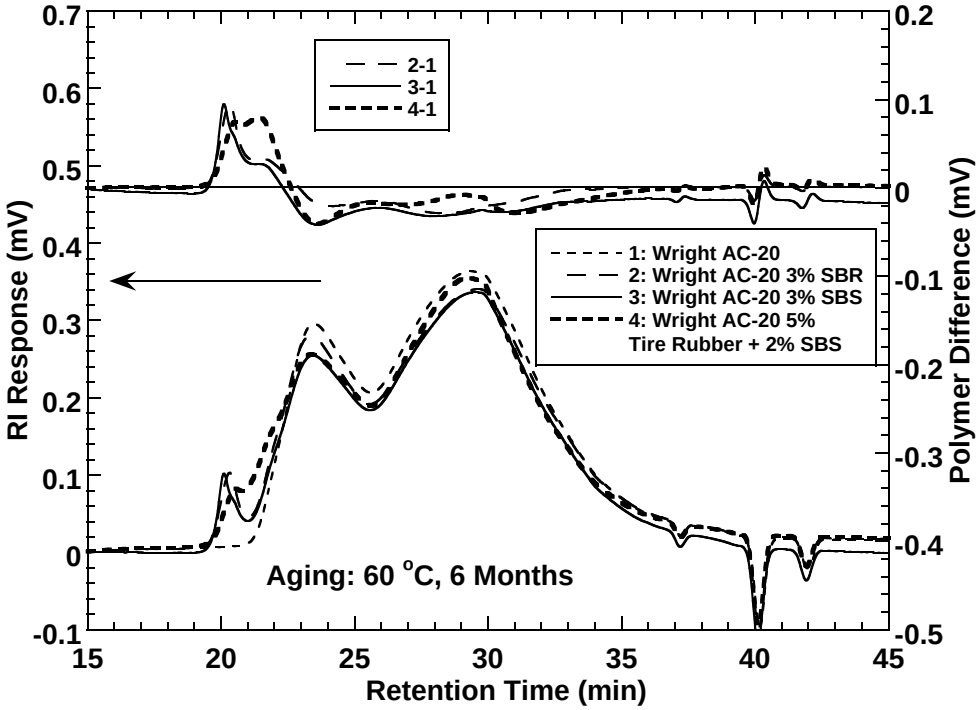

Figure 5-2b. SEC Chromatograms for Wright AC-10/SBR or SBS: Aged 6 Months

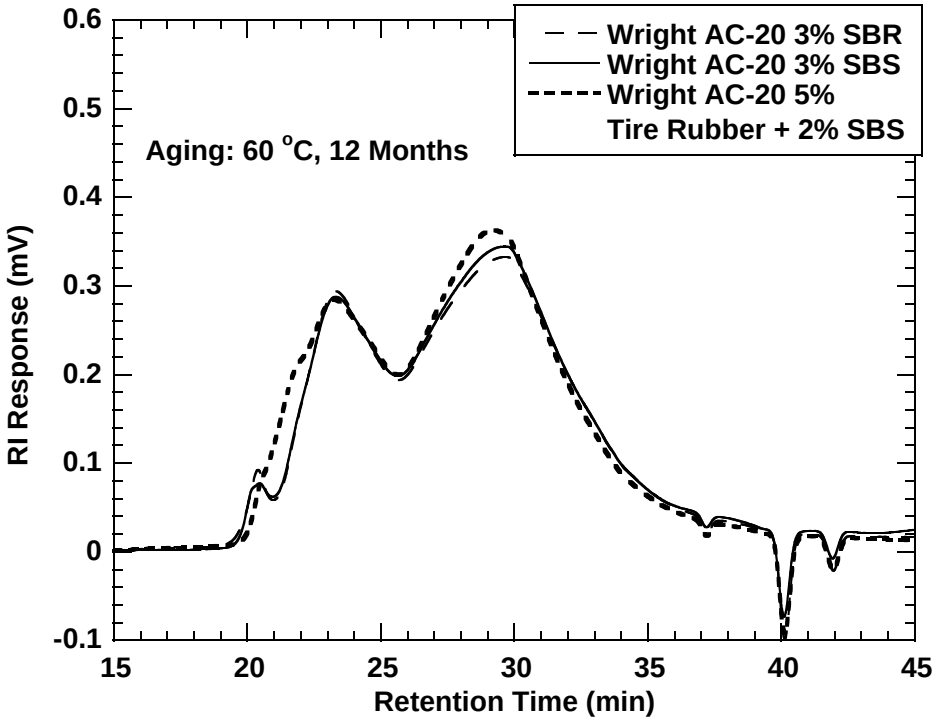

Figure 5-2c. SEC Chromatograms for Wright AC-10/SBR or SBS: Aged 12 Months.

After 6 months aging at 60 °C, three prominent differences between Figure 5-2b and Figure 5-2a are evident. First, the asphaltene peak has increased dramatically in size and shifted earlier in time. This phenomenon is the result of production of more asphaltene from naphthene and polar aromatics and from an increase in the size of the asphaltene structures due to increasing molecular interactions (Mullins and Sheu, 1998). Second, the polymer peak has shifted to a later time, indicating that the large polymer molecules decompose to smaller ones. Third, there is almost no difference between SBS (3 percent) peak and SBR peak (3 percent). By a full 12 months aging (Figure 5-2c), the polymer peak almost merges into the asphaltene peak, meaning that the polymers have been further decomposed. In addition, there is almost no difference between the asphaltenes peaks in Figures 5-2b and 5-2c. While this might be attributed to minimal asphaltene growth in subsequent aging, the HS value of about five would argue against this. It may be more likely that large "asphaltene" growth in the first 6 months actually is due to a combination of degraded polymer and asphaltene and that further aging actually reduces the polymer contribution as asphaltenes continue to grow.

Figures 5-3a and 5-3b are SEC chromatograms for the PG70 group aged for 0 and 6 months at 60 °C, respectively. From the bottom chromatogram, we can see that with the increase in tire rubber concentration, the asphaltene peak decreases. Our explanation is that tire rubber particles can adsorb asphaltene, and some rubber particles are larger than the filter pore (0.45 μm), so they could not go though the filter and GPC could not measure these large particles. The upper spectrum indicates that tire rubber particles are larger than asphaltene.

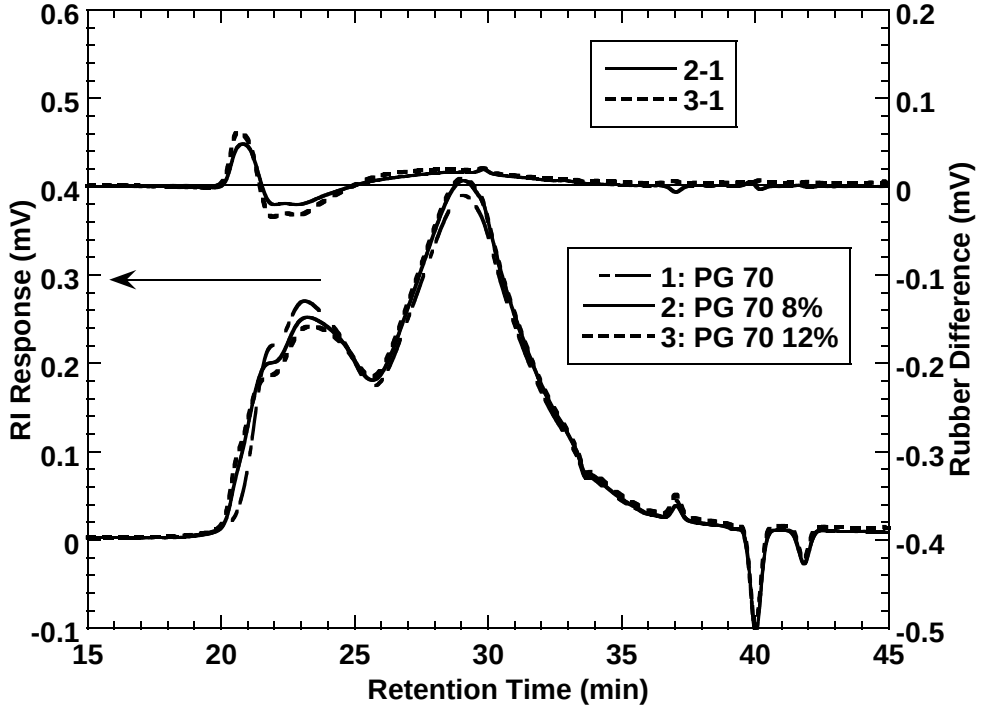

Figure 5-3a. SEC Chromatograms of a PG-70/HC-CRM: Unaged.

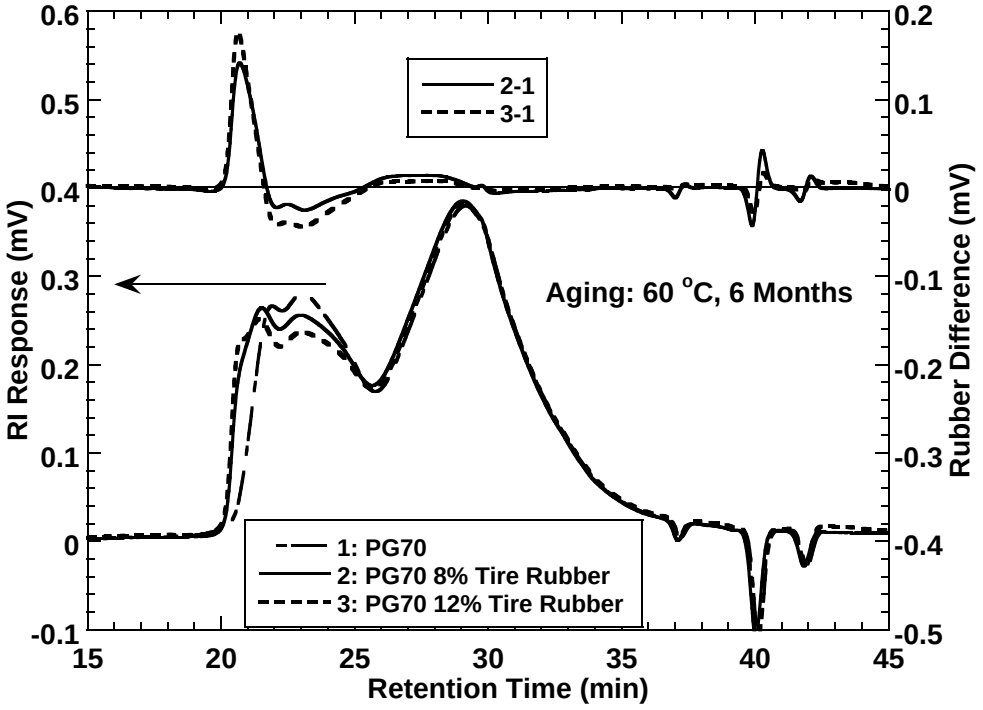

Figure 5-3b. SEC Chromatograms of a PG-70/HC-CRM: Aged 6 Months.

After 6 months aging (Figure 5-3b), the asphaltene peak increases and moves to the left slightly, meaning these asphalts have not produced much asphaltene upon aging. The upper spectrum indicates that the height of the tire rubber peak increases with aging. Our explanation is that during the aging procedure, oxygen could break down rubber particles so that more tire rubber particles pass through the filter. As a result, the rubber concentration in the SEC sample increases.

Conclusion

Polymer-modified binders tend to have a lower hardening rate than their corresponding base asphalts. The extent of decrease in hardening rate is different for different base asphalts and occurs due to the combined effects of aging on oxidation rate and hardening susceptibility. Modified binders also have a lower oxidation rate than their base materials, but the difference is not as large as that of hardening rate, and there are even some exceptions. Finally, modified binders have lower hardening susceptibility compared with their base materials, and in some cases the results can be dramatic. Chapter 6 presents additional results on oxidation and hardening of asphalts and modified asphalts.

With oxidative aging the asphaltene content in binders increases, and modifiers such as SBR, SBS, and tire rubber degrade to smaller molecules. The impact of this degradation and other effects of aging polymer-modified asphalts on binder properties are discussed further in the next sections.

EFFECT OF POLYMER MODIFIERS AND OXIDATION ON RHEOLOGICAL PROPERTIES

Abstract

The effect of different polymer modifiers and long-term aging on rheological properties of asphalt binders is presented. Modifiers include diblock poly(styrene-butadiene) rubber , triblock poly(styrene-butadiene-styrene), and tire rubber.

The addition of polymer to unmodified asphalt can lead to a higher complex modulus at high pavement temperature and a lower stiffness at low pavement temperature, meaning polymer modification can bring better rutting (high-temperature permanent deformation) and thermal cracking (low-temperature failure) resistance to pavement. Also polymer-modified binders have broader relaxation spectra than their base asphalts. The existence of a plateau region in loss tangent master curves of modified asphalts indicates the formation of a polymeric network. In addition, polymer additives impart more non-Newtonian properties to base asphalts. Aging increases the complex modulus (especially at high temperatures), decreases the phase angle, lowers the ductility, and damages the polymer network in binders. Aging can also decrease phase angle and destroy the polymeric network inside binders. Finally, aging can broaden the relaxation spectrum of asphalt binders.

Only one linear region where stress increases with elongation exists for unmodified asphalt binders. However, for modified binders, there is an additional region characteristic of the polymer network. SBR-modified asphalt binders can extend longer but build smaller stress than SBS-modified samples due to stronger interaction between SBS and asphalt components and the higher modulus of the polymer network.

With aging, the asphaltene content in binders increases, and modifiers such as SBR and SBS molecules degrade. The result is a reduction in the polymer benefit.

Introduction

Polymer modification of asphalt led to superior rutting resistance compared to the straight asphalt, and it was explained that SBS incorporated in binders could help to form a polymeric network structure that led to enhanced performance, especially at elevated temperatures (Bouldin and Collins, 1992; Lu and Isacsson, 1999). In addition, the formation of a polymeric network depends on both asphalt source and polymer type (Newman, 1998). Gahvari (1997) investigated the effect of SBR, SBS, and poly(styrene-ethylene-butylene-styrene) (SEBS) on the rheology of pavement asphalt and found that the addition of polymers into straight asphalt could decrease their temperature sensitivity and loss tangent and also broaden their relaxation spectra. Another study found that the addition of from 3 to 6 percent polymer into asphalt cement could result in higher viscosity and lower penetration, improved elasticity, and adhesion and tensile characteristics (Dhalaan et al., 1992). Apart from the beneficial environmental impact of the disposal of degrading wastes by recycling rather than by dumping, the introduction of waste tire rubber into asphalt results in a series of improvements, including resistance to fatigue cracking, greater flexibility at low temperatures, improved elasticity, greater adhesion, and higher aging resistance (Ista and Choquet, 1992).

The aging of polymer-modified asphalts is another important issue. Polymer-modified binders were aged for a short time with different methods, and it was found that aging resulted in the degradation of polymer additives (Lu and Isacsson, 1999) and improved elasticity of binders (Newman, 1998).

There are some studies about the effect of aging on the rheology of polymer-modified binders, but they address short-term (hot-mix) aging rather than long-term aging that is more relevant to pavement durability. Also there is no detailed research on the effect of polymer modification on extensional flow and failure of asphalt binders, an important issue to thermal and fatigue cracking in pavements. These two issues are assessed in this section.

Experimental Methodology

Materials

The unmodified asphalt is an AC-20, and polymer additives include diblock poly

(styrene-b-butadiene) rubber (SBR), triblock poly (styrene-b-butadiene-b-styrene) (SBS), and ground tire rubber well-cured in the asphalt.

Aging Method

All asphaltic materials were aged at 60 °C in a controlled environmental room for 6 months to simulate long-term road aging of approximately 4.5 years (Jemison et al., 1992). Aging at 60 °C was selected to approximate the temperature at which the bulk of pavement oxidation occurs. Higher temperatures, while speeding the process, do not accurately duplicate the balance of reactions that occur, and this is likely to be especially significant for polymer-modified materials.

Test Methods

Dynamic shear properties were measured with a Carri-Med CSL500 dynamic shear rheometer. Measurements were conducted at five temperatures: 0, 10, 25, 40, and 60 °C and frequencies from 0.1 to 100 rad/s, and the time-temperature superposition principle was used to construct master curves for complex modulus G^* and loss tangent tan δ (phase angle δ).

Ductility was obtained at 15 °C and an extensional speed of 1 cm per minute in accordance with ASTM D113-86 (1994). The ductility sample has a 3 cm initial gauge length and a tapered throat. Ductility is recorded as the amount of extension in centimeters of the asphalt specimen before break. Force ductility measurements were obtained at 4 °C and 1 cm per minute elongation speed. In this case the specimen was similar to the ductility specimen except that the initial gauge length, while still 3 cm in length, had a uniform cross-section 1 cm by 0.5 cm. A strain gauge measured force up to 100 Newton and this measurement was used to estimate stress as a function of extension ratio.

A Waters GPC system was used to measure the molecular size distribution of the asphaltic materials.

Results and Discussion

1. Effect of Modifiers on Dynamic Shear Modulus

An AC-20 asphalt binder was selected for study, and it was modified by the supplier with 3 percent SBR, 3 percent SBS, and 5 percent tire rubber plus 2 percent SBS. Figure 5-4a shows the dynamic shear modulus (G^*) master curves for the base and modified asphalt binders at a reference temperature of 0 °C. Compared with their base, modified binders showed a marked increase in the complex modulus at low angular frequency (high temperature). This means that the addition of polymers into asphalt makes it stiffer at high temperature, and as a result, polymer-modified binders have better rutting resistance than their base. At high angular frequency (low temperature), the trend is opposite: the addition of polymer brings a lower

stiffness to asphalt binder to make it easier to deform, and this will bring better thermal cracking resistance to the pavement. However, the effect of polymer on asphalt binder at high temperature is much more obvious than that at low temperature. At high temperature, the addition of 5 percent tire rubber plus 2 percent SBS increased the complex modulus approximately 10 times, but at low temperature it decreased the complex modulus by only about 15 percent.

Polymers vary in their ability to change the complex modulus. Comparing 3 percent SBR and 3 percent SBS for this base material, the SBR was somewhat more effective at increasing the base asphalt's stiffness at high temperature.

Figure 5-4a also indicates the effect of polymer modification on the slope of complex modulus master curve (Gahvari, 1997). Over almost the entire frequency range, the addition of polymers into the base asphalt brings a considerable decrease in the slope of complex modulus master curve. This decrease in the slope means the polymer-modified asphalt binders have improved temperature susceptibility over the unmodified binder with respect to G*.

Figure 5-4b shows the effect of 6 months of aging at 60 °C relative to the unaged materials in Figure 5-4a and indicates that oxidative aging increases G*, especially at high temperatures (low frequency). At low temperature (high frequency), the change in G* is relatively small with aging. As a result, the slope of G* versus ω curve decreases with aging, meaning that aging makes the asphalt binder less temperature sensitive in G*. Note that these effects are true of both the modified and unmodified materials.

2. Effect on Phase Angle

Loss tangent is another very important rheological parameter for asphalt binders. The desired effect of polymer modification is to provide a polymer network that imparts elastic stability at higher temperatures, and this is indicated by a decrease in loss tangent (Tayebali et al., 1992). Figure 5-5a shows loss tangent master curves for the unaged AC-20 series. It is clear that except for the high angular frequency (low temperature) region, the addition of polymers to asphalt decreases the loss tangent (or phase angle) value significantly, meaning that these polymers bring elasticity to the base asphalt. SBR is more effective than SBS in this regard, and AC-20 modified with 5 percent tire rubber plus 2 percent SBS has the lowest phase angle due to the inclusion of the more elastic tire rubber.

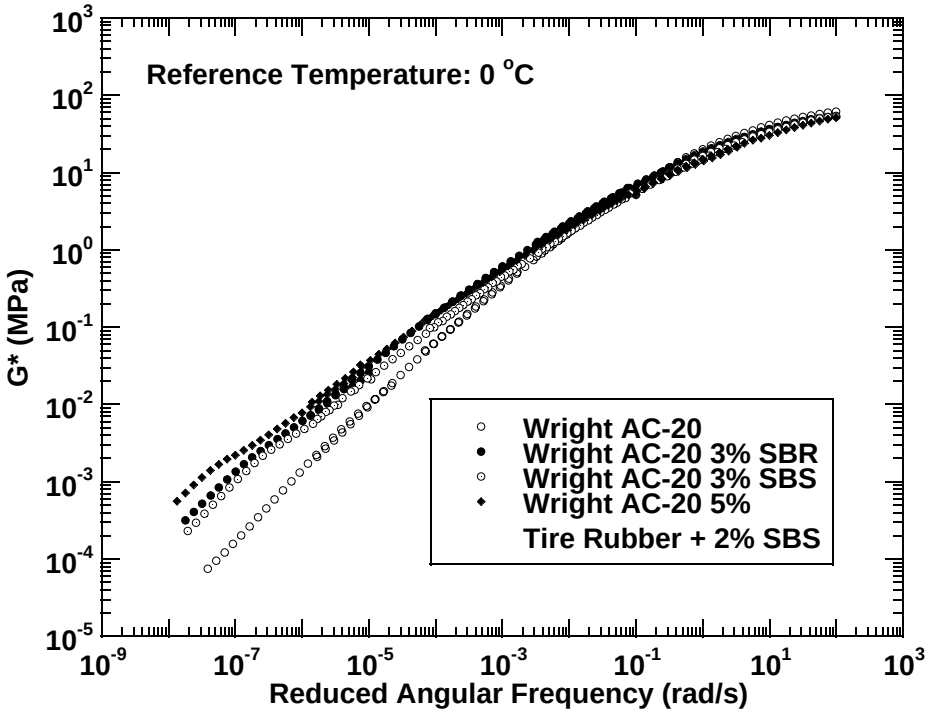

Figure 5-4a. G* Master Curves at 0 °C: Unaged.

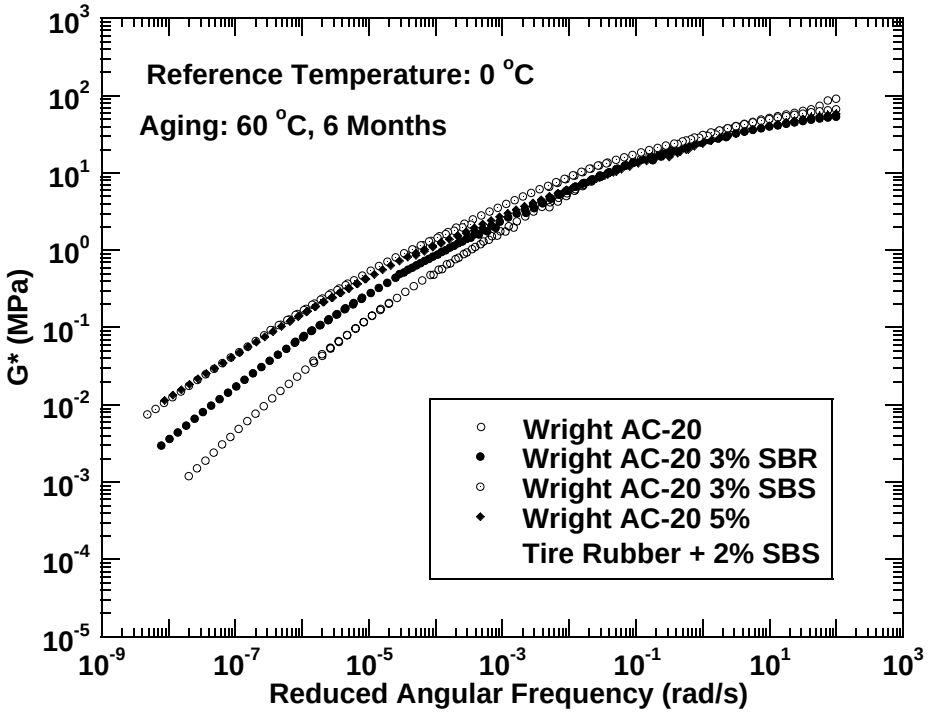

Figure 5-4b. G* Master Curves at 0 °C: Six Months Aging at 60 °C.

Figure 5-5a also indicates that the addition of polymer brings a plateau region to the loss tangent master curves over the intermediate angular frequency range (approximately from 10^{-6} to 10^{-3} rad/s at the 0 °C reference temperature). A true plateau region is absent for the SBR and SBS-modified AC-20, but for the asphalt modified with 5 percent tire rubber plus 2 percent SBS, there is a well-defined plateau region, suggesting the formation of a strong polymer network (Goodrich, 1988; Collins et al. 1991).

Aging results in a significant shift of the entire loss tangent (also phase angle) curve in the direction of more elastic (G′ increases even more than G″) behavior (Figure 5-5b). Also, the plateau region becomes less pronounced, suggesting that the polymer network has been damaged by oxidation.

3. Effect on Relaxation Spectrum

According to Anderson et al. (1992), polymer modifiers can extend the relaxation processes to longer times. Figure 5-6a shows the relaxation spectra for this AC-20 series. Derivation of the spectra was based on the procedure of Ferry (1980). Experimental data indicate that the inclusion of polymer into base asphalt results in a broader relaxation spectrum. In addition, the broadening effect of polymer modification on relaxation spectrum of asphalt binders is a function of polymer type, and AC-20 with 5 percent tire rubber plus 2 percent SBS has the broadest spectrum in this series. The reason for longer relaxation time for modified binders is that the polymer modification results in an increase in both in-phase and out-of-phase components of G*, but the relative amounts of increase are different; polymer modification enhances elasticity more than viscosity.

Figure 5-6b shows relaxation spectra after 6 months of aging. The spectra at longer times are shifted upward, indicating that aging makes asphalts more solidlike (Ferry, 1980).

4. Effect on Shift Factor

Anderson et al. (1994) found that for asphalt cements, the temperature dependence of the viscoelastic behavior, as indicated by the shift factors determined from construction of master curves, can be represented by the WLF equation above the defining temperature, T_d:

$$\log a(T)_d = -C_1(T-T_d)/(C_2+T-T_d) \qquad (5\text{-}4)$$

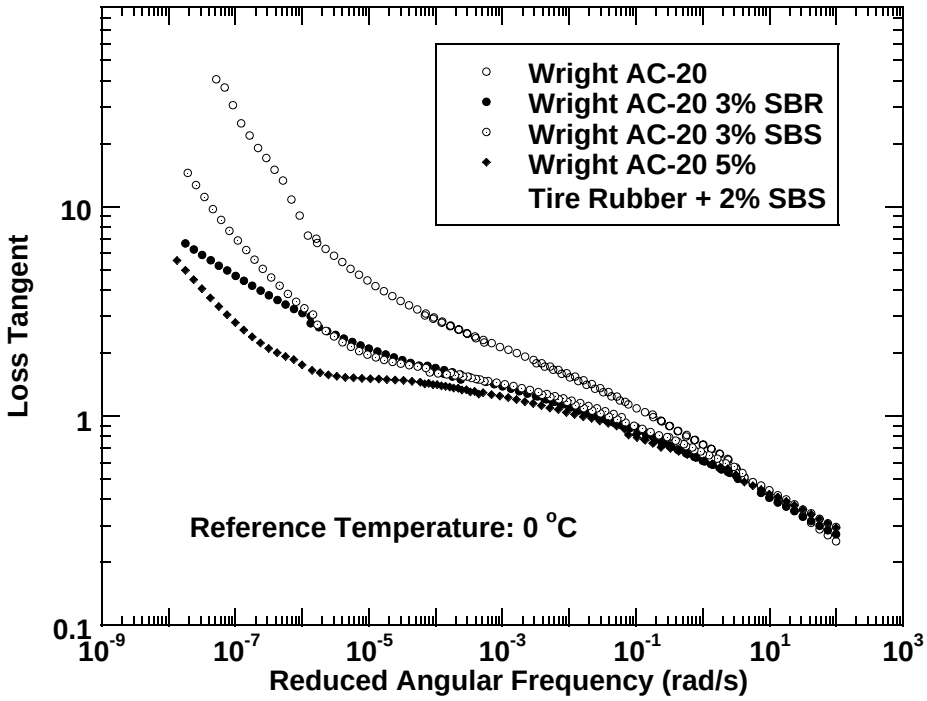

Figure 5-5a. Loss Tangent Master Curves at 0 °C: Unaged.

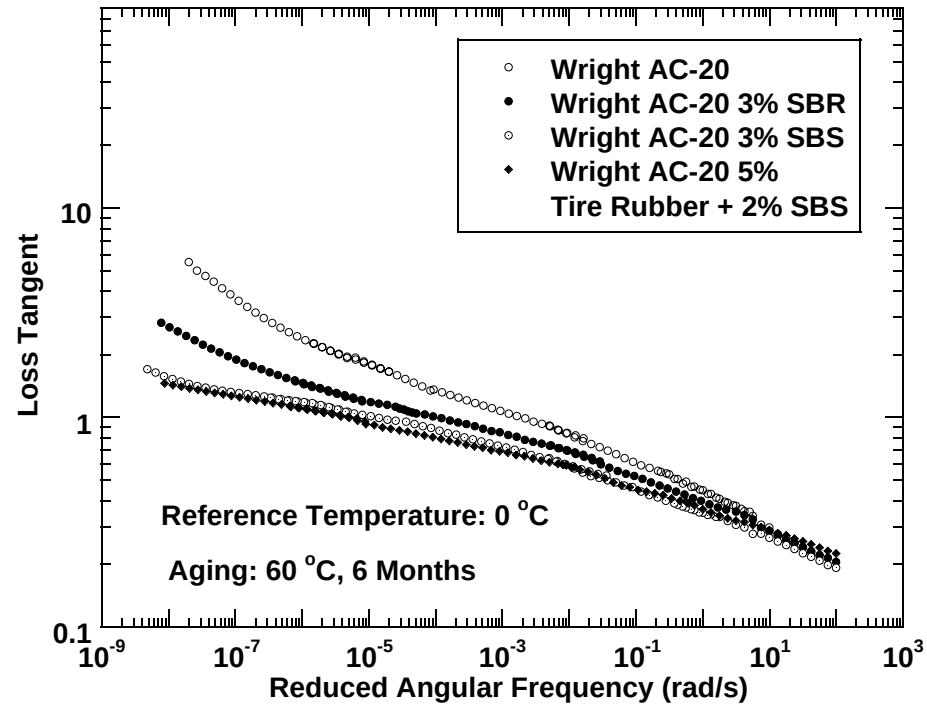

Figure 5-5b. Loss Tangent Master Curves at 0 °C: Six Months Aging at 60 °C.

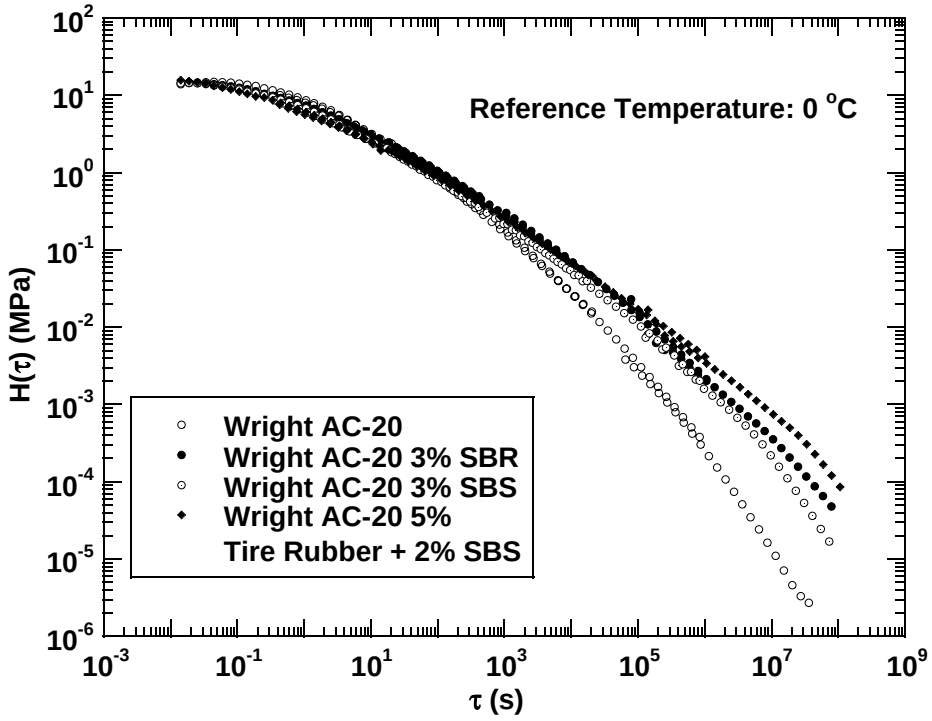

Figure 5-6a. Relaxation Spectra at 0 °C: Unaged.

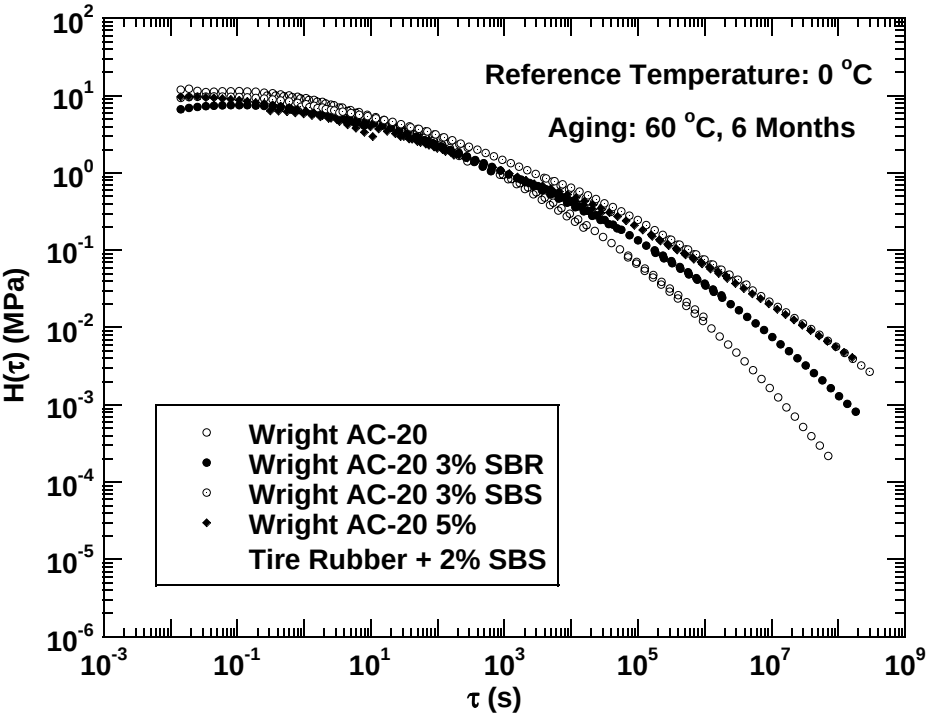

Figure 5-6b. Relaxation Spectra at 0 °C: Six Months Aging at 60 °C.

where $a(T)_d$ is the shift factor relative to the defining temperature; C_1 and C_2 are experimental constants; T is temperature (°C or K); and T_d is the defining temperature, a characteristic parameter for each asphalt cement.

Anderson et al. (1994) analysis on SHRP asphalts found that the values of C_1 and C_2 could be approximated by the fixed values 19 and 92, respectively. As an approximation, these constants were also assumed for the AC-20 series, although it would be reasonable to assume that other values might be more appropriate, especially for the polymer-modified materials. From experimentally determined values of the shift factor, the WLF equation was used to estimate the best value of T_d for each material, using the fixed values of C_1 and C_2. Figure 5-7a is the comparison between the WLF equation and the experimental shift factor values. The values of T_d are shown in the legend for each material. There is some difference between the model and the experimental data, and this may be the result of using universal values for the two constants C_1 and C_2.

Aging does not have much effect on shift factor a(T) (Table 5-2, Figure 5-7b, c). The defining temperature T_d for the aged SHRP asphalts is the average value for the PAV-aged binders, as reported by Anderson et al. (1994).

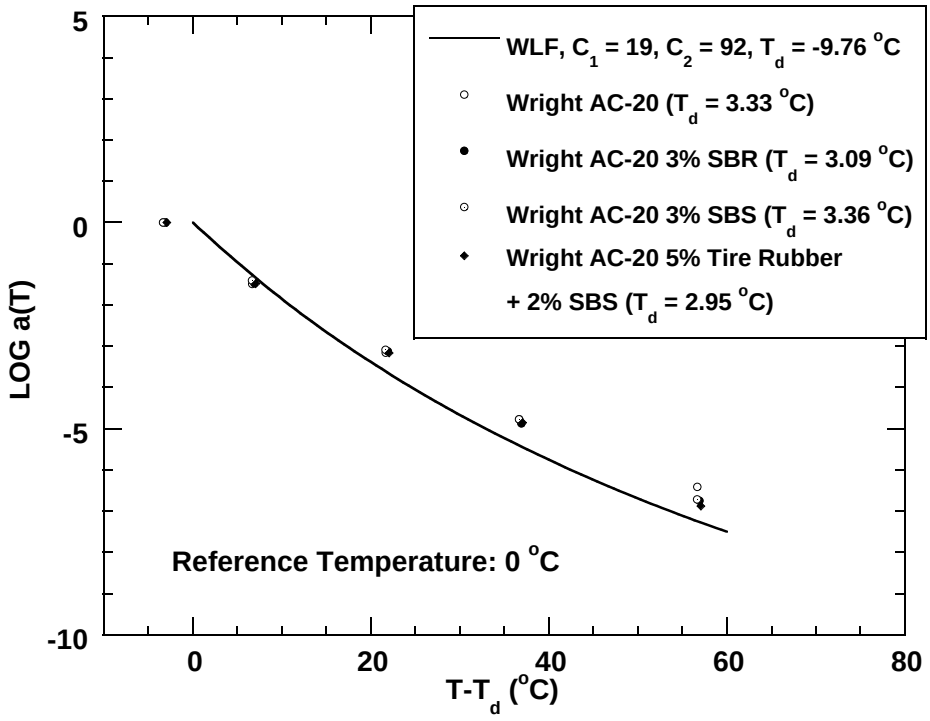

Figure 5-7a. Shift Factors Variation with Temperature for 0 °C Master Curves: Unaged.

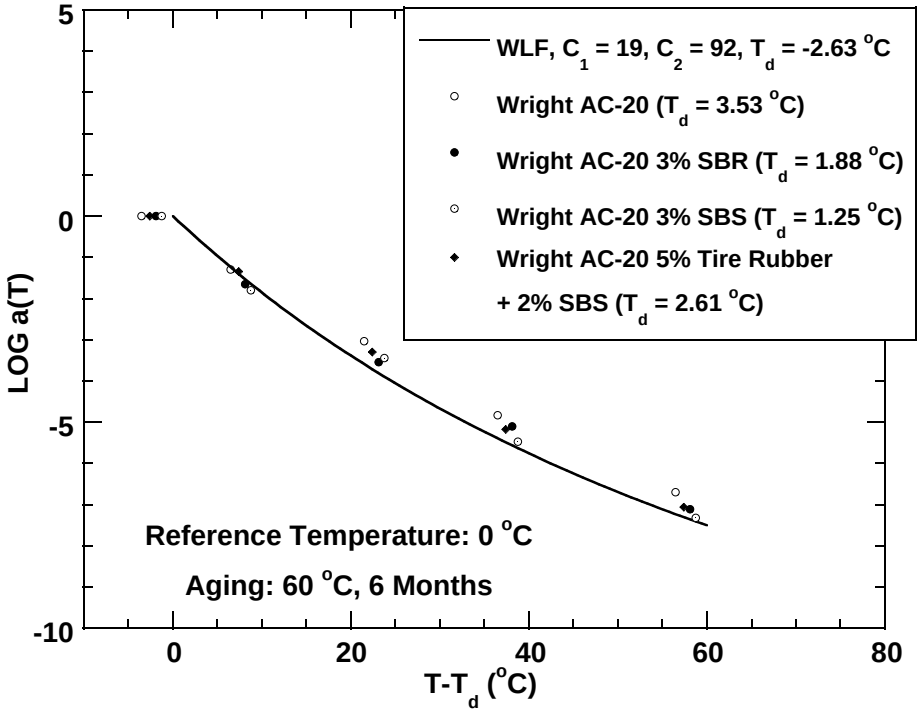

Figure 5-7b. Shift Factors Variation with Temperature for 0 °C Master Curves: Aged Six Months at 60 °C.

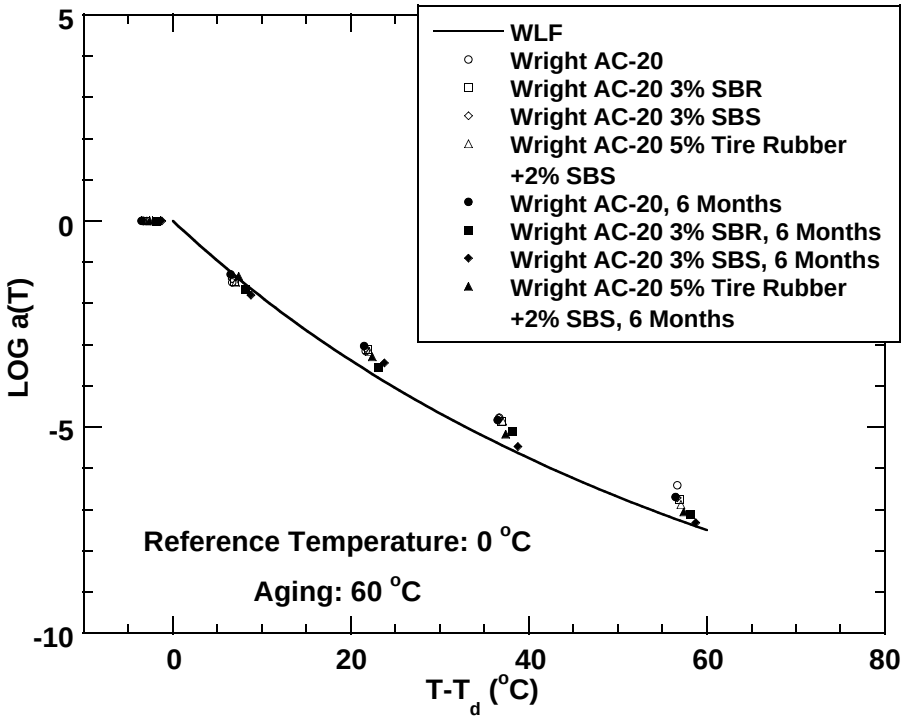

Figure 5-7c. Shift Factors Variation with Temperature for 0 °C Master Curves: All.

Table 5-2. Effect of Modifiers and Aging on Asphalt Shift Factors.

Material	Temperature (°C)				
	0	10	25	40	60
Wright AC-20	1.00	3.24×10^{-2}	6.92×10^{-4}	1.68×10^{-5}	3.87×10^{-7}
Wright AC-20 6 months	1.00	5.07×10^{-2}	9.24×10^{-4}	1.48×10^{-5}	2.00×10^{-7}
Wright AC-20 3% SBR	1.00	3.38×10^{-2}	7.54×10^{-4}	1.34×10^{-5}	1.29×10^{-7}
Wright AC-20 3% SBR 6 months	1.00	2.25×10^{-2}	2.89×10^{-4}	7.92×10^{-6}	7.73×10^{-8}
Wright AC-20 3% SBS	1.00	3.93×10^{-2}	8.20×10^{-4}	1.69×10^{-5}	1.93×10^{-7}
Wright AC-20 3% SBS 6 months	1.00	1.58×10^{-2}	3.60×10^{-4}	3.36×10^{-6}	4.79×10^{-8}
Wright AC-20 5% tire rubber plus 2% SBS	1.00	3.28×10^{-2}	6.83×10^{-4}	1.40×10^{-5}	1.33×10^{-7}
Wright AC-20 5% tire rubber plus 2% SBS 6 months	1.00	4.56×10^{-2}	5.07×10^{-4}	6.75×10^{-6}	8.70×10^{-8}

5. Effect on the Frequency Dependence of η_o^*

Figure 5-8 indicates the frequency dependence of the complex viscosity of this AC-20 series of asphalts. For both the unaged and aged samples, polymer modification results in an extension in non-Newtonian behavior to lower frequencies. In addition, aging alone can increase the non-Newtonian behavior. Also, modifiers have different abilities to increase the non-Newtonian property of asphalt binders. For the unaged group, the neat asphalt displays a reasonably Newtonian behavior, and the dynamic viscosity does not change much with the angular frequency. Both 3 percent SBR and 3 percent SBS impart almost the same extent of non-Newtonian property into the neat binders. But for the asphalt modified with 5 percent tire rubber plus 2 percent SBS, due to the presence of more elastic tire rubber particles, it displays a much more non-Newtonian property. Oxidative aging will produce asphaltene from polar aromatics inside asphalt binder, and asphaltene is a kind of solid particle. As a result, aged asphalt will display more non-Newtonian property than an unaged one. Figure 5-8 shows that after 6 months of aging at 60 °C, even the neat AC-20 begins to show apparent non-Newtonian behavior. For aged modified binders, there will be two opposite effects as to their non-Newtonian property. The first one is that the aging will produce more elastic asphaltene particles, and this will increase the content of non-Newtonian property. The second one is that the oxidative degradation of polymeric additives will decrease the content of non-Newtonian behavior. The experimental data show that the first effect is predominant.

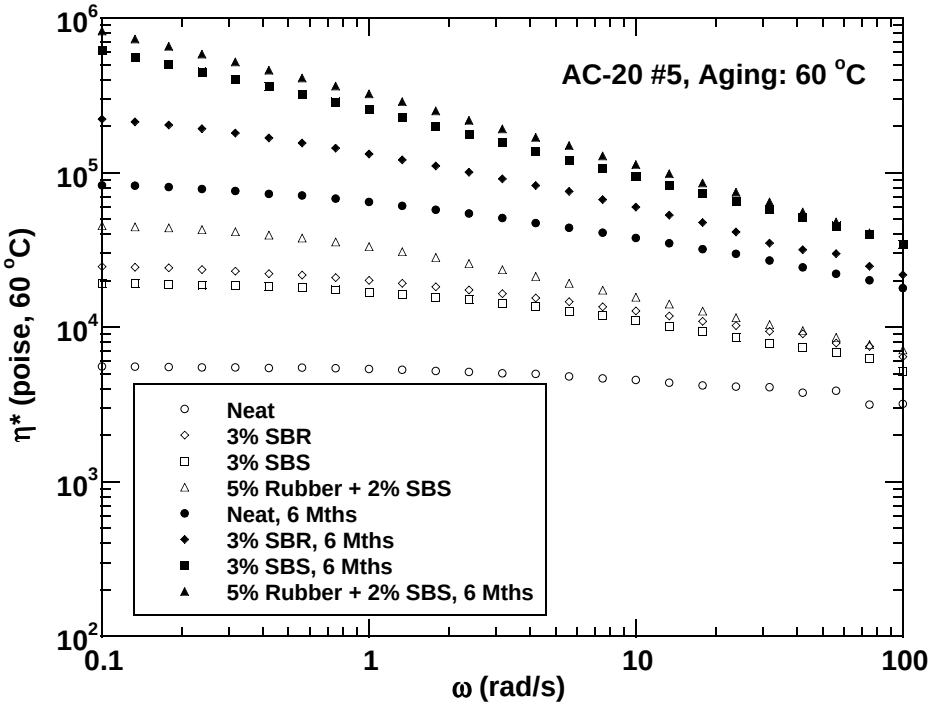

Figure 5-8. Shift in Complex Viscosity Behavior with Aging at Low Frequency.

Effect of Aging on Modifiers

Linde and Johansson (1992) aged SBS-modified asphalt at 200 °C for various times and found that after a few hours, there was a significant change in the polymer phase. After 24 hours, almost all of the original SBS had been degraded to a lower molecular size. The asphalt phase showed opposite behavior as larger molecular size fractions were formed.

Figures 5-2a and 5-2b, presented earlier, are SEC chromatograms for this AC-20 group aged for 0 and 6 months at 60 °C, respectively. Each of these figures include two sets of chromatograms: the upper chromatograms are differences between modified and unmodified asphalt chromatograms, and the bottom chromatograms are the corresponding complete SEC chromatograms. In these complete chromatograms, the three peaks (from left to right) correspond to modifiers (polymers), asphaltenes, and maltenes. The larger molecular size polymer elutes from the column before the asphaltenes. Note also that for the material containing ground-tire rubber the polymer peak consists of two peaks. The first peak is believed to be primarily SBS, based upon the material with 3 percent SBS modifier only, while the second peak is well-cured ground tire rubber, i.e., rubber that is small enough to pass through the 0.45 μm pre-column filter.

After 6-months aging at 60 °C, there are several apparent differences between Figures 5-2a and 5-2b. First, the asphaltene peak increases dramatically with aging. This phenomenon results from the production of more asphaltene from naphthene and polar aromatics and from the increase in asphaltene associations (Liu et al. 1998a, Mullins and Sheu, 1998). Secondly, the SBS peak shifts somewhat to later times and decreases dramatically in size, indicating that the polymer molecules decompose to smaller ones. The SBR peak also shifts to the right, but the shift is not as apparent as that of SBS. Third, the upper difference chromatograms indicate that the height of the second polymer peak, the tire rubber peak, increases with aging. We believe that this is the result of oxidation serving to digest more of the rubber to the point that it passes through the prefilter and on to the column (Chipps, 2001).

Effect of Modifiers on Extensional Properties of Asphalt Binders

We found that the addition of modifiers to asphalt binders could significantly increase their ductility. In addition, the effect of the polymer became more pronounced with increasing polymer content (Srivastava et al., 1992). Our experimental data confirm these trends. However, we also found that modifiers can improve binder ductility. The effect is dramatic for lightly-aged materials but diminishes with increased aging to the point that eventually the polymer benefit is gone (Table 5-3). This decrease could be the result of polymer degradation with aging, as seen in Figure 5-2. However, it also could be the result of the underlying asphalt binder stiffening with aging, resulting in failure that the polymer can't overcome. This hypothesis suggests that when the base asphalt is stiff enough, it will fail regardless of the presence of the polymer.

With the significant caveat that our data are limited, SBS-modified binders have lower ductility than SBR-modified ones (Table 5-3), especially at the beginning of oxidation. SBR is the abbreviation for diblock poly(styrene-butadiene) rubber. SBS represents triblock poly(styrene-butadiene-styrene). These molecular structures are shown below.

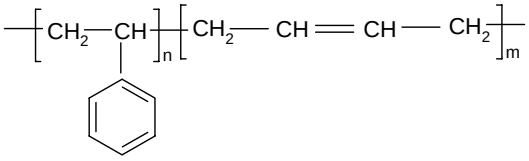

Diblock poly (styrene-b-butadiene) rubber (SBR)

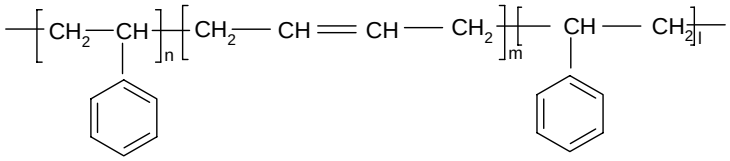

Triblock poly (styrene-b-butadiene-b-styrene) (SBS)

The different elongation properties of SBR-modified and SBS-modified binders could be explained by the different chemical structures of SBR and SBS and the difference in their interactions with asphalt components. The difference in these two polymers is that SBS has two polystyrene blocks, compared to one polystyrene block in SBR. This extra polar and rigid polystyrene block makes the polymer system more resistant to deformation (Linde and Johansson, 1992). In addition, more polar groups in the polymer mean larger interactions between the polymer molecules and asphaltenes and polar aromatics. As a result, the interaction between SBS and asphalt likely is greater than that between SBR and asphalt. So it is more difficult for SBS-modified asphalt to flow and thus stresses that arise from deformation are less easily relieved..

Table 5-3. Effect of Modifiers on Ductility (15 °C, 1 cm/min) of Asphalt Binders.

	Aging Time (months at 60 °C, 1 atm air)				
Material	2	4	6	9	12
Wright AC-20	6.35	5.6	4.6	3.53	2.5
Wright AC-20 3% SBR	39.42	24.35	17.53	6.85	2.3
Wright AC-20 3% SBS	22.13	19.12	13.32	10.7	2.93
Wright AC-20 5% tire rubber plus 2% SBS	16.73	9.17	5.32	3.37	2

Force ductility measurements can provide more details about the effect of modifiers on elongation of asphalt binders. Figure 5-9a shows the effect of SBS and tire rubber plus SBS on the elongation properties of asphalt Wright AC-20. SBR is not included on the graph because the AC-20 modified with 3 percent SBR began to neck down at an extension ratio around four, and stress could not be calculated after this point.

The stress-elongation curve for SBS-modified asphalt and polymer-modified materials in general, may be described in four stages. i) Initially, the unmodified and modified binders behave very similarly and stress is linear with elongation ratio. According to Shuler et al. (1987), in this region, stress arises mainly from deformation of the asphalt itself; the modifier's contribution is very small. Consequently, the initial slope of the stress-extension ratio curve in the linear region will be referred to as "asphalt modulus." ii) Upon additional extension, stress first reaches a maximum value (yield stress) and then begins to decline because of the flow of asphalt specimen. The yield stress of polymer-modified asphalts is a little bit higher than that of the straight asphalt. iii) With further elongation, polymer molecules also extend, and at the same time, these molecules reorientate themselves along the direction of elongation (Kaufman, 1978). This results in an increase in stress arising from the polymer deformation that compensates for the decrease in stress due to the flow of asphalt. These two opposite effects produce an approximately flat region designated as "C" in Figure 5-9a. iv) As deformation proceeds, the

reorientation of polymer molecules continues and increases the crystallinity of the polymer domain, resulting in further increases in stress, as shown in region "E" in Figure 5-9a. In this region, stress is linear with elongation again, and the slope is smaller than "asphalt modulus." This slope is called the "asphalt-polymer modulus" (Lu and Isacsson, 1999). The slope difference comes from the difference in molecular interactions. The "asphalt modulus" is the result of interactions between asphalt components, and these interactions include primary bonding, but also strong polar bonding and the effect of suspended solids (asphaltenes). However, the "asphalt-polymer modulus" is from the interaction between asphalt components and polymer molecules, which are mainly weaker secondary bonds. Note also that the "asphalt-tire rubber-SBS modulus" is larger than "asphalt-SBS modulus." Region D (not shown) is a transition between regions C and E.

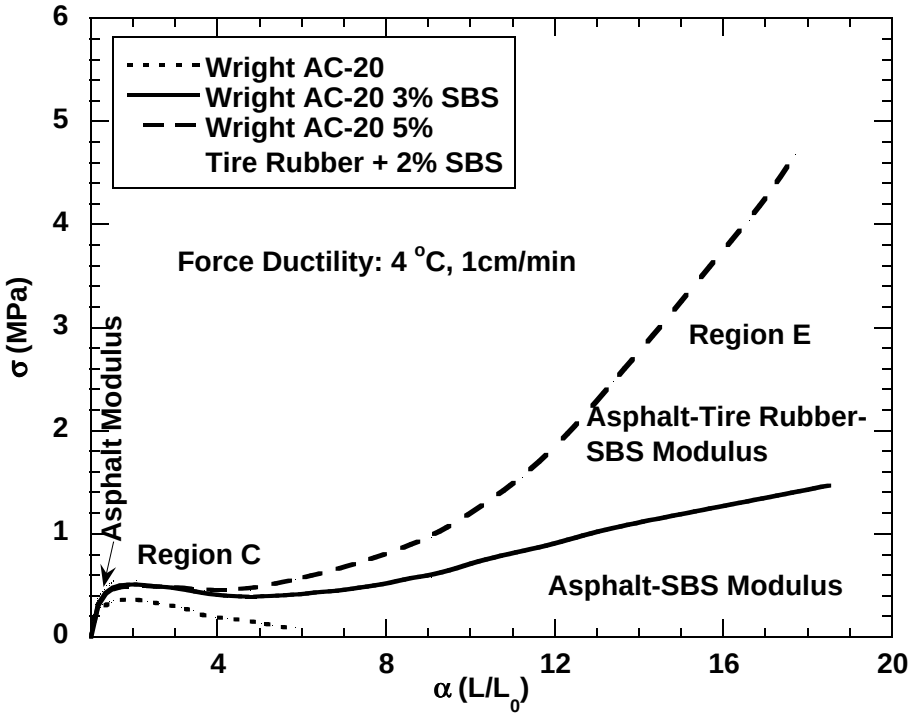

Figure 5-9a. Stress-Elongation Curves at 4 °C: Unaged.

In spite of the significant effect that polymers can have on extensional properties, these effects deteriorate with oxidative aging. Figure 5-9b indicates that after 6 months aging at 60 °C, there is almost no difference remaining between the unmodified and modified binder ductilities and failure stresses, measured at 4 °C.

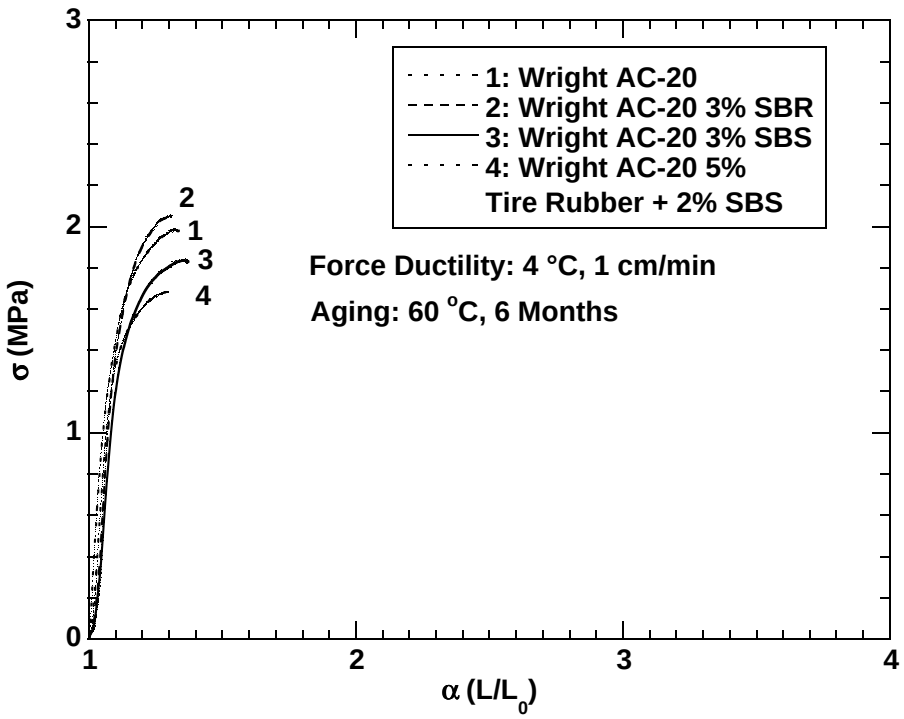

Figure 5-9b. Stress-Elongation Curves at 4 °C: Six Months Aging at 60 °C.

Conclusion

Polymer modification can improve asphalt binder physical properties at both high and low temperatures. However, the benefits tend to be greater to rutting resistance than to improved thermal cracking. Polymer-modified binders have a broader relaxation spectrum than their base asphalt. The existence of a plateau region in loss tangent master curves of modified asphalts suggests the formation of a polymer network. In addition, polymeric additives make the asphalt complex viscosity a stronger function of frequency (shear rate) at high pavement temperatures.

Aging can improve the temperature susceptibility of asphalt binders. Aging can also make asphalt more elastic, damage the polymer network in binders, and result in an extended relaxation spectrum for asphalt binders. These effects result from increases in asphaltene content and degradation of modifiers such as SBR and SBS.

For unaged polymer modified binder, ductility is improved greatly over the unmodified base binder. This is due to the polymer having a lower elastic modulus than the asphalt or the polymer modified material having a higher failure stress, or both. However, with aging, the benefit from modifiers decreases.

RELATIONSHIPS BETWEEN DUCTILITY AND DSR PROPERTIES FOR MODIFIED ASPHALTS

In Chapter 4 we found that for unmodified asphalts ductility correlates well with the DSR parameter $G'/(\eta'/G')$. In addition, for different unmodified binders, this appears to be a universal correlation in the low-ductility region of aged binders. In the previous sections of this chapter we investigated oxidation of polymer modified asphalts and its impact on fundamental rheological properties. In this section we return to the ductility correlation and evaluate it for modified asphalts.

Methodology

Seventeen modified asphalt binders were compared and evaluated through a number of physical properties. The binders were aged at 204 °C (400 °F) by air blowing and at a second temperature, 60 °C (140 °F), in a controlled environment room to obtain properties ranging from those of a slightly aged material to one which would be near the end of its service life. The materials and their aging methods are summarized in Table 5-4.

The experimental methods were the same as for the unmodified asphalts of Chapter 4.

Results and Discussion

Relationship Between Ductility and G', η'/G'

In Chapter 4, consistent with the Maxwell model of linear viscoelasticity, asphalt ductilities measured at 15 °C and 1 cm/min were found to correlate with the DSR parameter $G'/(\eta'/G')$ for aged unmodified binders. Accordingly, this correlation was evaluated for the polymer-modified asphalts.

Figure 5-10 shows a map of G' versus η'/G' for polymer-modified materials measured at 15 °C, 0.005 rad/s. The general trend is similar to unmodified binders. As modified asphalt ages it also moves from the lower right to the upper left, and the ductility declines dramatically along this path. This map clearly shows that for modified asphalts, ductility is related to both η'/G' and G' (stiffness) of the material.

As an alternate way of viewing these same data, ductility is plotted versus the ratio of G' to (η'/G') (Figure 5-11). In comparison to the correlation for unmodified asphalts (Figure 4-12 and the line in Figure 5-11), there is significantly more scatter as well as deviation from the unmodified correlation. There is no linear relationship even in the low ductility region. Obviously, polymer-modified asphalts behave much differently from unmodified asphalts, consistent with the stress elongation curves shown in Figure 5-9a.

Figure 5-12 is another version of Figure 5-11, showing asphalts divided into three rather distinct groups (also shown by the boundary lines in Figure 5-11). The Fina group includes all modified Fina asphalts plus GSAC AC-10 three percent SBS. The Wright group includes all modified Wright asphalts. The UltraPave group includes modified TFA, Exxon, and UR asphalts. For all of the modified materials, for a given value of $G'/(\eta'/G')$, ductility is signficntly better than for the unmodified binders. With aging, all three groups move from the upper left to the lower right, with the differences between them, and also between the unmodified binders, decreasing with aging.

So, for the modified asphalts, there is no universal correlation between ductility and $G'/(\eta'/G')$. However, for different asphalts within the same group, ductility correlates reasonably well with $G'/(\eta'/G')$ (Figure 5-12).

Table 5-4. List of Modified Asphalts Studied.

Aging Method	Asphalt Binders
204 °C Airblowing:	Fina AC-5 with 2 percent SBR
	Fina AC-10 with 2 percent SBR
	GSAC AC-10 with 3 percent SBS
	Wright AC-10 with 2 percent, 3 percent SBR
	Wright AC-10 with 3 percent SBS
	Wright AC-20 with 3 percent SBR
	Wright AC-20 with 3 percent SBS
	Wright AC-20 with 5 percent Tire Rubber + 2 percent SBS
60 °C Environmental Room:	Exxon AC-30 with 3.5 percent SBR
	Fina AC-5 with 1 percent, 2 percent SBR
	Fina AC-10 with 1 percent, 2 percent SBR
	Fina AC-20 with 1 percent, 3.5 percent SBR
	GSAC AC-10 with 3 percent SBS
	Neste AC-20 with 3 percent SBR
	FTA AC-20 with 3 percent SBR
	Wright AC-10 with 2 percent, 3 percent SBR
	Wright AC-10 with 3 percent SBS
	Wright AC-20 with 3 percent SBR
	Wright AC-20 with 3 percent SBS
	Wright AC-20 with 5 percent Tire Rubber + 2 percent SBS
	UR AC-10 with 3 percent SBR

Effect of Polymeric Modifiers on Ductility of Asphalt Binders

It was found that the addition of polymeric additives made asphalts more ductile (Srivastava, 1992). Furthermore, when the ductility of the asphalt in a pavement decreased to the range of 3 to 5 cm, there was serious cracking that developed (Kandahl, 1977). Using a ductility of five cm as a critical value, the additional aging time beyond that of its unmodified base asphalt, for a modified asphalt to reach this critical ductility value we term the "modifier benefit."

Figure 5-13 indicates the modifier benefit for Fina AC-10 asphalt group. When its ductility is low enough due to aging, the logarithm of ductility is linear with aging time. For unmodified Fina AC-10, the aging time to reach the critical ductility value is 8.5 months in the environmental room, and for Fina AC-10 with 1 percent SBR and 2 percent SBR, the times are

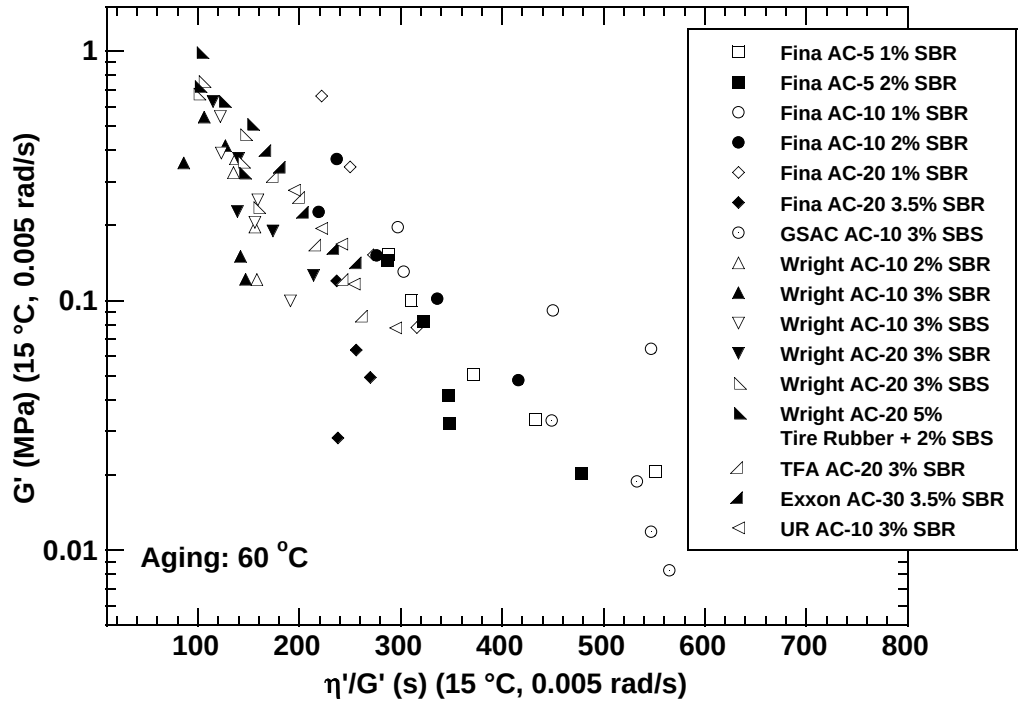

Figure 5-10. Ductility Map for Modified Asphalts.

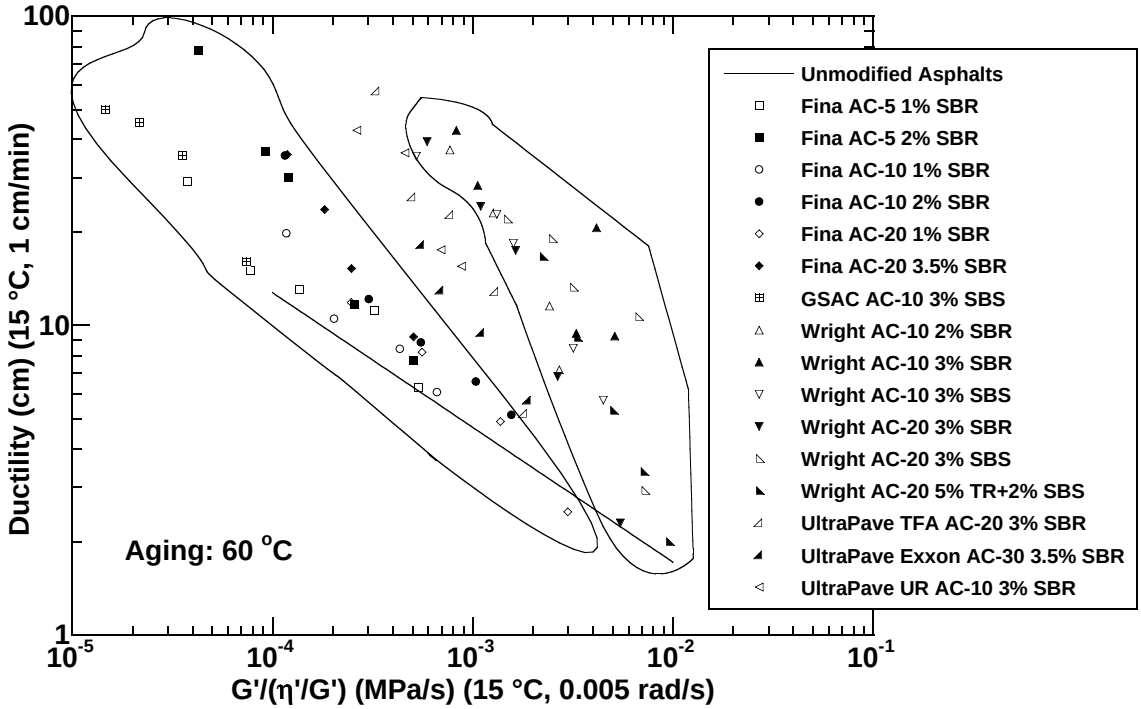

Figure 5-11. Ductility versus G′/(η′/G′) for Modified Asphalts.

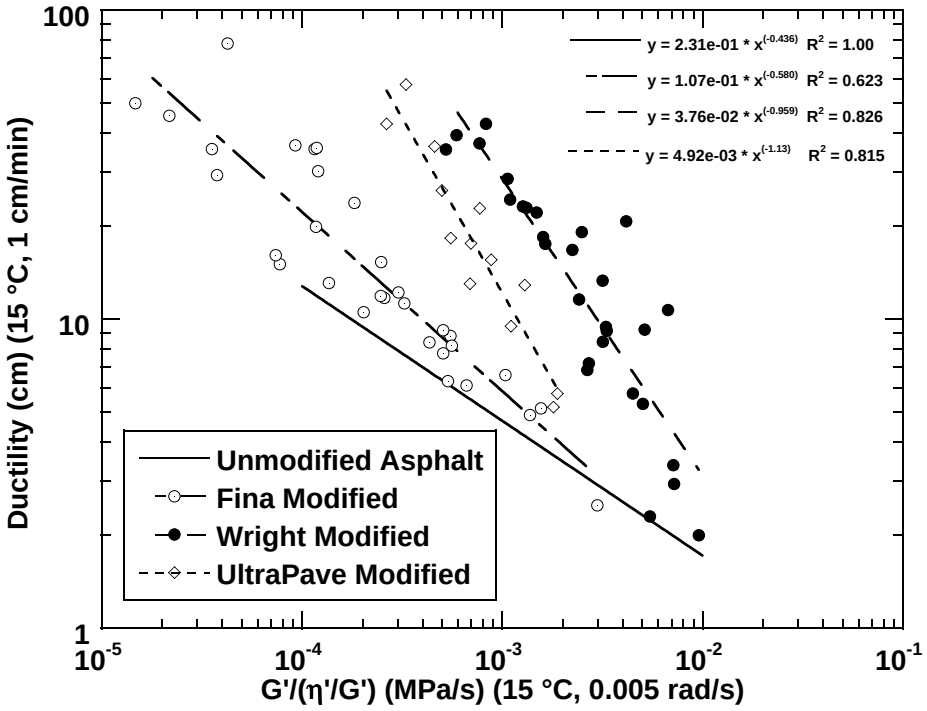

Figure 5-12. Ductiity versus G′/(η′/G′) for Modified Asphalt Groupings.

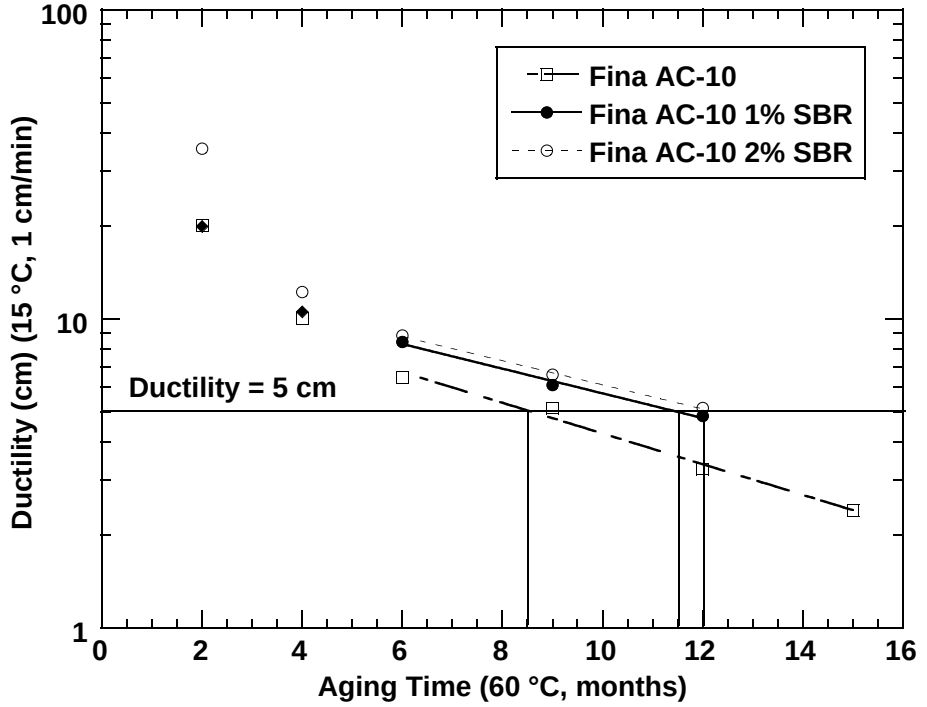

Figure 5-13. Effect of Modifiers on Ductility: Fina AC-10.

11.5 and 12 months, respectively. So for these data the benefits of 1 percent and 2 percent SBR for Fina AC-10 would be calculated as 3 and 3.5 months, respectively. For the Fina AC-20 group (Figure 5-14), the benefit of 1 percent SBR is calculated to be negative, -0.8 months, although this difference is almost certainly statistically insignificant, and 3.5 percent SBR produces a benefit of 5.8 months.

Table 5-5 is a summary of these calculated benefits for several unmodified and modified asphalts. Table 5-5 generally indicates that the addition of several percent of polymer modifiers can result in a benefit of from 2 to 6 months at 60 °C aging. Note, however, that this benefit is asphalt and modifier dependent The benefit values are also shown as a percent extension of aging time, relative to the base material.

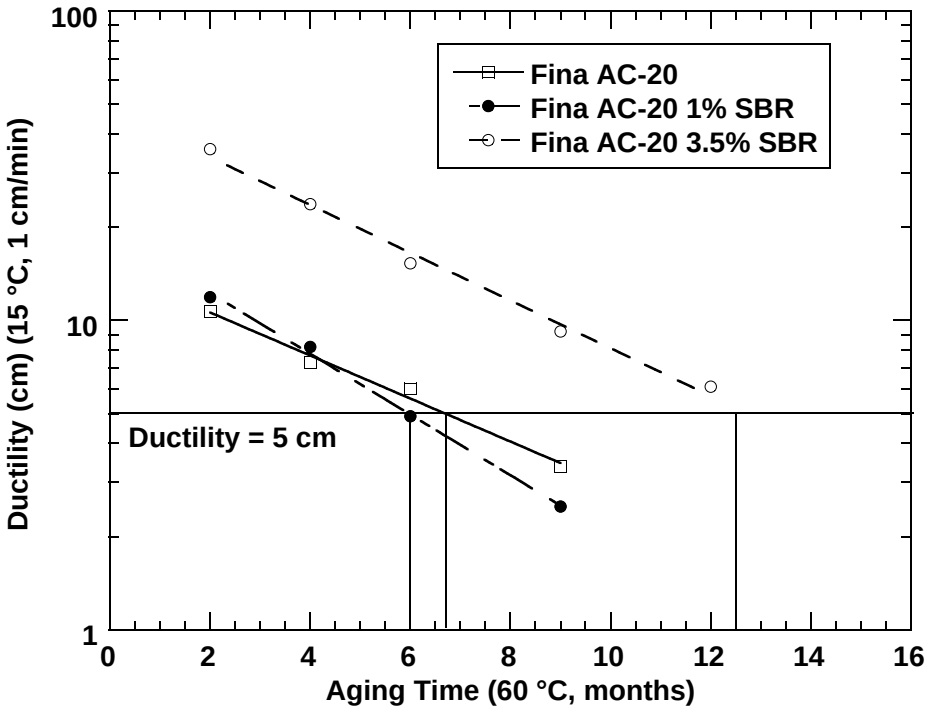

Figure 5-14. Effect of Modifiers on Ductility: Fina AC-20.

Table 5-5. Summary of Modifier Benefit on Ductility.

Sample	Aging Time to reach 5 cm ductility (months at 60 °C)	Modifier Benefit	
		(months)	(percent)
Fina AC-10	8.5	–	–
Fina AC-10 1% SBR	11.5	3.0	35
Fina AC-10 2% SBR	12.0	3.5	41
Fina AC-20	6.8	–	
Fina AC-20 1% SBR	6.0	-0.8	-12
Fina AC-20 3.5% SBR	12.5	5.7	84
Wright AC-10	7.75	–	–
Wright AC-10 2% SBR	14.0	6.2	80
Wright AC-10 3% SBR	13.3	5.5	71
Wright AC-10 3% SBS	13.0	5.3	68
Wright AC-20	5.0	–	–
Wright AC-20 3% SBR	9.8	4.7	94
Wright AC-20 3% SBS	9.8	4.7	94
Wright AC-20 5% Tire Rubber plus 2% SBS	7.0	2.0	40
Exxon AC-30	6.5	–	–
Exxon AC-30 3.5% SBR	10.0	3.5	54
TFA AC-20	9.0	–	–
TFA AC-20 3% SBR	12.8	3.7	41

Summary

For modified asphalts, there is no universal correlation between ductility and $G'/(\eta'/G')$, even in the low ductility region. However, there are reasonably good correlations between these two parameters for different asphalt groups.

Generally, the addition of several percent of polymer modifiers can result in a benefit of from 2 to 6 months continuous aging at 60 °C. In addition, this benefit is asphalt and modifier dependent.

CHAPTER 6. DEVELOPMENT OF AN AGING PROCEDURE

INTRODUCTION

The primary objective of this study has been the development of a procedure to identify asphalts that are particularly subject to failure resulting from oxidative hardening. To accomplish this two things are required: 1) an aging procedure to harden asphalts so that those most susceptible to oxidative hardening will fail the test, and 2) a test that correlates with pavement failure caused by binder hardening.

The aging procedure should age asphalts to the same relative extent as will occur in service, i.e., the best and worst asphalts in service should be best and worst in the test. This is particularly true with the worst, as it is the one that will be most likely to fail the test. It is, of course, highly desirable that the aging procedure require a relatively short time. Unfortunately, this introduces considerable difficulty into the choice of test conditions.

Strictly speaking, the problem is in theory intractable. Exhaustive data from prior studies and this one show that asphalts respond differently to temperature, pressure, and time so that a relatively rapidly hardening asphalt at road conditions may not be so at test conditions, and the reverse is also true. Using viscosity as a general surrogate for hardening, Equation 6-1 shows the mechanisms by which hardening occurs in the absence of diffusion resistance:

$$\ln \eta_t = \ln \eta_o + \Delta(\ln \eta_{ot}) + \Delta(\ln \eta_j) + r_\eta \cdot \text{time}, \qquad (6\text{-}1)$$

where η_o is the original viscosity, η_t is the viscosity at any time, $\Delta(\ln \eta_{ot})$ is the hardening in the hot-mix plant simulated by an oven test, $\Delta(\ln \eta_j)$ is the hardening that occurs in an early rapid "initial jump" stage, and r_η is the subsequent constant rate of hardening. This sequence is shown in Figure 6-1 in which η_{ot} is the viscosity after the oven test and η_j is the viscosity after the initial jump defined by the intercept of the constant-rate line. Region A will be defined as the time for the initial jump, and region B is a constant-rate region. If there is diffusional resistance, this rate will decline as the asphalt hardens. The first term is not a problem, as oven tests do a good job of simulating the hot-mix hardening (Jemison et al., 1991). The initial jump, however, is quite complex, being both asphalt dependent and pressure dependent. Interestingly, it is not temperature dependent. The oven test may reduce the initial jump but usually not nearly enough to eliminate it.

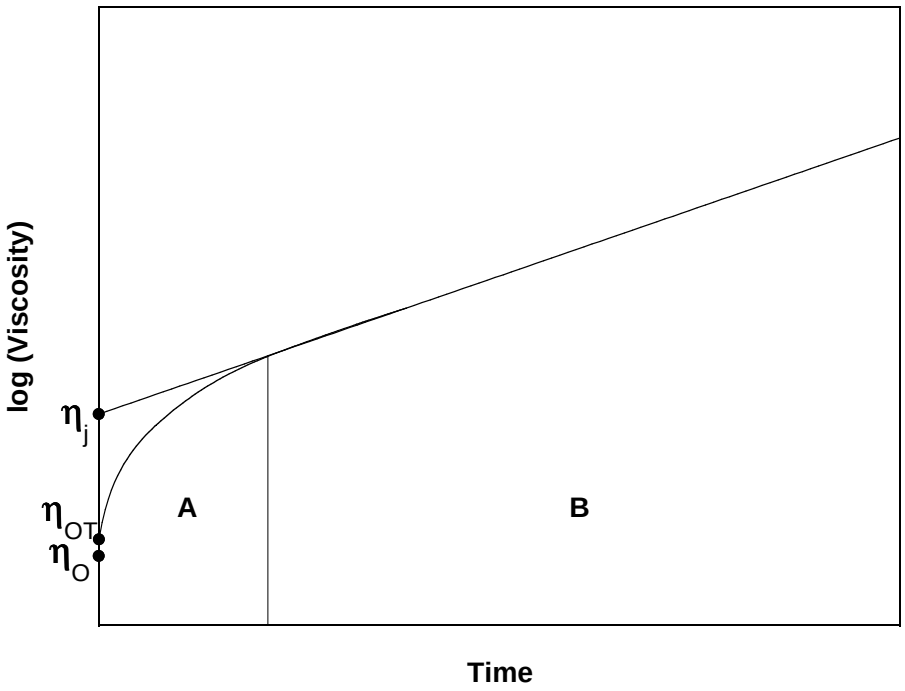

Figure 6-1. The Variation of Asphalt Viscosity with Aging.

Asphalt oxidative hardening is almost entirely caused by asphaltene formation (Lin et al., 1995, 1996, 1998), and the rate can be expressed as follows:

$$r_\eta = \frac{\partial \ln \eta}{\partial t} = \frac{\partial \ln \eta}{\partial AS} \cdot \frac{\partial AS}{\partial CA} \cdot \frac{\partial CA}{\partial t}, \qquad (6\text{-}2)$$

where $\partial \ln \eta / \partial AS$ is the impact of asphaltene (AS) increase on increasing viscosity and is affected by asphaltene size, which in turn is affected by maltene solvent power. $\partial AS / \partial CA$ is the rate at which carbonyl (CA) formation produces asphaltenes, and $\partial CA / \partial t$ is the rate of carbonyl formation. Carbonyl increase correlates linearly with oxidation (Liu et al., 1998b).

This can be simplified as

$$r_\eta = HS \cdot r_{CA}, \qquad (6\text{-}3)$$

where HS is the combination of the first two terms in Equation 6-2. This combination is remarkably constant as oxidation proceeds and is independent of oxidation temperature below about 100-110 ºC. It has a characteristic value for each asphalt except that it is pressure dependent. This term is called the hardening susceptibility (Lau et al. 1992; Domke, 1999).

The rate of carbonyl formation can be expressed by (Lin et al., 1996; Lin et al., 1998; Liu et al., 1997a)

$$r_{CA} = \frac{\partial CA}{\partial t} = AP^{\alpha} e^{-(E/RT)}, \qquad (6\text{-}4)$$

where A is the frequency (pre-exponential) factor, P is the pressure, α is the reaction order with respect to oxygen pressure, E is the activation energy, R is the gas constant, and T is the absolute temperature. Values of A, E, and α are very asphalt dependent, though A and E are generally correlated (Liu, 1996). Recent studies described in this report and in Domke et al. (2000) show that the activation energy, E, is also pressure dependent for many asphalts, and this dependence is a function of asphaltenes. The following equation summarizes these results:

$$\ln \eta_t = \ln \eta_{ot} + \Delta(\ln \eta_j)(P) + r_{CA}(T,P) \cdot HS(P) \cdot \text{time}. \qquad \text{(Early)}$$

As only one term is multiplied by time, this means that the relative rankings of asphalts from any accelerated aging procedure will change with the length of the test as well as with the temperature and pressure. Because of these complexities, the only recourse is to conduct accelerated aging at a variety of conditions and compare the results with long-term aging at or near road conditions. In this study, this long-term simulation was done in an environmental room held at 60 ºC (140 ºF). The asphalts were aged in thin films to minimize diffusion effects. All other tests were then compared as to relative rankings with results from the environmental room.

EARLY ENVIRONMENTAL ROOM COMPARISONS

The first task was to place an array of asphalts into the environmental room because aging at these conditions takes many months. Figure 6-2 shows the 60 ºC (140 ºF) viscosity of eight of these asphalts at various times after first subjecting them to RTFOT aging. The effect of time on relative rankings is readily apparent. At 50 days, which as shown in Chapter 3 of this report is more severe than the PAV, AAA-1 is best and AAF-1 is worst as ranked by viscosity. Asphalt AAF-1 appears to gradually improve with time, but its high initial jump is never completely offset. Asphalt AAD-1 loses ground continuously because of its high hardening rate. Asphalt AAG-1 gets increasingly relatively better with time because of its low hardening rate, as does Exxon AC-20.

COMPARISON OF POV AGING TO 60 ºC (140 ºF) AGING

Hardening rates (slopes of the lines shown) for the seven SHRP asphalts shown in Figure 6-2 are given in Table 6-1 along with POV hardening rates at five conditions of temperature and pressure. Hardening rates for the same asphalts in the 60 ºC (140 ºF) room are also tabulated.

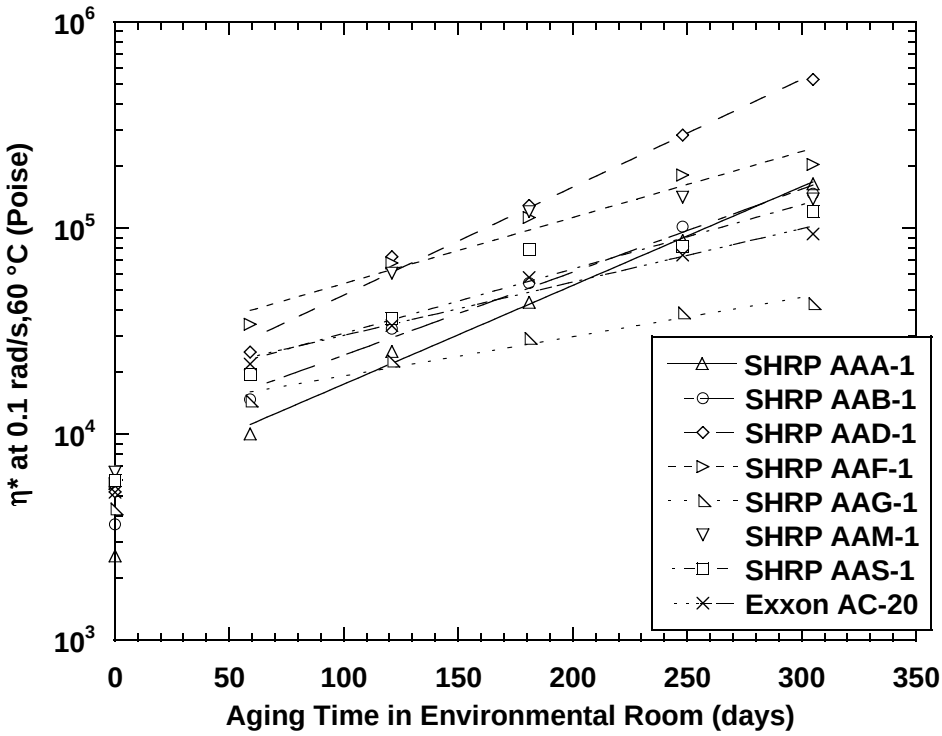

Figure 6-2. Hardening of Seven SHRP Asphalts in the 60 °C Environmental Room.

Unfortunately, the POV-aged asphalts were not subjected to RTFO aging before POV aging, while the 60 °C (140 °F) aged asphalts were. This will change both the initial jump and subsequent hardening rate to some extent. However, since the effects are not large, comparisons are still instructive.

To compare widely different rates, they were normalized by dividing each asphalt's rate in each set by the average rate for that group. These were then ordered from slowest to fastest rate, and percent deviation of POV values from 60 °C (140 °F) values were calculated and averaged for each POV condition. The results were generally as expected, with the average error increasing as the temperature and/or pressure are farther from 60 °C (140 °F) and 1 atm air (0.2 atm O_2). There are, however, a few large individual errors.

The same asphalts studied above were rerun in the PAV and POV after subjecting them to the RTFOT. Runs were made at a variety of temperatures and pressures as shown in Table 6-2, and samples were taken at 24, 48, and 72 hours. Both 60 °C (140 °F) limiting viscosity and the DSR function were determined. Table A-1 in Appendix A gives complete results.

As the environmental room data had been obtained previous to developing the DSR functions, it had not been measured. Subsequently, we found that these samples had further aged and the function could not be measured nor could it be calculated accurately from the data that had been obtained.

Table 6-1. Hardening Rate of SHRP Asphalts Aged at Various Conditions.

	POV 88 °C 1 atm Air Non-RTFO		POV 82 °C 1 atm Air Non-RTFO		POV 82 °C 1 atm O_2 Non-RTFO		POV 82 °C 4 atm O_2 Non-RTFO		POV 71 °C 20 atm O_2 Non-RTFO		Environmental Room 60 °C, 1 atm Air RTFO	
	HR (ln(poise)/day)	Rank	HR (ln(poise)/day)	Rank	HR (ln(poise)/day)	Rank	HR (ln(poise)/day)	Rank	HR (ln(poise)/day)	Rank	HR (ln(poise)/day)	Rank
AAA-1	0.1590	3	0.1028	6	0.1908	6	0.3673	7	0.2545	6	0.01103	6
AAB-1	0.1700	6	0.0945	5	0.1682	4	0.3633	6	0.1418	4	0.00927	5
AAD-1	0.2070	7	0.1212	7	0.2359	7	0.3487	5	0.2630	7	0.01204	7
AAF-1	0.1620	4	0.0805	4	0.1690	5	0.2999	4	0.1456	5	0.00737	4
AAG-1	0.0770	1	0.0447	1	0.0593	1	0.0820	1	0.0647	1	0.00438	1
AAM-1	0.1660	5	0.0734	2	0.1432	2	0.2017	2	0.1096	2	0.00660	2
AAS-1	0.1410	2	0.0789	3	0.1638	3	0.2946	3	0.1114	3	0.00718	3
Average	0.1546		0.0852		0.1615		0.2797		0.1558		0.00830	
Absolute Relative Error Compared to the ER Hardening Rate (%)												
AAA-1	22.9		9.5		11.4		1.6		22.4			
AAB-1	1.9		1.0		7.1		15.8		18.9			
AAD-1	8.1		2.3		0.3		14.4		15.9			
AAF-1	17.6		6.1		17.4		20.3		4.9			
AAG-1	6.0		0.9		30.7		44.6		21.7			
AAM-1	34.6		8.0		11.1		9.6		11.8			
AAS-1	5.0		6.7		16.8		21.3		17.6			
Average Error	13.7		4.9		13.6		18.2		16.2			

Table 6-2a. Rank and Absolute Error of Asphalts Based on Viscosity Aged at Various Conditions.

	Environmental Room at 253 days		Conventional PAV at 56 hours		PAV Thin Film 90 °C at 57 hours		POV 100 °C, 5 atm O_2 at 34 hours	
	$\eta^*_{60\ °C,\ 0.1\ rad/s}$ (poise)	Rank	$\eta^*_{60\ °C,\ 0.1\ rad/s}$ (poise)	Rank	$\eta^*_{60\ °C,\ 0.1\ rad/s}$ (poise)	Rank	$\eta^*_{60\ °C,\ 0.1\ rad/s}$ (poise)	Rank
AAA-1	94,918	3	193,613	4	124,436	4	159,786	3
AAB-1	100,240	4	206,657	5	110,332	2	167,663	4
AAD-1	300,000	7	300,000	7	300,000	7	300,000	7
AAF-1	166,724	6	153,616	3	243,502	6	264,184	6
AAM-1	129,486	5	219,780	6	199,662	5	195,577	5
AAS-1	92,909	2	133,760	2	113,165	3	139,375	2
Exxon AC-20	75,267	1	97,179	1	84,220	1	100,474	1
AAG-1	37,576		21,340		30,863		25,553	
TS2000 AC-20	-		587,892		293,715		377,464	
Absolute Error in Log Viscosity Compared to the ER Log Viscosity (%)								
AAA-1			6.2		0.4		4.5	
AAB-1			6.3		0.7		4.5	
AAD-1			0.0		0.0		0.0	
AAF-1			0.7		3.0		3.8	
AAM-1			4.5		4.7		3.5	
AAS-1			3.2		1.7		3.5	
Exxon AC-20			2.3		1.7		2.6	
Average Error			3.3		1.7		3.2	

Table 6-2b. Rank and Absolute Error of Asphalts Based on Viscosity Aged at Various Conditions.

	Environmental Room at 253 days		POV 110 °C, 1 atm O_2 at 45 hours		POV 100 °C, 1 atm O_2 at 77 hours		POV 93 °C, 1 atm O_2 at 119 hours	
	$\eta^*_{60\ °C,\ 0.1\ rad/s}$ (poise)	Rank	$\eta^*_{60\ °C,\ 0.1\ rad/s}$ (poise)	Rank	$\eta^*_{60\ °C,\ 0.1\ rad/s}$ (poise)	Rank	$\eta^*_{60\ °C,\ 0.1\ rad/s}$ (poise)	Rank
AAA-1	94,918	3	150,188	2	120,503	3	95,234	2
AAB-1	100,240	4	239,456	5	116,530	2	180,723	5
AAD-1	300,000	7	300,000	7	300,000	7	300,000	7
AAF-1	166,724	6	287,619	6	181,741	5	166,243	4
AAM-1	129,486	5	202,636	4	241,133	6	269,917	6
AAS-1	92,909	2	194,621	3	145,460	4	157,720	3
Exxon AC-20	75,267	1	120,232	1	89,172	1	89,482	1
AAG-1	37,576		21,821		19,678		24,701	
TS2000 AC-20	-		460,265		394,931		335,767	
Absolute Error in Log Viscosity Compared to ER Log Viscosity (%)								
AAA-1			4.0		2.1		0.0	
AAB-1			7.6		1.3		5.1	
AAD-1			0.0		0.0		0.0	
AAF-1			4.5		0.7		0.0	
AAM-1			3.8		5.3		6.2	
AAS-1			6.5		3.9		4.6	
Exxon AC-20			4.2		1.5		1.5	
Average Error			4.4		2.1		2.5	

Figure 6-3 is a plot of the DSR function versus 60 °C (140 °F) limiting viscosity. From the literature, we have chosen a critical ductility value of 3 cm/min measured at 15 °C. This corresponds to a function value of 0.003. From Figure 6-3, this is seen to very roughly correspond to a viscosity value of about 300,000 poise. For the 60 °C (140 °F) environmental room data and the PAV and POV data, times were calculated at which the hardest asphalt had reached 300,000 poise. In every case, this was asphalt AAD-1. Figure 6-2 shows that it requires 253 days for asphalt AAD-1 to reach this viscosity in the environmental room. The times for the POV and PAV runs are shown in Table 6-2 along with the corresponding viscosity for each asphalt.

For an ideal accelerated aging procedure, the viscosities of all POV- and PAV-aged asphalts would be the same as measured on the environmental room aged asphalts at 253 days. This is far from the case. The percent deviation in log viscosity from that in the environmental room is given for each asphalt along with the average deviation at each condition. This average excludes asphalt ABM-1, as the deviation was always large, but it hardened so little that its value was of no significance. We are, of course, most interested in the more rapidly hardening asphalts that are most likely to fail the test.

The thin-film PAV (film thickness of about 1 mm instead of the standard 3 mm) at 90° C (56 days) and the POV at 100° C and 1 atm O_2 (77 days) show the smallest average error. Since hardening varies logarithmically with time, percent error in log viscosity is reported. Unfortunately, asphalt AAM-1 has hardened much more at both of these conditions than in the

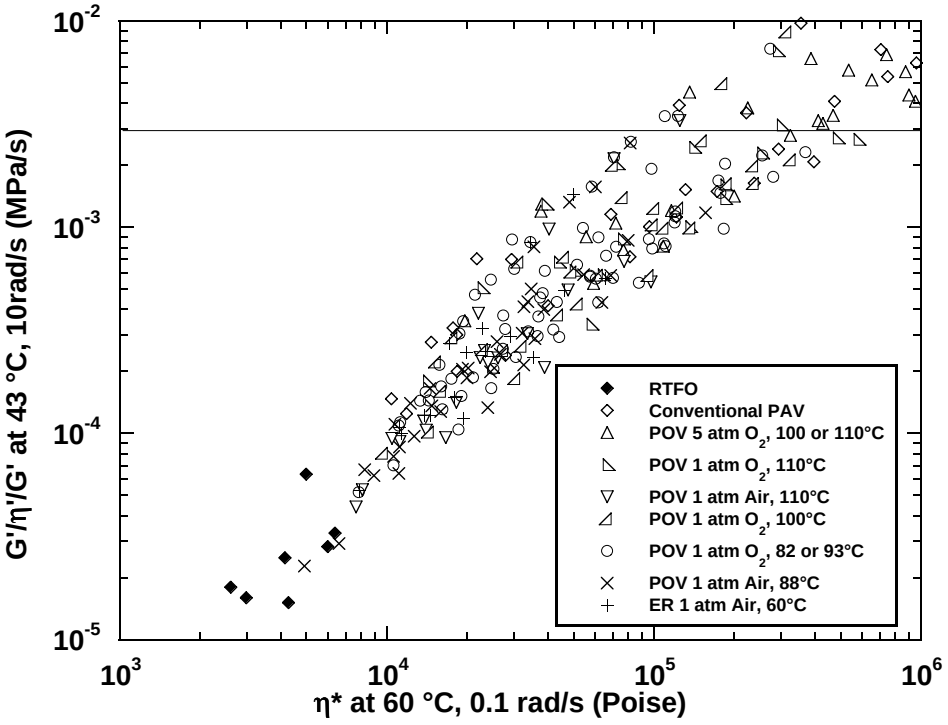

Figure 6-3. Relation Between G′/(η′/G′) and Complex Viscosity.

60° C room. In fact, no asphalt was a good match at both conditions. While asphalt AAF-1 hardens more than most, it is well behind asphalt AAD-1 at all conditions, while as we shall see, asphalt AAF-1 is consistently the worst performer when compared on the basis of the DSR function. A glance at Figure 6-3 indicates this is not too surprising in view of the scatter in the correlation of viscosity and the DSR functions.

Table 6-3 shows the DSR function for the same materials shown in Table 6-2, again corresponding to aging times that result in 300,000 poise for asphalt AAD-1. As discussed earlier, function values for the asphalts aged in the environmental room are not available. Here we see that asphalt AAF-1 is consistently the worst with respect to the function, while asphalt AAD-1 varies from next to hardest or seventh place to third place in the 90 °C thin-film PAV.

Table 6-3a. Rank of Function When Worst Asphalt Reaches 300,000 Poise.

	Conventional PAV 100 °C, 20 atm Air at 56 hours		PAV Thin Film 90 °C, 20 atm Air at 56 hours		POV 100 °C, 5 atm O_2 at 34 hours	
AAA-1	1.71×10^{-3}	3	9.92×10^{-4}	2	1.44×10^{-3}	4
AAB-1	2.62×10^{-3}	7	1.45×10^{-3}	4	2.13×10^{-3}	6
AAD-1	2.40×10^{-3}	6	2.27×10^{-3}	7	2.14×10^{-3}	7
AAF-1	6.77×10^{-3}	8	6.74×10^{-3}	8	7.32×10^{-3}	8
ABM-1	4.00×10^{-3}	1	8.76×10^{-4}	1	6.00×10^{-4}	1
AAM-1	2.25×10^{-3}	5	1.91×10^{-3}	6	1.10×10^{-3}	2
AAS-1	1.60×10^{-3}	2	1.12×10^{-3}	3	1.31×10^{-3}	3
Exxon AC-20	2.03×10^{-3}	4	1.49×10^{-3}	5	1.64×10^{-3}	5
TS2000 AC-20	2.91×10^{-3}		1.89×10^{-3}		2.27×10^{-3}	

Table 6-3b. Rank of Function When Worst Asphalt Reaches 300,000 Poise.

	POV 110 °C, 1 atm O_2 at 45 hours		POV 100 °C, 1 atm O_2 at 77 hours		POV 93 °C, 1 atm O_2 at 119 hours	
AAA-1	1.09×10^{-3}	2	1.04×10^{-3}	2	8.96×10^{-4}	2
AAB-1	2.36×10^{-3}	7	1.47×10^{-3}	4	2.93×10^{-3}	7
AAD-1	1.60×10^{-3}	3	2.05×10^{-3}	6	1.69×10^{-3}	4
AAF-1	6.35×10^{-3}	8	5.05×10^{-3}	8	7.95×10^{-3}	8
ABM-1	4.34×10^{-4}	1	3.73×10^{-4}	1	5.65×10^{-3}	1
AAM-1	1.78×10^{-3}	5	2.25×10^{-3}	7	2.47×10^{-3}	6
AAS-1	1.64×10^{-3}	4	1.47×10^{-3}	3	1.84×10^{-3}	5
Exxon AC-20	1.92×10^{-3}	6	1.50×10^{-3}	5	1.33×10^{-3}	3
TS2000 AC-20	2.39×10^{-3}		2.51×10^{-3}		2.28×10^{-3}	

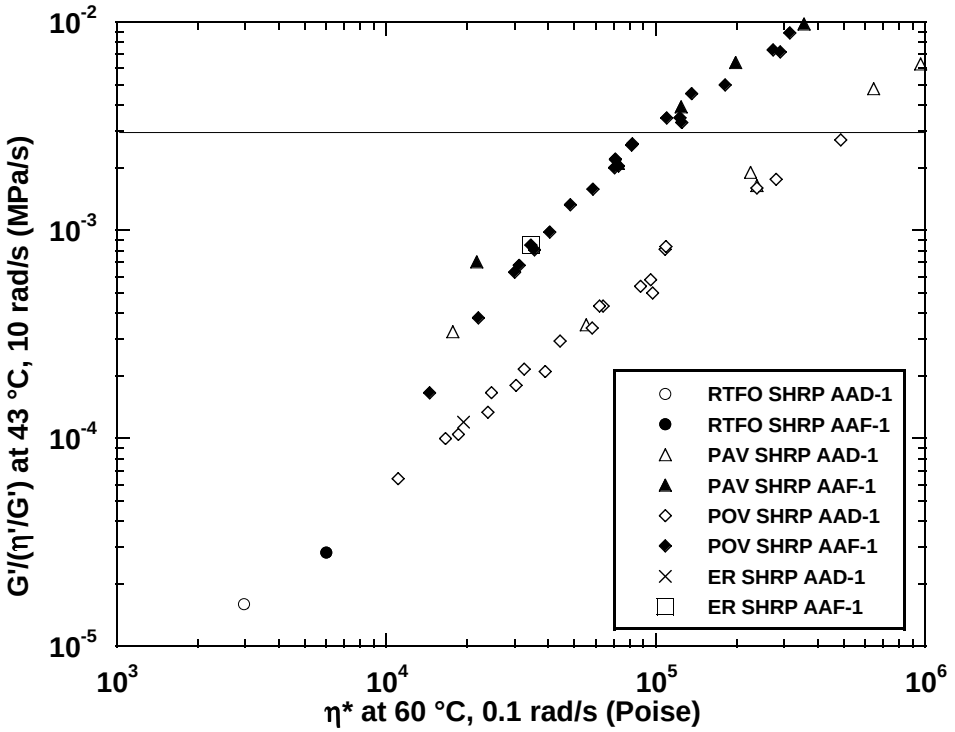

Figure 6-4. The Relation Between G′/(η′/G′) and Viscosity is Asphalt Dependent.

Figure 6-4 is a log-log plot of the DSR function versus viscosity for these two asphalts aged at 90 °C thin-film PAV and 100 °C and 1 atm O_2. It is discouraging when we compare the relative ranking for these two conditions that showed the smallest viscosity deviations. It is obvious that data on asphalts recovered from old roadways is needed to confirm that the DSR function correlates with pavement life.

In Figures 6-5 and 6-6, the DSR function is shown versus time for the two conditions discussed above. It is encouraging that asphalt AAF-1 crosses the critical value of 0.003 well ahead of the other asphalts at both conditions. It is sufficient that the procedure fail the right asphalts, not that it properly rank good asphalts.

One asphalt for which data were given in Tables 6-2 and 6-3 was the test section 2000. It was omitted from the above evaluation because it was not placed in the 60 °C (140 °F) environmental room soon enough. This is an air-blown asphalt that was modified by ground tire rubber, and preliminary results are given in TxDOT research report 1460-1 (Glover et al., 2000). The results here are for the unmodified base asphalt. With respect to viscosity, this asphalt was the worst performer at every condition, but as seen in Figure 6-5, it is an average performer in the thin-film PAV and well below asphalt AAF-1 in the POV at 100 °C (212 °F) and 1 atm O_2 (Figure 6-6). Figure 6-7 is a plot of log DSR function versus log viscosity for this asphalt. The viscosity is greater than 500,000 poise before it reaches the limiting value of the DSR function.

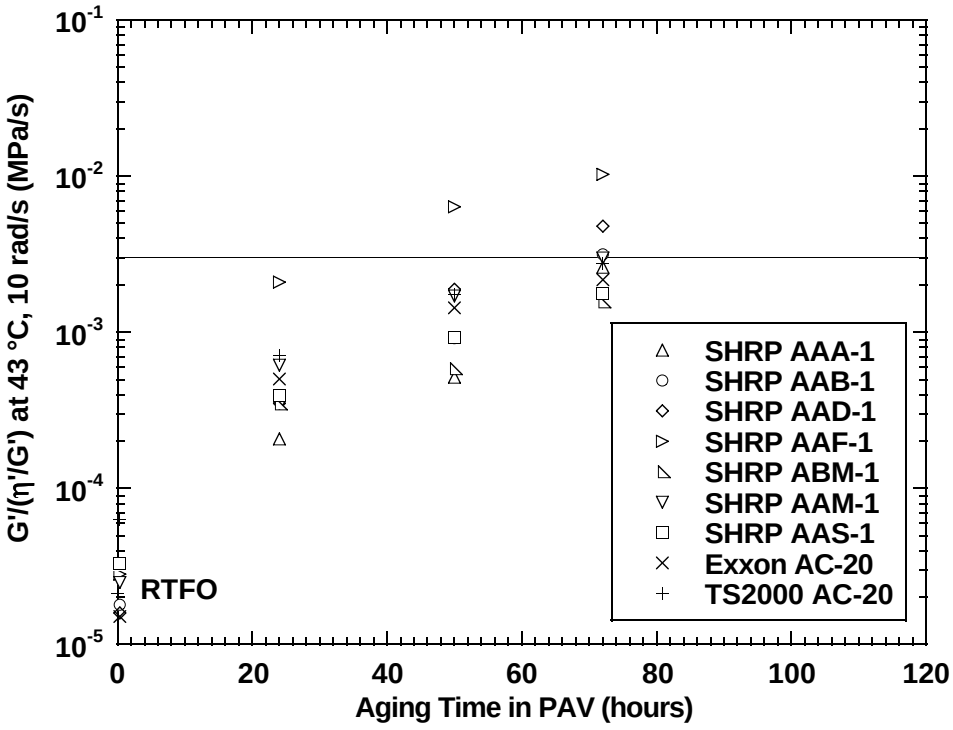

Figure 6-5. Thin-Film PAV Aging at 90 ºC, 200 atm Air.

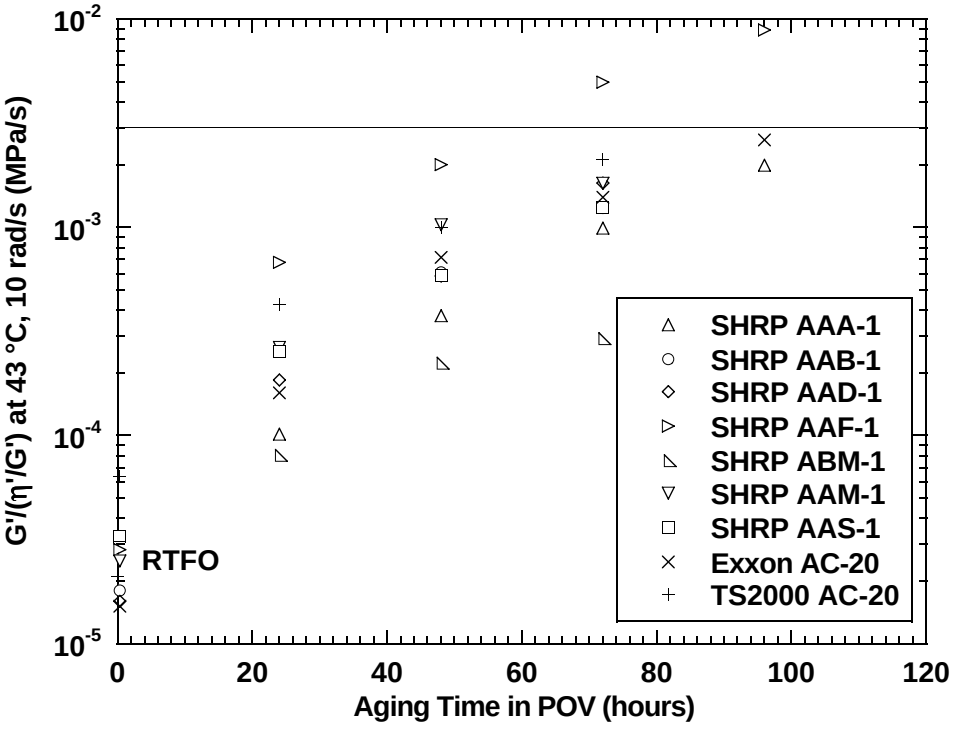

Figure 6-6. PAV Aging at 100 ºC and 1 atm O_2

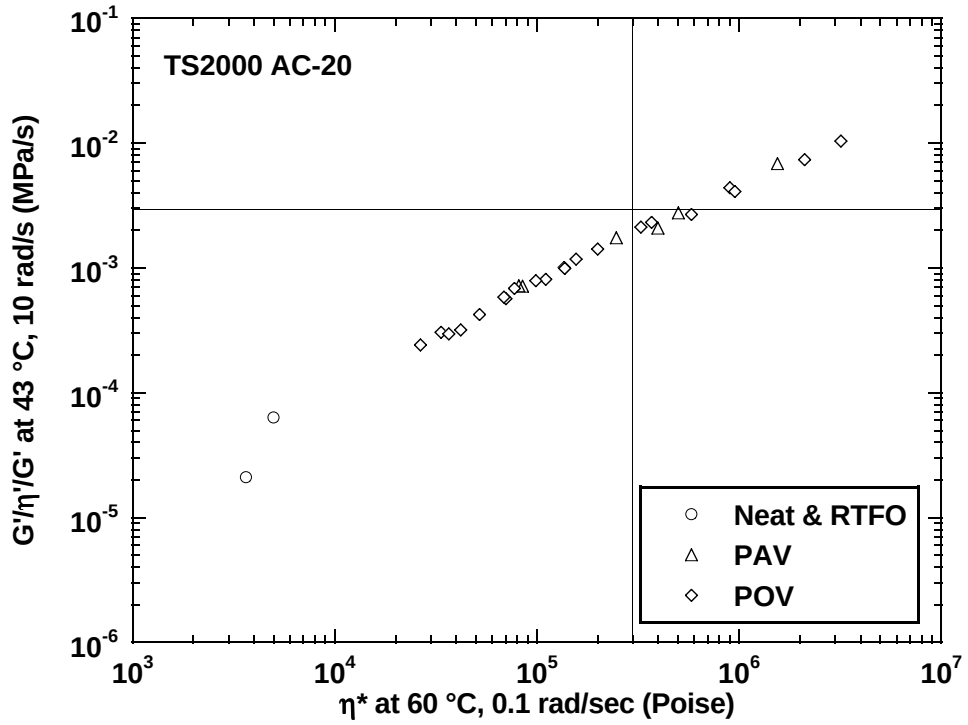

Figure 6-7. G′/(η′/G′) versus η* for TS 2000 AC-20.

COMPARISON OF LONGER PERIOD POV TO 60 ºC (140 ºF) AGING

As seen earlier in Table 6-1, POV conditions less removed from the environmental room conditions - lower temperature and pressure - tended to produce hardening rates that when normalized were relatively similar to those produced in the environmental room. For this reason, we decided to see if a test requiring longer times - lower temperature and/or pressure - would produce better results. Two conditions were chosen that had previously produced good results on the basis of hardening rates. These were 82 ºC (180 ºF) and 1 atm O_2 and 88 ºC (190 ºF) and 0.2 atm O_2, as in atmospheric air.

The viscosity results are given in Table 6-4. These data were taken over extended times and complete results are given in Appendix A, Table A-2. The data in Table 6-4 correspond to the times as shown that were required to harden asphalt AAD-1 to 300,000 poise. Surprisingly, the errors are quite large in spite of the less severe conditions. The 88 ºC (190 ºF) and 0.2 atm O_2 are the only conditions tested thus far that resulted in other asphalts hardening more than asphalt AAD-1. The DSR functions were calculated at the same times as the viscosities, and the results are also given in Table 6-4.

Values for both viscosity and DSR function are plotted versus time for both conditions in Figures 6-8 to 6-11. Once again, the considerable difference in results emphasizes the necessity of choosing the right property on which to base the test. If the DSR function is chosen rather than viscosity, the test time is reduced if the criterion is the time for the first asphalt to fail.

Table 6-4. Rank and Absolute Error of Asphalts Based on Viscosity of Long-Term Aging Conditions.

	Environmental Room 60 °C, 1 atm Air at 253 days	POV 88 °C, 0.2 atm O_2 at 661 hours				POV 82 °C, 1 atm O_2 at 394 hours			
	Viscosity at 60 °C, 0.1 rad/s (poise)	Viscosity at 60 °C, 0.1 rad/s (poise)	Rank	Function at 43 °C, 10 rad/s (MPa/s)	Rank	Viscosity at 60 °C, 0.1 rad/s (poise)	Rank	Function at 43 °C, 10 rad/s (MPa/s)	Rank
AAA-1	98,918	71,433	1	$1.29x10^{-3}$	3	110,576	2	$1.01x10^{-3}$	2
AAB-1	100,240	118,219	4	$2.25x10^{-3}$	4	191,035	3	$2.20x10^{-3}$	6
AAD-1	300,000	300,000	5	$2.28x10^{-3}$	5	300,000	7	$1.99x10^{-3}$	4
AAF-1	166,724	386,940	7	$3.20x10^{-3}$	8	278,074	6	$8.23x10^{-3}$	8
AAM-1	129,486	350,154	6	$5.70x10^{-4}$	7	268,223	5	$2.50x10^{-3}$	7
AAS-1	92,909	94,590	2	$8.06x10^{-4}$	2	191,731	4	$1.95x10^{-3}$	3
Exxon AC-20	75,267	95,490	3	$2.46x10^{-3}$	6	109,852	1	$2.15x10^{-3}$	5
ABM-1	37,576	21,253		$5.74x10^{-4}$	1	28,388		$7.81x10^{-4}$	1
TS2000 AC-20	-	779,925				377,679			
Absolute Error in Log Viscosity compared with ER Log Viscosity (%)									
AAA-1		2.5				1.3			
AAB-1		1.4				5.6			
AAD-1		0.0				0.0			
AAF-1		7.0				4.3			
AAM-1		8.5				6.2			
AAS-1		0.2				6.3			
Exxon AC-20		2.1				3.4			
Average		3.1				3.9			

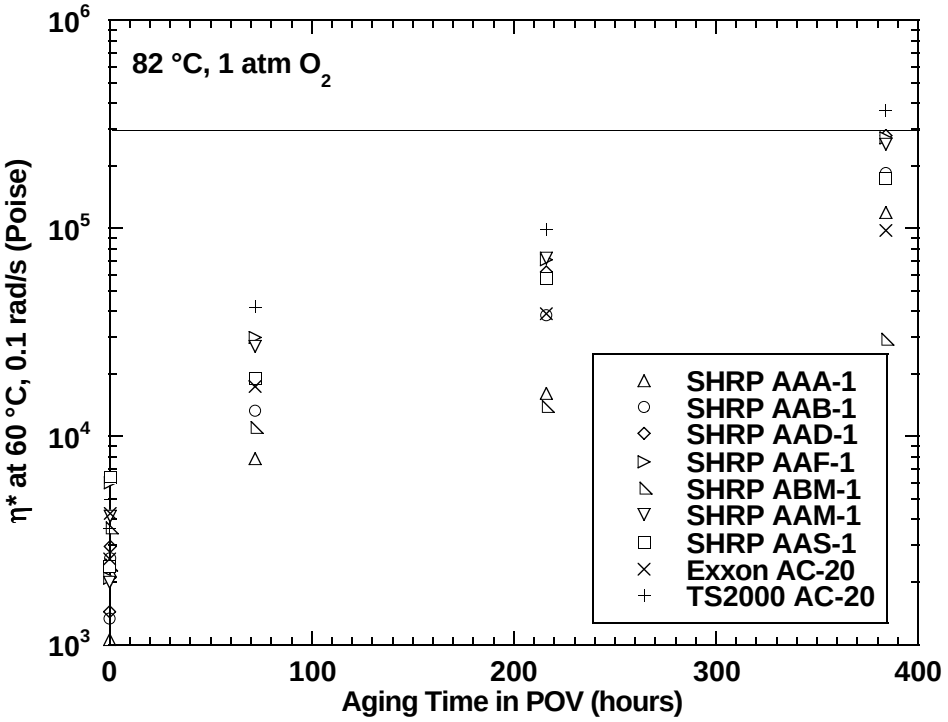

Figure 6-8. Variation of Viscosity with Aging Time at 82 ºC, 1 atm O_2.

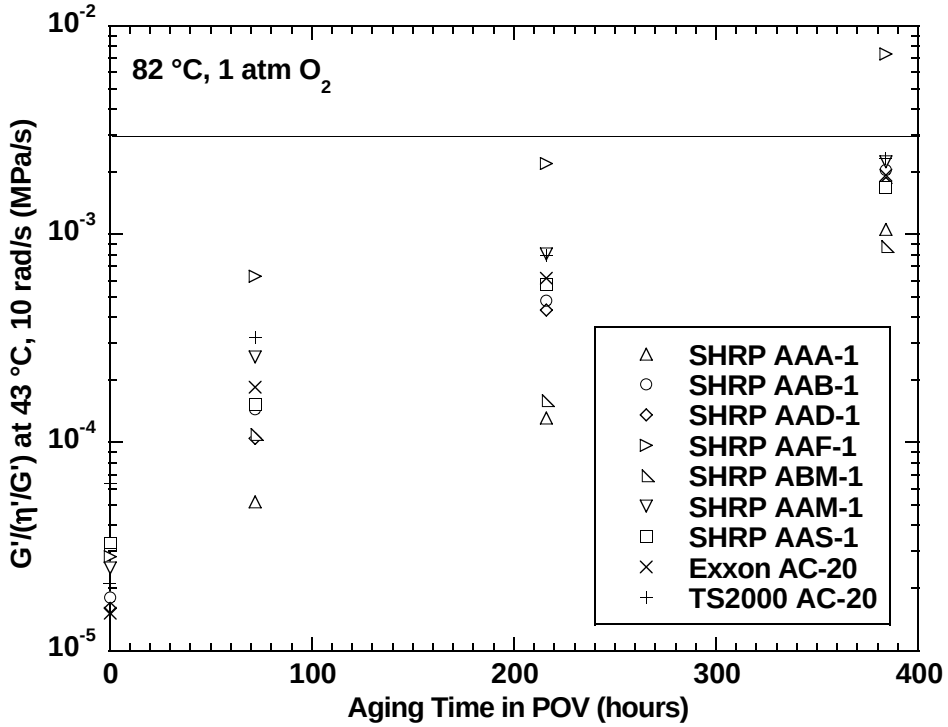

Figure 6-9. Variation of G′/(η′/G′) with Aging Time at 82 ºC, 1 atm O_2.

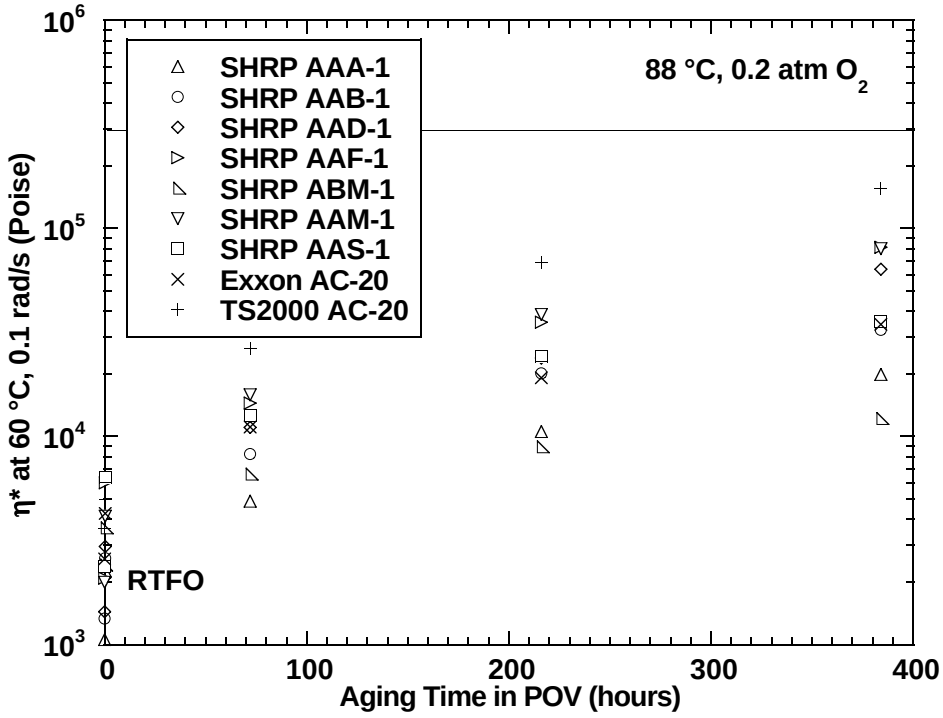

Figure 6-10. Variation of Viscosity with Aging Time at 88 °C, 0.2 atm.

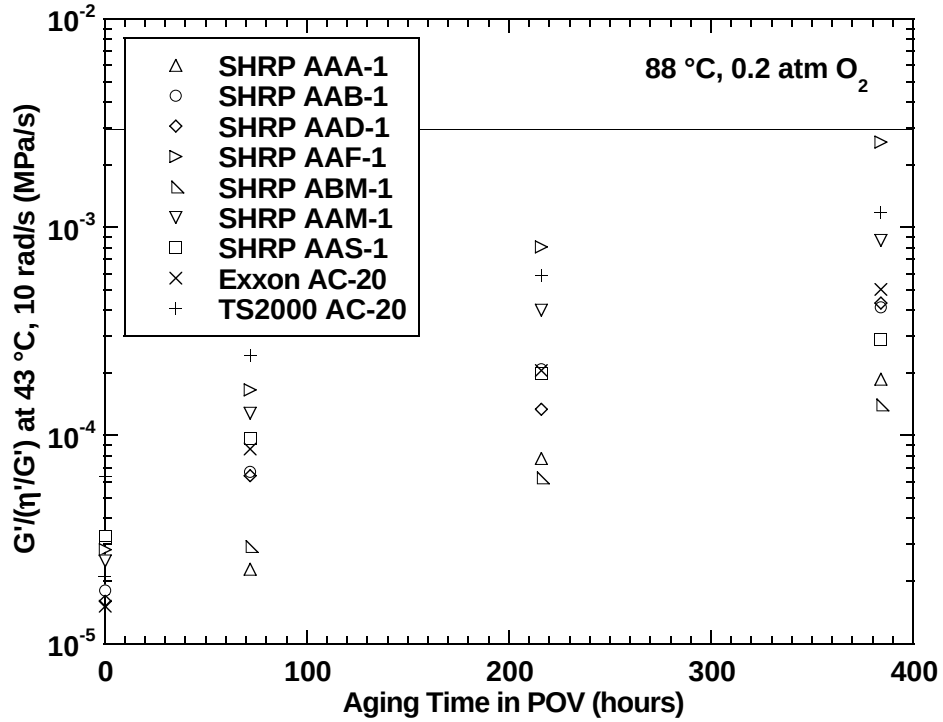

Figure 6-11. Variation in G′/(η′/G′) with Aging Time at 88 °C, 0.2 atm.

FURTHER ENVIRONMENTAL ROOM COMPARISONS

A second set of asphalts was aged in the 60 °C (140 °F) environmental room, consisting of the asphalts used in the ductility - DSR correlation described in Chapter 4. The values of the DSR function are given in Table 6-5 after 233 days, which was the time required for the first asphalt to reach the critical value chosen for this function of 0.003. This value corresponds to a ductility at 15 °C of 3 cm/min. Complete environmental room data for these asphalts are given in Table A-3 in Appendix A. In Figure 6-12 the DSR data are plotted versus time, and in Figure 6-13 the 60 °C (140 °F) viscosity is plotted versus time. Asphalt Fina PG 64-22 is the first to reach the critical DSR parameter of 0.003 and also the chosen viscosity parameter of 300,000 poise, although for this asphalt it took considerably longer to reach the viscosity limit.

Table 6-2 shows that the thin-film PAV at 90 °C (194 °F) and 20 atm air and the POV at 100 °C (212 °F) and 1 atm O_2 had the smallest deviation from the environmental room. Consequently, these asphalts were run at the same POV condition, and the thin-film PAV was also run but at 100 °C (212 °F) to reduce the time required.

Figure 6-14 shows the POV data (100 °C (212 °F) and 1 atm O_2) for the DSR function. It is interesting that the most rapidly hardening asphalt reached the critical DSR function value of 0.003 in about 52 hours, corresponding to the results for asphalt AAF-1 shown in Figure 6-6. Figure 6-15 shows that the first asphalt reached the critical viscosity of 300,000 poise in about the same time, but it was not the same asphalt.

Figure 6-16 shows the DSR function versus time for the PAV run (100 °C (212 °F) 20 atm air, 1 mm film). Here, the first asphalts reach the critical DSR function value of 0.003 in about 30 hours. Both runs seem to discriminate against the Wright AC-20 and Wright AC-10, though the latter is still well below the critical value. DSR functions for both of these runs at the critical times are given in Table 6-5 and complete data are given in Table A-4, Appendix A. Figure 6-17 shows viscosity versus DSR function for the second set of asphalts aged in the environmental room. It is very similar to the results for the first set shown in Figure 6-3

Percent error in the DSR function is calculated for each run, but GSAC AC-15P and Fina AC-10 and AC-20 are excluded, as they are so far below critical that their values are irrelevant. The average errors are close, but the big errors in the Wright asphalts distort the results. Because aging is logarithmic, the error in the log of the function is more meaningful, so these values are given. In this case, the POV error is smaller. The relative agreement of the two conditions with the environmental room is shown visually in Figures 6-18 and 6-19, where the PAV values at 30 hours and the POV at 52 hours are compared to the environmental room at 233 days. Agreement is very good for Fina PG64-22, especially for the POV, and this is fortunate in that the environmental room and POV show it as first to reach the critical value and it is very close in the PAV. Unfortunately, for both runs Wright AC-20 is very close to the critical value, while in the environmental room it is still well below this value. Overall, one can see that the POV data (100 °C (212 °F) and 1 atm O_2) are closer except for the Wright asphalts, but the difference is not great.

Table 6-5. Rank and Absolute Error of Asphalts Based on Function at Various Aging Conditions.

	Environmental Room at 233 hours		POV 100 °C, 1 atm O_2 at 52 hours			POV 100 °C, 20 atm Air at 30 hours		
	Function at 15 °C, 0.005 rad/s (MPa/s)	Rank	Function at 43 °C, 10 rad/s (MPa/s)	Rank	Absolute Log Error wrt ER (%)	Function at 43 °C, 10 rad/s (MPa/s)	Rank	Absolute Log Error wrt ER (%)
Exxon Base	1.80×10^{-3}	6	1.71×10^{-3}	5	0.9	1.25×10^{-3}	4	5.7
Fina PG64-22 Base	3.00×10^{-3}	7	3.19×10^{-3}	7	1.0	2.45×10^{-3}	6	3.5
Neste Base	9.14×10^{-4}	2	1.19×10^{-3}	2	3.7	1.04×10^{-3}	1	1.9
TFA Base	1.25×10^{-3}	3	1.05×10^{-3}	1	2.6	1.46×10^{-3}	5	2.3
United Ref Base	1.29×10^{-3}	4	1.26×10^{-3}	3	0.4	1.06×10^{-3}	2	3.1
Wright AC-10	7.03×10^{-4}	1	1.70×10^{-3}	4	12.2	1.22×10^{-3}	3	7.6
Wright AC-20	1.78×10^{-3}	5	2.65×10^{-3}	6	6.3	2.52×10^{-3}	7	5.5
Average Error for Hardest 7 Asphalts					3.9			4.2
Fina AC-5	4.02×10^{-4}		1.96×10^{-4}		9.2	1.55×10^{-4}		12.2
Fina AC-10	5.08×10^{-4}		3.90×10^{-4}		3.5	2.28×10^{-4}		10.5
GSAC AC-15P Base	5.71×10^{-5}		5.83×10^{-5}		0.2	7.22×10^{-5}		2.4

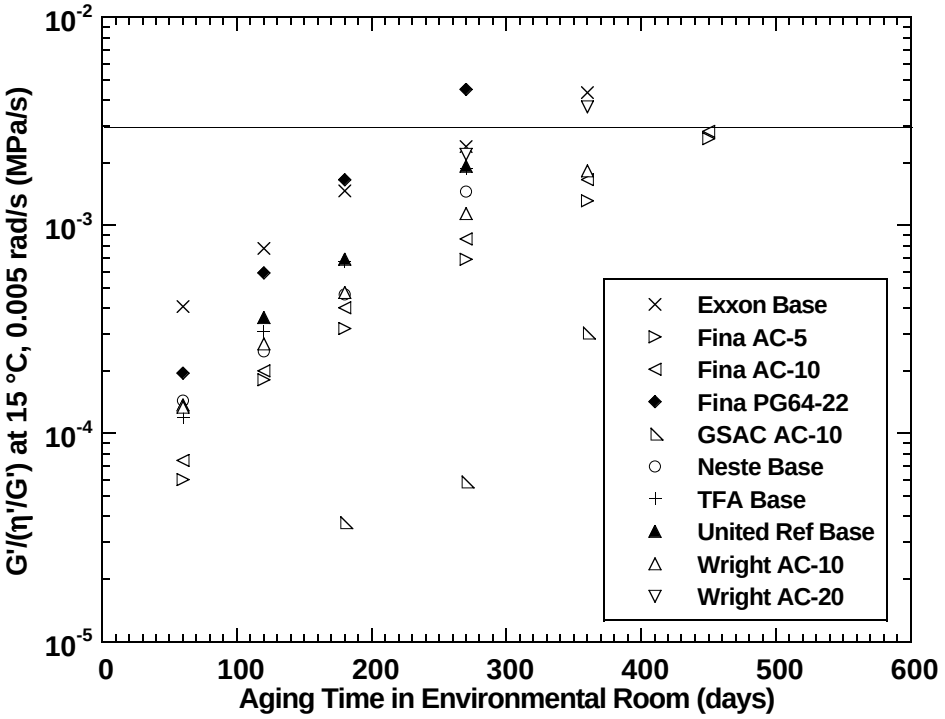

Figure 6-12. Change of G′/(η′/G′) with Aging Time in Environmental Room.

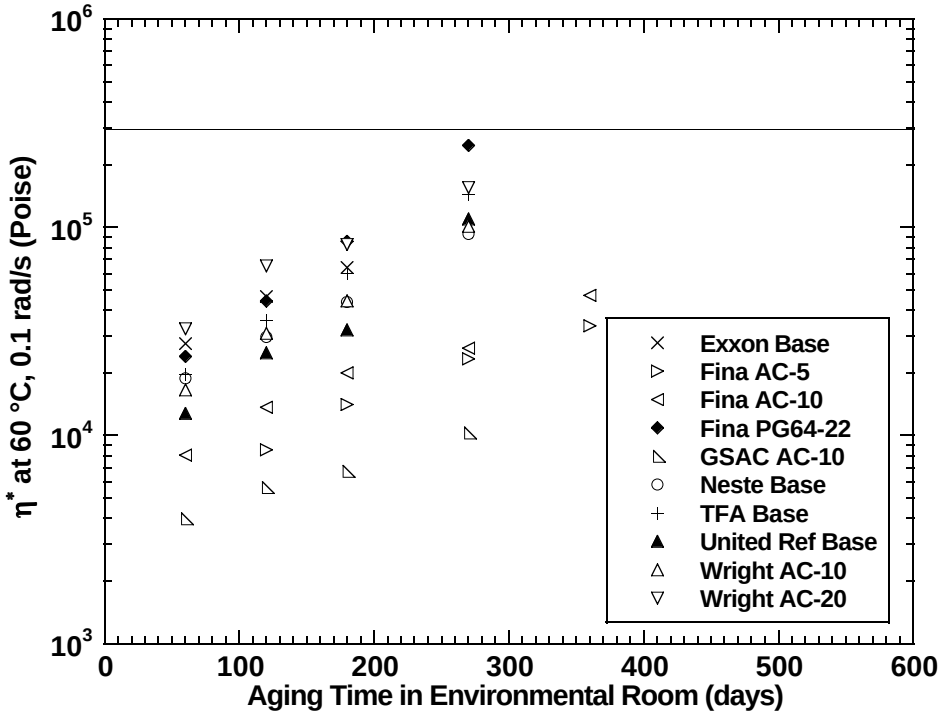

Figure 6-13. Change of η* with Aging Time in Environmental Room.

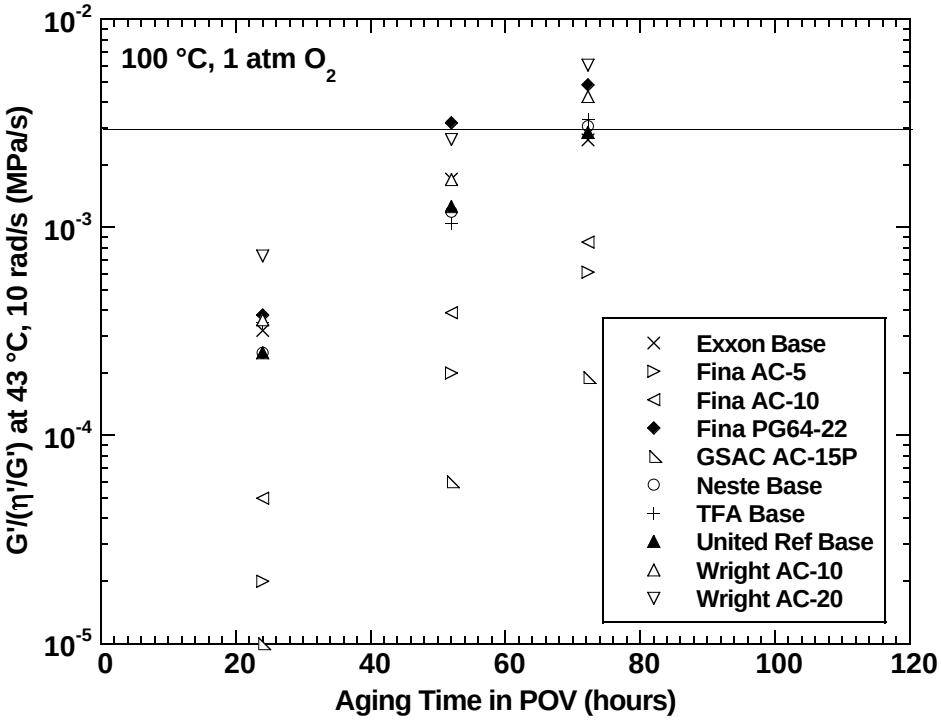

Figure 6-14. Change of G′/(η′/G′) with Aging Time at 100 °C, 1 atm O_2.

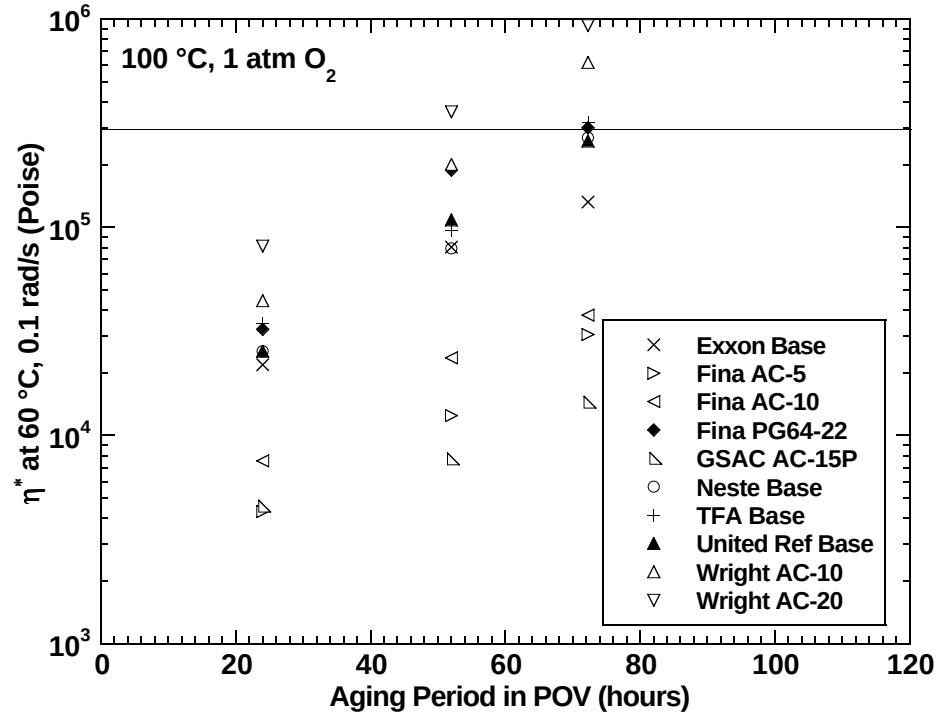

Figure 6-15. Change of η* with Aging Time at 100 °C, 1 atm O_2.

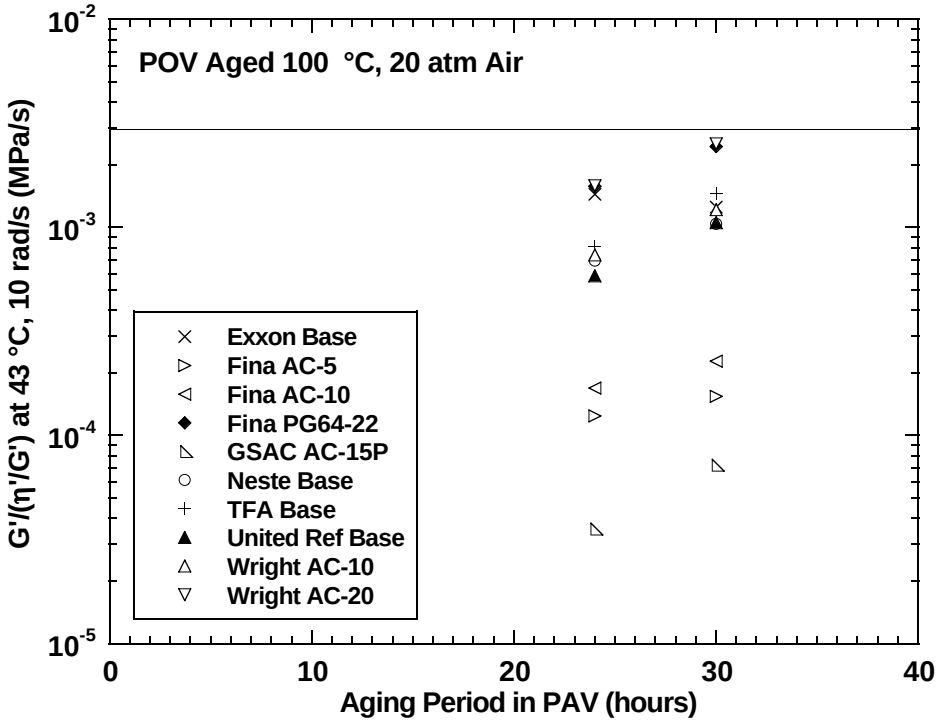

Figure 6-16. Change of G′/(η′/G′) for Thin Films with Aging Time in the PAV.

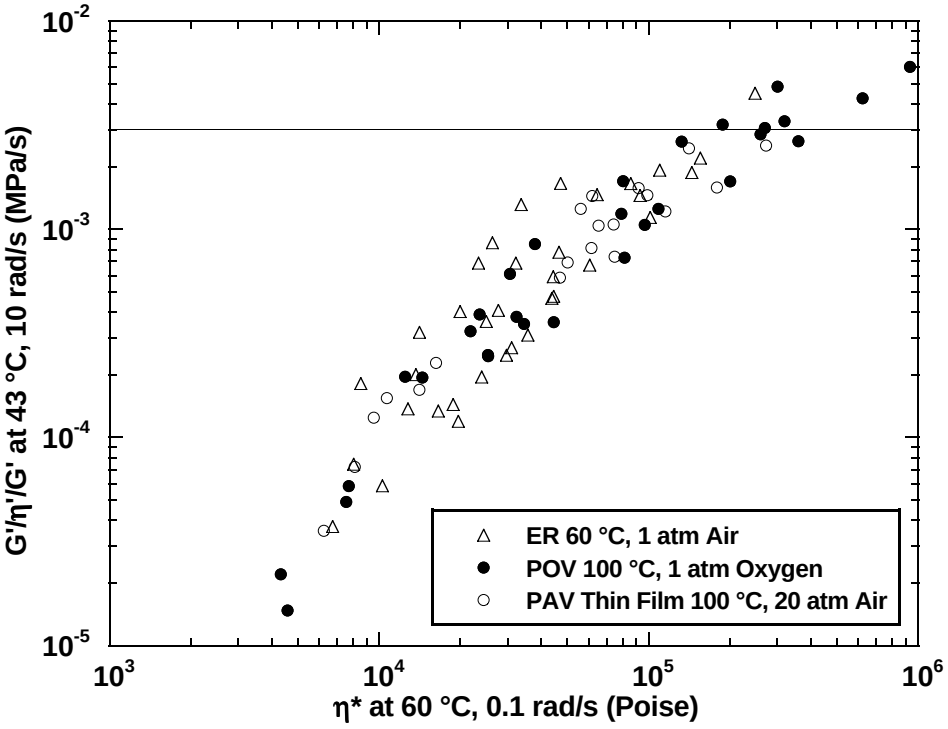

Figure 6-17. Relation Between G′/(η′/G′) and Viscosity for Several Aging Methods.

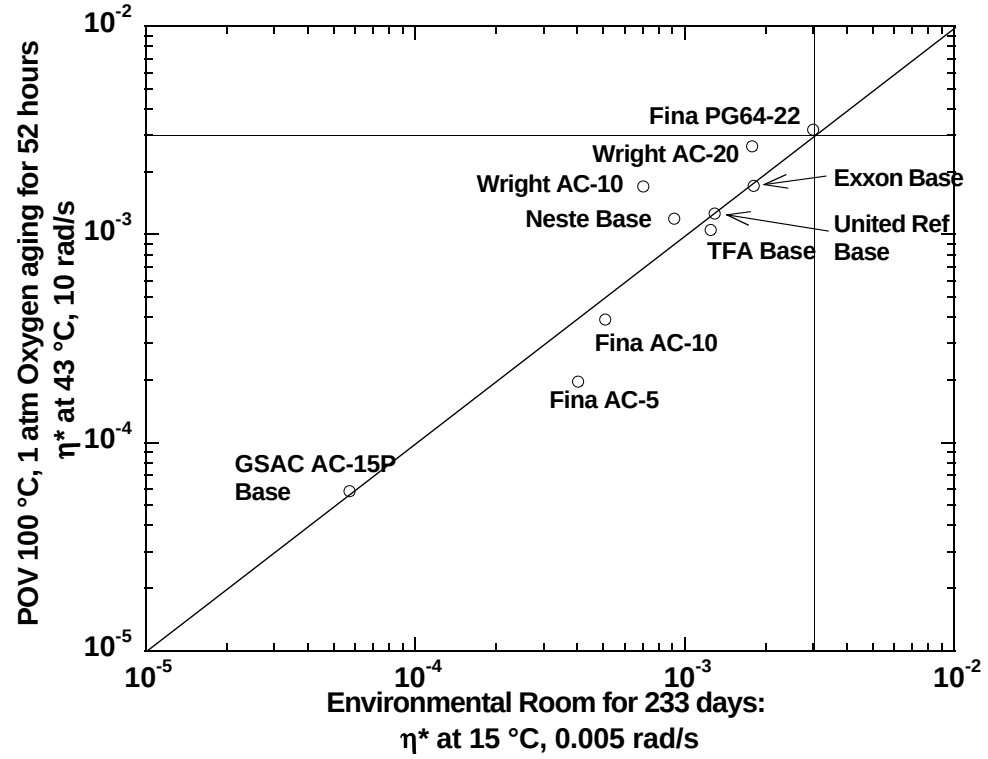

Figure 6-18. Comparison of ER Aging with PAV Aging: η*.

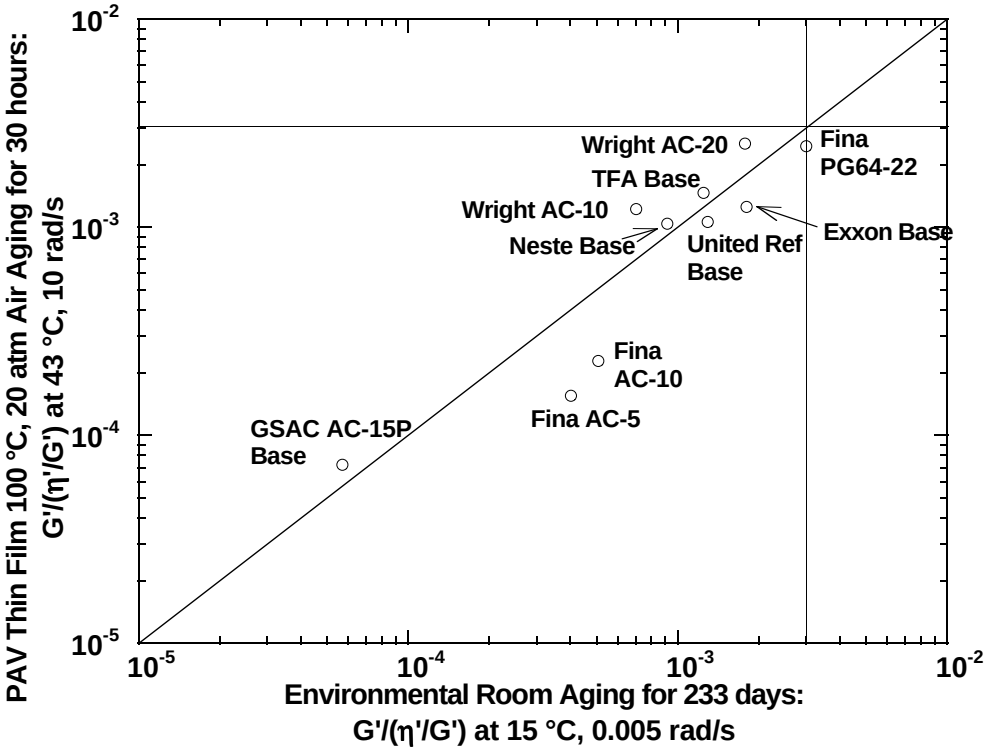

Figure 6-19. Comparison of ER Aging with PAV Aging: G′/(η′/G′).

RUNS INCLUDING MODIFIED AND BASE ASPHALTS

A series of runs were made with the following asphalts; the asphalts in the left column are the base materials.

Unmodified Materials	**Modified Materials**
TS 2000 AC-20	TS 2000 12% rubber
Exxon base	Ultrapave (Exxon base)
Fina PG 64-22	Fina PG 64-28
United Refinery Base	Ultrapave (UR base)
Wright AC-20	Wright AC-20 3% latex

Ultrapave (Exxon base) and Fina PG 64-28 contain 3.5% SBR latex, while Ultrapave (UR Base) contains 3% SBR latex, as does the Wright material. The TS 2000 asphalts are the control and 12% tire rubber containing material used in the TxDOT project 1460 test sections from 2000.

Good results had been obtained at 100 ^{o}C (212 ^{o}F) and 1 atm O_2, so this was repeated except air was used at 5 atm to obtain the same O_2 partial pressure. The results are listed in Table 6-6 at 77 hours of aging along with rankings and error when compared to the 60 ^{o}C (140 ^{o}F) environmental room at 233 days. Only eight of the asphalts were run in the environmental room. The values of the DSR function versus time are shown in Figure 6-20 for the unmodified asphalts. Asphalts AAD-1 and AAF-1 were also included to gain continuity with previous runs with mostly SHRP asphalts.

Surprisingly, 77 hours were required for the first asphalt to reach the crditical DSR function value of 0.003, while in the previous runs at 100 ^{o}C (212 ^{o}F) and 1 atm O_2, Figures 6-6 and 6-14, only about 52 hours were required. Figure 6-21 is a comparison of the DSR function at 77 hours for the current run with the 52-hour results using 1 atm O_2. The agreement is not bad, although Fina PG 64-22 has improved from worst to third from worst. It seems far from obvious that the presence of the inert nitrogen would slow the reaction to this extent. The increase in average error for the unmodified asphalts is not surprising, as only five of them were run here and there and this includes the Wright asphalts that always exhibit large errors.

Table 6-6. Rank and Absolute Error of Base and Modified Asphalts Based on the Function.

	Environmental Room at 233 hours		POV 100 °C, 20 atm Air at 26 hours			POV 100 °C, 5 atm Air at 77 hours		
	Function measured at 15 °C, 0.005 rad/s (MPa/s)	Rank	Function measured at 43 °C, 10 rad/s (MPa/s)	Rank	Absolute Log Error wrt ER (%)	Function measured at 43 °C, 10 rad/s (MPa/s)	Rank	Absolute Log Error wrt ER (%)
AAD-1	-		4.52×10^{-4}			5.87×10^{-4}		
AAF-1	-		3.11×10^{-3}			2.76×10^{-3}		
TS2000 AC-20	-		1.11×10^{-3}			1.84×10^{-3}		
Exxon Base	1.80×10^{-3}	6	1.39×10^{-3}	4	4.2	1.88×10^{-3}	5	0.7
Fina PG64-22 Base	3.00×10^{-3}	8	2.78×10^{-3}	7	1.3	2.14×10^{-3}	6	5.8
United Ref Base	1.29×10^{-3}	3	7.31×10^{-4}	2	8.6	1.20×10^{-3}	3	1.1
Wright AC-20	1.78×10^{-3}	5	2.96×10^{-3}	8	8.0	3.41×10^{-3}	7	10.3
Average Error					5.5			4.5
TS2000 12% Rubber	-		5.26×10^{-4}			6.47×10^{-4}		
UltraPave PG70-22 (Exxon Base)	1.36×10^{-3}	4	1.82×10^{-3}	6	4.4	1.77×10^{-3}	4	4.0
Fina PG64-28 3.5% Latex	3.83×10^{-4}	1	3.07×10^{-4}	1	2.8	3.15×10^{-4}	1	2.5
UltraPave PG70-22 (United Ref Base)	7.67×10^{-4}	2	1.34×10^{-3}	3	7.7	5.96×10^{-4}	2	3.5
Wright AC-20 3% Latex	2.22×10^{-3}	7	1.52×10^{-3}	5	6.2	6.57×10^{-3}	8	17.8
Overall Average Error					5.4			5.7

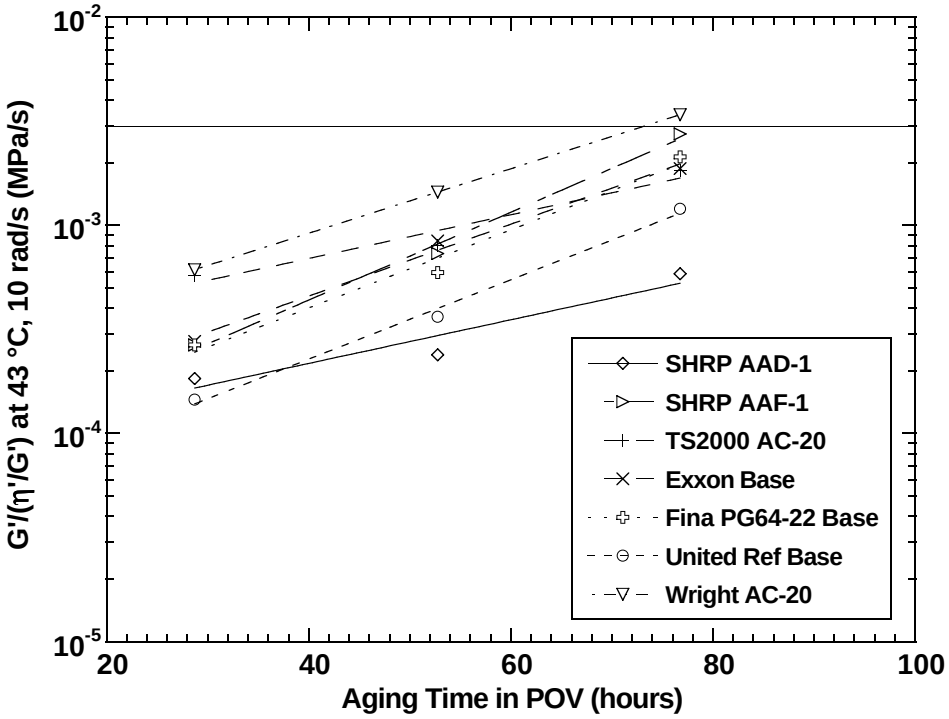

Figure 6-20. Change in G′/(η′/G′) with Aging Time: POV at 100 °C, 5 atm Air.

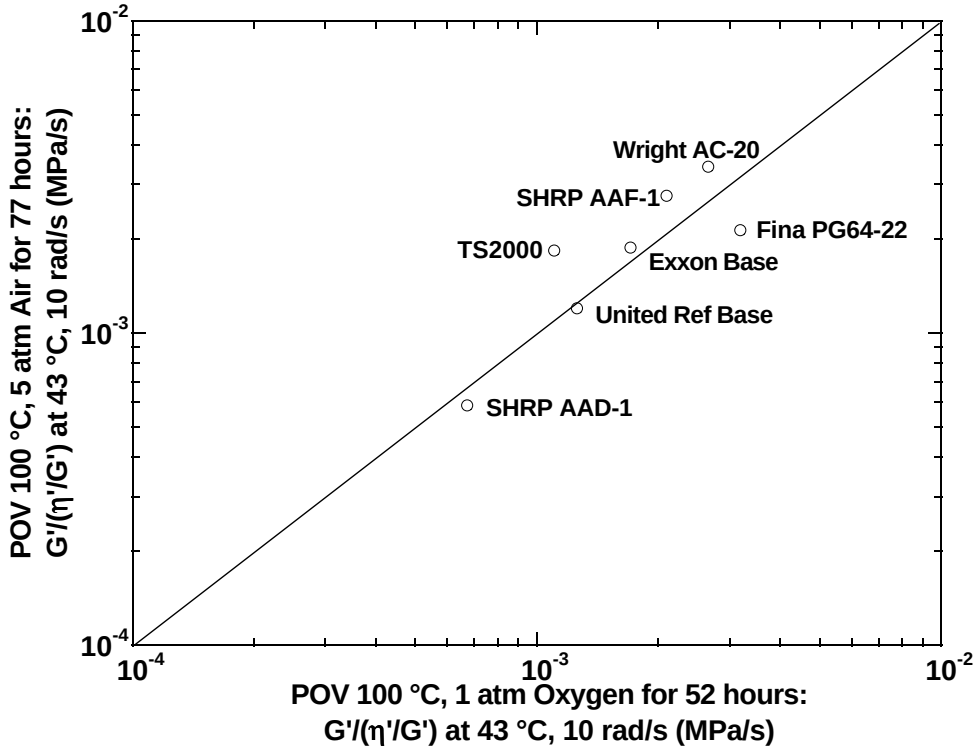

Figure 6-21. Comparison of POV Aging: 5 atm Air, 77 Hours versus 1 atm O_2, 52 Hours.

Figure 6-22 compares POV aging at 100 °C (212 °F) and 5 atm to environmental room aging for the modified asphalts and their base asphalts for the asphalts for which data at both conditions are available. The modified asphalts appear to behave fairly well as far as aging is concerned. Figure 6-23 shows the DSR function versus aging time for all five modified asphalts and their base asphalts. The aging of the Fina asphalt is much improved by modification, and it is significantly improved for the TS 2000 asphalt. The United Refinery and Exxon asphalts do not change much, and the Wright asphalt appears to have suffered significantly by modification. This is deceptive. Referring to Figures 5-11 and 5-12, showing how ductility varies with the DSR function, the Wright modified asphalts have a much higher ductility at given values of the DSR function. For all modified asphalts, the ductility is better than that of the base asphalt for a given function value; therefore, if the decline in function with aging is improved by the modifier, then the ductility is definitely improved. The reverse is not necessarily so and particularly not for the Wright asphalts. Complete data, viscosity, and function are given at the aging times shown in Figures 6-20 and 6-23 in Appendix A, Table A-5.

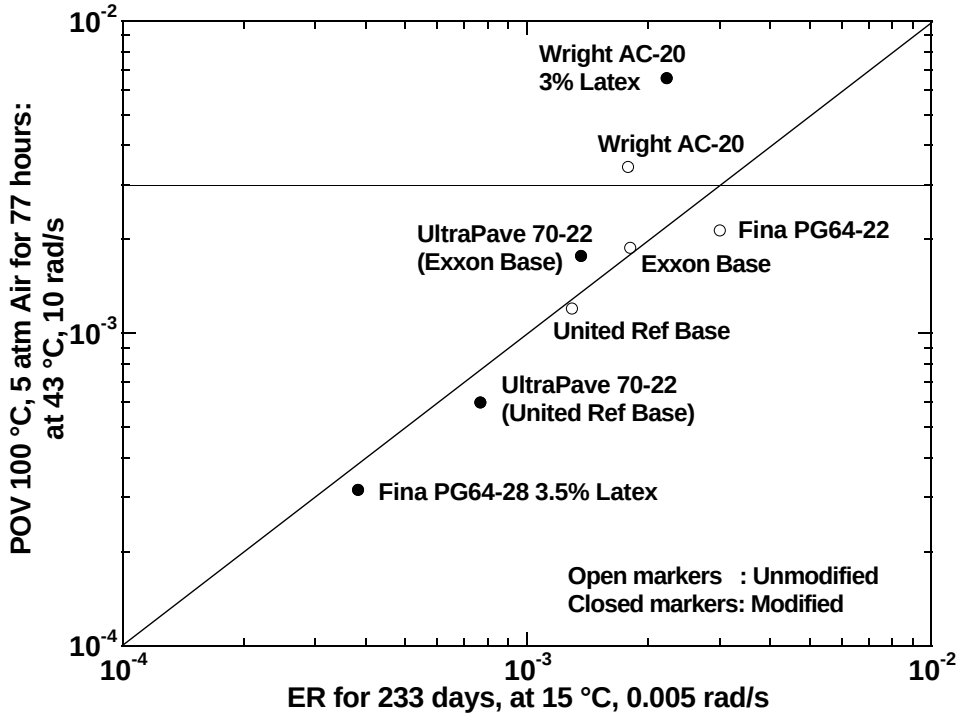

Figure 6-22. Comparison of POV (100 °C, 5 atm Air, 77 Hours) and ER (233 Days) Aging.

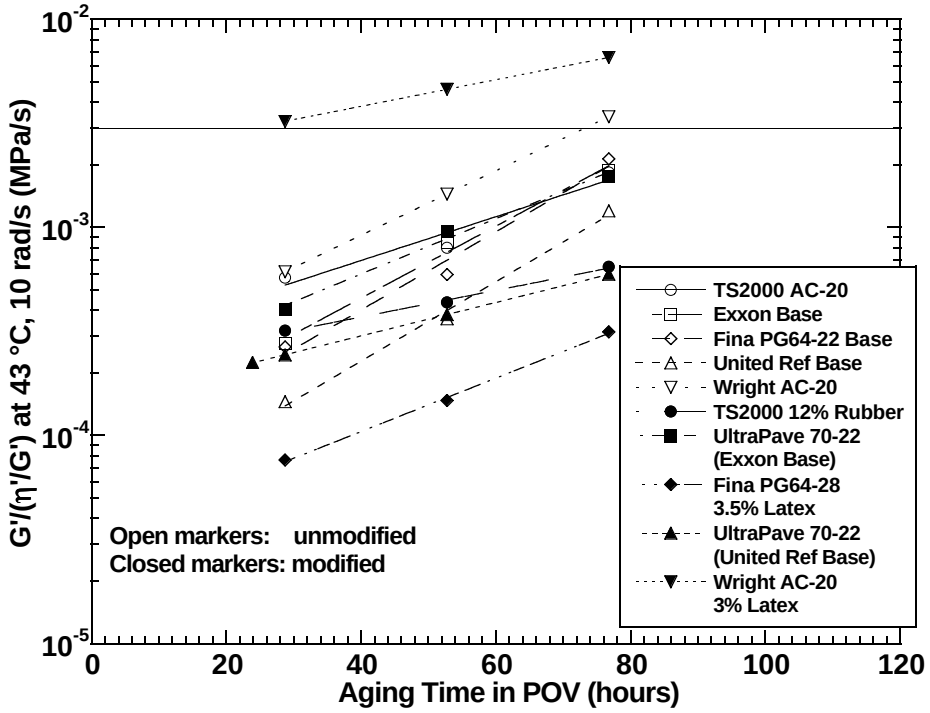

Figure 6-23. Effect of Modifiers on G′/(η′/G′) Aging at 100 °C, 5 atm Air.

The results in Table 6-5 for the run at 100 °C (212 °F) and 20 atm air were also promising, so they were repeated for the same materials, modified and unmodified, as were run in the 100 °C (°F), 5 atm air run. Runs were made at 26 and 30 hours. However, there was trouble with the pressure on the apparatus, and the 30-hour run was lost and results for the 26-hour run are suspect, as they do not fit with the two previous runs at 24 and 30 hours. The 26-hour data are shown in **Table 6-6** and the error compared to the environmental room is poorer than the 100 °C (212 °F), 5 atm run. All three PAV runs at 100 °C (212 °F) and 20 atm air are shown in Figure 6-24.

In summary, we observe the following results. In the last runs, PG 64-22 and Wright AC-20 asphalts were limiting in all cases but, as shown in Figures 6-18, 6-19, and 6-22, Wright asphalt is high compared to the environmental room and is not a good guide. On the other hand, Fina PG 64-22 tends to err the other way. For the SHRP asphalts, asphalt AAF-1 nearly always reached the critical DSR function value first. In the thin-film PAV at 90 °C (194 °F), it reached the value in 26 hours (Figure 6-5). In the POV at 100 °C (212 °F) and 1 atm O_2 (Figure 6-6), it was about 57 hours. For the latter run asphalts, PG 64-22 reached the critical value in 52 hours at 100 °C (212 °F) and 1 atm O_2 (Figure 6-14). In the POV at 100 °C (212 °F) and 20 atm air (Figure 6-16), it is seen that both Wright asphalt AC-20 and Fina PG 64-22 reach the critical value in slightly over 30 hours. Finally, at 100 °C and 5 atm air, both Wright AC-20 and AAF-2 require about 77 hours to reach the critical value.

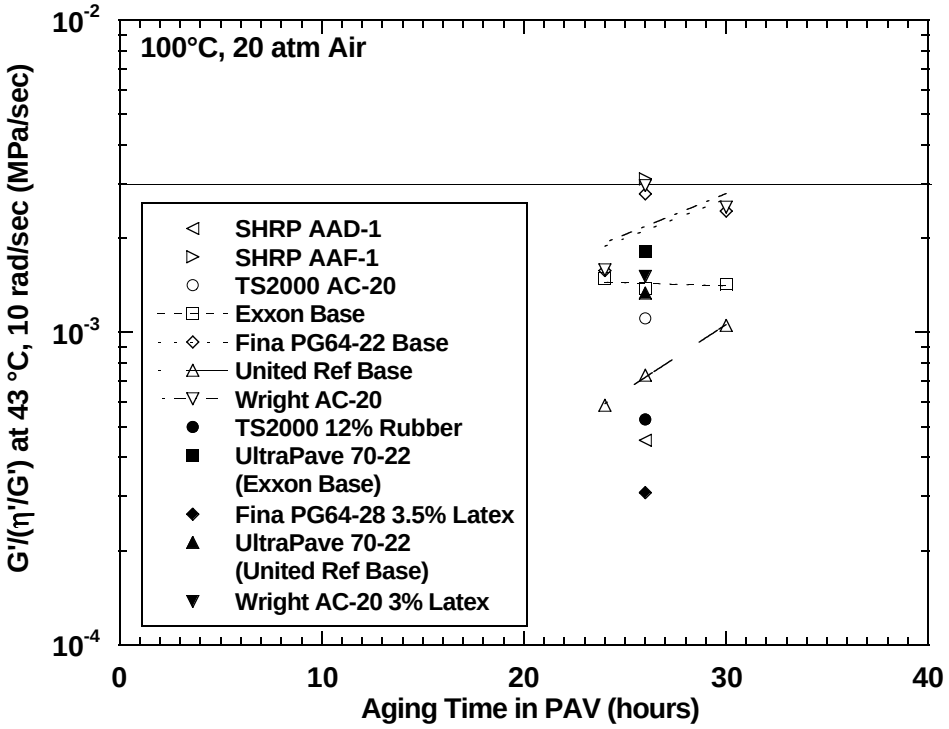

Figure 6-24. Thin-Film PAV Hardening Rates.

As suspected, the results for modified asphalts give very inconclusive results. As shown in previous studies, the aging of modified asphalts is even more complicated than that of unmodified asphalts, and the results in Chapter 4 show that the DSR-ductility correlation is not valid for modified asphalts. Even so, since the ductility is always higher than is indicated by the function, if the modifier also appears to slow the aging, it is very likely that it is decreasing the deterioration of the asphalt.

AGING BY AIR BLOWING

An attempt was made to replace the PAV with an airblowing procedure so that RTFOT and PAV aging could be accomplished in the same apparatus. Some of this is discussed in Chapter 3, dealing with the study of aging on low-temperature properties. As this represented a considerable effort, it will be further briefly discussed here.

The apparatus is described in Chapter 3 and is shown in Figure 3-2. Various combinations of air flow, mixer rpm, and mixer design were investigated, and the results are rather impressive except for two serious problems: first, operating a mixer unit overnight poses both safety and design issues, and second, as seen in Chapter 3, the carbonyl area at a given viscosity was different from that obtained in the environmental room. As both are oxidizing at 1 atm, studies have shown that the carbonyl to viscosity ratio should be the same.

Figure 6-25 is part of a study to attempt to use air blowing at 163 ºC (325 ºF) to simulate the RTFOT. In TxDOT project 0-1742, a similar apparatus was developed to simulate the

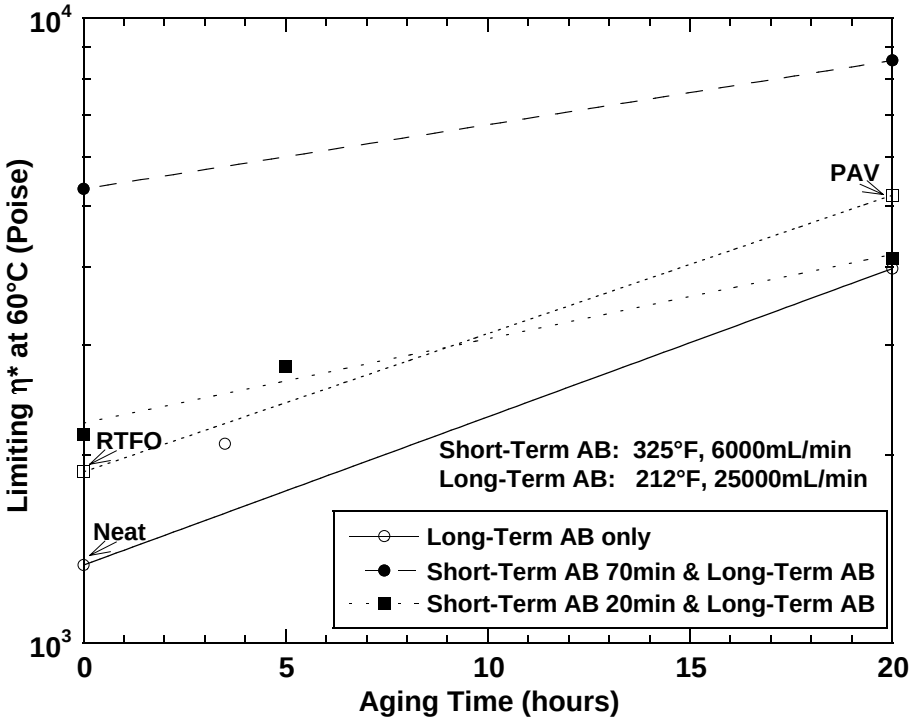

Figure 6-25. Simulation of RTFOT Aging in Air-Blowing Apparatus.

hot-mix operation and it required 30 minutes, whereas Figure 6-25 indicates that 20 minutes is sufficient at these conditions. The difference is a higher rpm and air-flow rate.

In Table 6-7, results are given for a number of asphalts. They were first air blown for 20 minutes at 163 °C (325 °F) at 6 L/min to simulate the RTFOT and then at 100 °C (212 °F) and 24 L/min to simulate the PAV. We see that PAV viscosities were reached at times ranging from less than 20 hours for asphalt AAS-1 to about 30 hours for asphalt AAG-1. These times should not all agree with the PAV time of 20 hours because the difference in pressure changes the relative hardening rates of the asphalts. The remarkable thing is that similar aging rates have been achieved at 1 atm as obtained in the PAV at 20 atm. This shows that the PAV is extremely limited by diffusion.

CONCLUSION

Many aging conditions have been investigated and compared to environmental room aging at 60 °C (140 °F) and 1 atm air. As suspected, no condition is able to accurately accelerate the aging rates so that the relative rates of hardening are the same as the simulated road condition in the environmental room. It is encouraging, however, that the same asphalts failed the DSR parameter at a large number of conditions, and this was true at conditions that do not require an extended aging time. We are therefore confident that we can specify a procedure that reasonably identifies asphalts that experience excessive oxidative hardening that is likely to lead to premature roadway failure.

Table 6-7. Viscosities of Airblown Asphalts

	Limiting 60°C Viscosity (Poise)								
Airblow Time	Exxon AC-10 [a]	Exxon AC-20 [a]	AAA-1 [a]	AAB-1 [a]	AAD-1 [a]	AAF-1 [a]	AAG-1 [b]	AAM-1 [a]	AAS-1 [a]
0	1,287	2,305	1,130	1,569	1,479	2,166	2,250	2,429	2,584
20 minutes	2,158	4,090	2,337	4,076	4,374	5,128	3,827	6,196	6,372
RTFO equivalent									
5 hours	2,776								
10 hours			4,274	8,005	10,828	14,810	6,574		15,361
20 hours	4,132	23,900	6,895	14,947	23,827	26,128	8,240		28,820
30 hours			10,105	24,771	95,587	45,900	10,340		50,488
40 hours			15,450	51,652	594,000	136,000	10,910		99,745
50 hours			26,310	112,351	-	252,000	15,403		264,000
Conventional RTFO + PAV	5,211		11,940	18,070	29,310	25,760	10,370		22,530

a : Aging condition is 163 °C, 1600 rpm, 6 L air/min (short-term) and 100 °C, 1600 rpm, 24 L air/min (long-term).
b : Aging condition is 163 °C, 1550 rpm, 6 L air/min (short-term) and 100 °C, 1550 rpm, 24 L air/min (long-term).

CHAPTER 7. WATER SUSCEPTIBILITY

We conducted a brief study of water susceptibility to make sure that modifiers did not adversely affect the water resistance of asphalt mixes and to see if there was any relation between water susceptibility of unmodified asphalts and PG grade and hardening tendencies.

The asphalts included the control and two levels of CRM asphalts (project 1460 test section 2000) SHRP asphalts AAA-1 and ABM-1, Wright asphalt AC-10 and Wright AC-10 modified with 3 percent SBR latex, and Wright AC-30P, which is Wright AC-10 modified with 3 percent SBS. The mix design is shown in Table 7-1. Binder content was 5.1 percent and no lime was used. Lottman's were run in accordance with Tex 531-C, "Prediction of Moisture Induced Damage to Bituminous Paving Materials Using Molded Specimens."

The results are shown in Figures 7-1 and 7-2. The modifiers seem to help the dry strength except for SBS, but wet strength less so. Rubber at 12 percent and 3 percent SBR seemed to give some improvement in the TSR ratio, while 8 percent rubber and SBS were slightly deleterious. In general, it appears that modifiers will have only a minor effect on water susceptibility.

The most striking effect is the superiority of asphalt ABM-1. Continuous PG grades as well as DSR functions as obtained in Chapter 8 for asphalts aged at 100 ^{o}C (212 ^{o}F), 1 atm O_2 and 52 hours are listed in Table 7-2 for the unmodified asphalts. At least for this small sample, no connection between grade, DSR function, or water susceptibility is discernible, except that ABM-1 has a good DSR function, the best wet and dry strength, and the worst grade span. These relations do not continue for the other asphalts, however.

Table 7-1. Aggregate Gradation and Materials for the Laboratory Specimens.

	Colo Materials D Rock Hunter		Colo Materials F Rock Hunter		Gifford-Hill Wash Scr. New Braunfels		Young Matls Sand Riverbend		Source 6 Aggr. Num 6 Lab Num 6		Total % 100.0			
Sieve Size	Bin#1 39.4	Total %	Bin#2 21.2	Total %	Bin#3 29.3	Total %	Bin#4 10.1	Total %	Bin#5 0.0	Total %	Cum. Pass	TxDOT Specs.	Ind. Ret.	Cum. Ret.
1"	100.0	39.4	100.0	21.2	100.0	29.3	100.0	10.1	100.0	0.0	100.0	100 - 100	0.0	0.0
7/8"	100.0	39.4	100.0	21.2	100.0	29.3	100.0	10.1	100.0	0.0	100.0	100 - 100	0.0	0.0
5/8"	99.5	39.2	100.0	21.2	100.0	29.3	100.0	10.1	100.0	0.0	99.8	98 - 100	0.2	0.2
3/8"	76.4	30.1	100.0	21.2	100.0	29.3	100.0	10.1	100.0	0.0	90.7	85 - 100	9.1	9.3
#4	6.0	2.3	70.7	14.9	99.5	29.2	100.0	10.1	100.0	0.0	56.5	50 - 70	34.2	43.5
#10	2.4	0.9	7.6	1.6	72.0	21.1	100.0	10.1	100.0	0.0	33.7	32 - 42	22.8	66.3
#40	1.9	0.7	2.6	0.5	22.6	6.7	99.3	10.0	100.0	0.0	17.9	11 - 26	15.8	82.1
#80	1.7	0.7	2.2	0.5	8.6	2.5	12.8	1.3	100.0	0.0	5	4 - 14	12.9	95
#200	0.8	0.3	0.7	0.1	4.1	1.2	0.5	0.1	100.0	0.0	1.7	1 - 6	3.3	98.3

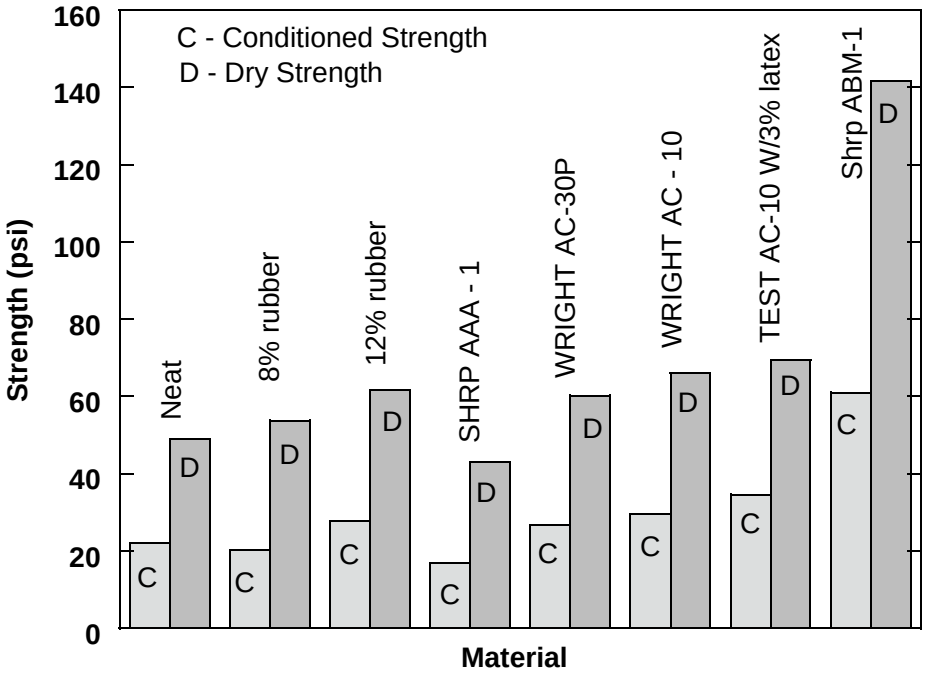

Figure 7-1. Dry and Conditioned Strengths for the Laboratory Specimens.

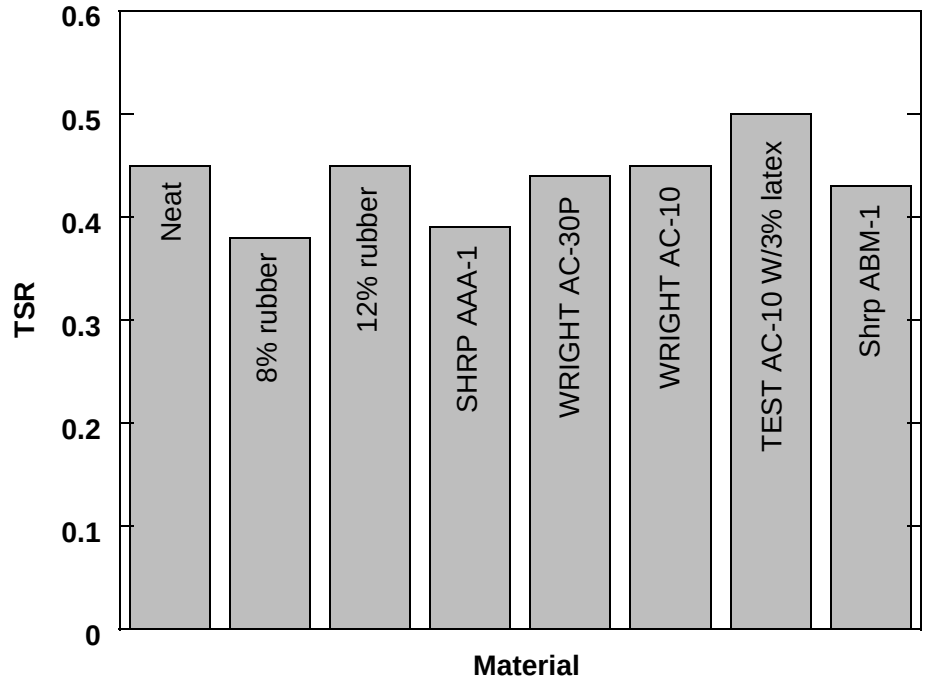

Figure 7-2. Tensile Strength Ratios for the Laboratory Specimens.

Table 7-2. Comparison of PG Grade Span and DSR Function.

Asphalt	DSR Function	Continuous Grade	Grade Span
AAA-1	3.77×10^{-4}	60-33	93
ABM-1	1.93×10^{-4}	66-14	80
TS 2000	1.10×10^{-3}	68-29	97
Wright AC-10	1.70×10^{-3}	61-29	90

CHAPTER 8. RECOMMENDED TEST PROCEDURE FOR PREDICTING AGE-RELATED CRACKING OF ASPHALTS

The purpose of this protocol is to provide a test to identify asphalts that might be expected to fail prematurely as a result of rapid loss of ductility on aging. The test includes the following steps: first the asphalt is subjected to RTFOT or SAFT (stirred air-flow test) aging to simulate the hot-mix operation, then it is subjected to longer term aging to simulate road aging. Finally, the asphalt is analyzed with the DSR and the function G'/(η'/G') is determined at 43 °C (109 °F) and 10 rad/s, which was shown in Chapter 5 to correlate well with ductility measured at 15 °C and 1 cm/min. A critical value of the ductility of 3 cm was chosen because the literature indicates that few, if any, pavements can survive at this value. This corresponds to a DSR function of 0.003.

As discussed in Chapter 4, we conducted an extensive study of various aging conditions to find a condition that correlates reasonably well with low-temperature atmospheric pressure aging as measured in the 60 °C (140 °F) environmental room. At the same time, the conditioning must be such that the test time is reasonable. Based on these studies, we recommend a first choice and an alternate. The first is the standard PAV except that the asphalt is deposited in a thin film and the aging time is longer. The second is also conducted in the PAV with asphalt deposited in a thin film, but the PAV is filled with oxygen at low pressure and the aging time is longer still. We realize that there may be an objection to using pure oxygen even at low pressure, but this is included because conditions at or near these values gave consistently better results.

UNMODIFIED ASPHALTS

Recommended Procedure

Test Equipment: standard PAV; 4 cm by 7 cm aluminum trays; DSR.

Test Conditions: 100 °C, 20 atm air for 28 hours.

Sample Preparation: 2.4 grams of asphalt are weighed into a 4 cm by 7 cm aluminum tray. The tray is heated slightly to obtain a uniformly thick film of asphalt in the tray. This produces an asphalt film approximately 0.857 mm thick.

Operation: Two trays will fit in each of the PAV shelves. Once the vessel is loaded and sealed, operation is identical to the standard PAV procedure except that the aging time is 28 hours.

Measurement of the DSR Function: Sufficient asphalt is removed from the tray, and G′ and η′ are measured at 43 °C and 10 rad/s and the function G′/(η′/G′) is calculated.

Evaluation: If the value of G′/(η′/G′) is larger than 0.003 MPa/s, the asphalt fails.

Alternate Procedure

The equipment and sample preparation are the same, but operating conditions are 100 ºC, 1 atm oxygen with an aging time of 52 hours. The function measurement and evaluation are unchanged.

Comment

These procedures are tentative, as insufficient replication has been made at each condition, and more asphalts, especially those likely to fail, should be tested. In the meantime, it would be informative to routinely run these tests, as it will be found that asphalts that have the same performance grade may perform quite differently on the test. It may also be found that some unmodified asphalts with high upper PG grade will perform poorly in the test.

PROCEDURE FOR MODIFIED ASPHALTS

We are not recommending a definite pass-fail procedure for modified asphalts. It is clearly shown in Chapter 5 that the DSR-ductility correlation does not hold for modified asphalts because their fundamental rheology is so different from conventional materials. It has also been shown that accelerated aging procedures are even less reliable for these materials (Glover, et al., 2000). Even so, these measurements could be useful for modified asphalts.

As seen in Chapter 5, all modified asphalts have ductilities better than those indicated for unmodified asphalts at a given value of the DSR function. The difference is small for small amounts of modifier but quite large for some materials, especially the modified Wright asphalts. If the aging procedure indicates a lower aging rate (of questionable reliability), it is very likely that the modifier is slowing the decrease in ductility and increasing ultimate life.

CHAPTER 9. SUMMARY OF INVESTIGATIONS, FINDINGS, AND RECOMMENDATIONS

This project was designed to answer questions about the adequacy of Superpave specifications and in particular to find a specification superior to the $G^*\sin\delta$ function which does not satisfactorily predict fatigue cracking. There was also concern that the PAV might not accurately simulate hardening of in-service asphalt pavements. With the increasing use of modifiers there is concern about the applicability of Superpave specifications to these materials, and also about the effect of modifiers on water susceptibility.

We addressed all of these questions in this project with emphasis on finding a DSR-derived function that could be reliably used to protect against cracking resulting from excessive oxidative hardening and subsequent fatigue. The literature contains data that indicate that ductility measured at lower temperatures such as 10-15 ^{o}C (50-59 ^{o}F) correlates well with the conditions of old roadways, so a correlation was needed between ductility and DSR measurements.

SUMMARY OF INVESTIGATIONS

This project was a comprehensive study directed at developing an improved method of screening asphalt binders for long-term pavement performance. This work involved a fresh look at asphalt binder oxidation methods, the effect of binder aging on Superpave performance properties, especially low-temperature BBR S and m, and especially the role of other properties important to durability and that are not included in Superpave. Specifically, this work included

- fundamental studies of asphalt oxidation, especially of the effect of oxygen pressure on asphalt hardening rates, important for understanding the suitability of accelerated aging procedures such as the PAV;

- studies of the suitability of the PAV as a conditioning procedure for assessing long-term binder durability;

- studies of the effect of aging on low-temperature asphalt properties;

- investigations to develop an appropriate DSR physical property that relates to long-term binder durability in pavements and that can be readily measured with existing DSR equipment;

- investigations of the impact of polymer modifiers on binder properties and on binder durability;

- extensive studies of accelerated aging methods to determine an appropriate procedure for conditioning asphalt to simulate long-term pavement aging with combined objectives of

accurately representing aging while at the same time being able to be performed in a reasonable length of time; and

- investigations of the effect of modifiers on water susceptibility.

SUMMARY OF FINDINGS

- An excellent correlation was found for unmodified asphalts between ductility (at 15 °C, 1 cm/min) below 10 cm and the DSR function $G'/(\eta'/G')$. This was coupled with a new aging procedure in a tentative specification which should guard against failure caused by premature asphalt hardening and consequent fatigue cracking. This method should be a good predictor of asphalt resistance to failure due to oxidative hardening. The developed method is not adequate for modified asphalts.

- The correlation was originally developed for DSR measurements at 15 °C and 0.005 rad/s. These conditions were shifted to 43 °C and 10 rad/s by using the time-temperature superposition principle to produce a method that is easily accessible to standard laboratory rheological equipment and methods.

- The recommended aging procedure uses the PAV apparatus but is modified by taking advantage of the higher average aging rate when the asphalt is aged in thiner films. This, combined with a somewhat longer aging, results in more extended binder aging and thus a more rigorous test of durability than the standard PAV method. At the same time, the resulting rankings of aged materials is more representative of rankings that are obtained from aging at atmospheric air pressure and 60 °C.

  In theory, replacing pavement-condition aging with a procedure accelerated with higher temperature and pressure is an intractable problem because of variation in the response of different asphalts to temperature and pressure, but a wide variety of conditions were tested and compared to relative hardening rates in a 60 °C (140 °F) environmental room. Asphalts were aged in both the standard PAV and our POV (pressure oxygen vessel) apparatus. Aging conditions were evaluated on the basis of time and relative deviation from the environmental room results, which required months of aging.

- For modified asphalts, the results were complex. Generally for a given value of the DSR function, the ductility was better than indicated by the DSR function correlation for unmodified asphalts. Larger amounts of modifier produced increasing values of ductility for a given function value. This was very asphalt dependent, however, so no general correlation could be found.

- For modified asphalts, the force-ductility method showed that modifiers change the extensional behavior of binders by providing stabililty to the binder under flow and, in some cases, by increasing the failure stress of the binder. These effects can result in

much improved binder ductility for unaged or lightly aged binders.

- As modified binders oxidize, the asphalt hardens and the improvement to ductility imparted by modifiers decreases. After enough aging, the improvement is gone and modified binders perform no better than their aged unmodified counterpart. Nevertheless, modifiers appear to provide added life to binders. A critical issue remains as to whether the life extension is cost effective and will rely on the actual extension and the cost of modification.

- Ductility and aging results indicate that polymer modifiers generally improve asphalt aging but the amount of improvement is modifier and asphalt dependent.

- SBS or SBR at small concentrations (1 percent) do not have much beneficial effect on binder hardening.

- Low temperature properties, BBR and direct tension, were measured for asphalts aged in the standard PAV procedure and in the environmental room. The properties for PAV-aged asphalts agreed remarkably well with the properties obtained after 38 days in the environmental room, though longer times in the PAV did not correlate as well with any specific longer time in the environmental room.

- The PAV can be eliminated and BBR run after the RTFOT (or alternative hot-mix aging procedure) with only a small error that can be estimated based on values of $G^*/\sin\delta$ at 18 °C.

- Water susceptibility was determined for several asphalts with and without modifiers, and the results indicated that the modifiers did not greatly affect the water susceptibility.

RECOMMENDATIONS

Recomendations of this project arise from the need to evaluate implementing the proposed procedures, to verify assumptions of the proposed durability evaluation method, and to better understand the interactions of modifiers and asphalt. Specific recommendations are:

- TxDOT should start evaluating the test procedure to become familiar with it and with the performance of various asphalts, preliminary to implementation;

- the DSR function criterion should be evaluated (calibrated) with unmodified binders extracted and recovered from pavements of known fatigue cracking and adjusted as appropriate;

- TxDOT should evaluate using the abbreviated procedure for determining low-temperature Superpave properties immediately after the hot-mix aging test, without PAV

conditioning;

- polymer modification should be further studied to understand the cause of the benefit degradation that occurs due to aging and whether this can be improved by adjusting asphalt composition;

- the effect of asphalt composition on polymer benefit should be studied;

- the effect of modifier on binder failure stress should be studied to obtain a better understanding of this phenomenon.

CHAPTER 10. REFERENCES

Anderson, D.A., and T.W. Kennedy. (1993) Development of SHRP Binder Specification. *Proc. Assoc. Asphalt Paving Technol.*, Vol. 62, pp. 481-507.

Anderson, D.A., D.W. Christensen, and H. Bahia. (1991) Physical Properties of Asphalt Cement and the Development of Performance-Related Specifications. *Proc. Assoc. Asphalt Paving Technol.*, Vol. 60, pp. 437-475.

Anderson, D.A., D.W. Christensen, R. Dongre, M.G. Sharma, J. Runt, and P. Jordhal. (1990) Asphalt Behavior at Low Service Temperatures. *FHWA-RD-88-078*, Federal Highway Administration, McLean, VA.

Anderson, D.A., D.W. Christensen, H.U. Bahia, R. Dongre, M.G. Sharma, C.E. Antle, and J. Button. (1994) *Binder Characterization and Evaluation, Volume 3: Physical Characterization*. SHRP A-369, Strategic Highway Research Program/National Research Council. Washington, D.C., p 31.

Anderson, D.A., D.W. Christensen, R. Roque, and R.A. Robyak. (1992) Rheological Properties of Polymer Modified Emulsion Residue. In ASTM STP 1108: *Polymer Modified Asphalt Binders*, K.R. Wardlaw and S. Shuler (Eds.), American Society for Testing and Materials, San Antonio, TX., pp. 20-34.

Anderson, D.I., D.E. Peterson, and M. Wiley. (1976) Characteristics of Asphalts as Related to the Performance of Flexible Pavements. *Research Report No. UDOT-MR-76-6*, State of Utah Department of Transportation.

Asphalt Institute. (1994) Performance Graded Asphalt Binder Specification and Testing. *SuperPave series No. 1 (SP-1)*.

ASTM D113-86. (1994) Standard Test Method for the Ductility of Bituminous Materials. Annual Book of ASTM Standards, Vol. 04.03, pp. 23-25.

ASTM D4124. (1994) Standard Test Methods for Separation of Asphalt into Four Fractions. Annual Book of ASTM Standards, Vol. 04.03, pp. 432-437.

Bahia, H.U., and D.A. Anderson. (1993) Glass Transition Behavior and Physical Hardening of Asphalt Binders. *Proc. AAPT*, Vol. 62, p. 93.

Boudart, M. (1991) *Kinetics of Chemical Process*; Butterworth-Heinemann, Stoneham, MA.

Bouldin, M.G., and J.H. Collins. (1992) Influence of Binder Rheology on Rutting Resistance of Polymer Modified and Unmodified Hot Mix Asphalt. In ASTM STP 1108: *Polymer Modified*

Asphalt Binders, K.R. Wardlaw and S. Shuler (Eds.), American Society for Testing and Materials, San Antonio, TX., pp. 55-60.

Bouldin, M.G., J.H. Collins, and A. Berker. (1991) Rheology and Microstructure of Polymer/Asphalt Blends. *Rubber Chemistry and Technology*, Vol. 64, pp. 577-600.

Chaffin, J.M., M. Liu, R.R. Davison, C.J. Glover, and J.A. Bullin. (1997) Supercritical Fractions as Asphalt Recycling Agents and Preliminary Aging Studies on Recycled Asphalts. *Ind. Eng. Chem. Res.*, Vol. 36 (3), pp. 656-666.

Chipps, J.F. (2001) *The Industrial Manufacture of Tire Rubber-Modified Asphalts with Enhanced Rheological Performance and Improved Longevity*. Ph.D. Dissertation, Texas A&M University, College Station, TX.

Christensen, D. W. and D. A. Anderson. (1992) Interpretation of Dynamic Mechanical Test Data for Paving Grade Asphalt Cements. *J. Am. Assoc. Paving Technol.*, Vol. 61, pp. 67-98.

Clark, R.C. (1958) Practical Results of Asphalt Hardening on Pavement Life. *Proc. Assoc. Asphalt Paving Technol.*, Vol. 27, pp. 196-208.

Collins, J.H., M.G. Bouldin, R. Gelles, and A. Berker. (1991) Improved Performance of paving Asphalts by Polymer Modification. *Proc. Assoc. Asphalt Paving Technol.*, Vol. 60, p. 43-79.

Corbett, L.W. (1979) Dumbbell Mix for Better Asphalt. *Hydrocarbon Processing*, Vol. 58, pp. 173-177.

Davison, R.R., J.A. Bullin, C.J. Glover, B.L. Burr, H.B. Jemison, A.L.G. Kyle, and C.A. Cipione. (1989) Development of Gel Permeation Chromatography, Infrared and Other Tests to Characterize Asphalt Cements and Correlate with Field Performance. *Research Report No. 458*, Texas State Dept. of Highways and Public Transportation.

Davison, R.R., J.A. Bullin, C.J. Glover, J.R. Stegeman, H.B. Jemison, B.L. Burr, A.L. Kyle, and C.A. Cipione. (1991) Design and Manufacture of Superior Asphalt Binders. *FHWA/TX-91/1155-1F*.

Dhalaan, M.A., F. Balghunaim, I.A. Dhubaib, and A.S. Noureldin. (1992) Field Trials with Polymer Modified Asphalts in Saudi Arabia. In ASTM STP 1108: *Polymer Modified Asphalt Binders*, K.R. Wardlaw and S. Shuler (Eds.), American Society for Testing and Materials, San Antonio, TX., pp. 203-223.

Domke, C.H. (1999) *Asphalt Compositional Effects on Physical and Chemical Properties*. Ph.D. Dissertation, Texas A&M University, College Station, TX.

Domke, C.H., R.R. Davison, and C.J. Glover. (1999) Effect of Oxidation Pressure on Asphalt Hardening Susceptibility. *Transp. Res. Rec.*, Vol. 1661, pp. 114-121.

Domke, C.H., Davison, R.R., and Glover, C.J. (2000) Effect of Oxygen Pressure on Asphalt Oxidation Kinetics. *Ind. Eng. Chem. Res.*, Vol. 39 (3), pp. 592-598.

Domke, C.H., R.R. Davison, C.J. Glover, and J.A. Bullin. (1997) The Effect of Asphaltenes on SHRP Superpave™ Specifications. Presented at Symposium #635 "Advances in the Chemistry of Asphaltene and Related Substances," at the 5th North American Chemical Congress, Cancun, Mexico, November 11-15.

Domke, C.H., M. Liu, R.R. Davison, J.A. Bullin, and C.J. Glover. (1997) Study of Strategic Highway Research Program Pressure Aging Vessel Procedure Using Long-Term, Low-Temperature Aging Experiments and Asphalt Kinetics. *Trans. Res. Rec.*, Vol. 1586, pp. 10-15.

Doyle, P.C. (1958) Cracking Characteristic of Asphalt Cement. *Proc. Assoc. Asphalt Paving Technol.*, Vol. 27, pp. 581-597.

Ferry, J.D. (1980) *Viscoelastic Properties of Polymers*, 3rd edition, John Wiley & Sons, New York, p. 82.

Fromm, H.J., and W.A. Phang. (1970) Temperature Susceptibility Control in Asphalt Cement Specifications. *Report IR 35*, Ontario Department of Highways.

Gahvari, F. (1997) Effect of Thermoplastic Block Copolymers on Rheology of Asphalt. *J. of Materials in Civil Engineering*, pp. 111-116.

Gallagher, K.P, H.U. Gahia, J.D. Guerra, and J. Keating. (1996) Influence of Air-Blowing on the Performance-Related Properties of Paving Asphalt. *Transp. Res. Rec.*, Vol. 535, p. 29.

Glover, C.J., R.R. Davison, J.A. Bullin, C.K. Estakhri, S.A. Williamson, T.C. Billiter, J.F Chipps, J.S. Chun, P. Juristyarini, S.E. Leicht, and P. Wattanachai. (2000) A Comprehensive Laboratory and Field Study of High Cure Asphalt-Rubber Materials. Texas Dept. of Transp. Research Report No. 1460.

Goodrich, J.L (1988) Asphalt and Polymer Modified Asphalt Properties Related to the Performance of asphalt Concrete Mixes. *Proc. Assoc. Asphalt Paving Technol.*, Vol. 57, p. 116-175.

Halstead, W.J. (1963) The Relation of Asphalt Ductility to Pavement Performance. *Proc. Assoc. Asphalt Paving Technol.*, Vol. 32, pp. 247-270.

Halstead, W.J. (1984) Relation of Asphalt Chemistry to Physical Properties and Specifications. *Research Report No. FHWA/VA-84/85*, Virginia Department of Highways and Transportation.

Harper, C.A. (1996) *Handbook of Plastics, Elastomers, and Composites*, 3rd edition, McGraw-Hill, p. 5, 12.

Harrigan, E.T., R.B. Leahy, and J.S. Youtcheff (Eds). (1994) *The SUPERPAVE Mix Design System Manual of Specifications, Test Methods, and Practices*. Strategic Highway Research Program/National Research Council. Washington, D.C.

Heukelom, W. (1966) Observations on the Rheology and Fracture of Bitumens and Asphalt Mixes. *Proc. Assoc. Asphalt Paving Technol.*, Vol. 36, pp. 358-396.

Hills, J.F., and D. Brien. (1966) The Fracture of Bitumens and Asphalt Mixes by Temperature Induced Stresses. Discussion in *Proc. Assoc. Asphalt Paving Technol.*, Vol. 35, pp. 292-309.

Hoare, T.R., and S. Hesp. (2000) Low-Temperature Fracture Testing of Asphalt Binders: Regular and Modified Systems. *Transp. Res. Rec.*, Vol. 1728, p. 36.

Huang, S-C, M. Tia, and B.E. Ruth. (1996). Laboratory Aging Methods for Simulation of Field Aging of Asphalts. *J. of Materials in Civil Engineering*, Vol. 8 (3), pp. 147-152.

Hubbard, P., and H. Gollomb. (1937) The Hardening of Asphalt with Relation to Development of Cracks in Asphalt Pavements. *Proc. Assoc. Asphalt Paving Technol.*, Vol. 9, pp. 165-194.

Hveem, F.N., E. Zube, and J. Skog. (1963) Proposed New Tests and Specifications for Paving Grade Asphalts. *Proc. Assoc. Asphalt Paving Technol.*, Vol. 32, p. 2.

Ista, E.J., and F.S. Choquet. (1992) The Determination of Bitumen and Recycled Tire Rubber Content in Rubberized Asphalt Road Mixtures. In ASTM STP 1108: *Polymer Modified Asphalt Binders*, K.R. Wardlaw and S. Shuler (Eds.), American Society for Testing and Materials, San Antonio, TX., pp. 224-233.

Jamieson, I.L., and M.M. Hattingh. (1970) The Correlation of Chemical and Physical Properties of Bitumens with Their Road Performance. *Australian Road Research Conf. Proc.*, Vol. 5, pp. 293-324.

Jemison, H.B., B.L. Burr, R.R. Davison, J.A. Bullin, and C.J. Glover. (1992) Application and Use of the ATR, FTIR Method to Asphalt Aging Studies. *Fuel Sci. and Technol. Int'l.*, Vol. 10, pp. 795-808.

Jemison, H.B., R.R. Davison, C.J. Glover, and J.A. Bullin. (1991) Evaluation of Standard Oven Tests for Hot-Mix Plant Aging. *Transp. Res. Rec.*, Vol. 1323, pp. 77-84.

Jemison, H.B., R.R. Davison, C.J. Glover, and J.A. Bullin. (1995) Fractionation of Asphalt Materials by Using Supercritical Cyclohexane and Pentane. *Fuel Sci. And Technol. Int'l.*, Vol. 13 (5), pp. 605-638.

Jennings, P.W., and J.A. Pribanic. (1985) The Expanded Montana Asphalt Quality Study Using High Pressure Liquid Chromatography. *Research Report FHWA/MT-85/001*, State of Montana Department of Highways.

Jennings, P.W., J.A. Pribanic, W. Campbell, K.R. Dawson, and R.B. Taylor. (1980) High Pressure Liquid Chromatography as a Method of Measuring Asphalt Composition. *Research Report FHWA-MT-7930*, State of Montana Department of Highways.

Kandhal, P.S. (1977) Low-Temperature Ductility in Relation to Pavement Performance. In ASTM STP 628: *Low-Temperature Properties of Bituminous Materials and Compacted Bituminous Paving Mixtures*, C.R. Marek (Ed.), American Society for Testing and Materials, Philadelphia, PA, pp. 95-106.

Kandhal, P.S., and W.C. Koehler. (1984) Significant Studies on Asphalt Durability: Pennsylvania Experience. *Transp. Res. Rec.*, Vol. 999, pp. 41-50.

Kandhal, P.S., and M.E. Wenger. (1973) Evaluation of Properties of AC-20 Asphalt Cements. *Transp. Res. Rec.*, Vol. 468, pp. 56-64.

Kanhal, P.S., and M.E. Wenger. (1975) Asphalt Properties in Relation to Pavement Performance. *Transp. Res. Rec.*, Vol. 544, pp. 1-13.

Kaufman, H.S. (1978) *Introduction to Polymer Science and Technology: an SPE Textbook.* John Wiley & Sons, New York, NY, p. 312**.**

Kumar, A., and R.K. Gupta. (1998) *Fundamentals of Polymers*. McGraw-Hill, New York, NY.

Larson, R.G. (1999) *The Structure and Rheology of Complex Fluids*. Oxford University Press, New York, NY, p. 107.

Lau, C.K., K.M. Lunsford, C.J. Glover, R.R. Davison, and J.A. Bullin. (1992) Reaction Rates and Hardening Susceptibilities as Determined from POV Aging of Asphalts. *Transp. Res. Rec.*, Vol. 1342, pp. 50-57.

Lee, D.Y. (1968) Development of a Laboratory Durability Test for Asphalt. *HRB Report*, Vol. 231, p. 34.

Lee, D.Y. (1973) Asphalt Durability Test Correlations in Iowa. *Hwy. Res. Rec.*, Vol. 468, pp. 43-60.

Lee, D.Y., and R.J. Huang. (1973) Weathering of Asphalts as Characterized by Infrared Multiple Internal Reflection Spectra. *Anal. Chem.*, Vol. 46, p. 2242.

Lesueur, D., J.-F. Gerard, P. Claudy, J.-M. Letoffe, J.P. Planche, and D. Martin. (1996) A Structure-Related Model to Describe Asphalt Linear Viscoelasticity. *J. Rheology,* Vol. 40 (5), pp. 813-836.

Lewandowski. L.H. (1994) Polymer Modification of Paving Asphalt Binders. *Rubber Chemistry and Technology,* Vol. 67, pp. 447-480.

Lin, M.S., C.J. Glover, R.R. Davison, and J.A. Bullin. (1995a) The Effects of Asphaltenes on Asphalt Recycling and Aging. *Transp. Res. Rec.*, Vol. 1507, pp. 86-95.

Lin, M.-S., J.M. Chaffin, R.R. Davison, C.J. Glover, and J.A. Bullin. (1998) A New Suspension Viscosity Model and Its Application to Asphaltene Association Thermodynamics and Structures. O.C. Mullins, E.Y. Sheu (Eds.). In *Structures and Dynamics of Asphaltenes,* Plenum Press, New York, NY, pp. 267-302.

Lin, M.-S., J.M. Chaffin, M. Liu, C.J. Glover, R.R. Davison, and J.A. Bullin. (1996) The Effect of Asphalt Composition on the Formation of Asphaltenes and Their Contribution to Asphalt Viscosity. *Fuel Sci. and Technol. Int'l*, Vol. 14 (1&2), pp. 139-162.

Lin, M.S., K.M. Lunsford, C.J. Glover, R.R. Davison, and J.A. Bullin. (1995b) The Effects of Asphaltenes on the Chemical and Physical Characteristics of Asphalts. In *Asphaltenes: Fundamentals and Applications*, E.Y. Sheu and O.C. Mullins (Eds.), Plenum Press, New York, NY, pp. 155-176.

Linde, S., and U. Johansson. (1992) Thermo-Oxidative Degradation of Polymer Modified Bitumen. In ASTM STP 1108: *Polymer Modified Asphalt Binders*, K.R. Wardlaw and S. Shuler (Eds.), American Society for Testing and Materials, San Antonio, TX., pp. 244-253.

Liu, M. (1996) *The Effects of Asphalt Fractional Composition on Properties.* Ph.D. Dissertation, Texas A&M University, College Station, TX.

Liu, M., J.M. Chaffin, R.R. Davison, C.J. Glover, and J.A. Bullin. (1997a) Reactivity of Asphalt Supercritical Fractions. *Ind. Eng. Chem. Res.*, Vol. 36 (6), pp. 2177-2183.

Liu, M., J. M. Chaffin, R. R. Davison, C. J. Glover, and J. A. Bullin. (1998a) Changes in Corbett Fraction Composition During Oxidation of Asphalt Fractions. *Transp. Res. Rec*., Vol. 1638, pp. 40-46.

Liu, M., M.A. Ferry, R.R. Davison, C.J. Glover, and J.A. Bullin. (1998b) Oxygen Uptake as Correlated to Carbonyl Growth in Aged Asphalts and Asphalt Corbett Fractions. *Ind. Eng. Chem. Res.*, Vol. 37, pp. 4669-4674.

Liu, M., M.S. Lin, J.M. Chaffin, R.R. Davison, C.J. Glover, and J.A. Bullin. (1997b) Compositional Optimization for a Superior Asphalt Binder. *Petroleum Sci. and Technol.*, Vol. 15 (1&2), pp. 471-493.

Liu, M., M.S. Lin, J.M. Chaffin, R.R. Davison, C.J. Glover, and J.A. Bullin. (1998c) Oxidation Kinetics of Asphalt Corbett Fractions and Compositional Dependence of Asphalt Oxidation. *Petroleum Science and Technology,* Vol. 16 (7&8), pp. 827-850.

Liu, M., K.M. Lunsford, R.R. Davison, C.J. Glover, and J.A. Bullin. (1996) The Kinetics of Carbonyl Formation in Asphalt. *AIChE J.*, Vol. 42 (4), pp. 1069-1076.

Lu X., and U. Isacsson. (1999) Chemical and Rheological Characteristics of Styrene-Butadiene-Styrene Polymer-Modified Bitumens. *Transp. Res. Rec.*, Vol. 1661, pp. 83-92.

Lunsford, K.M. (1994) *The Effect of Temperature and Pressure on Laboratory Oxidized Asphalt Films with Comparison to Field Aging*. Ph.D. Dissertation, Texas A&M University, College Station, TX.

Madrid, R.C. (1997) *Compositional Evaluation of Asphalt Binder Recycling Agents*. M.S. Thesis, Texas A&M University, College Station, TX.

Martin, K.L., R.R. Davison, C.J. Glover, and J.A. Bullin. (1990) Asphalt Aging in Texas Roads and Test Sections. *Transp. Res. Rec.*, Vol. 1269, pp. 9-19.

McCrum, N.G., C.P. Buckley, and C.B. Bucknall. (1997) *Principles of Polymer Engineering,* 2nd Edition, Oxford Science Publications, p. 140.

McLeod, N.W. (1972) A 4-Year Survey of Low Temperature Transverse Pavement Cracking on Three Ontario Test Roads. *Proc. Assoc. Asphalt Paving Technol.*, Vol. 41, pp. 424-493.

Mullins, O.C., and E.Y. Sheu. (1998) *Structures and Dynamics of Asphaltenes,* Plenum Press, New York, NY.

Muncy, H.W., G.N. King, and J.B. Prudhomme. (1987) Improved Rheological Properties of Polymer-Modified Asphalts. In ASTM STP 941: *Asphalt Rheology: Relationship to Mixture*. O.E. Briscoe (Ed.), American Society for Testing and Materials, Nashville, TN., pp. 146-165.

Newman, J.K. (1998) Dynamic Shear Rheological Properties of Polymer-Modified Asphalt Binders. *Journal of Elastomers and Plastics*, Vol. 30, pp. 245-263.

Petersen, J.C. (1984) Chemical Composition of Asphalt as Related to Asphalt Durability-State-of-the-Art. *Transp. Res. Rec.*, Vol. 999, pp. 13-30.

Petersen, J.C. (1998) A Dual, Sequential Mechanism for the Oxidation for Petroleum Asphalts. *Pet. Sci. & Tech.*, Vol. 16, p. 1023.

Petersen, J.C., J.F. Branthaver, R.E. Robertson, P.M. Harnsberger, J.J. Duvall, and E.K. Ensley. (1993) Effects of Physicochemical Factors on Asphalt Oxidation Kinetics. *Transp. Res. Rec*., Vol. 1391, p. 1.

Peterson, G.D., R.R. Davison, C.J. Glover, and J.A. Bullin. (1994) Effect of Composition on Asphalt Recycling Agent Performance. *Transp. Res. Rec.*, Vol. 1436, pp. 38-46.

Pfeiffer, J.P., and R.N.J. Saal. (1940) *J. Phys. Chem.*, Vol. 44, p. 139.

Quddus, M.A., S.N. Sarwar, and F. Khan. (1995) The Chemical Composition of Catalytic Air Blown Asphalt. *Fuel*, Vol. 74, p. 684.

Readshaw, E.E. (1972) Asphalt Specifications in British Columbia for Low Temperature Performance. *Proc. Assoc. Asphalt Paving Technol.*, Vol. 43, pp. 562-581.

Reese, R.E. (1997) Properties of Aged Asphalt binder Related to Asphalt Concrete Fatigue Life. *Proc. Assoc. Asphalt Paving Technol*., Vol. 66, 604-632.

Reese, R.E., and J.L. Goodrich. (1993) California Desert Test Road - a Step Closer to Performance Based Specifications. *Proc. Assoc. Asphalt Paving Technol.*, Vol. 62, pp. 247-313.

Shuler, T.S., J.H. Collins, and J.P. Kirkpatrick. (1987) Polymer-Modified Asphalt Properties Related to Asphalt Concrete Performance. In ASTM STP 941: *Asphalt Rheology: Relationship to Mixture,* O.E. Briscoe (Ed.), American Society for Testing and Materials, Nashville, TN., pp. 179-193.

Skog, J. (1967) 'Setting' and Durability Studies on Paving Grade Asphalts. *Proc. Assoc. Asphalt Paving Technol.*, Vol. 36, pp. 387-420.

Srivastava, A., P.C. Hopman, and A.A. Molenaar. (1992) SBS Polymer Modified Asphalt Binder and Its Implications on Overlay Design. In ASTM STP 1108: *Polymer Modified Asphalt Binders*, K.R. Wardlaw and S. Shuler (Eds.), American Society for Testing and Materials, San Antonio, TX, pp. 309-329.

Stegeman, J.R., R.R. Davison, C.J. Glover, and J.A. Bullin. (1991) Supercritical Fractionation and Reblending to Produce Improved Asphalts. *Proceedings of the International Symposium: Chemistry of Bitumens*, Rome, Italy, Vol. 1, pp. 336-381.

Stoffels, S.M., R. Roque, and T. Farwana. (1994) Evaluation and Field Validation of Proposed SHRP Binder Specification for Thermal Cracking. *Transp. Res. Rec.*, Vol. 1436, pp. 1-10.

Strategic Highway Research Program. (1993) *SHRP Materials Reference Library: Asphalt Cements: A Concise Data Compilation*, National Research Council, Washington D.C.

Tayebali, A.A., J.L. Goodrich, J.B. Sousa, and C.L. Monismith. (1992) Influence of the Rheological Properties of Modified Asphalt Binders on the Load Deformation Characteristics of the Binder-Aggregate Mixtures. In ASTM STP 1108: *Polymer Modified Asphalt Binders*, K.R. Wardlaw and S. Shuler (Eds.), American Society for Testing and Materials, San Antonio, TX, pp. 77-96.

Texas Department of Transportation. (1995) Prediction of Moisture Induced Damage to Bituminous Paving Materials Using Molded Specimens. *Manual of Testing Procedures*. Section 10. Tex-531-C.

Vallerga, B.A., and W.J. Halstead. (1971) The Effect of Field Aging on Fundamental Properties of Paving Asphalts. *Highway Research Record*, Vol. 361, pp. 71-92.

Vassiliev, N.Y. (2001) *Studies of Asphalt Air Blowing and Development of a New Air Blowing Technique for Simulation of Asphalt Short-Term Aging*. M.S. Thesis, Texas A&M University, College Station, TX.

Welborn, J.Y. (1984) Physical Properties as Related to Asphalt Durability: State of the Art. *Transp. Res. Rec.*, Vol. 999, pp. 31-36.

Welborn, J.Y., E.R. Oglio, and J.A. Zenewitz. (1966) A Study of Viscosity-Graded Asphalt Cements. *Proc. Assoc. Asphalt Paving Technol.*, Vol. 35, pp. 19-60.

Williams, M. L., R. F. Landel, and J. F. Ferry. (1955) The Temperature Dependence of Relaxation Mechanisms in Amorphous Polymers and Other Glass Forming Liquids. *J. Am. Chem. Soc.*, Vol. 77, pp. 3701-3707.

APPENDIX A

TABLES OF AGING STUDIES DATA

Table A-1 (a).

	Conventional PAV			PAV Thin Film 90 °C			POV 100 °C, 5 atm O_2		
	24 hours	48 hours	72 hours	24 hours	50 hours	72 hours	24 hours	48 hours	72 hours
$\eta^*_{60\ °C,\ 0.1\ rad/s}$ (poise)									
AAA-1	10,390	121,400	750,900	23,040	69,830	325,700	59,360	653,800	3,030,000
AAB-1	14,640	131,200	720,100	30,700	74,590	221,600	71,990	535,900	2,741,000
AAD-1	17,680	237,300	961,500	55,190	224,900	643,600	108,400	1,271,000	6,379,000
AAF-1	21,700	124,400	355,200	72,740	198,200	419,900	135,900	680,800	1,894,000
ABM-1	11,830	18,240	29,270	18,830	24,980	42,130	19,570	37,950	50,590
AAM-1	40,110	172,300	474,300	61,720	176,300	321,700	116,200	412,400	886,400
AAS-1	27,780	96,100	292,500	38,680	91,750	187,100	76,780	323,700	852,500
Exxon AC-20	18,330	69,030	221,600	32,810	74,660	125,300	55,740	224,200	740,000
TS2000 AC-20	81,310	397,000	1,549,000	84,990	246,800	500,700	199,800	900,900	3,186,000
Function									
AAA-1	1.48×10^{-4}	1.12×10^{-3}	5.39×10^{-3}	2.08×10^{-4}	5.17×10^{-4}	2.62×10^{-3}	5.35×10^{-4}	5.21×10^{-3}	6.38×10^{-2}
AAB-1	2.78×10^{-4}	1.53×10^{-3}	7.34×10^{-3}	3.66×10^{-4}	9.17×10^{-4}	3.15×10^{-3}	1.05×10^{-3}	5.78×10^{-3}	1.82×10^{-2}
AAD-1	3.26×10^{-4}	1.64×10^{-3}	6.31×10^{-3}	3.52×10^{-4}	1.89×10^{-3}	4.80×10^{-3}	8.12×10^{-4}	8.55×10^{-3}	3.51×10^{-2}
AAF-1	7.06×10^{-4}	3.93×10^{-3}	9.84×10^{-3}	2.10×10^{-3}	6.39×10^{-3}	1.03×10^{-2}	4.54×10^{-3}	1.47×10^{-2}	2.70×10^{-2}
ABM-1	1.25×10^{-4}	3.02×10^{-4}	6.91×10^{-4}	3.48×10^{-4}	5.86×10^{-4}	1.57×10^{-3}	3.53×10^{-4}	1.34×10^{-3}	2.10×10^{-3}
AAM-1	4.17×10^{-4}	1.50×10^{-3}	4.14×10^{-3}	6.18×10^{-4}	1.71×10^{-3}	3.01×10^{-3}	5.35×10^{-4}	3.29×10^{-3}	5.92×10^{-3}
AAS-1	2.40×10^{-4}	1.01×10^{-3}	2.38×10^{-3}	3.93×10^{-4}	9.35×10^{-4}	1.79×10^{-3}	7.79×10^{-4}	2.77×10^{-3}	6.09×10^{-3}
Exxon AC-20	2.01×10^{-4}	1.16×10^{-3}	3.60×10^{-3}	5.04×10^{-4}	1.44×10^{-3}	2.18×10^{-3}	9.01×10^{-4}	3.79×10^{-3}	1.10×10^{-2}
TS2000 AC-20	7.21×10^{-4}	2.08×10^{-3}	6.86×10^{-3}	7.15×10^{-4}	1.75×10^{-3}	2.76×10^{-3}	1.42×10^{-3}	4.39×10^{-3}	1.04×10^{-2}

Table A-1 (b).

	POV 110 °C, 1 atm O_2			POV 100 °C, 1 atm O_2			POV 93 °C, 1 atm O_2		
	24 hours	48 hours	72 hours	24 hours	48 hours	72 hours	24 hours	48 hours	72 hours
$\eta^*_{60\ °C,\ 0.1\ rad/s}$ (poise)									
AAA-1	24,640	184,100	1,712,000	14,400	43,900	109,000	10,590	25,080	30,410
AAB-1	50,200	299,900	1,846,000	22,970	49,190	100,600	14,350	27,760	51,520
AAD-1	58,130	485,600	1,890,000	30,360	95,730	237,400	24,560	44,150	87,880
AAF-1	72,800	289,800	2,196,000	31,200	70,290	181,100	34,470	58,490	81,910
ABM-1	14,190	22,680	39,430	9,695	15,300	17,650	11,200	15,740	18,680
AAM-1	72,260	184,600	972,500	32,030	99,230	188,000	33,830	60,630	95,720
AAS-1	63,960	253,200	733,600	27,320	61,790	123,600	21,030	36,890	57,730
Exxon AC-20	43,860	140,900	441,900	15,990	46,140	76,620	15,960	27,260	37,490
TS2000 AC-20	136,200	580,800	2,106,000	51,980	137,300	326,300	36,670	70,220	110,600
Function									
AAA-1	2.10×10^{-4}	1.38×10^{-3}	9.46×10^{-3}	1.02×10^{-4}	3.77×10^{-4}	9.92×10^{-4}	7.02×10^{-5}	2.06×10^{-4}	2.35×10^{-4}
AAB-1	6.16×10^{-4}	3.14×10^{-3}	1.21×10^{-2}	2.56×10^{-4}	6.08×10^{-4}	1.24×10^{-3}	1.45×10^{-4}	3.22×10^{-4}	6.58×10^{-4}
AAD-1	3.42×10^{-4}	2.72×10^{-3}	8.27×10^{-3}	1.85×10^{-4}	5.85×10^{-4}	1.63×10^{-3}	1.66×10^{-4}	2.94×10^{-4}	5.39×10^{-4}
AAF-1	2.04×10^{-3}	7.21×10^{-3}	2.92×10^{-2}	6.80×10^{-4}	2.00×10^{-3}	5.00×10^{-3}	8.48×10^{-4}	1.58×10^{-3}	2.61×10^{-3}
ABM-1	1.79×10^{-4}	5.12×10^{-4}	1.32×10^{-3}	8.03×10^{-5}	2.23×10^{-4}	2.92×10^{-4}	1.13×10^{-4}	2.15×10^{-4}	3.05×10^{-4}
AAM-1	8.77×10^{-4}	1.61×10^{-3}	5.77×10^{-3}	2.65×10^{-4}	1.03×10^{-3}	1.63×10^{-3}	3.13×10^{-4}	5.64×10^{-4}	8.79×10^{-4}
AAS-1	5.88×10^{-4}	2.30×10^{-3}	4.94×10^{-3}	2.53×10^{-4}	5.88×10^{-4}	1.24×10^{-3}	1.87×10^{-4}	3.70×10^{-4}	5.83×10^{-4}
Exxon AC-20	6.78×10^{-4}	2.45×10^{-3}	6.65×10^{-3}	1.60×10^{-4}	7.17×10^{-4}	1.40×10^{-3}	1.69×10^{-4}	3.74×10^{-4}	4.58×10^{-4}
TS2000 AC-20	1.01×10^{-3}	2.68×10^{-3}	7.39×10^{-3}	4.25×10^{-4}	9.95×10^{-4}	2.13×10^{-3}	2.97×10^{-4}	5.69×10^{-4}	8.12×10^{-4}

Table A-2.

	POV 88 °C, 0.2 atm O_2			POV 82 °C, 1 atm O_2		
	72 hours	216 hours	384 hours	72 hours	216 hours	384 hours
η^* measured at 60 °C, 0.1 rad/s (poise)						
AAA-1	4,904	10,580	19,910	7,834	16,140	119,600
AAB-1	8,247	20,130	32,580	13,330	38,290	184,700
AAD-1	11,070	23,880	63,850	18,540	61,910	279,600
AAF-1	14,490	35,490	81,340	29,990	70,830	272,500
ABM-1	6,605	8,946	12,230	11,070	13,980	29,430
AAM-1	15,890	38,640	80,100	27,180	72,120	254,500
AAS-1	12,650	24,410	35,810	19,020	57,610	174,300
Exxon AC-20	11,140	19,170	34,650	17,440	39,010	97,880
TS2000 AC-20	26,580	68,780	156,100	41,970	98,690	369,300
Function measured at 43 °C, 10 rad/s						
AAA-1	2.28×10^{-5}	7.76×10^{-5}	1.86×10^{-4}	5.19×10^{-5}	1.31×10^{-4}	1.06×10^{-3}
AAB-1	6.68×10^{-5}	2.08×10^{-4}	4.13×10^{-4}	1.44×10^{-4}	4.80×10^{-4}	2.04×10^{-3}
AAD-1	6.41×10^{-5}	1.34×10^{-4}	4.33×10^{-4}	1.05×10^{-4}	4.33×10^{-4}	1.76×10^{-3}
AAF-1	1.66×10^{-4}	8.06×10^{-4}	2.57×10^{-3}	6.30×10^{-4}	2.19×10^{-3}	7.37×10^{-3}
ABM-1	2.93×10^{-5}	6.26×10^{-5}	1.40×10^{-4}	1.09×10^{-4}	1.59×10^{-4}	8.76×10^{-4}
AAM-1	1.28×10^{-4}	4.01×10^{-4}	8.66×10^{-4}	2.57×10^{-4}	8.06×10^{-4}	2.23×10^{-3}
AAS-1	9.71×10^{-5}	1.99×10^{-4}	2.89×10^{-4}	1.52×10^{-4}	5.76×10^{-4}	1.69×10^{-3}
Exxon AC-20	8.62×10^{-5}	2.06×10^{-4}	5.04×10^{-4}	1.85×10^{-4}	6.15×10^{-4}	1.93×10^{-3}
TS2000 AC-20	2.42×10^{-4}	5.86×10^{-4}	1.18×10^{-3}	3.19×10^{-4}	7.92×10^{-4}	2.32×10^{-3}

Table A-3.

	Aging Time in Environmental Room (60 °C, 1 atm Air)						
	2 months	4 months	6 months	9 months	12 months	15 months	22 months
η* measured at 60 °C, 0.1 rad/s (poise)							
Exxon Base	27,690	46,520	64,280				
Fina AC-5		8,543	14,100	23,390	33,640		
Fina AC-10	8,039	13,680	19,980	26,290	47,100		
Fina PG64-22 Base	24,010	44,260	85,760	247,800			
GSAC AC-15P Base	3,977	5,617	6,726	10,290			
Neste Base	18,840	29,710	43,700	92,890			
TFA Base	19,660	35,630	60,400	144,500			
United Ref Base	12,790	24,970	32,130	109,700			
Wright AC-10	16,570	31,010	44,380	101,200			
Wright AC-20	32,590	65,380	82,650	155,400			
Function measured at 15 °C, 0.001 rad/s							
Exxon Base	4.08×10^{-4}	7.76×10^{-4}	1.47×10^{-3}	2.40×10^{-3}	4.35×10^{-3}		
Fina AC-5	6.02×10^{-5}	1.82×10^{-4}	3.20×10^{-4}	6.89×10^{-4}	1.31×10^{-3}	2.62×10^{-3}	7.55×10^{-3}
Fina AC-10	7.44×10^{-5}	2.01×10^{-4}	4.03×10^{-4}	8.63×10^{-4}	1.66×10^{-3}	2.84×10^{-3}	
Fina PG64-22 Base	1.95×10^{-4}	5.92×10^{-4}	1.66×10^{-3}	4.50×10^{-3}			
GSAC AC-15P Base			3.74×10^{-5}	5.86×10^{-5}	3.04×10^{-4}		
Neste Base	1.44×10^{-4}	2.48×10^{-4}	4.67×10^{-4}	1.45×10^{-3}			
TFA Base	1.20×10^{-4}	3.11×10^{-4}	6.73×10^{-4}	1.88×10^{-3}			
United Ref Base	1.37×10^{-4}	3.62×10^{-4}	6.88×10^{-4}	1.93×10^{-3}			
Wright AC-10	1.34×10^{-4}	2.70×10^{-4}	4.77×10^{-4}	1.14×10^{-3}	1.83×10^{-3}		
Wright AC-20				2.20×10^{-3}	3.72×10^{-3}		

Table A-4.

	POV 100 °C, 1 atm O_2			POV 100 °C, 20 atm Air	
	24 hours	52 hours	72.25 hours	24 hours	30 hours
η^* measured at 60 °C, 0.1 rad/s (poise)					
Exxon Base	21,850	80,450	132,400	61,750	55,920
Fina AC-5	54,710	12,490	30,630	9,550	10,700
Fina AC-10	958,300	23,640	37,880	14,110	16,270
Fina PG64-22 Base	255,400	188,300	317,900	91,750	141,200
GSAC AC-15P Base	66,200	7,724	14,470	6,237	8,123
Neste Base	192,000	79,310	269,800	40,040	65,220
TFA Base	231,300	96,700	319,400	61,390	98,980
United Ref Base	146,500	108,600	260,100	46,850	74,220
Wright AC-10	161,700	200,600	621,900	74,870	115,300
Wright AC-20	260,400	359,200	932,200	179,300	272,500
Function measured at 43 °C, 10 rad/s					
Exxon Base	3.24×10^{-4}	1.71×10^{-3}	2.64×10^{-3}	1.45×10^{-3}	1.25×10^{-3}
Fina AC-5	2.20×10^{-5}	1.96×10^{-4}	6.11×10^{-4}	1.24×10^{-4}	1.55×10^{-4}
Fina AC-10	4.91×10^{-5}	3.90×10^{-4}	8.49×10^{-4}	1.69×10^{-4}	2.28×10^{-4}
Fina PG64-22 Base	3.80×10^{-4}	3.19×10^{-3}	4.91×10^{-3}	1.58×10^{-3}	2.45×10^{-3}
GSAC AC-15P Base	1.48×10^{-5}	5.83×10^{-5}	1.94×10^{-4}	3.56×10^{-5}	7.22×10^{-5}
Neste Base	2.46×10^{-4}	1.19×10^{-3}	3.07×10^{-3}	6.93×10^{-4}	1.04×10^{-3}
TFA Base	3.51×10^{-4}	1.05×10^{-3}	3.30×10^{-3}	8.14×10^{-4}	1.46×10^{-3}
United Ref Base	2.49×10^{-4}	1.26×10^{-3}	2.86×10^{-3}	5.85×10^{-4}	1.06×10^{-3}
Wright AC-10	3.58×10^{-4}	1.70×10^{-3}	4.26×10^{-3}	7.38×10^{-4}	1.22×10^{-3}
Wright AC-20	7.32×10^{-4}	2.65×10^{-3}	6.03×10^{-3}	1.59×10^{-3}	2.52×10^{-3}

Table A-5.

	POV 100 °C, 5 atm Air			
	24 hours	29 hours	52.75 hours	76.75 hours
η^* measured at 60 °C, 0.1 rad/s (poise)				
SHRP AAD-1		29,010	32,690	87,200
SHRP AAF-1		28,400	33,820	90,610
TS2000 AC-20		59,760	92,600	240,100
Exxon Base		20,400	39,040	86,220
Fina PG64-22 Base		26,950	45,090	127,100
United Ref Base		16,010	32,090	93,840
Wright AC-20		64,020	144,700	387,100
TS2000 12% Rubber		52,820	54,370	66,560
UltraPave PG70-22 (Exxon Base)		25,980	34,000	78,830
Fina PG64-28 3.5% Latex		13,470	17,710	24,000
UltraPavePG70-22 (United Ref	23,510	21,130	27,650	36,168
Base)		139,500	174,400	217,964
Wright AC-20 3% Latex				
Function measured at 43 °C, 10 rad/s				
SHRP AAD-1		1.84×10^{-4}	2.40×10^{-4}	5.87×10^{-4}
SHRP AAF-1		6.40×10^{-4}	7.35×10^{-4}	2.76×10^{-3}
TS2000 AC-20		5.75×10^{-4}	8.00×10^{-4}	1.84×10^{-3}
Exxon Base		2.78×10^{-4}	8.44×10^{-4}	1.88×10^{-3}
Fina PG64-22 Base		2.67×10^{-4}	5.94×10^{-4}	2.14×10^{-3}
United Ref Base		1.46×10^{-4}	3.64×10^{-4}	1.20×10^{-3}
Wright AC-20		6.14×10^{-4}	1.45×10^{-3}	3.41×10^{-3}
TS2000 12% Rubber		3.20×10^{-4}	4.36×10^{-4}	6.47×10^{-4}
UltraPave PG70-22 (Exxon Base)		4.06×10^{-4}	9.62×10^{-4}	1.77×10^{-3}
Fina PG64-28 3.5% Latex		7.63×10^{-5}	1.48×10^{-4}	3.15×10^{-4}
UltraPavePG70-22 (United Ref	2.25×10^{-4}	2.44×10^{-4}	3.82×10^{-4}	5.96×10^{-4}
Base)		3.24×10^{-4}	4.62×10^{-3}	6.57×10^{-3}
Wright AC-20 3% Latex				